Universidade do Minho

Escola de Engenharia

Jorge Manuel Jardim da Silva

The role of interfacial elasticity on the rheological behaviour of polymer blends

Tese de Doutoramento em Ciência e Engenharia de Polímeros
Área de conhecimento de Ciência de Materiais Poliméricos

Trabalho efectuado sob a orientação de

Doutor João Maia

Doutora Ana Vera Machado

Junho de 2009

ACKNOWLEDGMENTS

I´ll be eternally grateful to all of those that, during this period, personally and professionally very enriching, helped and encourage me.

First, I would like to thank my supervisors, João Maia and Ana Vera Machado, for their help, their patience and for the motivation they transmitted to me, mainly in the difficult moments.

I would also like to thank Paula Moldenaers, Peter Van Puyvelde and all members of the Applied Rheology and Polymer Processing group of the Katholieke Universiteit Leuven, where some experiments were performed, that contributed to my stay in Belgium being very fruitful and pleasant.

Chapter 5 of this thesis was result of a collaboration with the Polymer Group of University of Coruña and I am especially grateful to Ana Ares for this collaboration as well as for her friendship.

Thanks are also due to academic staff, researchers, technicians and administrative staff of the Department of Polymer Engineering of the University of Minho that helped me along this path. To name a few: J. A. Covas, Olga Carneiro, Miguel Nóbrega, Fernando Duarte, Gaspar Cunha, Conceição Paiva, Ferrie Van Hattum, Loic Hilliou, Susana Filipe, Vitor Barroso, Renato Reis, Joana Barbas, Eva Barroso, Patrícia Rebelo, Liliana Santos, Diana Krasteva, Carla Leer, Ricardo Andrade, Albano Teixeira, Rachelle Musampa, Paulo Teixeira, Gabriela Azevedo, Pedro Marques.

Thanks are also due to my family, my father João and my sister Alexandra for their continued support. I´m also grateful to my girlfriend, Marlene, for her love during these five years.

Finally, I thank the Foundation for Science and Technology–FCT for awarding me a PhD Fellowship (grant BD/12833/2003) within the framework of Programa Operacional"Ciência, Tecnologia, Inovação" (POCTI) and Programa Operacional Sociedade da Informação (POSI) of the 3nd European Support Board (2000–2006).

I dedicate this thesis to the memory of my Mother, Maria da Conceição Gonçalves Jardim, who sadly passed away during its preparation.

The role of interfacial elasticity on the rheological behaviour of polymer blends

ABSTRACT

Blending polymers allows materials with enhanced properties to be developed with much less effort than that required to synthesize a completely new polymer.

The main advantages of the polymers blends are *a)* the fact that they can be compounded on standard industrial equipments, e.g., twin-screw extruders and *b)* by merely changing the blend composition a wide range of materials properties can be reached.

The market of polymer blend based materials has increased continuously in recent times. Nowadays, a significant fraction of all produced plastics are processed as blends. For example, in 2001, approximately 10% of all thermoplastics and 75% of all elastomers were processed as blends [Ehrenstein (2001)]. Polymer blends find applications in many areas such as automotive industry, lawns and gardens, medicine, building and construction, packaging, among others.

However most polymers are immiscible and thus the use of compatibilizers is necessary to improve the final properties of the materials. The optimization of these final properties depends strongly on knowledge of the behavior of the polymer blends during processing, when they are subjected to complex flows.

In this thesis the influence of the compatibilization of polymer blends on their rheological behavior was investigated. First, a commercial blend of PA6/EPM, non-compatibilized and compatibilized with EPM-g-MA, with high viscosity and elasticity ratio was studied. Stress relaxation experiments, both in shear and extension, showed that the introduction of the compatibilizer leads to a large increase of the relaxation time. The observation of the morphology frozen during extension tests seemed to indicate that the droplets of the highly compatibilized blends are more deformed than the droplets of the non-compatibilized one.

To clarify these results and better understand the relative importance of relaxation of the droplets and relaxation of the interfaces in this kind of compatibilized blends, high viscosity ratio blends of PMMA/PS/PSOX were prepared. These blends, which are optically transparent, allow the use of

Small Angle Light Scattering (SALS) when the concentration of the blend is low enough. Thus, the deformation of the droplets in transient shear flows could be evaluated. Contrary to the non-compatibilized one, the blend with functionalized PS shows a droplet deformation on the vorticity direction, which is an indication of an increase in the elasticity of the interface. A larger relaxation time is also observed. In this case, the increase of relaxation time is related with stress relaxation at and in the interfaces.

The role of the elasticity of the interface became quite clear when PP/EVOH blends, non-compatibilized and compatibilized with Na^+ were tested. In this case the elasticity of the interface is negligible and it was observed that the Na^+ compatibilizer does not alter drastically the relaxation behavior after a step deformation.

O papel da elasticidade interfacial no comportamento reológico de misturas de polímeros

RESUMO

Misturar polímeros permite o desenvolvimento de materiais com melhores propriedades com menor esforço do que seria necessário para sintetizar um polímero completamente novo.

As principais vantagens das misturas de polímeros são a) o facto de poderem ser compostas em equipamentos industriais rotineiros, p.e., extrusoras de duplo-fuso e b) permitirem atingir uma vasta gama de propriedades através da simples alteração da composição da mistura.

O mercado de materiais baseados em misturas de polímeros tem aumentado continuamente nos últimos anos. Hoje, uma fracção significativa de todos os plásticos produzidos é misturas de polímeros. Por exemplo, em 2001, aproximadamente 10% de todos os termoplásticos e 75% de todos os elastómeros eram processados como misturas [Ehrenstein (2001)]. As misturas de polímeros encontram aplicações em muitas áreas tais como a indústria automóvel, agricultura, medicina, construção e embalamento, entre outras.

Contudo, a maioria dos polímeros são imiscíveis e então é necessário utilizar compatibilizadores para aumentar as propriedades finais dos materiais. A optimização destas propriedades finais depende, em boa medida, do conhecimento do comportamento das misturas de polímeros durante o processamento quando sujeitas a escoamentos.

Nesta tese foi investigada a influência da compatibilização nas propriedades reológicas das misturas de polímeros. Inicialmente foi estudada uma mistura comercial de PA6/EPM, não compatibilizada e compatibilizada com EPM-g-MA, com altas razões de viscosidade e elasticidade. As experiências de relaxação de tensões, em corte e em extensão, mostraram que a introdução do compatibilizador conduz a um grande aumento do tempo de relaxação. A observação da morfologia congelada durante um ensaio extensional pareceu indicar que as gotas das misturas mais compatibilizadas se deformam mais do que as gotas das misturas não compatibilizadas.

Tendo em vista clarificar estes resultados e obter uma melhor compreensão da importância relativa da relaxação das gotas e das interfaces neste tipo de misturas compatibilizadas, foram preparadas misturas de PMMA/PS/PSOX com alta razão de viscosidade. Estas misturas, que são opticamente transparentes, permitem o uso da técnica Difracção de Luz de Baixos Ângulos, *Small Angle Light Scattering*, (SALS), quando a concentração da mistura é suficientemente baixa. Assim, foi possível avaliar a deformação das gotas em escoamentos de corte transientes. Contrariamente ao que acontece na mistura não compatibilizada, as gotas da mistura funcionalizada com PS exibem uma deformação na direcção da vorticidade, a qual é uma indicação do aumento da elasticidade da interface. Neste caso o aumento do tempo de relaxação está relacionado com a tensão de relaxação nas interfaces.

Finalmente foi testada uma mistura de PP/EVOH, não compatibilizada e compatibilizada com Na^{+}. Neste caso a compatibilização não aumenta significativamente a elasticidade da interface e portanto, a relaxação depois da aplicação de um escoamento de corte não é alterada.

TABLE OF CONTENTS

LIST OF SYMBOLS AND ABREVIATIONS

PA6	Polyamide-6
EPM	Ethene-propene rubber
EPM-g-MA	Anhydride Maleic grafted Ethene-propene Rubber
MA	Maleic Anhydride
PMMA	Poly-methylmethacrylate
PS	Polystyrene
PSOX	Oxazoline Functionalized Polystyrene
PP	Polypropylene
EVOH	Ethylene-vinyl alcohol copolymer
SEM	Scanning Electron Microscope
SALS	Small Angle Light Scattering
$2\mathbf{D}$	Rate-of-deformation tensor
$\boldsymbol{\tau}$	Stress tensor
$\dot{\gamma}$	Shear rate
η	Zero shear viscosity
p	Viscosity ratio
Ca	Capillary number
α	Interfacial tension
Ca_{crit}	Critical capillary number
Q	Interfacial area per unit of volume
q_{ij}	Anisotropy tensor

ω	Angular frequency
η^*	Complex viscosity
G^*	Complex modulus
G'	Storage modulus
G''	Loss modulus
ϕ	Volume fraction of dispersed phase
R_v	Volume average radii
R_n	Number average radii
ε_H	Hencky strain
$\dot{\varepsilon}$	Strain rate
Tr	Trouton ratio
η_E^+	Transient uniaxial extensional viscosity
M	Torque
E	Uniaxial relaxation modulus
E_N	Normalized uniaxial relaxation modulus

LIST OF FIGURES

CHAPTER 1

CHAPTER 2

CHAPTER 3

CHAPTER 4

CHAPTER 5

LIST OF TABLES

LIST OF PUBLICATIONS AND COMMUNICATIONS

This thesis gave origin to the following publications and communications:

Papers in international journals

Silva, J. M., A. V. Machado and J. M. Maia, "Transient rheological behaviour of PA6/EPM/EPM-g-MA blends," Advanced Materials Forum Iii, Pts 1 and 2 vol.514-516, 853-857 (2006).

Silva, J., A. V. Machado and J. Maia, "Rheological behavior of compatibilized and non-compatibilized PA6/EPM blends", Rheol Acta 46, 1091-1097 (2007).

Ares, A., J. Silva, J. Maia, L. Barral and M. Abad, "Rheomechanical and morphological study of compatibilized PP/EVOH blends." (2009) *Submitted to* Rheologica Acta.

Silva, J., A. V. Machado, P. Moldenaers, J. Maia, "The effect of interfacial properties on the deformation and relaxation behavior of PMMA/PS blends" (2009) *Submitted to* Journal of Rheology.

Silva, J., A. V. Machado, P. Moldenaers, J. Maia, "The role of interfacial elasticity on the rheological behavior of polymer blends", Korea-Australia Rheology Journal (2009) *In press*.

Papers in national journals

Silva, J., A. V. Machado and J. Maia, "Rheological behaviour of high-viscosity emulsions: A comparison between the predictive capabilities of several theoretical models", e-rheo.pt 4, 64-71 (2004).

Communications in international meetings

Silva, J. M., A. V. Machado and J. M. Maia, "Rheological behaviour of high-viscosity emulsions: A comparison between the predictive capabilities of several theoretical models", IBERHEO 2004 - Progress in Rheology of Biological and Synthetic Polymer Systems, Beja, Portugal, September (2004), *poster presentation*.

Silva, J. M., A. V. Machado and J. M. Maia, "Transient rheological behaviour of PA6/EPM/EPM-g-MA blends", Materiais 2005 – XII Portuguese Materials Society Meeting and II International Materials Symposium, , University of Aveiro, Aveiro, Portugal, March (2005), *poster presentation*.

Silva, J. M., A. V. Machado and J. M. Maia, "Transient rheological behaviour of PA6/EPM/EPM-g-MA blends", AERC 2005 – 2nd Annual European Rheology Conference, Grenoble, France, April (2005), *poster presentation*.

Silva, J. M., A. V. Machado and J. M. Maia, "Nonlinear viscoelasticity of PA6/EPM/EPM-g-MA blends", PPS-2005 – America's Regional Meeting, Quebec, Canada, August (2005), *poster presentation*.

Silva, J. M., A. V. Machado and J. M. Maia, "Rheological behaviour of compatibilazed and non-compatibilazed PA6/EPM blends", AERC 2006 – 3rd Annual European Rheology Conference, Hersonisos - Crete, Greece, April (2006), *oral presentation*.

Silva, J., A. V. Machado, P. Moldenaers, J. Maia, "Deformation and relaxation of PMMA/PS and PMMA/PSOX blends", ICR 2008 - XVth International Congress on Rheology, Monterey – California, USA, August (2008), *oral presentation*.

Silva, J., A. V. Machado, P. Moldenaers, J. Maia, "Effect of the oxazoline groups on the deformation and relaxation of PMMA/PS blends", IBEREO 2008 – Iberian Meeting on Rheology, Madrid, Spain, September (2008), *oral presentation*.

Silva, J., A. V. Machado, P. Moldenaers, J. Maia, "The role of interfacial elasticity on the rheological behavior of polymer blends", 20th Anniversary Symposium of the Korean Society of Rheology, Seoul, Korea, August (2009), *invited presentation*.

Book chapters/Proceedings with ISBN

Silva, J. M., A. V. Machado and J. M. Maia, "Rheological behaviour of high-viscosity emulsions: A comparison between the predictive capabilities of several theoretical models", in Progress in Rheology of Biological and Synthetic Polymer Systems, Ed. A. C. Diogo, N. B. Alvarenga, J. Canada, S. Ferro Palma and J. Dias, Instituto Politécnico de Beja, Beja, Portugal, (2004), 77-82.

Silva, J., A. V. Machado, P. Moldenaers, J. Maia, "Deformation and relaxation of PMMA/PS and PMMA/PSOX blends", in American Institute of Physics Conference Proceedings 1027 - The XVTH International Congress on Rheology, Ed. Albert Co, L. Gary Leal, Ralph H. Colby, and Jeffrey Giacomin, American Institute of Physics, Melville, New York, (2008), 872-874.

ABOUT THE THESIS FORMAT

This thesis is divided in six chapters, each of which contains sections and subsections. **Chapter 1** presents both the introduction and state-of-the-art to the subject of rheology of non-compatibilized and compatibilized polymer blends. In the beginning of the chapter concepts such as miscibility, compatibility, compatibilization and compatibilizer are introduced. The different compatibilization types and the morphologies that can be founded in polymer blends are also discussed. The behavior of polymer blends in shear and extensional flows are reviewed separately in two sections (1.4 and 1.5) of Chapter 1. The Subsection 1.4.3, in particular, compares the predictions of several theoretical rheological models for immiscible polymer blends. It is adapted from Silva *et al.* (2004). In the last section of the chapter the main motivations for this work are discussed.

Chapter 2 is concerned with rheometry. Analogously to Chapter 1, shear and extensional rheometry are discussed in different sections. The techniques and type of rheometers used in this work are presented.

In **Chapter 3** commercial blends of PA-6/EPM compatibilized with EPM-g-MA are studied in both morphological and rheological point of views. This chapter is adapted from the paper Silva *et al.* (2007).

Pursuing the issues arose in the previous chapter, in **Chapter 4** a different, model blend is investigated. Here the compatibilization is achieved by introduction of additional physical interactions. Chapter 4 is adapted from Silva *et al.* (2009a).

To confirm the conclusions of previous chapters in **Chapter 5,** which is adapted from Ares *et al.* (2009), blends of PP/EVOH compatibilized with ionomers are discussed.

In last chapter the relationships between rheology and compatibilization type are explored and the final conclusions are drawn.

CHAPTER 1

Introduction and state-of the art

Note: Section 1.4.3 was adapted from *Silva, J., A. V. Machado and J. Maia, "Rheological behaviour of high-viscosity emulsions: A comparison between the predictive capabilities of several theoretical models", e-rheo.pt 4, 64-71 (2004).* [Appendix A]

1.1 POLYMER BLENDS

Blending polymers allows materials with enhanced properties to be developed with much less effort than what is required to synthesize a new polymer from a new monomer.

The main advantages of blending polymers are *a)* the fact that blends can be compounded on standard industrial equipments, e.g., twin-screw extruders and *b)* by changing the blend composition, a wide range of materials properties can be reached.

The market of polymer blend based materials has increased continuously in recent years. Nowadays, a significant fraction of all produced plastics are prepared as blends. For example, in 2001, approximately 10 % of all thermoplastics and 75 % of all elastomers were prepared as blends [Ehrenstein (2001)]. Polymer blends find applications in many areas, such as the automotive industry, lawns and gardens, medicine, building and construction, packaging, among others.

The basic thermodynamics of polymer mixtures follows the same rules as those of other molecules. Indeed, all of the phase behavior displayed by polymer blends can be found in small molecule mixtures. It can be found miscibility in polymer blends as well as in blends of smaller molecules. However, contrary to the blends of small molecules, it is rare to find true solubility in mixtures of two polymers and in the immiscible ones the kinetic of phase separation is slow. Due to the differences between the general polymer blends behavior and the mixtures of other kinds

of molecules the language used in the polymer blends field is slightly different. For example, instead of thermodynamic solubility the term *miscibility* is normally employed.

Two polymers are miscible if the free energy of mixing, which is a function of the chemical structure of the polymers (e.g., molecular weight, its distribution, copolymer composition) and thermodynamic variables, such as temperature, pressure and blend composition, is negative. A pair of polymers which are immiscible as a 50/50 blend might be miscible as a 95/5 blend under the same conditions.

Since the 1960's it is known that the addition of specific blocks or grafted polymers to an immiscible polymer blend is able to enhance their interfacial properties promoting *compatibility*. It is important to note that miscibility and compatibility is not the same thing. While the former has a strict thermodynamic meaning ($\Delta G_{mix} \leq 0$), the latter is defined in operational terms. A blend may be more or less compatible depending on its miscibility. A "completely compatible" system is thus a miscible one [Utracki (2002)].

From a technical point of view, it is quite important to promote the compatibility of immiscible polymer blends. Immiscible blends usually have coarse and unstable morphology and consequently bad mechanical properties. The *compatibilization* decreases the interfacial tension and hence the scale of phase separation of the components. As a result the morphology becomes more stable and the mechanical properties are improved.

How the degree of compatibility of a blend is measured or determined depends to some extent on why one is interested in the blend, often in terms of what application it might have. The scale on which the polymers are mixed, that is, the size of separated phase domains provides a good measure of compatibility. In fact, domain size and growth are system responses to the thermodynamic driving forces of phase separation. In this work the morphology is used as a compatibility measurement in Chapter 3.

The substances added to a blend with the purpose of increase its degree of compatibility are named *compatibilizers*. A compatibilizer is a type of polymeric surfactant that should be found at the interface between the phases.

Several strategies of compatibilization will be discussed in the next section.

1.2 STRATEGIES OF COMPATIBILIZATION

Over the last years, compatibilization has become a usual practice to enhance adhesion between the two phases and stabilize the morphology. There are many routes to promote the compatibility of immiscible polymer blends. Here only four strategies of compatibilization (the most relevant to this work) will be discussed: addition of premade grafted and block copolymers, "in-situ" formation of a copolymer, introduction of specific interactions and addition of ionomers.

1.2.1. Addition of premade grafted and block copolymers

The remarkable progress reported in polymerization techniques during the last decades allows the main molecular characteristic features of block and grafted copolymers to be changed in a systematic way, e. g. molecular architecture, composition and molecular weight. In many cases it has been possible to synthesize copolymers that have "affinity" with both phases of the polymer blend and thus act as compatibilizers.

Diblock copolymers (Figure 1.1a) can be added to homopolymers, which have identical repeat units or are chemically similar to each segment of the copolymer. This type of compatibilized blends can be designated as a "A/B/A-B" system.

Another approach is to use A-C diblock copolymers to overcome the compatibility gap between some A/B polymer pairs, provided that C is miscible with B, so that the diblock is an "enthalpic acting copolymer". Less common, but also possible, is to compatibilize the A/B blend with a C-D diblock copolymer, where A and B are miscible with C and D, respectively ("A/B/C-D system").

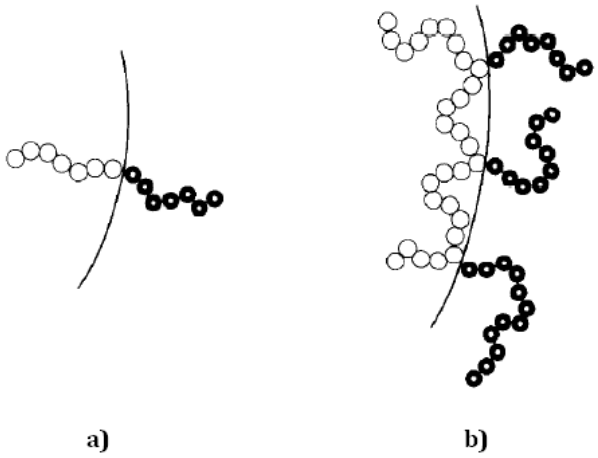

Figure 1.1 – Compatibilization by addition of a copolymer at the interface of a heterogeneous polymer blend *a)* diblock and *b)* grafted.

Figure 1.1b shows a schematic representation of a grafted copolymer acting as a compatibilizer. Grafted copolymers are another possible route to control of the phase morphology and the mechanical properties of immiscible polymer blends.

1.2.2. "In-situ" compatibilization

The addition of a reactive polymer, miscible with one blend component and reactive with the functional groups of the second blend component results in "in-situ" compatibilization (Figure 1.2), i.e. formation of a copolymer at the interface. Usually reactive polymers can be generated by free radical copolymerization or by melt grafting of reactive groups on chemically inert polymer chains. When compared with the addition of premade block or grafted copolymers this technique has some advantages and some drawbacks. The block or grafted copolymer is generated at the interface, where it is necessary to act as a compatibilizer. Nevertheless, because the reaction takes place primarily in the interfaces during blending, it is difficult to control the rate of formation, the amount, and the molecular architecture of the compatibilizer.

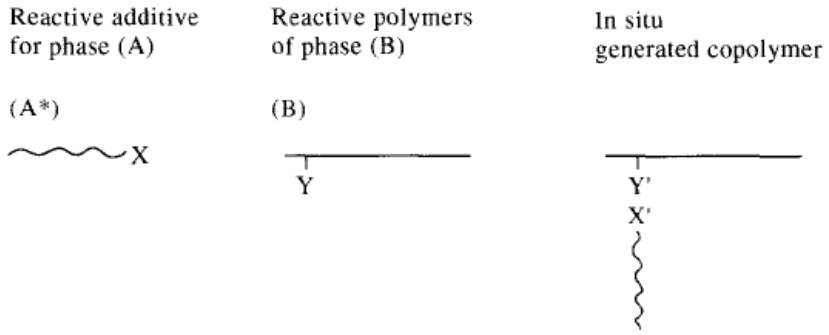

Figure 1.2 – Schematic example of a block copolymer precursor (A*) that can be added to a blend of immiscible polymer (A) and polymer (B), as well as the formed copolymer. Adapted from .Koning *et al.* (1998).

EXAMPLE The terminal amine groups of PA-6 can react with maleic anhydride groups of the modified polyolefins to generate a copolymer at the interface (Figure 1.3). This type of compatibilization will be used in Chapter 3 to compatibilize PA-6 and ethene-propene-monomer (EPM) using a small amount of EPM grafted with maleic anhydride.

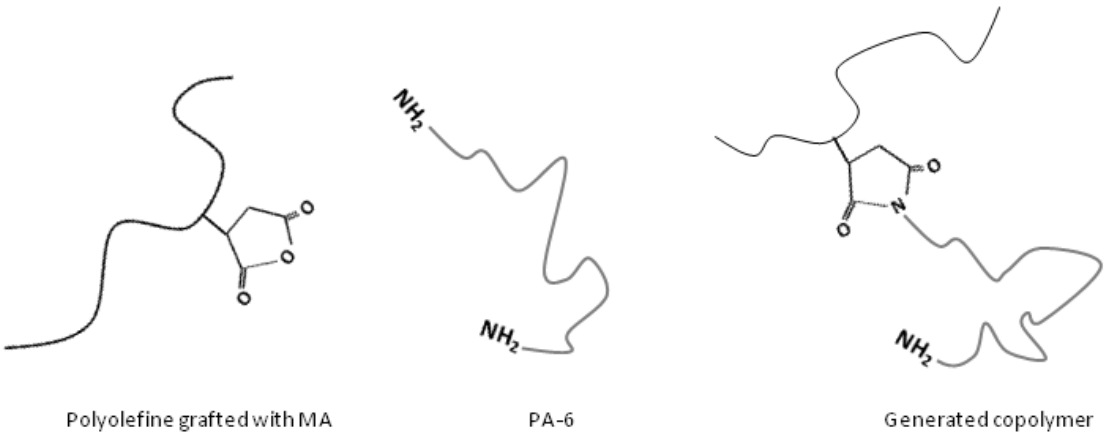

Figure 1.3 – "In-situ" compatibilization of PA-6 and polyolefine.

.

1.2.3. Introduction of specific interactions

Achieving compatibilization via specific interactions differs from the compatibilization strategies discussed above. Specific interactions are introduced into the blend by chemical modification of the blend components with suitable functional groups. No third polymeric or low molecular weight compound is added to the blend.

The introduction of specific interactions between polymer chains may result in a decrease of the Gibbs energy of mixing, and thus in a higher compatibility between the polymers. Even for polymer combinations with very large differences in polarity, a certain degree of compatibility between the two phases can be induced, resulting in a refinement of the blend morphology. When the interaction energy is too high and not localized, the interfacial tension may decrease to the point where molecular miscibility can be observed.

Both, the number of interactions per polymer chain and the strength of the individual interactions are important. The energy of interactions varies according to their type increasing in the following order: van der Waals interactions < dipole-dipole interactions < electron-acceptor complex formation ≈ hydrogen bonding ≈ ion-dipole interactions < ion-ion-interactions.

EXAMPLE A case where the compatibilization can be achieved by introduction of hydrogen bonding is given as an example. Blends of the commodity polymer PS are of commercial interest. The compatibility of PS with a variety of hydrogen acceptor containing polymers, such as PMMA, PEMA, SAN, PC, PPO, PVME, PSU, PET, PA´s and PDMS can be improved by the copolymerization of the styrene with *p*-(hexafluoro-2-hydroxy-isopropyl)styrene. The electron withdrawing effect of the six fluorine atoms results in a relatively strong acidic character of the hydroxyl group. As a result, hydrogen bonding of this modified PS with hydrogen acceptor containing polymers is possible, resulting in complete miscibility for PS with high hydroxyl content. For lower hydroxyl contents, partially miscible or compatible, heterogeneous blends are expected to be formed [Koning *et al.* (1998)].

1.2.4. Addition of ionomers

Ionomers are polymeric species carrying a relatively low number of pedant ionic groups per molecule. Usually, the ionic groups results from neutralization of sulphonic acid or carboxylic acid groups. Either monovalent (e.g. Na^+ , K^+) or divalent (e.g. Zn^{2+}) metal cations are used as counterions. Sulphonic acid or carboxylic acid groups are introduced into the polymer chains by copolymerization or chemical modification of existing polymers. The ionic group tends to associate into multiplets, which at sufficiently high concentrations can associate into clusters. Multiplets and clusters act as physical crosslinks between polymer chains, which promotes compatibility. However, at elevated temperatures the ionic groups lose their attractions (Figure 1.4).

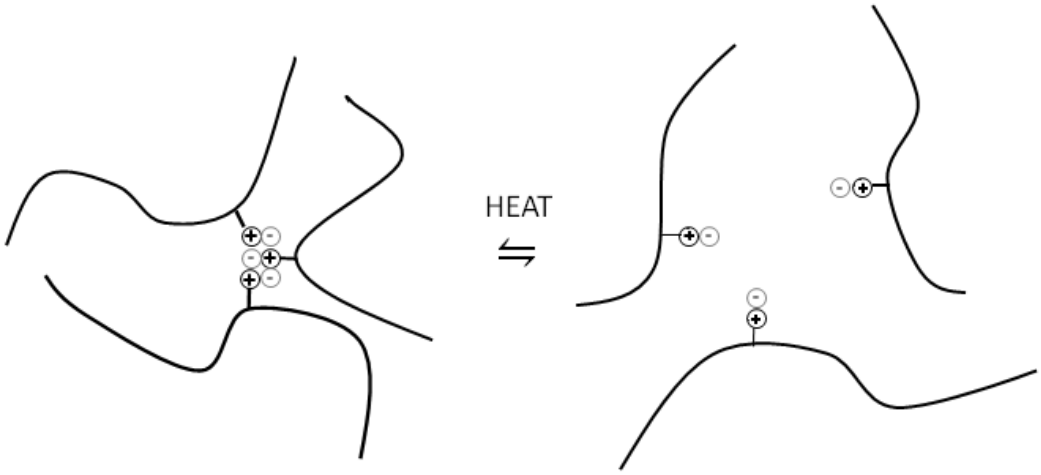

Figure 1.4 – Multiplets and clusters act as physical crosslinks between polymer chains. At elevated temperatures, these ionic crosslinks become reversible.

Thus, one way to improve the compatibility is to add an ionomer based in one of the immiscible polymers. This leads to the formation of ion-dipole interactions which may be strong enough to generate a kind of grafted copolymer at the interface. If both components of a A/B blend are apolar both A and B based ionomers can be required for compatibilization.

EXAMPLE Immiscible blends of PP/EVOH can be compatibilized with an ethylene-methacrylic acid based ionomer. As will be seen in Chapter 5 the addition of this Na^+ ionomer significantly improves compatibility.

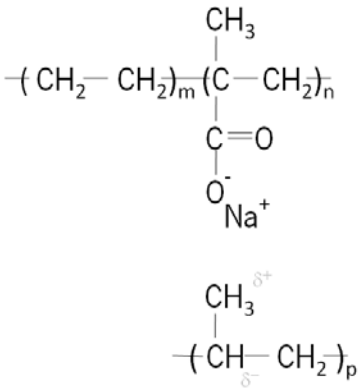

Figure 1.5 – Ethylene methacrylic based ionomer interacts with the polypropylene promoting compatibility in PP/EVOH blends.

As stated before, compatibilization leads to a finer and stable morphology and hence to an improvement of the final properties of the blends. However, in order to obtain polymeric materials with the desirable properties is necessary to know the behavior of the blends during processing, namely, how the microstructure changes when subjected to flow.

1.3 EVOLUTION OF MORPHOLOGY DURING FLOWS

The mixing of immiscible fluids can lead to blends with several morphologies, with the exact size and shape of the microstructure depending on the processing history and on the materials and their relative amounts. In the case of two phase systems the most common morphologies are: spherical droplet in matrix, fibrillar, lamellar and co-continuous (Figure 1.6). During the mixing process four main phenomena can occur: deformation, breakup, coalescence and orientation.

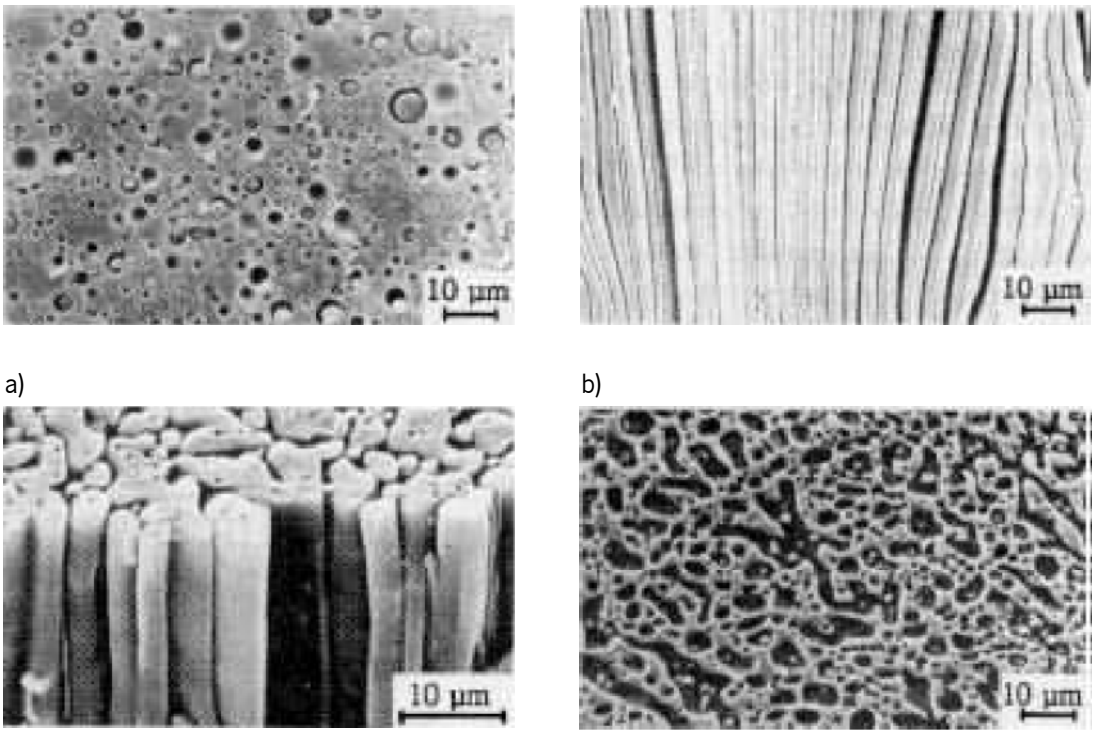

Figure 1.6 - Examples of the most common morphologies in the immiscible polymer blends. (a) droplet in matrix (b) lamellar (c) fibrillar (d) co-continuous morphology. From Wetzel (2001).

In this work attention will be focused on blends with a droplet-matrix morphology. When a blend with this type of morphology is subject to a sudden flow the droplets will deform, orient, and possibly break up. If inertial effects, fluid elasticity, interfacial reactions, concentration effects and buoyancy effects are neglected the droplets response will be determined by the nature of the flow and by two adimensional quantities: the *viscosity ratio*, p, and the *capillary number*, Ca. The viscosity ratio is defined as $p = \eta_d / \eta_m$. η_d is the viscosity of the dispersed phase and η_m is the viscosity of the matrix. The subscripts d and m will be used throughout the text to associate quantities to the disperse phase and matrix, respectively. The capillary number of a blend with spherical droplets of radius R is given by

$$Ca = \frac{E \eta_m R}{\alpha} \tag{1.1}$$

where α is the *interfacial tension* and E is the scalar rate of deformation.

The capillary number is the ratio of viscous stresses, which tend to deform the dispersed phase, to interfacial tension stresses, which tend to relax the morphology. It can act via three mechanisms: retracting nonspherical droplets toward a spherical shape, breaking up extended droplets into smaller spheres and coalescing small droplets to make larger ones. It is possible that even after cessation of the flow the morphology changes by action of interfacial tension.

In the following sections the behavior of the polymer blends when subjected to shear and extensional flows will be discussed.

1.4 POLYMER BLENDS IN SHEAR FLOWS

A fluid can be subjected to different types of flows. Shear flow is the most common type of flow studied in rheology since it is relatively easy to perform in laboratory. Moreover shear flows are very relevant in some industrial processes, such as extrusion.

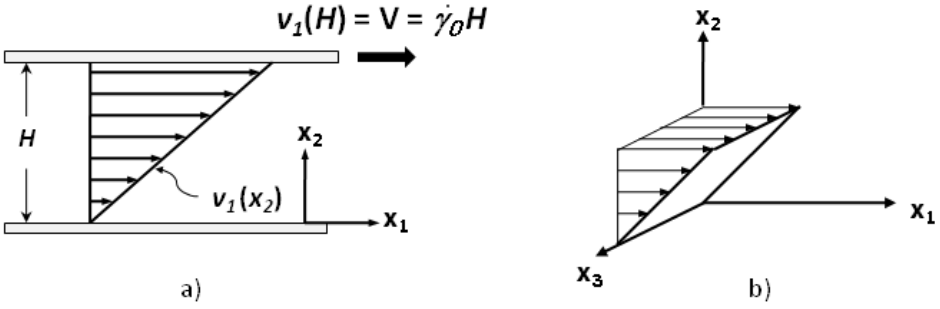

Figure 1.7 – Flow field in simple shear. *a)* Velocity profile in 2D. *b)* Velocity field in 3D.

In simple shear flow, layers of fluid slide past each other and do not mix (Figure 1.7a). The flow is rectilinear and the velocity only varies in one direction, x_2 in the Figure 1.7. The velocity profile for simple shear flow is defined in Cartesian coordinates as

$$v = \begin{pmatrix} v_1 \\ v_2 \\ v_3 \end{pmatrix} = \begin{pmatrix} \dot{\gamma}_{21} x_2 \\ 0 \\ 0 \end{pmatrix} \tag{1.2}$$

Shear flows may be produced in many ways and it is standard practice to call the flow direction the 1-direction, with the 2-direction reserved for the direction in which the velocity changes (the gradient direction) and the 3-direction called the neutral direction, since flow neither occur in this direction nor changes in this direction (Figure 1.7b). $\dot{\gamma}_{21}$ is called the *shear rate* and is equal to the derivative $\partial v_1 / \partial x_2$.

To describe a flow is useful to write the *rate-of-deformation tensor*, $2\mathbf{D}$. In terms of velocity gradient it can be defined as

$$2\mathbf{D} \equiv \nabla v + \left(\nabla v\right)^T \tag{1.3}$$

$$= \begin{pmatrix} \frac{\partial v_1}{\partial x_1} & \frac{\partial v_2}{\partial x_1} & \frac{\partial v_3}{\partial x_1} \\ \frac{\partial v_1}{\partial x_2} & \frac{\partial v_2}{\partial x_2} & \frac{\partial v_3}{\partial x_2} \\ \frac{\partial v_1}{\partial x_3} & \frac{\partial v_2}{\partial x_3} & \frac{\partial v_3}{\partial x_3} \end{pmatrix} + \begin{pmatrix} \frac{\partial v_1}{\partial x_1} & \frac{\partial v_1}{\partial x_2} & \frac{\partial v_1}{\partial x_3} \\ \frac{\partial v_2}{\partial x_1} & \frac{\partial v_2}{\partial x_2} & \frac{\partial v_2}{\partial x_3} \\ \frac{\partial v_3}{\partial x_1} & \frac{\partial v_3}{\partial x_2} & \frac{\partial v_3}{\partial x_3} \end{pmatrix} \tag{1.4}$$

Thus, in the case of simple shear flow, the rate-of-deformation tensor becomes,

$$2\mathbf{D} \equiv \begin{pmatrix} 0 & 0 & 0 \\ \dot{\gamma}_{21} & 0 & 0 \\ 0 & 0 & 0 \end{pmatrix} + \begin{pmatrix} 0 & \dot{\gamma}_{21} & 0 \\ 0 & 0 & 0 \\ 0 & 0 & 0 \end{pmatrix} \tag{1.5}$$

$$= \begin{pmatrix} 0 & \dot{\gamma}_{21} & 0 \\ \dot{\gamma}_{21} & 0 & 0 \\ 0 & 0 & 0 \end{pmatrix} \tag{1.6}$$

It should be noticed that the shear rate is independent of the position (not a function of x_1, x_2 or x_3) for simple shear flow as defined by the velocity field in Eqn. (1.2).

The main aim of rheology is to relate the rate-of-deformation with the stresses that act on the fluid. These stresses are usually represented by a second order tensor with nine components

$$\boldsymbol{\tau} = \begin{pmatrix} \tau_{11} & \tau_{12} & \tau_{13} \\ \tau_{21} & \tau_{22} & \tau_{23} \\ \tau_{31} & \tau_{32} & \tau_{33} \end{pmatrix} \tag{1.7}$$

This tensor, called the *stress tensor*, contains all the information about the state of stress at a point of the fluid. Given a general component of the stress tensor, τ_{ij}, the first subscript, i, refers to the direction of normal vector to the plane on which the stress is acting. The second subscript, j, is the direction of the stress. Figure 1.8 exemplifies this concept showing the stress components acting on a surface of a cubic element.

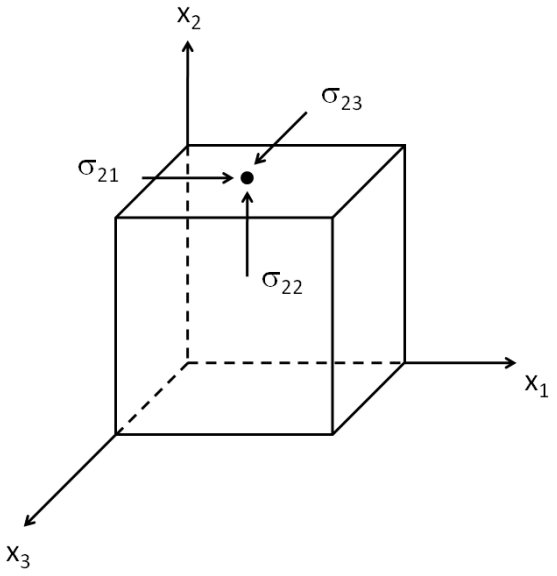

Figure 1.8 – Stresses acting on a surface of a cubic element.

In the so-called *Newtonian fluids* the relations between stress and rate-of-deformation are relatively easy to establish. Based in experimental observations Newton proposed, in 1687, for the first time a constitutive equation. He observed that on incompressible fluids the shear stress, τ_{21}, was directly proportional to the gradient of the velocity.

$$\tau_{21} = \eta\dot{\gamma}_{21} \tag{1.8}$$

where η is the *Newtonian viscosity*. This equation gives the relationship between shear stress and velocity gradient in shear flows only. From the principles of fluid mechanicals, a more general relation, who is valid for any type of flow, was deduced later.

$$\boldsymbol{\tau} = \eta 2\mathbf{D} \tag{1.9}$$

This is the Newtonian constitutive equation for Newtonian incompressible fluids. Eqn. (1.8) is a special case of Eqn. (1.9) when simple shear flow is considered. In fact, the Eqn. (1.8) can be obtained substituting Eqn. (1.6) in the Newtonian constitutive equation and noting that the stress tensor is symmetric in shear flows. However, the behavior of most fluids is not predicted by the Newtonian constitutive equation. Such fluids are called *non-Newtonian fluids*. Even a blend of two immiscible Newtonian fluids has in general a non-Newtonian behavior.

Characterizing non-Newtonian fluids is more complicated than characterizing Newtonian fluids. When a shear flow $\dot{\gamma}_{21}$, for example, is imposed to a Newtonian fluid the stress tensor will only have one nonzero component, τ_{21}. Thus, from τ_{21} and the imposed shear rate $\dot{\gamma}_{21}$, it is possible to calculate the viscosity $\eta = \tau_{21}/\dot{\gamma}_{21}$, which is all the material information needed to specify the constitutive equation. However, when a non-Newtonian fluid is subjected to a shear flow, normal stresses (τ_{11}, τ_{22} and τ_{33}) will appear and in general the viscosity, η, will be a

function of the applied shear rate. So, it is not easy to obtain constitutive equations for these fluids. In general the material properties are functions of kinematic parameters such as $\dot{\gamma}_{21}$.

In the previous paragraphs only the stresses due to the deformation of the fluid have been considered. Nevertheless, all fluids are subjected to a *thermodynamic pressure*, p. This pressure is isotropic (acts equally in all directions) and normal (perpendicular) to a surface. Mathematically it can be described by

$$\mathbf{p} = \begin{pmatrix} p & 0 & 0 \\ 0 & p & 0 \\ 0 & 0 & p \end{pmatrix} = p\mathbf{I} \tag{1.10}$$

where $\mathbf{I}$ is the identity tensor. In fact the fluids are subjected to a total stress tensor $\mathbf{\Pi}$ defined as,

$$\mathbf{\Pi} = \begin{pmatrix} \tau_{11} + p & \tau_{12} & \tau_{13} \\ \tau_{21} & \tau_{22} + p & \tau_{23} \\ \tau_{31} & \tau_{32} & \tau_{33} + p \end{pmatrix} = \boldsymbol{\tau} + \mathbf{P} \tag{1.11}$$

A problem arises from the difficulty to measure p. If p is not known it is impossible to separate it from normal stress measurements. This is important since for non-Newtonian fluids subjected to a shear flow the components τ_{11}, τ_{22} and τ_{33} are nonzero. To overcome this problem rheologists consider *normal-stress differences* (N_1 and N_2) instead of normal stresses (τ_{11}, τ_{22}, τ_{33}). If normal-stress differences are measured then p vanishes, since they are defined as:

$$N_1 = \tau_{11} - \tau_{22} \tag{1.12}$$

$$N_2 = \tau_{22} - \tau_{33} \tag{1.13}$$

In the present discussion is particularly important to introduce the concept of viscoelasticity.

VISCOELASTICITY When a Newtonian fluid is instantaneously deformed, for example in shear, the stress will relax to zero as soon as strain becomes constant [according to Eqn. (1.8)]. On the other hand, in a non-Newtonian fluid the stress will relax over a significant time. This time-dependent response is call *viscoelasticity*.

If stress relaxation data is converted to a relaxation modulus

$$G(t) = \frac{\tau(t)}{\gamma} \tag{1.14}$$

all the data for small strains fall on the same curve. This linear dependence of stress relaxation on strain, Eqn. (1.14), is called *linear viscoelasticity*. For larger strain, the relaxation modulus is no longer independent of strain. The relaxation modulus is defined as above, but now depending on the strain.

$$G(t,\gamma) = \frac{\tau(t,\gamma)}{\gamma} \tag{1.15}$$

This is known as *nonlinear* viscoelastic behaviour. Thus, for a particular material, in the viscoelastic region strain varies linearly with stress.

Some kinematic parameters that characterize the rheological behaviour of fluid, the so-called *rheological material functions*, will be presented next. The shear-flow material functions herein described are usually used in the study of polymer blends and are measured and used in this work.

STEADY SHEAR If a constant shear rate is applied to a material, $\dot{\gamma}_{21}(t) = \dot{\gamma}_0$, after some time a steady-state flow will be obtained. In this case the shear stress will become constant in time. Thus, the viscosity is defined as:

$$\eta\left(\dot{\gamma}\right)=\frac{\tau_{21}}{\dot{\gamma}_0} \tag{1.16}$$

For non-Newtonian fluids the viscosity is a function of the shear rate. The zero-shear viscosity is defined as

$$\lim_{\dot{\gamma}\to 0}\eta\left(\dot{\gamma}\right)\equiv\eta_0 \tag{1.17}$$

So, in practical terms the zero-shear viscosity is the viscosity determined at very low shear rates.

STRESS RELAXATION Some information about the relaxation properties of polymer blends may be obtained by observing how the steady-state stresses in shear flow relax when the flow is stopped. The cessation of steady shearing is represented by the equation:

$$\dot{\gamma}_{21}\left(t\right)=\begin{cases}\dot{\gamma}_0 & t<0\\ 0 & t\geq 0\end{cases} \tag{1.18}$$

In general the time-dependent material function for shear-stress decay after cessation of steady shear vary with $\dot{\gamma}$.

$$\eta^{-}\left(t,\dot{\gamma}\right)=\frac{\tau_{21}}{\dot{\gamma}_0} \tag{1.19}$$

Instead of this material function, in this work the normalized shear stress relaxation is used

$$\tau^{-}_{21,N}\left(t,\dot{\gamma}\right)=\frac{\tau_{21}}{\tau_{21}(t=0)} \tag{1.20}$$

As will be seen in the next chapters, this material function gives important information about polymer blends.

SMALL AMPLITUDE OSCILLATORY SHEAR (SAOS) The next set of material functions present is routinely used to characterize complex fluids namely polymer blends. Here, the shear rate is a periodic function

$$\dot{\gamma}_{21}(t) = \dot{\gamma}_0 \cos \omega t \tag{1.21}$$

where ω is the frequency of the cosine function and $\dot{\gamma}_0$ is the constant maximum amplitude of the shear-rate function. This flow is always carried out in a cone-and-plate or parallel-plate rheometer (see Chapter 2). It can be shown that it is necessary to apply the shear rate of Eqn. (1.21) to deform the material sinusoidally according to

$$\gamma_{21}\left(0,t\right) = \gamma_0 \sin \omega t \tag{1.22}$$

where $\gamma_0 = \dot{\gamma}_0 / \omega$ is the strain amplitude. In the linear viscoelastic region of the material the shear stress that is produced will be a sine wave with the same frequency as the input strain wave. However, usually it will not be in phase with the input strain. Then, it can be written as

$$\tau_{21}\left(t\right) = \tau_0 \sin\left(\omega t + \delta\right) \tag{1.23}$$

where the quantity δ is the phase angle which gives the phase difference between the strain wave and the stress response. To define the material functions for SAOS is useful expand the preceding equation.

$$\begin{aligned}\tau_{21}(t) &= \tau_0 \sin(\omega t + \delta) \\ &= \tau_0 (\sin\omega t \cos\delta + \sin\delta \cos\omega t) \\ &= (\tau_0 \cos\delta)\sin\omega t + (\tau_0 \sin\delta)\cos\omega t \end{aligned} \quad (1.24)$$

In this expression it is possible to see that there is a portion of the stress wave that is in phase with the imposed strain (i.e., proportional to $\sin\omega t$) and a portion of the stress wave that is in phase with the imposed strain rate (proportional to $\cos\omega t$). To understand the importance of this it should be recalled that for Newtonian fluids stress-shear response is proportional to the imposed shear rate while for perfect elastic solids stress-shear is proportional to the imposed strain. Thus, the stress response in SAOS [Eqn. (1.24)] contains both a part that is fluid-like (proportional to $\dot{\gamma}_{21}$) and an elastic part (proportional to γ_{21}). Therefore, the SAOS experiment is ideal for probing materials that show both viscous and elastic properties, i.e., *viscoelastic materials*.

The material functions for SAOS, the storage modulus $G'(\omega)$ and the loss modulus, $G''(\omega)$ are defined as follows:

$$\frac{\tau_{21}}{\gamma_0} = G' \sin\omega t + G'' \cos\omega t \quad (1.25)$$

$$G'(\omega) = \frac{\tau_0}{\gamma_0}\cos\delta \quad (1.26)$$

$$G''(\omega) = \frac{\tau_0}{\gamma_0}\sin\delta \quad (1.27)$$

G' is equal to the amplitude of the portion of the stress wave that is in phase with the strain divided by the amplitude of the strain wave. G'' is defined analogously as the amplitude of the portion of the stress wave that is out of phase with the strain wave, divided by the amplitude of the strain wave. Hence, the storage modulus, G', is related to the elastic energy storage by the material while the loss modulus G'' is related to the viscous response of the fluid. It is common to use other material functions, although the information that they contain is already present in the dynamic moduli (G' and G''). For example, the loss tangent, defined as

$$\tan\delta = \frac{G''}{G'} \tag{1.28}$$

expresses the relation between the viscous and elastic responses of the material at a given solicitation frequency.

Another material function used in this work is the complex viscosity. It can be expressed as a function of dynamic moduli as,

$$\left|\eta^*\right| = \sqrt{\left(\frac{G'}{\omega}\right)^2 + \left(\frac{G''}{\omega}\right)^2} \tag{1.29}$$

The complex viscosity can be very useful to compare steady shear viscosities with complex viscosities. Furthermore, there is an empirical relation, the Cox-Merz rule, which states that for equal values of the shear rate, $\dot{\gamma}\left(\mathrm{s}^{-1}\right)$, and the angular frequency, $\omega\left(\mathrm{rad.s}^{-1}\right)$, the steady shear and the complex viscosity have equal values.

$$\eta\left(\dot{\gamma}\right) = \left|\eta^*\left(\omega\right)\right|; \qquad \text{with } \dot{\gamma}=\omega \tag{1.30}$$

The Cox-Merz rule has been verified for a large number of fluids. It was found that some polymer blends agree with this empirical rule. The Cox-Merz rule will be applied to blends in Chapter 3.

The behaviour of the polymer blends in shear flows will be discussed in the next section.

1.4.1. Model blends

The rheological behavior and morphology development of dilute blends of Newtonian components subjected to shear flows is well-known.

As was stated in 1.3, under certain conditions (if inertial effects, fluid elasticity, interfacial reactions, concentration effects and buoyancy effects are neglected) the response of the droplets will be determined by the nature of the flow, capillary number and viscosity ratio only. There are critical values to the capillary number above which the droplets will breakup. The critical capillary number, Ca_{crit}, was measured by Grace (1982) for Newtonian droplets. Figure 1.9, which shows the critical capillary number as a function of the viscosity ratio, results from an empirical fit to Grace's data by Debruijn (1991):

$$\log Ca_{crit} = -0.506 - 0.995\log p + 0.124\left(\log p\right)^2 - \frac{0.115}{\log p - \log 0.408} \quad (1.31)$$

The deformation of a droplet and the mode in which it will breakup depends on the capillary number. For example, when $Ca \ll 1$, the steady shape is slightly ellipsoidal, with the long axis oriented at 45° to the flow. As the capillary number increases, the steady-state deformation increases, and the droplet axis shifts toward the flow direction. If Ca is slight greater than Ca_{crit} the breakup mode depends on the viscosity ratio. For $p \ll 1$ the droplet assumes a pointed sigmoidal shape and small droplets are released from the ends (tip streaming). For $p \approx 1$ the central portion of the droplet gradually necks until the droplet breaks into two daughter droplets, with small satellite droplets in between. In the case of $Ca \gg Ca_{crit}$ the droplet stretches into a slender fibril, which subsequently breaks up by a capillary-wave instability (Rayleigh instability).

Other remarkable aspect that can be seen in the Figure 1.9 is the impossibility of breaking up droplets in shear flows for viscosity ratios exceeding 4.

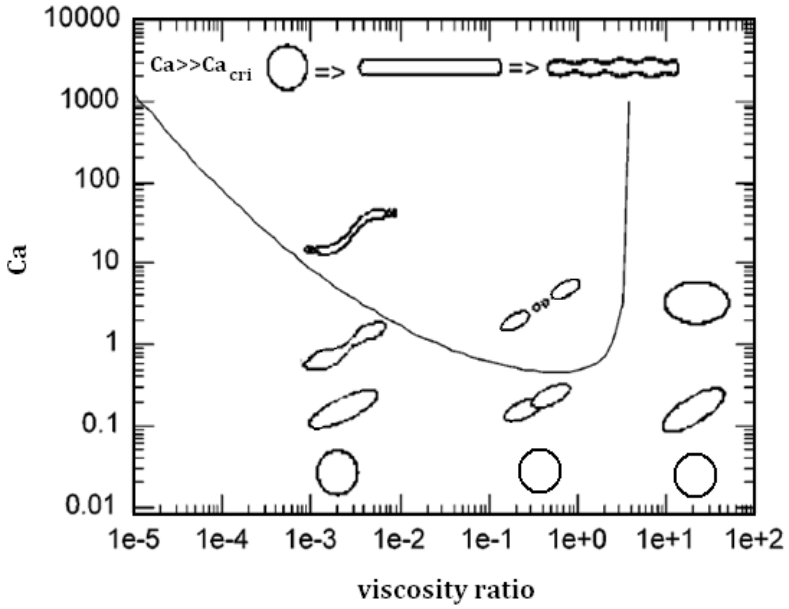

Figure 1.9 - Critical capillary number for breakup in simple shear flow. Taken from Tucker and Moldenaers (2002).

To describe the dynamics of a Newtonian droplet in a Newtonian matrix, theoretical models as well as numerical simulations have been proposed. Since numerical simulations fall outside of the scope of this work only theoretical models will be discussed here.

Based on the elasticity solution of Eshelby (1957), Wetzel and Tucker (2001) developed an analytical solution that applies to a single ellipsoidal droplet of any shape when interfacial tension equals zero. The solution applies to small as well as large deformations, when $Ca >> 1$. Later this model was extended to include the interfacial tension effect [Jackson and Tucker (2003)]. Other models have been developed, namely by Maffettone and Minale (1998). Although there is good agreement between these models and the experimental data they can only be used in very dilute systems since the concentration will affect the deformation and relaxation of the individual droplets.

Although the behavior of blends with Newtonian components in shear flows is relatively well understood, the same is not true for real blends due to the additional effects that come into play. In fact, blends with industrial interest are generally constituted by viscoelastic components, concentrated and often compatibilized. Next, some progresses in the attempt to understand the influence of these factors on the behavior of the blends subjected to shear flows will be reviewed.

1.4.2. 'Real' blends – effects of concentration and elasticity

Generally, industrial blends are not so diluted that concentration effects can be neglected. More concentrated systems are difficult to treat theoretically, but despite of this, some coarse grained models were developed to take into account the relatively high volume fractions of the dispersed phase.

Doi and Ohta (1991) made the first attempt to tackle the rheology of the concentrated systems. The Doi and Otha model and a modified version of it, introduced by Lee and Park (1994), to account for a mismatch in the viscosities of polymers will be discussed in next subsection.

Additionally, industrial blends are often constituted by viscoelastic components. The effect of non-Newtonian properties of the components, such as, a shear rate dependent viscosity and normal stress differences on the rheological and morphological behavior of the blends is not completely understood. Although there are additional difficulties introduced by these effects, some experimental and theoretical results exist in the literature. Most of the studies on the influence of the viscoelasticy of the components concern a single droplet immersed in a matrix.

From the experimental data available in the literature it can be noticed that the droplet elasticity leads to less deformed and more stable droplets than in the Newtonian case Mighri *et al.* (1998).

In the case of Newtonian droplets in a viscoelastic matrix, in shear, the experimental studies show that deformation of the droplets and their degree of orientation in the flow direction, as well as the critical capillary number and breakup time, increased with increasing elasticity of the matrix fluid [Guido *et al.* (2003a), Guido *et al.* (2003b), Mighri *et al.* (1998), Sibillo *et al.* (2004)].

There are also studies for systems in which both phases are viscoelastic. Droplet widening in the neutral direction of a shear flow when isolated polypropylene droplets were sheared in a highly viscoelastic polystyrene matrix was observed by Levitt *et al.* (1996). The effect was associated with the large differences in elasticities between the droplets and the matrix. In fact, some studies [Hobbie and Migler (1999), Mighri and Huneault (2001), Migler (2000)] show that highly elastic droplets can align in the neutral direction rather than in the flow direction. This phenomenon will be observed in Chapter 4.

Theoretical investigations on droplet deformation in viscoelastic blends are difficult to perform due to the complex rheological properties of viscoelastic components. Despite this, Greco (2002) suggested a model for steady droplet deformation (that is second order in *Ca*) where both components are second-order liquids. This model was experimentally verified by Guido *et al.* (2003a) and Guido *et al.* (2003b), especially for the orientation of a Newtonian droplet in a viscoelastic matrix. Maffettone and Greco (2004) suggested a modified ellipsoidal model on the basis of the Newtonian MM model [Maffettone and Minale (1998)]. This modified ellipsoidal model does a good job in predicting the steady droplet deformation. However, the model is unable to quantitatively capture the relaxation process of the droplet. Another viscoelastic model was suggested by Yu *et al.* (2004), which considered the transient deformation/relaxation processes under small deformations. The model predicts that the steady droplet deformation in a viscoelastic system under a small capillary number is the same as in the Newtonian system, and the elasticity of the droplet/matrix accelerates/decelerates the initial droplet deformation. Moreover, the relaxation process with small initial deformation after shear can be quantitatively captured. The main limitation of this model is that it is constrained to small capillary numbers. Using a nonequilibrium thermodynamics approach another models have been proposed, namely by Dressler and Edwards (2004) and Yu *et al.* (2005).

For real blends, semi-concentrated and constituted by viscoelastic fluids, theoretical analyses are available in some simple cases. For small amplitude oscillatory flows, the Palierne model [Palierne (1990)] has been widely used. Due to the presence of the interfaces, the immiscible binary blends shows a higher elasticity at low frequencies than the individual components of the

blends [Graebling *et al.* (1993), Oosterlinck *et al.* (2005)]. The higher value of elasticity of the blends can result in the presence of a secondary plateau in the curve of the storage modulus vs frequency for low frequencies. In many cases, the Palierne model correctly predicts the dynamic modulli of the blends. Thus, G' has been used to determine the size of dispersed droplets in a blend [Jansseune *et al.* (2000), Vinckier *et al.* (1996)]. The Palierne as will as other models such as Bousmina [Bousmina (1999)], Doi and Otha and Lee and Park models will be discussed and compared in the next section.

1.4.3. Theoretical modeling

The development of models to predict the rheological behavior of emulsions started some decades ago. In the early 50's, Oldroyd, using the pioneer works of Einstein (1906) and Taylor (1932), developed a model [Oldroyd (1955), Oldroyd (1953)] that included time-dependent effects to describe the rheology of diluted emulsions. The fluids were assumed to be Newtonian and the droplet deformation small. The most interesting extension of the Oldroyd emulsion model is that proposed by Palierne (1990), who analyzed the linear viscoelastic behaviour of non-dilute emulsions of viscoelastic droplets in a viscoelastic matrix. Dipole-type particles interactions were considered and effects of particle size distribution were included. The Palierne model describes the complex modulus, G_b^*, of viscoelastic emulsions as a function of the complex moduli of both phases (G_m^* for the matrix and G_d^* for the droplets), the ratio of the interfacial tension and the droplet size and the size distribution, as follows:

$$G_b^* = \frac{1+3\sum_i \phi_i H_i^*(\omega)}{1-2\sum_i \phi_i H_i^*(\omega)} G_m^*(\omega) \tag{1.32}$$

with

$$H_i^*(\omega)=\frac{4\left(\frac{\alpha}{R_i}\right)\left[2G_m^*(\omega)+5G_d^*(\omega)\right]+\left[G_d^*(\omega)-G_m^*(\omega)\right]\left[16G_m^*(\omega)+19G_d^*(\omega)\right]}{40\left(\frac{\alpha}{R_i}\right)\left[G_m^*(\omega)+G_d^*(\omega)\right]+\left[2G_d^*(\omega)+3G_m^*(\omega)\right]\left[16G_m^*(\omega)+19G_d^*(\omega)\right]}$$

(1.33)

where α is the interfacial tension and ϕ_i is the volume fraction of particles with radius R_i.

Starting from the model of Kerner (1956), for a rheological behaviour of a composite of two elastic bodies, Bousmina (1999) derived another expression for G_b^*

$$G_b^*=G_m^*\frac{2\left(G_d^*+\alpha/R\right)+3G_m^*+3\phi\left(G_d^*+\alpha/R-G_m^*\right)}{2\left(G_d^*+\alpha/R\right)+3G_m^*-2\phi\left(G_d^*+\alpha/R-G_m^*\right)} \qquad (1.34)$$

where R is the mean radius of the dispersed phase.

A third model was proposed by Doi and Ohta (1991). They considered the interface between the two phases and derived a semiphenomenological kinetic equation to describe the time evolution of interfacial area per unit of volume (Q) and its anisotropy (q_{ij}) in a given flow field. The interfacial area and its anisotropy are defined as follows:

$$Q=\frac{1}{V}\int dS \qquad (1.35)$$

$$q_{ij}=\frac{1}{V}\int dS\left(n_i n_j-\tfrac{1}{3}\delta_{ij}\right) \qquad (1.36)$$

where n_i denotes the unit normal vector to the interfaces, V the total system volume, and dS an interface element. The constitutive equation obtained by Doi and Otha was later modified by Lee and Park (1994) to account for a mismatch in the viscosities of the polymers. They proposed the following constitutive equations:

$$\sigma_{ij} = \left(1 + \frac{6\left(\eta_d - \eta_m\right)}{10\left(\eta_d + \eta_m\right)}\phi\right)\eta_m\dot{\gamma}_{ij} - \alpha q_{ij} - P\delta_{ij} \tag{1.37}$$

$$\begin{aligned}\frac{\partial}{\partial t}q_{ij} = -q_{ik}d_{kj} - q_{jk}d_{ki} - \frac{2}{3}\delta_{ij}d_{lm}k_{lm} - \frac{Q}{3}\left(d_{ij} + d_{ji}\right) + \frac{q_{lm}d_{lm}}{Q}q_{ij} \\ -\lambda\frac{\alpha}{\eta_m}Qq_{ij} - \lambda\nu\frac{\alpha}{\eta_m}\left(\frac{q_{lm}q_{lm}}{Q}\right)q_{ij}\end{aligned} \tag{1.38}$$

$$\frac{\partial}{\partial t}Q = -d_{ij}q_{ij} - \lambda\mu\frac{\alpha}{\eta_m}Q^2 - \lambda\nu\frac{\alpha}{\eta_m}q_{ij}q_{ij} \tag{1.39}$$

where η_m is the zero-shear viscosity of matrix, η_d is the zero-shear viscosity of inclusions, P is the hydrostatic pressure, λ is the total relaxation parameter, μ the size relaxation, ν the shape relaxation. The μ parameter is associated to coalescence and so it can be considered zero in small amplitude oscillatory flow because the deformation of dispersed phase is small. Other considerations suggested $\nu = 1 - \phi$, for the same type of flow.

Several researchers [Covas *et al.* (2000), Zhao and Macosko (2002)] have reported a negative deviation behaviour (NDB), *i.e.*, when the values of both G' and G'' of the blends are lower than those of either the components (see Chapter 2). In the next subsection, the predictions of several models will be analysed and compared in terms of their predictive capabilities of both the viscoelastic and NDB of the blends.

1.4.3.1 Influence of emulsion parameters on the Palierne model

We start by considering a two fluids emulsion and supposing that both fluids have a Maxwel-type behaviour according to,

$$G_b^* = \frac{i\omega\eta}{1+i\omega\lambda} \tag{1.40}$$

Also, we will start from typical values of the constants and will vary them in order to study the influence of each of them on the viscoelastic behaviour. The initial values of the constants are $\lambda_m = \lambda_d = 0.1\text{s}$, $\eta_m = \eta_d = 10^6$ Pa.s, $\alpha = 10$ mN/m, $\phi = 0.2$. Furthermore, we shall assume that all droplets have same radius, $R = 1\ \mu$m.

Figure 1.10 shows that the plateau modulus in G' decreases in value but is extended to lower frequencies with increasing radius of the particles of the dispersed phase. The effect of interfacial tension is the opposite since from Eqn. (1.33) depends on α/R_i. No significant effects in G'' can be noticed.

On the contrary and as expected, the increase of volume fraction of the disperse phase leads to an increase of the G' plateau, as can be seen in Figure 1.11. A slight increase of G'' at low frequencies is also shown.

In order to study the influence of the viscosity ratio between the dispersed phase and the matrix, the viscosity of the latter was kept constant at 10^6 Pa.s and that of the former was changed from a minimum of 10^5 Pa.s to a maximum of 10^8 Pa.s, thus yielding a ratio varying between 0.1 and 100. Figure 1.12 shows clearly that there is a marked influence of the viscosity ratio on the value of the plateau in G', which is shifted to lower frequencies and decreases with increasing viscosity ratio.

Finally, when the relaxation time of the disperse phase increases, the G' plateau also increases, Figure 1.13, which was expected due to the increased elasticity levels.

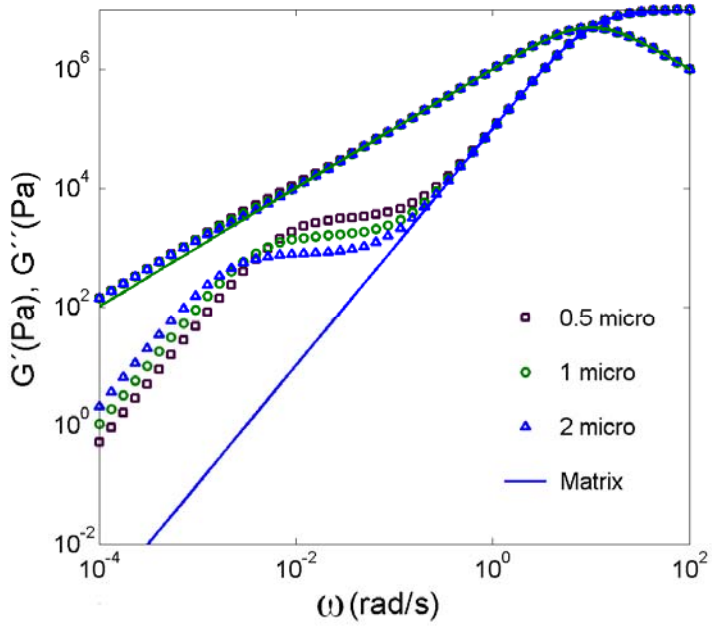

Figure 1.10 - Dynamic moduli vs frequency. Effect of variation of radius of inclusions (micro=μm).

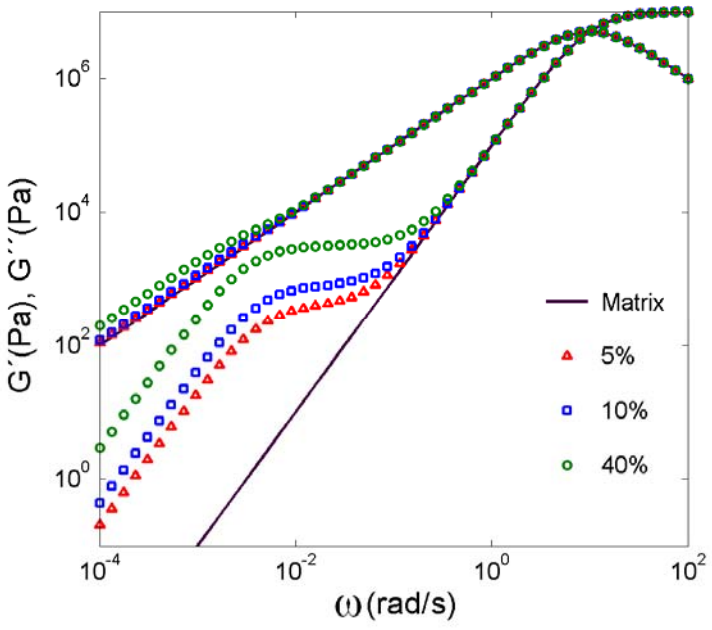

Figure 1.11 - Dynamic moduli vs frequency. Effect of variation of volume fraction of the disperse phase.

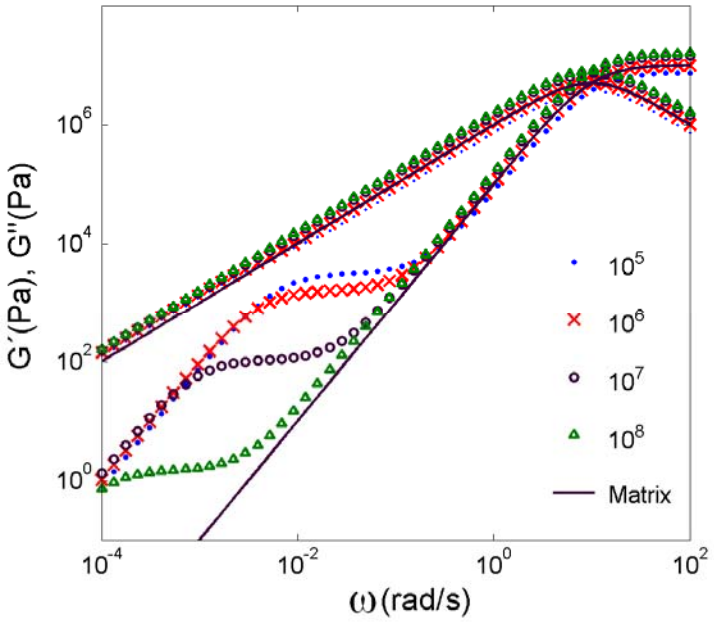

Figure 1.12 - Dynamic moduli vs frequency. Effect of the zero-shear viscosity of the dispersed phase.

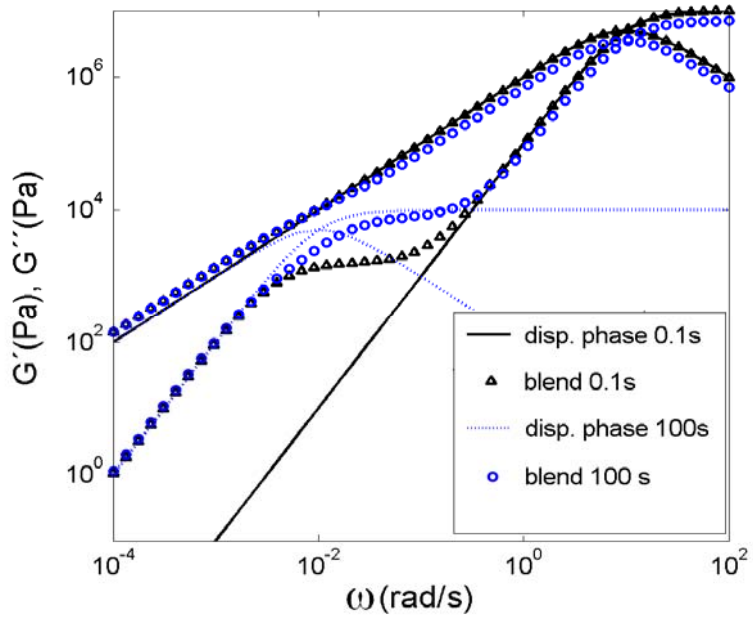

Figure 1.13 - Dynamic moduli vs frequency. Effect of relaxation time of dispersed phase.

1.4.3.2 Comparison between the Palierne and Lee-Park models

Both the Bousmina and the Palierne models give very similar predictions for typical values of the parameters [Bousmina (1999)], which is not the case with the predictions of the Lee-Park model. These models will be compared varying different parameters.

In the Lee-Park model, the interfacial area, Q, is related to the particle radius by:

$$Q = \frac{6\phi}{R} \tag{1.41}$$

Figure 1.14 shows, for both radii, that the plateau modulus in G' predicted by the Lee-Park model is higher than that predicted by the Palierne model.

Regarding other parameters, the Lee-Park model predicts a higher value for plateau in G', for different values of interfacial tension (Figure 1.15) and shows lower sensibility to variations of the viscosity ratio and volume fraction of dispersed phase than the Palierne model.

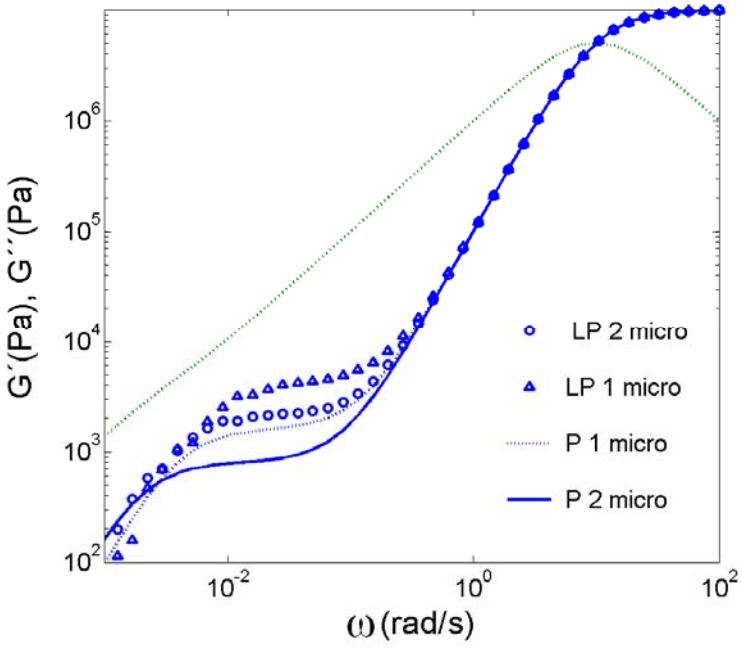

Figure 1.14 - Dynamic moduli vs frequency. Comparation of models predictions for different radius of inclusions. (micro = μm , PL- Lee-Park model, P- Palierne model, $\lambda = 0.6$)

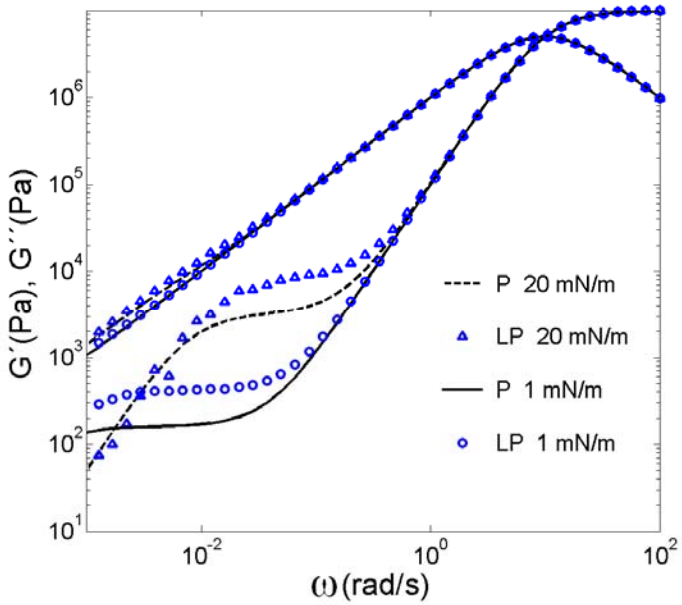

Figure 1.15 - Dynamic moduli vs frequency. Comparation of models predictions for different values of interfacial tension. (PL- Lee-Park model, P- Palierne model, $\lambda = 0.6$)

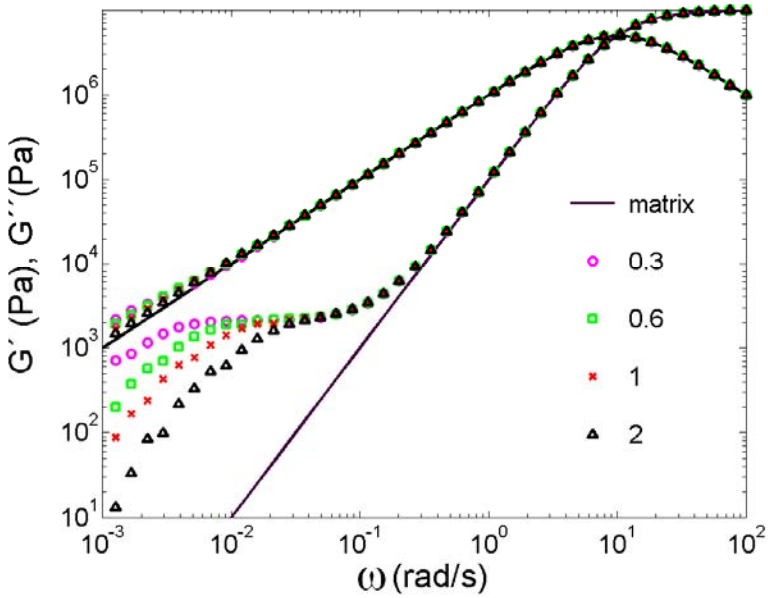

Figure 1.16 - Dynamic moduli vs frequency. Effect of the λ parameter (total relaxation parameter).

Contrarily to the Palierne model, the Lee-Park model has an adjustable parameter: the relaxation total, λ. In Figure 1.16 it is shown that this parameter affects the width of the G' plateau; when λ increases the width of the plateau modulus in G' decreases.

None of the models is able to predict the rheological proprieties of blends that show a negative deviation behaviour (NBD) that is often seen occurs when slippage at the polymer interfaces occurs. In fact, all the models assume continuity on the interfaces and fail in these cases. Recently, Adhikari and Goveas (2004), modifying a Palierne theory, calculated the rheological proprieties for dilute polymer emulsions considering a slip effect. However, this modification to the original Palierne theory is not valid for concentrated polymer emulsions, such as typical polymer blends and, thus, this still constitutes an open problem.

As was mentioned in section 1.2, in order to improve blend properties, the use of the compatibilizers has become a generalized practice. In the next section the effect of the compatibilizers in the rheological behavior of the blends in shear will be discussed.

1.4.4. Compatibilized blends

The addition of compatibilizers suppresses droplet coalescence [Van Hemelrijck *et al.* (2004), Van Puyvelde *et al.* (2001)] and reduces or eliminates interfacial slip. For example, Van Puyvelde *et al.* (2003), studying PA-6/EPR blends, observed a negative deviation from the log-additivity rule. It was observed that the addition of compatibilizer suppresses slip and significantly increases the viscosity of the blend. Their studies support the hypothesis that the interfacial slip is due to loss of entanglements in the interfacial region. The scaling laws of Doi and Ohta (1991) for the shear stress were verified experimentally by Iza *et al.* (2001) for PS/HDPE blends physically compatibilized with copolymers. However, these authors verified that N_1 does not scale with $\dot{\gamma}$ but with $\dot{\gamma}^{\alpha}$, where α is close to 2. Moreover, it was demonstrated that the amount of compatibilizer, as well as its structure, drastically affects the rheological response to a sudden imposition of a shear rate. Macaubas *et al.* (2005), using blends of PP/PS compatibilized with a linear triblock copolymer (styrene-ethylene-butylene-styrene, SEBS), observed that the scaling laws are not valid for the shear stress. They formulated a model using the ideas of Doi and Ohta

(1991), Lacroix *et al.* (1998), and Bousmina *et al.* (2001) that was able to predict the behaviour of non-compatibilized blends for a single step shear. However, the model does not predict the behaviour of compatibilized blends.

Compatibilizers influence the characteristics of the interfaces, thereby changing the rheology of the blends. There are several experimental studies that present the experimental evidence of an additional relaxation time, τ_β , in the compatibilized blends. That relaxation time can be attributed to the relaxation of Marangoni stresses tangential to the interface between the dispersed and matrix phase [Riemann *et al.* (1997), Van Hemelrijck *et al.* (2004)]. These Marangoni stresses are induced by the presence of a gradient of compatibilizer concentration at the interface, which induces a gradient of interfacial tension [Van Hemelrijck *et al.* (2004), Van Puyvelde *et al.* (2001)]. Considering non-isotropic interfacial stress in the Palierne model both the relaxation time τ_s , due to the shape relaxation of the droplets, and τ_β can be calculated [Jacobs *et al.* (1999)]. This full version of Palierne model has showed a good agreement with some experimental data of compatibilized blends [Yee *et al.* (2007); Huo *et al.* (2007); Shi *et al.* (2002); Asthana and Jayaraman (1999)].

1.5 POLYMER BLENDS IN EXTENSIONAL FLOWS

Contrarily to the shear flows, extensional flows do not include nonzero off-diagonal components in the rate-of-deformation tensor, 2**D**. There are three types of simple extensional flows: uniaxial, biaxial and planar extensional flows. Here, only uniaxial extensional flow will be described since, in this work, in terms of extensional behaviour only uniaxial flows are investigated. Moreover, in almost all of the few studies about polymers blends subjected to extensional flows this is the type of flow used. In fact, uniaxial extensional flow is very important in polymer processing operations such as fiber spinning and injection moulding. In terms of velocity profile this flow is described as

$$v = \begin{pmatrix} v_1 \\ v_2 \\ v_3 \end{pmatrix} = \begin{pmatrix} \dot{\varepsilon} x_1 \\ -\frac{\dot{\varepsilon}}{2} x_2 \\ -\frac{\dot{\varepsilon}}{2} x_3 \end{pmatrix}, \ \dot{\varepsilon}>0 \tag{1.42}$$

$\dot{\varepsilon}$ is called the extensional rate and for uniaxial extensional flows $\dot{\varepsilon}$ is positive. This type of flow can be exemplified stretching a sample of fluid of cylindrical shape (Figure 1.17). The flow pattern that this velocity profile describes is three dimensional, with a strong stretch occurring in the x_1-direction and contraction occurring equally in the x_2 and x_3-directions. The velocity field is more complicated than the velocity field in shear flows since in uniaxial extensional flow the velocity components are nonzero in all three directions for most points. Only on the coordinate axes is one of the velocity components zero. The only point not moving at all is the particle located at (0, 0, 0); this is called the stagnation point.

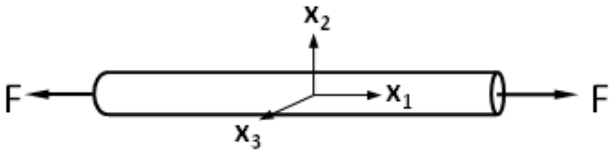

Figure 1.17 - Uniaxial extension of a cylindrical rod and coordinate system.

From Eqn. (1.42) it is easy to conclude that in uniaxial extensional flow, if $\dot{\varepsilon}$ does not vary in time, the velocities of fluid particles are continuously changing as the flow progress. Inversely, in simple shear flow (described in the previous section) the velocities of fluid particles are constant in time if shear rate, $\dot{\gamma}$, does not depends on the time.

From Eqn (1.3) the strain-of-deformation tensor, $2\mathbf{D}$, for the uniaxial extensional flow can be deduced.

$$2\mathbf{D} = \begin{pmatrix} 2\dot{\varepsilon} & 0 & 0 \\ 0 & -\dot{\varepsilon} & 0 \\ 0 & 0 & -\dot{\varepsilon} \end{pmatrix} \tag{1.43}$$

A comparison of this tensor with Eqn. (1.6) shows that shear and extensional flow differ qualitatively in the form of rate-of-deformation tensor. In fact this tensor is diagonal and thus has no shear components.

The extensional material functions that will be measured in this work will be presented next.

EXTENSIONAL STRESS GROWTH In elongational stress growth experiments a constant extension rate is applied, i.e., $\dot{\varepsilon}(t) = \dot{\varepsilon}_0 = \text{constant}$. For these flows, constant stress differences are measured. Thus, the uniaxial extensional viscosity is defined as

$$\eta_E^+(t, \dot{\varepsilon}_0) = \frac{\tau_{11} - \tau_{22}}{\dot{\varepsilon}_0} \tag{1.44}$$

More details about the meaning of this equation and the experimental procedure followed in this work to measure this viscosity will be given in Chapter 2.

In steady extensional flows where $\dot{\varepsilon}(t) = \dot{\varepsilon}_0 = \text{constant}$ it is also common to use the Hencky strain, defined as

$$\varepsilon_H = \dot{\varepsilon}_0 t = \ln \frac{l}{l_0} \tag{1.45}$$

There is an interesting relation between the shear and extensional viscosities in the linear viscoelastic regime. According to this relation, called the Trounton ratio, for low strain rates or small strains the uniaxial extensional viscosity is 3 times the transient growth viscosity in shear, i.e., $\eta_E^+(t, \dot{\varepsilon}) / \eta^+(t, \dot{\varepsilon}) = 3$.

STRESS RELAXATION AFTER AN EXTENSIONAL STEP STRAIN After the application of an uniaxial extensional flow during a very short interval of time the stress relaxation is measured. Therefore,

the kinematics of this experiment can be described by Eqn. (1.42) with the extension rate of the form

$$\dot{\varepsilon}(t) = \lim_{\xi \to 0} \begin{cases} 0 & t<0 \\ \dot{\varepsilon}_0 & 0 \le t<\xi \\ 0 & t \ge \xi \end{cases} \tag{1.46}$$

The extensional strain imposed on the fluid is $\varepsilon_0 = \dot{\varepsilon}_0 \xi$. Then, the uniaxial (tensile) relaxation modulus can be defined as

$$E(t, \varepsilon_0) = \frac{\tau_{11} - \tau_{22}}{e^{2\varepsilon_0} - e^{-\varepsilon_0}} \tag{1.47}$$

In this thesis the normalized tensile relaxation modulus is used.

$$E_N(t, \varepsilon_0) = \frac{E(t, \varepsilon_0)}{E_{max}(\varepsilon_0)} \tag{1.48}$$

The experimental procedure used in this work to measure stress relaxation after an extensional step strain will be discussed in Chapter 2.

In the next subsections the behaviour of polymer blends when subjected to extensional flows will be reviewed.

1.5.1. Non-compatibilized blends

Polymer blends in extensional flows have not been as studied as in shear flows. The main reason for this is probably the experimental difficulties associated to these experiments. Despite this, there are some studies available, mainly concerning non-compatibilized blends.

As in shear, in elongational flows there is a critical capillary number above which the droplets will break up. This subject was tackled experimentally by Grace (1982) using blends of Newtonian components. He determined the critical capillary number as a function of viscosity ratio. An important conclusion of his work was that extensional flow is more effective than simple shear flow in breaking-up droplets. For the same viscosity ratio, a smaller value of Ca_{crit} is obtained for elongational flows than for shear flows. It was also observed that, contrarily to simple shear flows, in extensional flows it is possible to break droplets at viscosity ratios lager than 4.

Delaby *et al.* (1996a) studied blends with well controlled number and size of droplets and viscosity ratios subjected to shear flows. The authors found that the droplet deforms less than the macroscopic deformation of the sample when it is more viscous than the matrix and more than the matrix (approximately 5/3 times) when it is less viscous, which is in agreement with the theories of Taylor (1934) and Cox (1969) for vanishing interfacial tension. Delaby *et al.* (1996a), Delaby *et al.* (1994), Delaby *et al.* (1996b), Delaby *et al.* (1995) also used Palierne's linear model to derive a first-order time evolution deformation of the droplet during start-up of flow. Mighri *et al.* (1997) used a convergent die to generate an apparent elongation flow and showed that the droplet deformation is also governed by the elasticity ratio, defined as the ratio between the relaxation time of the dispersed phase to that of the matrix. They observed that the droplet deformation increases with increasing elasticity of the matrix and decreases with increasing elasticity of the droplet.

The elongation and subsequent recovery of poly(methylmethacrylate)-polystyrene (PMMA/PS) blends, as well as the evolution of the morphology, were studied by Gramespacher and Meissner (1997) and, more recently, by Mechbal and Bousmina (2004) and Handge and Potschke (2004). Pronounced differences were observed in the recovery behaviour after melt elongation, that of the

blends being much larger than that of the blend components. The results suggest that there is a fast molecular recovery related with each component and a slow one associated with interfacial tension. In terms of elongation flow, Mechbal and Bousmina (2004) observed that behaviour of a PMMA/PS 95/5 blend is mainly dominated by the behaviour of the matrix. Oosterlinck et al. (2005), while studying PMMA/PS blends subjected to uniaxial elongation flows, verified that the extra stress due to droplet deformation can, in principle, be deduced from extensional rheological measurements. However, experimental studies about the morphological development of immiscible blends during uniaxial elongational flows are rare, and some aspects, mainly those concerned with the influence of elasticity, need to be clarified. Experimental studies on the behaviour of compatibilized blends in extensional flows, which will be the subject of next section, are even rarer.

1.5.2. Compatibilized blends

Mechbal and Bousmina (2007) studied the effect of the diblock copolymer addition on the rheology and morphology development during uniaxial elongation and during relaxation after cessation of flow on a PMMA/PS blend. They observed that when the concentration of the copolymer is above a critical value the droplets are less deformed due to local entanglements that resist deformation. These entanglements cause a slower relaxation too.

In most industrial cases a complex flow field, with both shear and elongational components, is present. However, only a few papers deal with blends behaviour in complex flows. These studies will not be reviewed in this text.

Knowledge of the behaviour of the polymer blends under flow is very important since it allows process control to be improved and thus also the properties of the final product. The rheological behaviour of an emulsion of two polymers depends on factors like the concentration of the dispersed phase or the elasticity ratios between the components. The combination of such variables can lead to a complex and difficult behaviour prediction. Moreover, the compatibilizers, whose use has become common in industry, have a large effect in the rheology of polymer blends.

1.6 OBJECTIVES

This work will focus on the effect of the compatibilizers on the rheology of polymer blends. More specifically, the aim is to understand the influence of the compatibilizer on the rheological behaviour of polymer blends with industrial interest and its relationship with morphology. The attention will be focused in concentrated blends with high viscosity ratios and droplet-matrix morphology. This kind of blends has a great practical interest and many questions remain open. In particular, how do the interfaces modified by the compatibilizer relax and what are the consequences in the rheological behaviour? Moreover, the studies concerning extensional rheology of polymer blends specially compatibilized polymer blends are extremely rare. An exhaustive rheological characterization will be persecuted in this work. Linear and non-linear (relaxation both in shear and extension) experiments will be performed. Additionally, in order to investigate the characteristics of the interfaces rheo-optical measurements will also be performed.

References

Adhikari, N. P. and J. L. Goveas, "Effects of slip on the viscosity of polymer melts", J. Polym. Sci. Pol. Phys. 42, 1888-1904 (2004).

Asthana, H. and K. Jayaraman, "Rheology of reactively compatibilized polymer blends with varying extent of interfacial reaction", Macromolecules 32, 3412-3419 (1999).

Bousmina, M., "Rheology of polymer blends: linear model for viscoelastic emulsions", Rheol. Acta 38, 73-83 (1999).

Bousmina, M., M. Aouina, B. Chaudhry, R. Guenette and R. E. S. Bretas, "Rheology of polymer blends: non-linear model for viscoelastic emulsions undergoing high deformation flows", Rheol. Acta 40, 538-551 (2001).

Covas, J. A., A. V. Machado and M. Van Duin, "Rheology of PA-6/EPM/EPM-g-MA blends along a twin-screw extruder", Adv. Polym. Tech. 19, 260-276 (2000).

Cox, R. G., "Deformation of a Drop in a General Time-Dependent Fluid Flow", J. Fluid Mech. 37, 601-& (1969).

Debruijn, R. A., "Deformation and breakup of drops in simple shear flows", PhD thesis, Eindhoven Univ. Technol. (1991).

Delaby, I., B. Ernst, D. Froelich and R. Muller, "Droplet deformation in immiscible polymer blends during transient uniaxial elongational flow", Polym. Eng. Sci. 36, 1627-1635 (1996a).

Delaby, I., B. Ernst, Y. Germain and R. Muller, "Droplet Deformation in Polymer Blends during Uniaxial Elongational Flow - Influence of Viscosity Ratio for Large Capillary Numbers", J. Rheol. 38, 1705-1720 (1994).

Delaby, I., B. Ernst and R. Muller, "Drop deformation in polymer blends during elongational flow", Journal of Macromolecular Science-Physics B35, 547-561 (1996b).

Delaby, I., D. Froelich and R. Muller, "Drop Deformation in Polymer Blends during Uniaxial Elongational Flow", Macromolecular Symposia 100, 131-135 (1995).

Doi, M. and T. Ohta, "Dynamics and Rheology of Complex Interfaces .1." J. Chem. Phys. 95, 1242-1248 (1991).

Dressler, M. and B. J. Edwards, "The influence of matrix viscoelasticity on the rheology of polymer blends", Rheol. Acta 43, 257-282 (2004).

Ehrenstein, G. W., *Polymeric Materials: Structure-Properties-Applications* (Hanser, Munich, 2001).

Einstein, "A new determination of molecular dimensions", Annalen der Physik 19, 289-306 (1906).

Eshelby, J. D., "The Determination of the Elastic Field of an Ellipsoidal Inclusion, and Related Problems", Proceedings of the Royal Society of London Series a-Mathematical and Physical Sciences 241, 376-396 (1957).

Grace, H. P., "Dispersion Phenomena in High-Viscosity Immiscible Fluid Systems and Application of Static Mixers as Dispersion Devices in Such Systems", Chemical Engineering Communications 14, 225-277 (1982).

Graebling, D., R. Muller and J. F. Palierne, "Linear Viscoelastic Behavior of Some Incompatible Polymer Blends in the Melt - Interpretation of Data with a Model of Emulsion of Viscoelastic Liquids", Macromolecules 26, 320-329 (1993).

Gramespacher, H. and J. Meissner, "Melt elongation and recovery of polymer blends, morphology, and influence of interfacial tension", J. Rheol. 41, 27-44 (1997).

Greco, F., "Drop deformation for non-Newtonian fluids in slow flows", J. Non-Newtonian Fluid Mech. 107, 111-131 (2002).

Guido, S., M. Simeone and F. Greco, "Deformation of a Newtonian drop in a viscoelastic matrix under steady shear flow - Experimental validation of slow flow theory", J. Non-Newtonian Fluid Mech. 114, 65-82 (2003a).

Guido, S., M. Simeone and F. Greco, "Effects of matrix viscoelasticity on drop deformation in dilute polymer blends under slow shear flow", Polymer 44, 467-471 (2003b).

Handge, U. A. and P. Potschke, "Interplay of rheology and morphology in melt elongation and subsequent recovery of polystyrene/poly(methyl methacrylate) blends", J. Rheol. 48, 1103-1122 (2004).

Hobbie, E. K. and K. B. Migler, "Vorticity elongation in polymeric emulsions", Physical Review Letters 82, 5393-5396 (1999).

Huo, Y. L., G. Groeninckx and P. Moldenaers, "Rheology and morphology of polystyrene/polypropylene blends with in situ compatibilization", Rheol. Acta 46, 507-520 (2007).

Iza, M., M. Bousmina and R. Jerome, "Rheology of compatibilized immiscible viscoelastic polymer blends", Rheol. Acta 40, 10-22 (2001).

Jackson, N. E. and C. L. Tucker, "A model for large deformation of an ellipsoidal droplet with interfacial tension", J. Rheol. 47, 659-682 (2003).

Jacobs, U., M. Fahrlander, J. Winterhalter and C. Friedrich, "Analysis of Palierne's emulsion model in the case of viscoelastic interfacial properties", J. Rheol. 43, 1495-1509 (1999).

Jansseune, T., J. Mewis, P. Moldenaers, M. Minale and P. L. Maffettone, "Rheology and rheological morphology determination in immiscible two-phase polymer model blends", J. Non-Newtonian Fluid Mech. 93, 153-165 (2000).

Kerner, E. H., "The Elastic and Thermo-Elastic Properties of Composite Media", Proceedings of the Physical Society of London Section B 69, 808-813 (1956).

Koning, C., M. Van Duin, C. Pagnoulle and R. Jerome, "Strategies for compatibilization of polymer blends", Progress in Polymer Science 23, 707-757 (1998).

Lacroix, C., M. Grmela and P. J. Carreau, "Relationships between rheology and morphology for immiscible molten blends of polypropylene and ethylene copolymers under shear flow", J. Rheol. 42, 41-62 (1998).

Lee, H. M. and O. O. Park, "Rheology and Dynamics of Immiscible Polymer Blends", J. Rheol. 38, 1405-1425 (1994).

Levitt, L., C. W. Macosko and S. D. Pearson, "Influence of normal stress difference on polymer drop deformation", Polym. Eng. Sci. 36, 1647-1655 (1996).

Macaubas, P. H. P., N. R. Demarquette and J. M. Dealy, "Nonlinear viscoelasticity of PP/PS/SEBS blends", Rheol. Acta 44, 295-312 (2005).

Maffettone, P. L. and F. Greco, "Ellipsoidal drop model for single drop dynamics with non-Newtonian fluids", J. Rheol. 48, 83-100 (2004).

Maffettone, P. L. and M. Minale, "Equation of change for ellipsoidal drops in viscous flow", J. Non-Newtonian Fluid Mech. 78, 227-241 (1998).

Mechbal, N. and M. Bousmina, "Effect of copolymer addition on drop deformation during uniaxial elongation and during relaxation after cessation of flow", Macromolecules 40, 967-975 (2007).

Mechbal, N. and M. Bousmina, "Uniaxial deformation and relaxation of polymer blends: relationship between flow and morphology development", Rheol. Acta 43, 119-126 (2004).

Mighri, F., A. Ajji and P. J. Carreau, "Influence of elastic properties on drop deformation in elongational flow", J. Rheol. 41, 1183-1201 (1997).

Mighri, F., P. J. Carreau and A. Ajji, "Influence of elastic properties on drop deformation and breakup in shear flow", J. Rheol. 42, 1477-1490 (1998).

Mighri, F. and M. A. Huneault, "Dispersion visualization of model fluids in a transparent Couette flow cell", J. Rheol. 45, 783-797 (2001).

Migler, K. B., "Droplet vorticity alignment in model polymer blends", J. Rheol. 44, 277-290 (2000).

Oldroyd, J. G., "The effect of interfacial stabilizing films on the elastic and viscous properties of emulsions", Proc Roy Soc A232, 567-577 (1955).

Oldroyd, J. G., "The elastic and viscous properties of emulsions and suspensions", Proc Roy Soc London A218, 122-132 (1953).

Oosterlinck, F., M. Mours, H. M. Laun and P. Moldenaers, "Morphology development of a polystyrene/polymethylmethacrylate blend during start-up of uniaxial elongational flow", J. Rheol. 49, 897-918 (2005).

Palierne, J. F., "Linear Rheology of Viscoelastic Emulsions with Interfacial-Tension", Rheol. Acta 29, 204-214 (1990).

Riemann, R. E., H. J. Cantow and C. Friedrich, "Interpretation of a new interface-governed relaxation process in compatibilized polymer blends", Macromolecules 30, 5476-5484 (1997).

Shi, D., Z. Ke, J. H. Yang, Y. Gao, J. Wu and J. H. Yin, "Rheology and morphology of reactively compatibilized PP/PA6 blends", Macromolecules 35, 8005-8012 (2002).

Sibillo, V., M. Simeone and S. Guido, "Break-up of a Newtonian drop in a viscoelastic matrix under simple shear flow", Rheol. Acta 43, 449-456 (2004).

Taylor, G. I., "The formation of emulsions in definable fluids of flow", Proceedings of the Royal Society of London. Series A 146, 501-523 (1934).

Taylor, G. I., "The Viscosity of a Fluid Containing Small Drops of Another Fluid", Proceedings of the Royal Society of London. Series A 138, 41-48 (1932).

Tucker, C. L. and P. Moldenaers, "Microstructural evolution in polymer blends", Annu. Rev. Fluid. Mech. 34, 177-210 (2002).

Utracki, L. A., Editor, *Polymer Blends Handbook - Vol. 1* (Kluwer Academic Publishers, Dordrecht, 2002).

Van Hemelrijck, E., P. Van Puyvelde, S. Velankar, C. W. Macosko and P. Moldenaers, "Interfacial elasticity and coalescence suppression in compatibilized polymer blends", J. Rheol. 48, 143-158 (2004).

Van Puyvelde, P., Z. Oommen, P. Koets, G. Groeninckx and P. Moldenaers, "Effect of reactive compatibilization on the interfacial slip in nylon-6/EPR blends", Polym. Eng. Sci. 43, 71-77 (2003).

Van Puyvelde, P., S. Velankar and P. Moldenaers, "Rheology and morphology of compatibilized polymer blends", Curr. Opin. Coll. Int. Sci. 6, 457-463 (2001).

Vinckier, I., P. Moldenaers and J. Mewis, "Relationship between rheology and morphology of model blends in steady shear flow", J. Rheol. 40, 613-631 (1996).

Wetzel, E. D., "Modeling flow-induced microstructure of inhomogeneous liquid-liquid mixtures ", PhD. thesis, University of Illinois at Urbana-Champaign (2001).

Wetzel, E. D. and C. L. Tucker, "Droplet deformation in dispersions with unequal viscosities and zero interfacial tension", J. Fluid Mech. 426, 199-228 (2001).

Yee, M., P. S. Calvao and N. R. Demarquette, "Rheological behavior of poly(methyl methacrylate)/polystyrene (PMMA/PS) blends with the addition of PMMA-ran-PS", Rheol. Acta 46, 653-664 (2007).

Yu, W., M. Bousmina, C. X. Zhou and C. L. Tucker, "Theory for drop deformation in viscoelastic systems", J. Rheol. 48, 417-438 (2004).

Yu, W., C. X. Zhou and M. Bousmina, "Theory of morphology evolution in mixtures of viscoelastic immiscible components", J. Rheol. 49, 215-236 (2005).

Zhao, R. and C. W. Macosko, "Slip at polymer-polymer interfaces: Rheological measurements on coextruded multilayers", J. Rheol. 46, 145-167 (2002).

CHAPTER 2

Rheometry: principles and devices used

In Chapter 1 shear and extensional flows were described and some material functions particularly important in the study of rheology of polymer blends were defined. In this chapter the devices used to measure the rheological material functions will be discussed. Such devices are called rheometers and can be divided in two major classes, according to the imposed flow type and quantities measured: shear and extensional rheometers.

2.1 SHEAR RHEOMETRY

The most common rheological characterization of the materials is performed in shear flows. Shear rheometers can be divided into two groups: *drag flows* in which shear is generated between a moving and a fixed solid surface, and *pressure-driven flows*, in which shear is generated by a pressure difference over a closed channel. For the study of the morphology or interfacial elasticity in polymer blends the use of rheometers of the first type, namely rotational rheometers, is desirable. Thus, rotational rheometry, in particular that resorting to the parallel-plate geometry used in this work, will be analysed.

2.1.1. Rotational Rheometry

There are several types of rotational rheometers. The most common are the concentric cylinder rheometer, the cone and plate rheometer and the parallel-plate rheometer. The former takes advantage in characterization of materials with low viscosity at high shear rates. Thus, it is not the most adequate to the polymer blends that will be studied. In comparison with the parallel-plate, the cone and plate rheometer has the advantage that allows N_1 to be measured and imposes a constant shear rate on all the sample. However, in the cone and plate rheometer it is difficult to load the samples, specially the most viscous ones. Moreover, the parallel-plate rheometer is preferable to determine the dynamic modulli, G' and G''. Hence, the experiments

in shear were performed in the parallel-plate rheometer. This will be studied in the more detail in the next paragraphs.

PARALLEL-PLATE RHEOMETER The parallel-plate apparatus is composed by two disks disposed parallel to each other (Figure 2.1). With one disk stationary and the other rotating at Ω, assuming no slip at these surfaces and neglecting inertial forces, the velocity vector written in $r\theta z$ coordinate system is

$$v = \begin{pmatrix} 0 \\ v_\theta \\ 0 \end{pmatrix}_{r\theta z} \tag{2.1}$$

with v_θ given by

$$v_\theta = \frac{r\Omega z}{h} \tag{2.2}$$

and, thus

$$\dot{\gamma}(r) = \frac{r\Omega}{h} \tag{2.3}$$

Then, it is possible to see that the shear rate is not constant in the radial direction. Obviously the shear stress varies also in the radial direction. The shear stress at the rim position $r = R$ can be related with the torque measured by the rheometer, M,

$$\tau_{21}(R) = \frac{M}{2\pi R^3}\left[3 + \frac{d\ln(M)}{d\ln\dot{\gamma}_R}\right] \tag{2.4}$$

where $\dot{\gamma}_R$ is the shear rate in the R position.

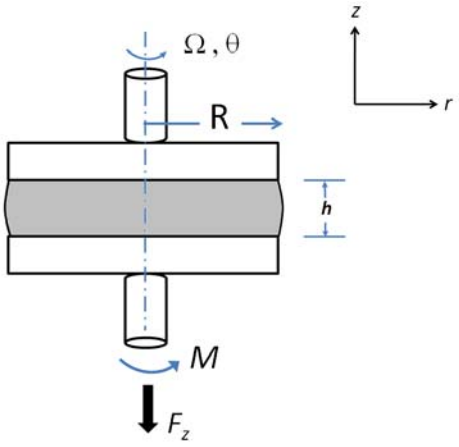

Figure 2.1 – Schematic of a parallel-plate rheometer.

Thus, to evaluate the shear stress for an unknown fluid, a sufficient amount of $\ln M$ versus $\ln \dot{\gamma}_R$ data must be taken to determine the derivative accurately. In practice this is not very difficult since many materials have power law regions and numerical software packages are readily available for handling the data. Furthermore, the derivative is generally less than 1, and then a 10% error results in less than 3% error in τ_{21} [Macosko (1994)].

If the tested fluid is Newtonian, $d\ln M/d\ln \dot{\gamma}_R = 1.0$ and the shear stress is simply

$$\tau_a(R) = \frac{2M}{\pi R^3} \tag{2.5}$$

This *apparent shear stress* is often used to calculate an apparent viscosity, since only a single torque measurement is required. However, a simple, approximate single point method was developed by Giesekus and Langer (1977). The idea is that the *true* and apparent shear stresses must be equal at some radial point. This occurs nearly at the same point, $r/R = 0.76$, for a wide range of liquids, i.e., those for which $d\ln M/d\ln \dot{\gamma}_R < 1.4$. Thus, the true viscosity is equal to the apparent viscosity evaluated at

$$\eta(\tau) = \eta_a(\tau_a) \pm 2\% \quad \text{for} \quad \tau = 0.76\,\tau_a \tag{2.6}$$

The main error sources in plate-plate rheometer are due to edge effects, shear heating and the possible existence of secondary flows. However, these errors can be minimized by operating the rheometer at small gaps.

2.2 EXTENSIONAL RHEOMETRY

As was seen in Chapter 1, extensional rheometry measurements are less common than shear measurements. This happens mainly because extensional experiments are harder to perform. However, it is known that the extensional properties are very sensible to changes in structure and are very important in many industrial processes.

Several types of rheometers, based in different flow geometries, have been proposed to generate purely uniaxial extensional flows.

2.2.1. Measuring the uniaxial extensional viscosity

In Section 1.5 it was seen that the simplest way to generate this kind of flow is to grab a rod of fluid on each end and pull it. However, before describing the experimental techniques that allow the uniaxial extensional viscosity to be measured it is necessary to fix the quantities to be measured or imposed to the sample.

To generate a steady uniaxial extension the velocity field should be given by Eqn. (1.35) or in cylindrical coordinates (see Figure 2.2)

$$v_x = \dot{\varepsilon} x \tag{2.7}$$

$$v_r = -\frac{1}{2}\dot{\varepsilon} r \tag{2.8}$$

Thus, the samples ends must move with velocity

$$v_{end} = \frac{\dot{\varepsilon} L}{2} \tag{2.9}$$

If it is assumed that the material is incompressible, it is possible to deduce the following expression for the variation of the radius of the sample:

$$R(t) = R_0 e^{-\frac{1}{2}\dot{\varepsilon} t} \tag{2.10}$$

where R_0 is the initial radius of the sample.

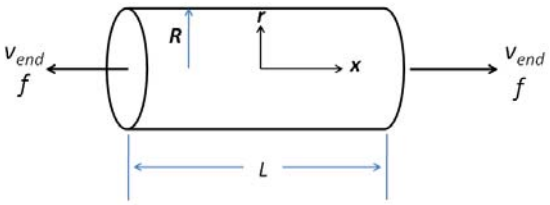

Figure 2.2 – A cylindrical sample being pulled at each end by a force f with a velocity v_{end}.

The stress that causes the sample to elongate is the normal stress difference $\tau_{xx} - \tau_{rr}$. If surface tension and other factors like gravity were ignored, then this stress is the force per unit area acting on the end of the sample (see Figure 2.2)

$$\tau_{xx} - \tau_{rr} = \frac{f}{A} \tag{2.11}$$

It is then possible to rewrite Eqn. (1.37) in terms of cylindrical coordinates.

$$\eta_E^+ = \frac{\tau_{xx} - \tau_{rr}}{\dot{\varepsilon}} \tag{2.12}$$

Most of the rheometers that perform uniaxial extension tests on highly viscous samples, such as polymer melts, can be classified in one of the following classes: varying length or fixed length. Although there are experimental difficulties inherent to each method, the concepts in which they underlie are very simple. In the varying length rheometers the ends of the sample are held by the clamps and pulled. In fixed length type rheometer the stretching of the sample is realized by rotating clamps. The rheometer used in this thesis is of the latter type.

THE MRR RHEOMETER In this work the extensional rheological measurements were performed on the MRR (Modified Rotational Rheometer) developed by Maia *et al.* (1999). The MRR is composed of a fixed clamp and a rotating clamp with two counter-rotating rollers (Figure 2.3) allowing simple uniaxial extensions at constant strain rates to be imposed. During the experiments the samples are immersed in a bath of silicone oil for the dual purpose of temperature control and sagging prevention. The silicone oil is selected in such away that the density of the oil matches that of the polymer (in order to compensate for gravitational effects) and its viscosity is low enough to minimise viscous drag on the sample. During this work samples with circular cross sections were used. In some cases it was necessary to increase the signal and thus samples with rectangular cross sections were done instead. Theses samples were prepared by compression moulding while the circular cross section ones were extruded. Sample preparation must be careful since a poor sample preparation may lead to the existence of impurities (such as trapped air) causing stress concentrations and, possibly, degradation (which may be non-negligible for experiments carried out at low strain rates). Hence, extrusion conditions were kept in such a way as to avoid the presence of instabilities. In compression moulding the press plates were cooled below T_g of the materials before samples were removed.

Nevertheless, special care was taken in rejecting the samples that did not have a perfect shape, or had pockets of trapped air inside.

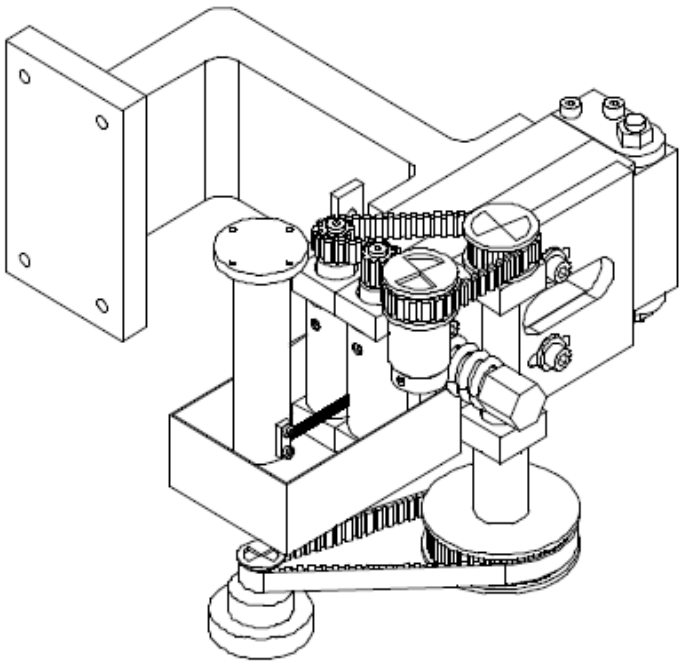

Figure 2.3 – General view of the MRR (Modified Rotational Rheometer). Taken from Barroso (2003).

In these types of rheometers it can happen that the cross section of the sample was not uniform throughout the experiment with the cross section becoming higher in the extremities. Barroso *et al.* (2002) have shown that the aspect ratio, L/D, used in this work, which ranged between approximately 13 and 20, is high enough for these end-effects to be negligible. In fact the effective length of each sample was 40 mm and the diameter varied between 2 and 3 mm. Nevertheless, the stretch uniformity was checked visually in all experiments resorting to video footage.

Sample loading is of extreme importance and, while the procedure in itself is straightforward, special care had to be taken in the process. Upon loading onto the rheometer, residual stresses were allowed to relax; once the measured torque decayed to zero any existing slack was removed,

which was followed by another waiting period for residual stress relaxation; only once the measured torque decayed to zero again would the experiment be started.

The effective strain rates were obtained by experimental fitting of the evolution in time of sample radius since Maia *et al.* (1999) found that effective strain rates different by up to 40% to those expected theoretically through the angular velocity of the rollers. This was achieved by resorting to video footage and fitting Eqn. (2.10) to the experimental data.

It is known that exist is the possibility of sample slip at the rollers. When slip starts occurring, the rate of change of the torque is expected to decrease (this corresponds to a lower 'effective' strain rate). In some cases, the measured torque becomes constant and so does the cross-section, and the sample does not fail at all during the experiment. Therefore, whenever a change in slope in the torque it was detected, it was taken as an indication of the onset of slip at the rollers and all further data was rejected.

The MRR allows performing not only startup extensional measurements but also stress relaxation after an extensional step strain. In these latter experiments a maximum theoretical step Hencky strain of approximately 0.3 units, i.e., a linear deformation of approximately 35% can be obtained over a period of less than ten hundredths of a second. The angular displacement of the rollers was measured for each step strain in order to determine apparent Hencky strains for any given experiment. In fact, those are not the real Hencky strains since the angular displacement of the rollers is not fully transferred to the samples it was said above. To calculate the true strain rates the calibrations developed by Barroso and Maia (2002) were used.

In stress relaxation after an extensional step strain experiments a crucial point that needs addressing is related to the shape and magnitude of the measured signal. Since the transition to the strained state and back to rest is very fast (of the order of a few hundredths of a second) and because of the particular form of the torque measuring head of the rheometer (in which an elastic torsion bar of known elastic constant is attached to the fixed clamp via a frictionless air bearing) it is expected that transients will appear in the output signal. In fact, after an initial overshoot, damped oscillations were observed in the torque measuring head. The reason for this

damping comes from the superposition of the signal originating from the self-damping of the elastic torsion bar of the measuring head to that of the true signal. To obtain the true signal upper and lower boundaries to the measured output were constructed (Figure 2.4). The functions of choice for the boundaries varied somewhat, since the only criterion was the evolution of the boundary points to be preserved, one of the most common choices was of the type

$$y = \frac{a + cx + ex^2 + gx^3 + ix^4 + kx^5}{1 + bx + dx^2 + fx^3 + hx^4 + jx^5} \tag{2.13}$$

The true relaxation signal was then assumed to be the average of two boundaries. More details on the experimental technique to measure the stress relaxation after an extensional step strain are given in Barroso and Maia (2002).

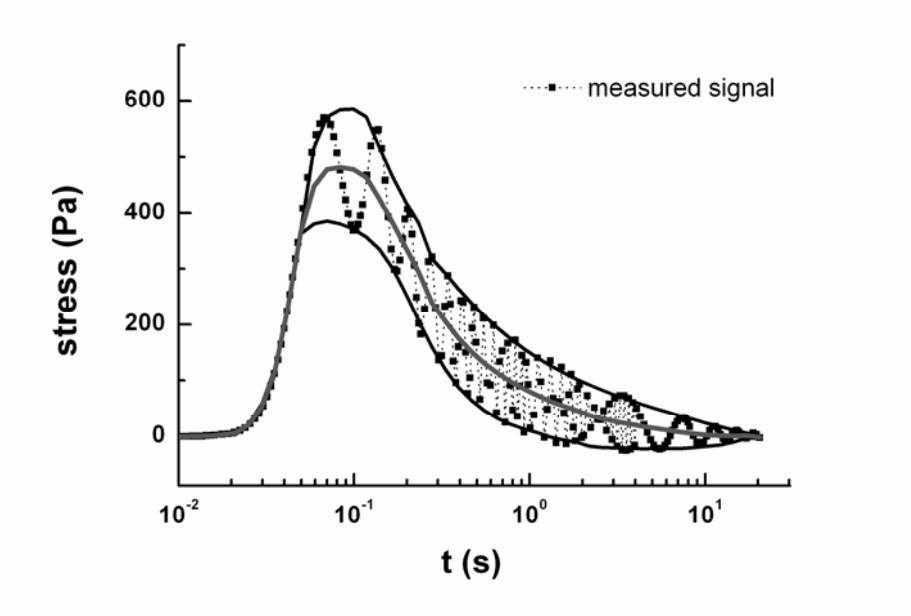

Figure 2.4 – Example of a stress relaxation experiment performed on a sample of PS (see Chapter 4). The true relaxation signal is determined after analysis of the upper and lower boundaries.

Reference

Barroso, V., "Viscoelasticity of Polymer Melts in Uniaxial Extension Flows", PhD. thesis, University of Minho (2003).

Barroso, V. C., J. A. Covas and J. M. Maia, "Sources of error and other difficulties in extensional rheometry revisited: commenting and complementing a recent paper by T. Schweizer", Rheol. Acta 41, 154-161 (2002).

Barroso, V. C. and J. M. Maia, "Evaluation by means of stress relaxation (after a step strain) experiments of the viscoelastic behavior of polymer melts in uniaxial extension", Rheol. Acta 41, 257-264 (2002).

Giesekus, H. and G. Langer, "Determination of Real Flow Curves of Non-Newtonian Liquids and Plastic Materials Using Method of Representative Viscosity", Rheol. Acta 16, 1-22 (1977).

Macosko, C. W., *Rheology: Principles, measurements, and applications* (VCH Publishers, New York, 1994).

Maia, J. M., J. A. Covas, J. M. Nobrega, T. F. Dias and F. E. Alves, "Measuring uniaxial extensional viscosity using a modified rotational rheometer", J. Non-Newtonian Fluid Mech. 80, 183-197 (1999).

CHAPTER 3

Commercial high viscosity/elasticity ratios blends: PA6/EPM/EPM-g-MA

A commercial polymer blend, which is constituted by a dispersed phase having a viscosity and an elasticity that exceeds more that 10 times the viscosity and elasticity of the matrix, will be the departure point for this work. Since polyamide-6 (PA-6) and ethene-propene-monomer (EPM) rubber are immiscible and their blend shows bad mechanical properties, compatibilization is usual. In this chapter compatibilized blends resulting from *in situ* compatibilization with EPM grafted with maleic anidrid (EPM-g-MA) will be studied. It particular, attention will be focused on the role of the *in situ* compatibilization of these materials, namely, whether the high viscosity, high elasticity droplets of the dispersed phase are viscoelastically deformed under flow and what the implications in the overall rheological behaviour of the materials are.

This chapter was adapted from *Silva, J., A. V. Machado and J. Maia, "Rheological behavior of compatibilized and non-compatibilized PA6/EPM blends", Rheol Acta 46, 1091-1097 (2007).* [Appendix B]

3.1 EXPERIMENTAL

3.1.1. Materials

Several blends of a commercial polyamide-6 (PA-6 Akulon K123), an ethene-propene rubber (EPM Keltan 740) and an ethene-propene rubber modified with maleic anhydride (EPM-g-MA ExxelorVA 1801, containing 0.49 wt% of MA, as determined by FT-IR) were prepared in a twin screw extruder, under the same process conditions (the screws rotating at 200 rpm, with a flow rate of 6 kg/h and set temperatures of 220–230°C in the barrel and 220°C at the die). The PA-6 content was kept constant in all blends, but the amount of modified rubber was varied in order to have different amounts of maleic anhydride in each blend and thus various amounts of

compatibilizer at the interface. The chemical and morphological characterizations were performed in a previous work [Machado et al. (1999)], some data being summarized in Table I and Table II. The volume (R_v) and number (R_n) average radii were calculated using Eqns. (3.1) and (3.2):

$$R_v = \frac{\sum_i n_i R_i^4}{\sum_i n_i R_i^3} \tag{3.1}$$

$$R_n = \frac{\sum_i n_i R_i^3}{\sum_i n_i} \tag{3.2}$$

where n_i = number of the droplets having radius R_i.

Blend (w/w/w)	PA-6 (wt%)	EPM (wt%)	EPM-g-MA (wt%)[1]	MA content of rubber phase (wt%)[2]
80/20/0	80	20	0	0
80/15/5	80	15	5	0.13
80/10/10	80	10	10	0.25
80/5/15	80	5	15	0.37
80/0/20	80	0	20	0.49

Table I – Blends composition.

[1] MA content of EPM-g-MA is 0.49 wt%.

[2] MA content of the rubber phase is the weight average of the combined EPM and EPM-g-MA rubber phases.

Blend (w/w/w)	R_v (μm)	R_n (μm)	R_v/R_n
80/20/0	17.6	5.6	3.1
80/15/5	8.25	1.28	6.5
80/10/10	2.35	1.18	2.0
80/5/15	1.78	1.11	1.6
80/0/20	0.36	0.20	1.8

Table II - Morphological characterization of the blends.

3.1.2. Shear rheometry

The rheological measurements in shear were performed in a Reologica Stress Tech HR rheometer, using a parallel plate geometry (diameter=25 mm) with a 1000 ± 1 μm gap. Samples were vacuum dried at 80°C during 12 h before each rheological experiment.

All oscillatory tests were performed at 3 different temperatures (240, 260, 280°C) in a nitrogen atmosphere, time sweep measurements at constant frequency having been performed in order to ensure that neither polymerization nor degradation occurred during the frequency sweep tests (Figure 3.1 and Figure 3.2).

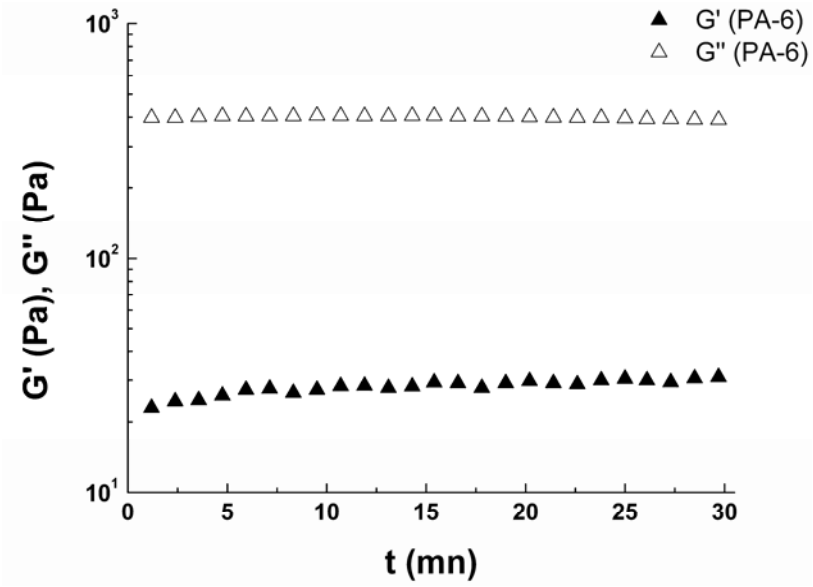

Figure 3.1 - Dynamic moduli of PA6 measured at a constant frequency (0.1 Hz) at 260 °C in a nitrogen atmosphere.

The stress relaxation experiments were performed at 240°C, in a nitrogen atmosphere; a shear rate of 0.1 s^{-1} during 250 s was applied, and the shear stress upon cessation of flow was measured. Since it is known that processing causes degradation (by chain scission/crosslinking) of the polyamide, in order to have comparable results for the PA-6 and the blends, the former was also extruded under the same conditions as the latter. Thus, all the results shown in this Chapter are not for virgin PA-6, but for extruded PA-6.

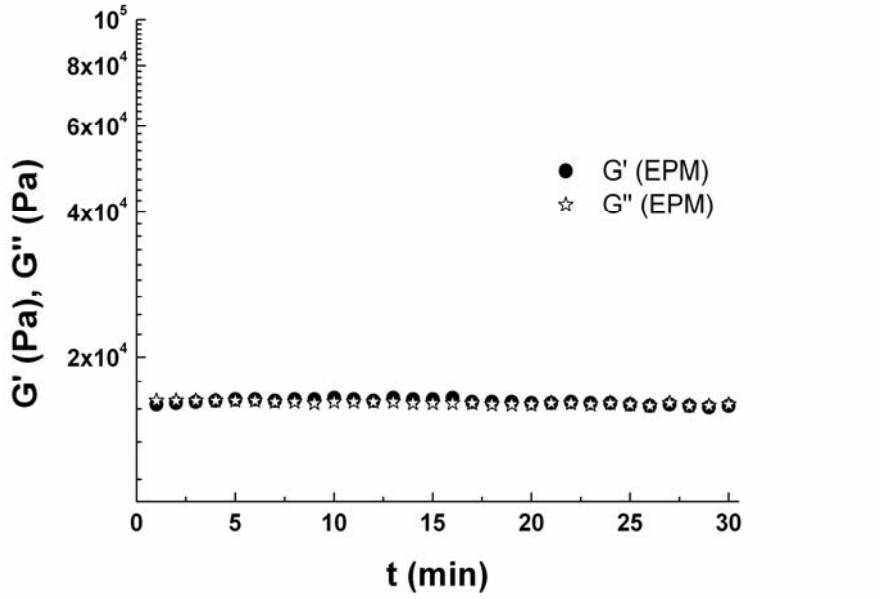

Figure 3.2 - Dynamic moduli of EPM measured at a constant frequency (0.1 Hz) at 240 °C.

3.1.3. Extensional rheometry

The extensional rheological measurements were performed on the modified rotational rheometer (MRR). For start-up extensional measurements extruded samples (either in a Leistritz twin-screw extruder -blends- or in a ROSAND RH8-2 capillary rheometer-EPM and EPM-g-MA) were used while for extensional relaxation experiments samples with rectangular cross section (about 3×2 mm) were prepared. All the samples were vacuum dried at 80°C during 12 h before the

corresponding rheological experiments. The temperature of silicone oil was 240°C. For details about the experimental technique see Subsection 2.2.1.

The main motivation for performing extensional rheometry experiments on these samples is related to the fact that their viscosity and elasticity ratios are very high (see below) and, therefore, any differences in rheological behaviour, especially due to interfacial phenomena, between the immiscible and the compatibilized blends are likely to be better seen in extensional flows than is shear [e.g., Oosterlinck *et al.* (2005)].

3.1.4. Morphology

In order to study the morphology of samples undergoing extensional deformations, the oil bath was rapidly removed during an experiment and the deformed sample was quenched in liquid nitrogen (the whole process takes only 2 to 3 seconds) while the deformation is still being imposed. This means that no significant morphological changes, such as droplet relaxation and/or coalescence, should occur during the quenching process. Once solidified, the samples were fractured longitudinally in liquid nitrogen, etched with boiling xylene to remove the rubber from the surface and gold plated; their morphology was studied using a Jeol JSM 6310F Scanning Electron Microscope.

3.2 RESULTS AND DISCUSSION

3.2.1. Linear viscoelasticity

Figure 3.3 and Figure 3.4 show the dynamic moduli of the blends and their components (PA-6, EPM, EPM-g-MA). Time-Temperature superposition was performed at a reference temperature of 260 °C for PA-6 and the blends. From the figures it is possible to observe that the $t-T$ superposition works well at high frequencies while at low frequencies there is some scatter in the data and it is possible that, especially at the higher temperatures, sample degradation set in. However, since the experiments were performed in a nitrogen atmosphere this is not very likely; in addition, since the scatter is not large enough to mask the qualitative behaviour of the G' and G'' curves, the option was made to keep the data.

The figures show that the blends have different qualitative behaviours depending on the amount of compatibilizer. At high frequencies all the blends except the one with the highest compatibilizer content show an effect commonly known as, Negative Deviation Behaviour, NDB, which originates in slip at the interfaces [Utracki (1983), Van Puyvelde *et al.* (2003)] due to poor or insufficient adhesion between the matrix and the dispersed phase. At low frequencies, an increase in the moduli of the blends can be noticed. This is especially noticeable at very low frequencies, where a plateau in G', which has been related to the size of the particles of the dispersed phase and the amount of compatibilizer at the interfaces [Riemann *et al.* (1997), Van Hemelrijck *et al.* (2004)] seems to develop.

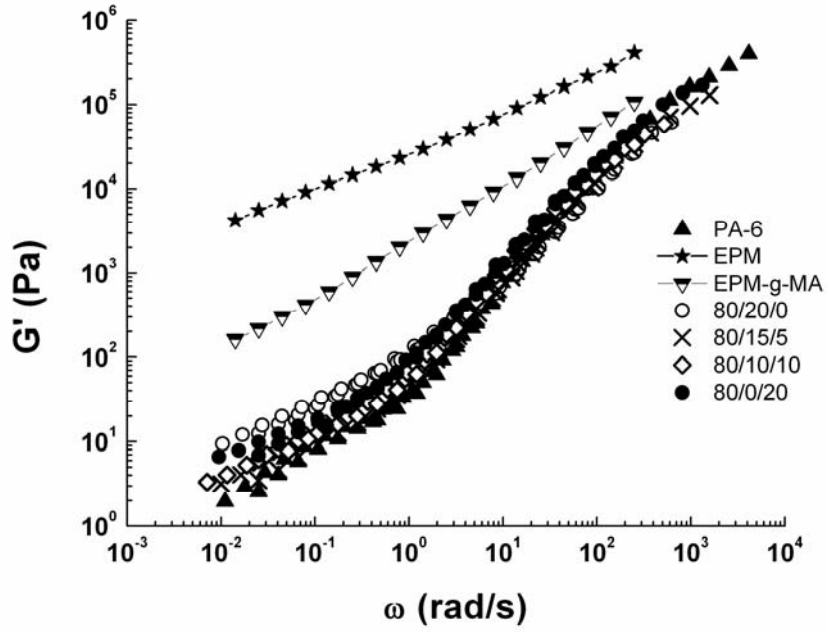

Figure 3.3 - Storage modulus for several blends of PA6/EPM/EPM-g-MA and their components.

Again, it could be argued that this plateau could also be attributed to changes in rheological properties of the components during the experiment, e.g., degradation. However, as shown in Figure 3.1 and Figure 3.2 the rheological behaviour of PA-6 and EPM remains very much constant in time at the timescale of the experiments.

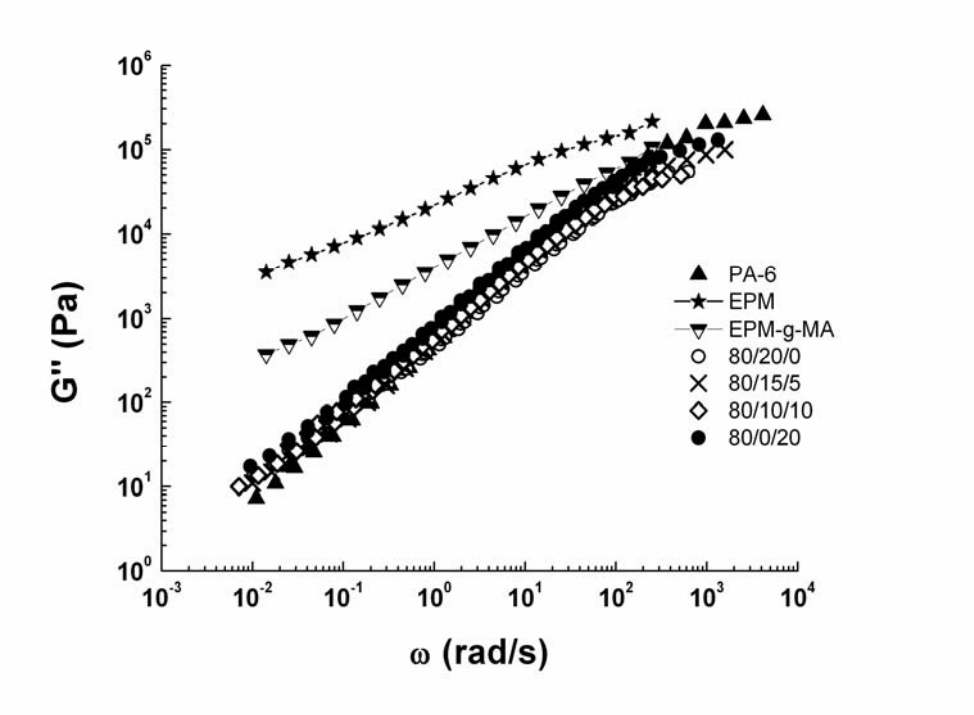

Figure 3.4 - Dissipative modulus for several blends of PA6/EPM/EPMg-MA and their components.

Since the viscosity ratios are very high (approximately 50 and 400 between PA6 and EPM, at 3×10^{-3} Hz) the Palierne model is not able to predict, even qualitatively, these results.

Figure 3.5 shows the transient Trouton ratios for all the materials in uniaxial extension (except PA6 that was not possible to test due to its low viscosity), the main features being:

a) All the materials show a pronounced strain-hardening, due to the existence of a rubber phase. In the non-compatibilised blend, the degree of strain-hardening is much smaller than in the remainder, which is a further indication of poor adhesion between the two phases.

b) The onset of strain-hardening is much lower (of the order $\varepsilon_H = 0.1$) for the non-compatibilised and the insufficiently compatibilised blends (EPM-g-MA content equal or lower than 10%) than for those with higher MA contents (of the order $\varepsilon_H = 1$). Again, this is presumably due to the better adhesion between the phases, *i.e.*, the presence of the rubber stabilizes the blend and increases the range of linear viscoelastic response (note that the onset of strain-hardening for the EPM and EPM-g-MA are very similar to those of the 15 and 20 % EPM-g-MA blends).

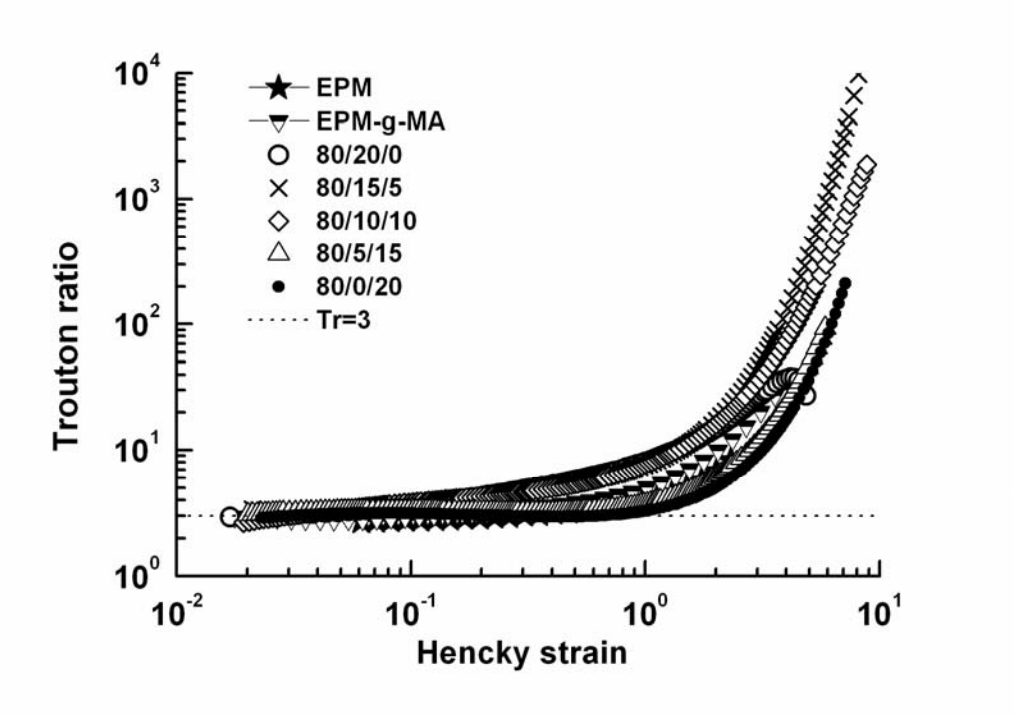

Figure 3.5 - Trouton ratios for all blends. Strain rates, $\dot{\varepsilon}$: 80/20/0, 0.10 s^{-1};80/15/5, 0.11 s^{-1}; 80/10/10, 0.16 s^{-1}; 80/5/15, 0.14 s^{-1}; 80/0/20, 0.13 s^{-1}; EPM, 0.10 s^{-1}; EPM-g-MA, 0.11 s^{-1}.

3.2.2. Stress relaxation after cessation of flow

Shear stress relaxation measurements (Figure 3.6) illustrated that all blends relax in two consecutive steps. The first (faster) step should be related with the relaxation of the PA-6 matrix and second (slower) step is probably due to relaxation of EPM and/or interfaces. In this case, particle size and interfacial adhesion play a determinant role in the shear stress relaxation function. For the compatibilized blends, the second relaxation time increases in duration with increasing amount of compatibilizer up to a EPM-g-MA content of 15%, which indicates that the effect is related with a better adhesion at the interfaces and saturates at 15% EPM-g-MA concentration. An interesting feature in Figure 3.6 is that the second relaxation time of the 80/15/5 blend is slightly shorter than the one of the non-compatibilized blend, which indicates that low compatibilizer amounts are enough to decrease significantly of the average size droplets but not to prevent the slip between the phases.

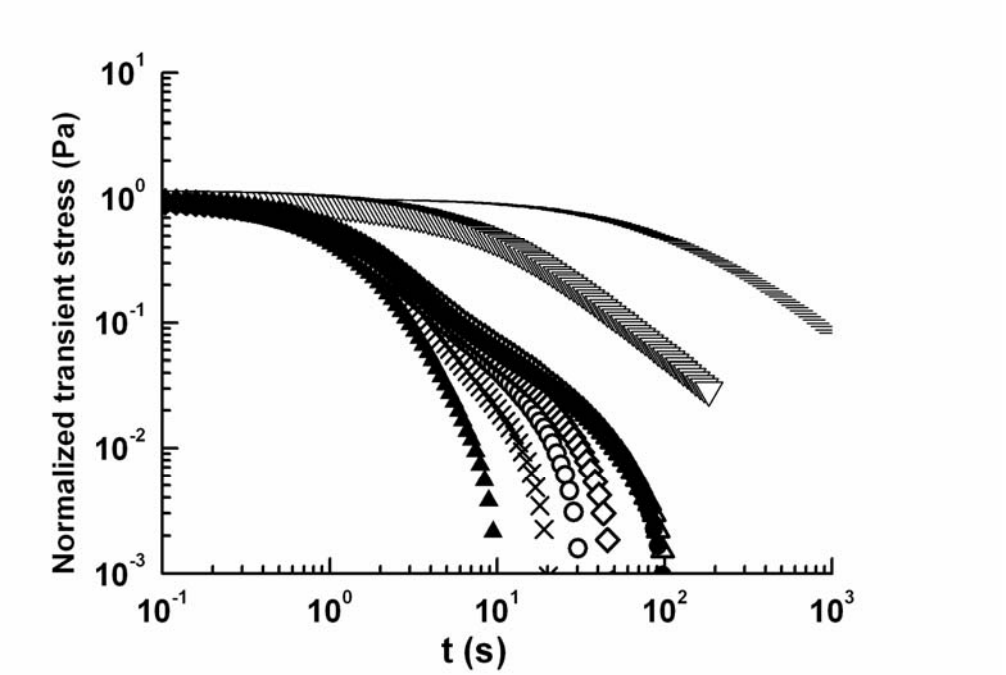

Figure 3.6 - Normalized transient stress for several blends of PA6/EPM/EPM-g-MA and their components after cessation of a shear flow of 0.1 s^{-1}. *Filled triangle* PA-6, *bar* EPM, *inverted open triangle* EPMg-MA, open circle 80/20/0, *cross* 80/15/5, *diamond* 80/10/10, *open triangle* 80/5/15, *filled circle* 80/0/20.

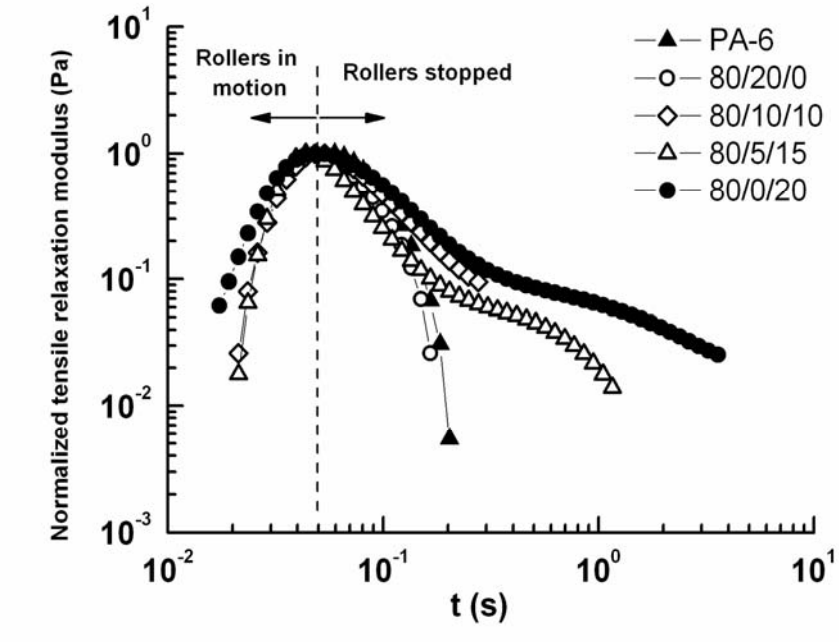

Figure 3.7 - Normalized relaxation modulus flow for the blends and their components. Strain rates are PA-6, 15.6 s^{-1}; 80/20/0, 0.98 s^{-1}; 80/10/10, 0.98 s^{-1}; 80/5/15, 0.24 s^{-1}; 80/0/20, 0.54 s^{-1}.

As in the shear relaxation experiments, in the extensional relaxation (after a step strain) experiments the compatibilized blends exhibits higher relaxation times (Figure 3.7). Once more, the fast relaxation time can be attributed to the PA-6 matrix and the slow one to the interface and/or rubber dispersed phase. This suggests that the presence of slip at the interface inhibits the deformation of dispersed phase droplets and that this effect is overcome with the addition of EPM-g-MA. However this needs to be confirmed by a morphological analysis of stretched samples on a SEM.

Representative results of the morphological analysis are depicted in Figure 3.8 and Figure 3.9 for the non-compatibilized and the highest compatibilizer content blends, respectively. Figure 3.8 shows the morphologies of the non-compatibilized blend, a) before extension and b) quenched during extension and the similarities are immediately apparent: in both cases droplets are essential spherical. Thus, there was no (or only negligible) deformation of the rubber phase upon extension, due to interfacial slip. In the compatibilized blend the average droplet size is much smaller, as would be expected, and the morphologies before (Figure 3.9a) and after (Figure 3.9b) extension are quite different. In the former case the expected spherical droplet morphology is seen and in the latter the droplets are very elongated, but still quite large. This is an indication that the compatibilizer was present in an enough content to make the drag force on the droplets overcome the resistance to flow/deformation of the rubber phase (note that the viscosity ratio is very high in these materials).

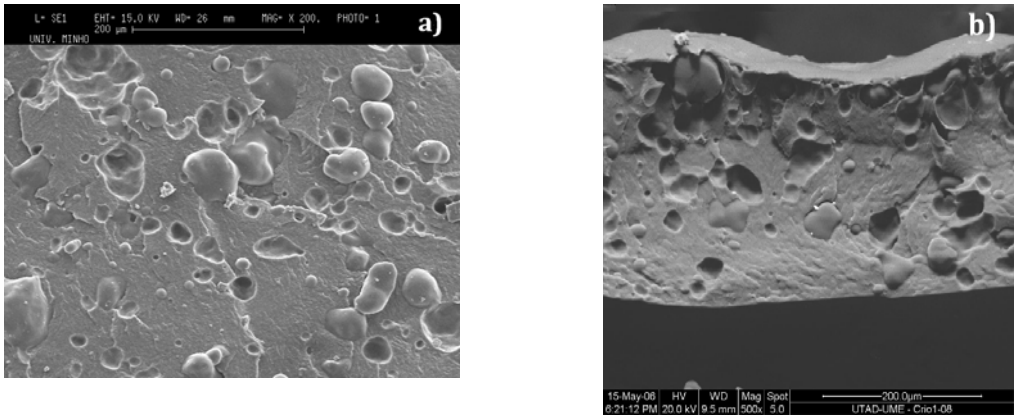

Figure 3.8 - SEM micrographs of the fracture surfaces of the 80/20/0 blend: **a** non-deformed sample and **b** after extension (the sample was stretched during 5 s at a strain rate of 0.08 s^{-1}).

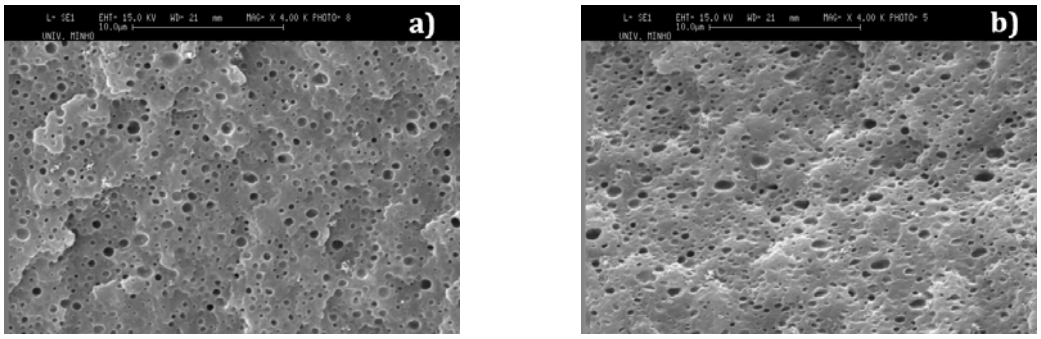

Figure 3.9 - SEM micrographs of the fracture surfaces of the 80/0/20 blend: **a** non-deformed sample and **b** after extension (the sample was stretched during 5 s at a strain rate of 0.08 s^{-1}).

3.3 SUMMARY

In the present chapter, the rheological proprieties of immiscible and compatibilized blends with high viscosity and elasticity ratios were studied. The reactive compatibilization, which was achieved by addiction of a modified EPM, led to a finer morphology. In rheological terms, it was found that the rubber droplets do not exhibit a rigid sphere-like behaviour. In fact, oscillatory shear, uniaxial extension and stress relaxation experiments (in both shear and extension) showed the existence of one relaxation time for the immiscible blend and two for the compatibilized ones that, in all cases, is more pronounced for higher compatibilizer contents. Together with SEM evidence of the existence of elongated droplets after extension for the compatibilized blends and spherical ones in the non-compatibilized ones, these results indicate that, despite the high viscosity and elasticity ratios, if high enough amounts of compatibilizer are added to the blend, interfacial slip is suppressed and a high enough adhesion between the phases is achieved for the high-viscosity dispersed phase to be deformed.

These results seem to indicate that the second relaxation is due to relaxation of the EPM droplets. But a main question arises. Is this small deformation of the droplets observed in compatibilized blends enough to justify the big increase of the second relaxation time? Or is there some more phenomenon occurring, namely at the interface, that justifies such observations? The

answer to these questions lies in the indirect visualization of the deformation of the droplets during the flow. This will be done in the next chapter.

References

Machado, A. V., J. A. Covas and M. Van Duin, "Chemical and morphological evolution of PA-6/Epm/Epm-g-MA blends in a twin screw extruder", J. Polym. Sci. Pol. Chem. 37, 1311-1320 (1999).

Oosterlinck, F., M. Mours, H. M. Laun and P. Moldenaers, "Morphology development of a polystyrene/polymethylmethacrylate blend during start-up of uniaxial elongational flow", J. Rheol. 49, 897-918 (2005).

Riemann, R. E., H. J. Cantow and C. Friedrich, "Interpretation of a new interface-governed relaxation process in compatibilized polymer blends", Macromolecules 30, 5476-5484 (1997).

Utracki, L. A., "Melt Flow of Polymer Blends", Polym. Eng. Sci. 23, 602-609 (1983).

Van Hemelrijck, E., P. Van Puyvelde, S. Velankar, C. W. Macosko and P. Moldenaers, "Interfacial elasticity and coalescence suppression in compatibilized polymer blends", J. Rheol. 48, 143-158 (2004).

Van Puyvelde, P., Z. Oommen, P. Koets, G. Groeninckx and P. Moldenaers, "Effect of reactive compatibilization on the interfacial slip in nylon-6/EPR blends", Polym. Eng. Sci. 43, 71-77 (2003).

CHAPTER 4

Model high viscosity ratio and high interfacial elasticity blends: PMMA/PS/PSOX

From the last chapter some questions remain open about the role of the compatibilizer at the interface on the relaxation mechanism in compatibilized polymer blend. One interesting way to access to some information about the microstructure during the flow is to use rheo-optic techniques like Small Angle Light Scattering (SALS). However, PA6/EPM/EPM-g-MA blends are not optically transparent, thus this technique could not be used. So, the study of the previous chapter will be complemented with the investigation of another system, this time optically transparent: PMMA/PS/PSOX blends. Here the effect of the introduction of a functional group (oxazoline) in the PS chain, PSOX, on the rheological properties of the interface will be investigated. These polymers are relatively inelastic, which allows the effect of the elasticity of the interface to be maximized, but still show relatively high viscosity ratios (between 2 and 4 at the relevant shear and extension rates) so that the dispersed phase deformation is relatively small.

This chapter was adapted from *Silva, J., A. V. Machado, P. Moldenaers, J. Maia, "The effect of interfacial properties on the deformation and relaxation behavior of PMMA/PS blends" (2009)* Submitted to *Journal of Rheology.* [Appendix C]

4.1 EXPERIMENTAL

4.1.1. Materials

The blend components are commercial grades of polymethylmethacrylate (PMMA, Altuglas VSE UVT, MFI 27g/10min at 230°C with 3.8Kg) and polystyrene (PS, Solarene G116, MFI 2.3g/10min at 200°C with 5Kg). The oxazoline functionalized polystyrene (PSOX, Epocros RPS-

1005, 6-10 g/10 min at 200°C with 5Kg) (Figure 4.1) was provided by Nippon Shokubai. In the PSOX the weight of oxazoline groups corresponds to 1.9% of the total weight.

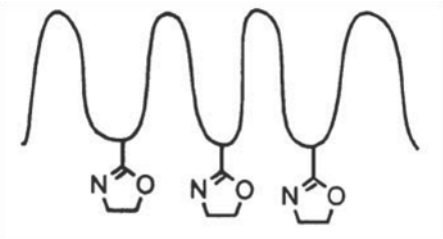

Figure 4.1 - Schematic diagram of a PS chain functionalized with oxazoline.

4.1.2. Compounding

A series of blends of PMMA/PS/PSOX were prepared in this work. The concentration of the PMMA matrix was keep constant (80 w/w%) while that of PS and PSOX were varied from a maximum of PS and no PSOX (80/20/0 PMMA/PS/PSOX) to the opposite situation, i.e., 20 w/w% of PSOX and no PS (80/0/20 PMMA/PS/PSOX). Moreover, two diluted blends (99/1/0 PMMA/PS/PSOX and 99/0/1 PMMA/PS/PSOX) were also prepared. A Haake batch mixer at a set temperature of 210 °C and a rotor speed of 80 rpm was used to compound the blends. The sample was removed from the mixer after a mixing time of 600 s.

4.1.3. Morphology

The morphology of all the blends was analyzed by SEM (Scanning Electron Microscopy). The samples were fractured in liquid nitrogen and then the PS/PSOX phase was removed in cyclohexane at 50°C during 1h. The morphology of the blends was studied, after gold plating the samples, using a Jeol JSM 6310F Scanning Electron Microscope.

4.1.4. Rheometry

The rheological measurements were performed with an ARES rheometer (TA Instruments). Samples were vacuum dried at 80°C during 12 h before each rheological experiment. Since

degradation may occur during blend preparation, in order to have comparable results for the pure components and the blends, the former was also subjected to the same processing conditions in the batch mixer.

Oscillatory tests were performed for the pure components and blends at 230°C, using a parallel-plate geometry with a $1000 \pm 1\ \mu m$ gap. For the samples with lowest moduli 50 mm plates were used in order to increase the signal, whilst for the remainder 25 mm diameter plates were used. Stress relaxation experiments after shear were performed at 230 °C using the same geometry; a shear rate of 0.1 s^{-1} during a time interval of 250 s, which is enough to reach the steady state, was applied and the evolution of the shear stress upon cessation of flow was measured.

The stress relaxation experiments in shear were performed at 230 °C again using a parallel-plate geometry (diameter=25 mm) with a $1000 \pm 1\ \mu m$ gap; a shear rate of $0.1 s^{-1}$ during 250s was applied and the evolution of the shear stress upon cessation of flow was measured.

The extensional rheological measurements were performed on the MRR (Modified Rotational Rheometer) at 205°C (the highest temperature at which the sample yielded a strong enough signal to be measured). For both extensional start-up and relaxation extensional experiments samples with rectangular cross-section (about 3×2 mm) were prepared. For details about the experimental technique see Subsection 2.2.1.

4.1.5. Small Angle Light Scattering (SALS)

Small angle light scattering measurements (SALS) were performed to study the deformation of the droplets and the interface. In SALS, light emerging from a He-Ne laser ($\lambda = 633$ nm) is sent through the sample that is contained within a Linkam shear cell (CSS 450). The anisotropy of the SALS patterns can be quantified calculating a second moment tensor from the measured light intensity on the 2D CCD array. Then, the anisotropy, ε, is given by the difference between the eigenvalues of this tensor [Borschig *et al.* (2000)]:

$$\varepsilon(\dot{\gamma},t) = \frac{\left[\left(\int d\vec{q}q_x q_x I(q,\dot{\gamma},t) - \int d\vec{q}q_y q_y I(q,\dot{\gamma},t)\right)^2 + 4\int d\vec{q}q_x q_y I(q,\dot{\gamma},t)^2\right]^{0.5}}{\int d\vec{q}I(q,\dot{\gamma},t)} \quad (4.1)$$

This calculation was done using SalsSoftware developed in K. U. Leuven. To avoid multiple scattering only dilute blends (99/1/0 and 90/0/1) were used in the SALS experiments. The experiments were performed at 230°C.

4.2 RESULTS AND DISCUSSION

4.2.1. Viscosity ratios of the pure components

Figure 4.2a shows the steady state and the complex viscosities of the pure components as functions of shear rate and frequency, respectively. These materials are thermorheologically simple and thus the Cox-Mertz rule is valid. Figure 4.2b shows the viscosity ratios between the two polystyrenes (with and without oxazoline) and the PMMA matrix at 230 °C. At low frequencies the viscosity ratios between PS and PMMA and PSOX and PMMA are 3.8 and 1.6, respectively. They decrease as the frequency increases reaching values approaching unity at high frequencies. This behaviour means that the stress relaxation experiments (which were performed after the imposition of a shear rate of 0.1 s^{-1}) were performed in blends of relatively high viscosity ratios.

4.2.2. Blend morphology

The morphology of the blends after the mixing process was analyzed by SEM. The blends with 20% dispersed phase show similar morphologies. They exhibit droplet-matrix morphology with similar droplet sizes, R_n varying between 0.3 and 0.4 μm and R_v/R_n between 1.6 and 1.8. The dilute blends (with 1% of dispersed phase), also show droplet-matrix morphology but with smaller droplet sizes (R_n=0.09 μm for both 99/1/0 and 99/0/1 and R_v/R_n=1.1 and 1.2 for 99/1/0 and 99/0/1, respectively).

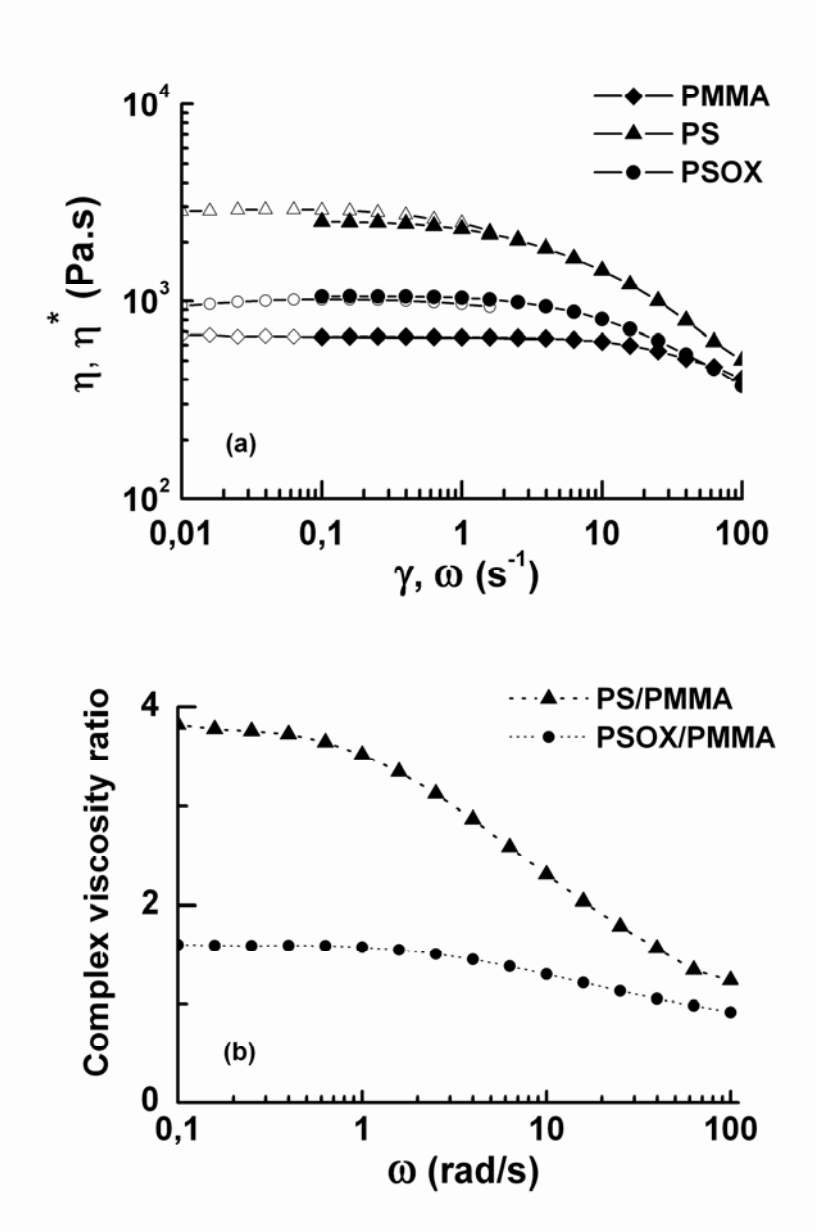

Figure 4.2 - (a) Viscosities of the pure components at 230°C. The open symbols are the steady shear viscosity; the full symbols are the complex viscosity. (b) Viscosity ratios at 230°C.

Since the process conditions were the same for all blends, the differences in the morphology of the diluted and concentrated blends is due to the fact that in the former are less prone to coalescence than the latter (in the uncompatibilized blends) because the probability of collision of two droplet is lower and because the dynamic equilibrium is established at lower droplet sizes [Grizzuti and Bifulco (1997), Vinckier *et al.* (1998)].

4.2.3. Linear Viscoelastic Behaviour

The dynamic storage and loss moduli of the three pure components and the concentrated blends, at 230°C, are shown in the Figures 4.3 a) and b) respectively. The PMMA/PS blend shows a shoulder in G', which is a typical behaviour for an immiscible polymer blend. Moreover, their dynamic moduli can be fitted to the Palierne model. In the blends containing modified polystyrene it was observed that the increase of PSOX concentration causes an increase of the dynamic moduli at low frequencies. In G' this increase is very large when the PSOX concentration goes from 7.5 to 10% wt and higher, thus indicating that there may exist a critical concentration of PSOX above which there are no significant changes in rheological behaviour as a function of %PSOX added. Moreover, the observed plateau (also previously observed by other authors in compatibilized blends, e.g., Yee et al. (2007), Sailer and Handge (2007) and Fahrlander et al. (2001)), suggests that the extra interactions at the interface play a crucial role in the rheological behaviour, inclusively being more important than the average size and size distribution of the dispersed phase. Thus, it seems that the amount of oxazoline has an important role in the elasticity of the interfaces.

This behaviour cannot be explained by the relaxation of droplets of the dispersed phase only. For example, if one tries to fit any form of the Palierne model to the data of the blends with higher concentrations of PSOX, the obtained values of the interfacial tension are totally unrealistic.

The elongational measurements, the results of which are depicted in Figure 4.4 for the samples with highest concentrations of PS and PSOX, show that while the 80/20/0 blend follows linear viscoelastic behaviour, the 80/0/20 blend exhibits strong strain hardening, which is in broad agreement with the results in oscillatory shear. Again the interfacial contribution in 80/0/20 blend clearly seems to be much higher than in case of 80/20/0 blend.

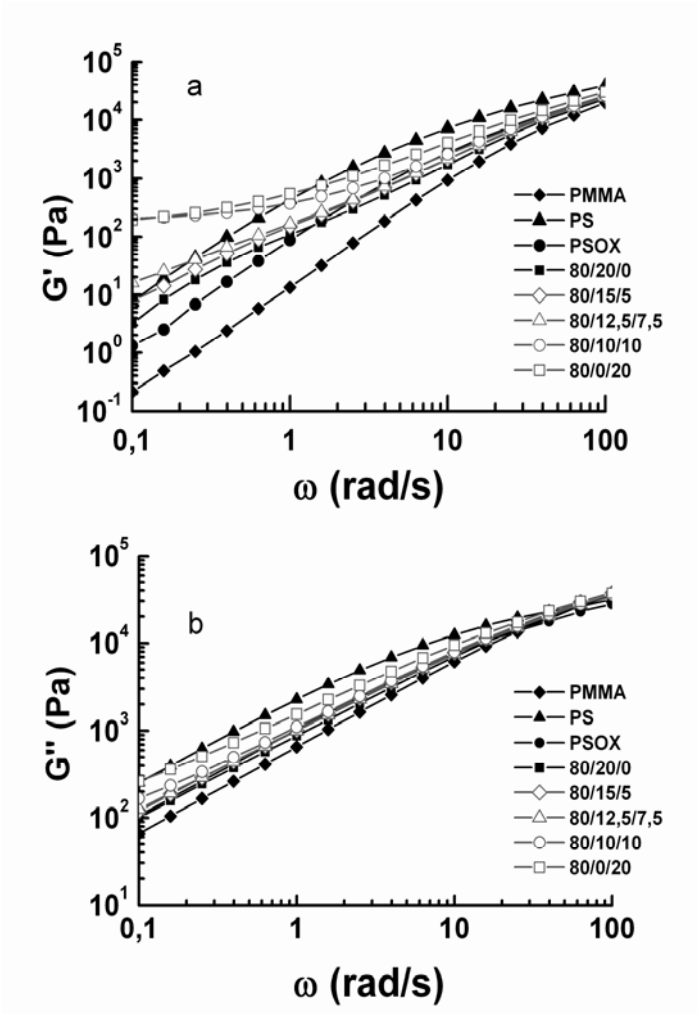

Figure 4.3 - Rheological shear behaviour of several concentrated blends of PMMA/PS/PSOX and their components. (a) Storage and (b) loss moduli.

These results indicate that some chemical reaction or additional physical interaction occur in blends containing PSOX. In order to study the possibility of the existence of new chemical species or interactions in PMMA/PSOX blends, a FTIR analysis was performed.

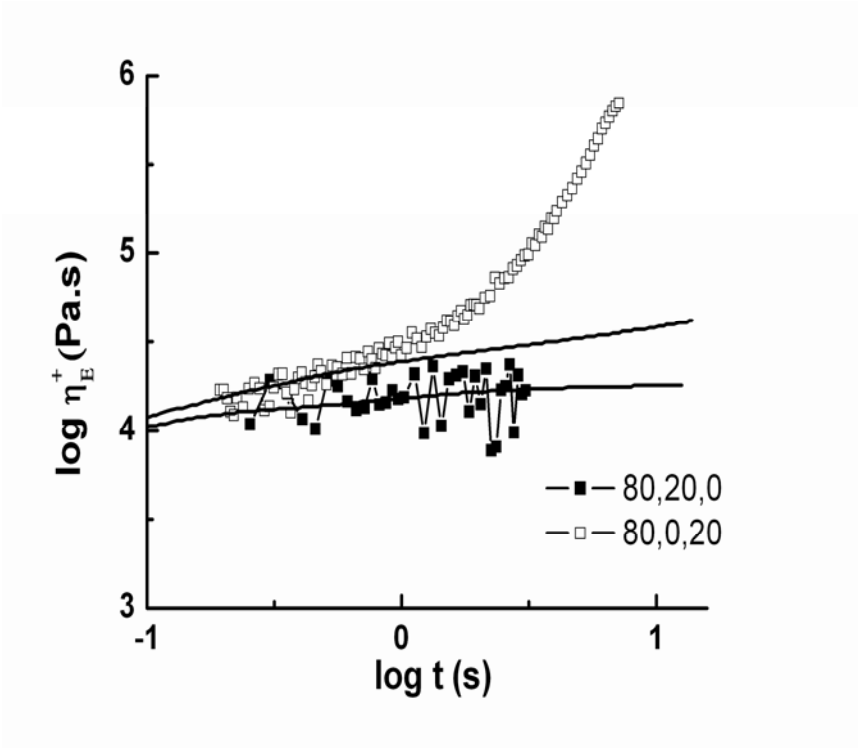

Figure 4.4 - Transient uniaxial extensional viscosity at 205°C for 80/20/0 and 80/0/20 blends (strain rates of 0,46 s^{-1} and 0,24 s^{-1} respectively) and corresponding curves (solid lines) for the linear viscoelastic regime.

4.2.4. FTIR

It is known that oxazaline groups react with carboxylic acids, acid anhydrides and phenolic hydroxyls. However, no chemical reaction is known to occur between oxazoline and methacrylate groups. To verify whether the introduction of PSOX leads to formation of new chemical species and to investigate the occurrence of new additional physical interactions between oxazoline and PMMA FTIR was used.

After compression of a small sample of each blend (80/20/0 and 80/0/20), FTIR spectra were recorded in transmittance mode (Figure 4.5). These are very similar, indicating that no reaction took place when oxazoline groups were present. Thus, from FTIR it is possible to state that during blending there was no formation of new chemical species at the interface, or the amount that could be formed was so low that can not be detected by this technique. Likewise, the spectra can not allow conclude the existence of additional physical interactions.

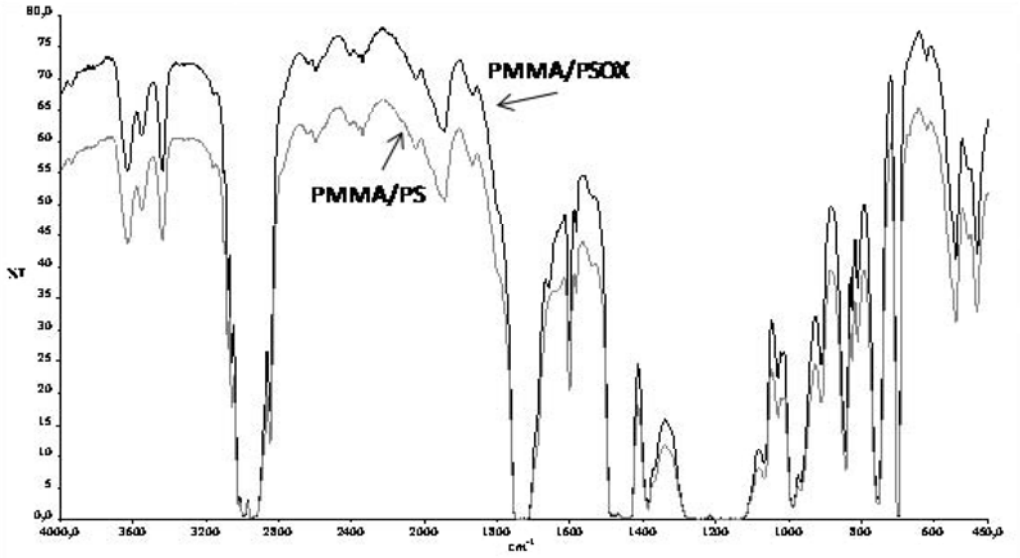

Figure 4.5 - FTIR spectra of PMMA/PS and PMMA/PSOX blends.

However, it is known that specific interactions between polymer chains result in a change of the mixing enthalpy, resulting in a decrease of the interfacial tension and increase in the interphase thickness [Koning *et al.* (1998)]. Thus, the occurrence of hydrogen bonds and Van der Waals interactions between PMMA and PSOX, for example, may play a compatibilizing role in the mixtures through the enhancement of the interactions at the interface.

4.2.5. Relaxation after cessation of flow

At this point is not clear whether the plateau at low frequencies in G' and strain hardening behaviour in extension observed for 80/0/20 blend is due to a larger deformation of the droplets and/or to existence of strong physical interactions at the interface of the 80/0/20 blend that are not present in the 80/20/0 blend. One way to determine for sure whether these results are really due to interfacial effects is to perform stress relaxation experiments after flow and compare the relaxation kinetics of the PMMA/PS blend and the blends containing PSOX.

The aim is to test the elasticity of the interfaces while deforming the disperse phase droplets as little as possible. Hence, stress relaxation experiments after a step uniaxial extension and shear were performed. The results for the former (see Figure 4.6) show that the 80/20/0 blend follows

essentially the relaxation of matrix, as expected, while the blend with PSOX shows a second relaxation process. At long times the relaxation modulus of the 80/0/20 blend becomes higher than the relaxation modulus of the PSOX dispersed phase. Thus, this clearly shows that there is strong stress build-up at the interface in these systems that may even surpass that inside the droplets. This effect was attributed in Chapter 3 to the long term relaxation of the highly elastic disperse phase, but clearly the present results indicate that the interface may play at least a similar role. Mechbal and Bousmina (2007) investigating compatibilized blends also observed that much slower stress relaxation is obtained at higher copolymer compatibilizer concentrations, i.e., above a critical concentration of saturation of the interface. This effect was attributed to entanglements in the interfaces.

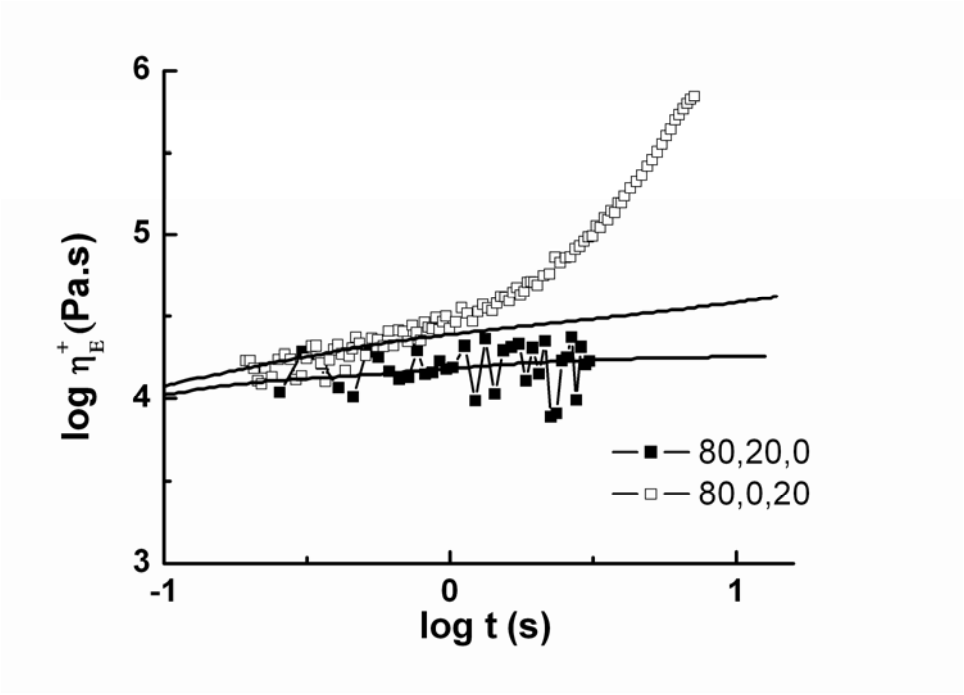

Figure 4.6 - Normalized transient extensional stress for concentrated blends of PMMA/PS/PSOX and their components after cessation of a step extension, at 205°C. The time is normalized by that corresponding to maximum stress and the stress is normalized by its maximum. In legend are the Hencky strains applied to each sample.

The results for the relaxation behaviour after steady shear, for a number of blends with varying PS and PSOX ratios, [Figure 4.7 a)] indicate that, at long times, all blends relax slower than the

pure components which is a consequence of the relaxation of the dispersed phase and/or interfaces. The blend without PSOX (80/20/0) shows a well-defined two-step relaxation process: a first fast relaxation due to the molecular relaxation of the PMMA matrix followed by a second one slower related with the shape relaxation of the PS droplets. With the introduction of the PSOX the relaxation in two-steps becomes less evident. In fact the shape of the curves and the increase of the relaxation times indicate that there are additional relaxation mechanisms (interfacial relaxation) which are characteristic of compatibilized blends (an additional relaxation time was predicted indirectly by Van Hemelrijck *et al.* (2004), Van Puyvelde *et al.* (2001) from the calculation of the relaxation spectra of compatibilized blends).

Figure 4.7 b) shows the time necessary for the reduced relaxation modulus to decrease to 2% of the original value (dubbed, for simplicity, "relaxation" time) vs. the concentration of PSOX. It is clear that the increase of the "relaxation" time with increase of concentration of PSOX is not linear. At very low PSOX concentrations the relaxation decreases slightly relatively to that of the immiscible blend but then increases rapidly between 5 w/w% and 10 w/w%, at which point it becomes independent of the concentration of PSOX in the dispersed phase. Like the results in storage modulus, these also reveal the existence of a critical concentration for PSOX (the existence of a critical concentration for compatibilizer was reported by Mechbal and Bousmina (2007)). Moreover, the blends above the critical concentration exhibit a very slow relaxation process lasting of the order of several minutes. Again, these results are consistent with the plateau in G' observed in the linear viscoelastic measurements. Even neither new chemical bonds (see FTIR results above) nor significant morphological changes were found, these results indicate that PSOX is indeed acting as a compatibilizer, albeit a physical one.

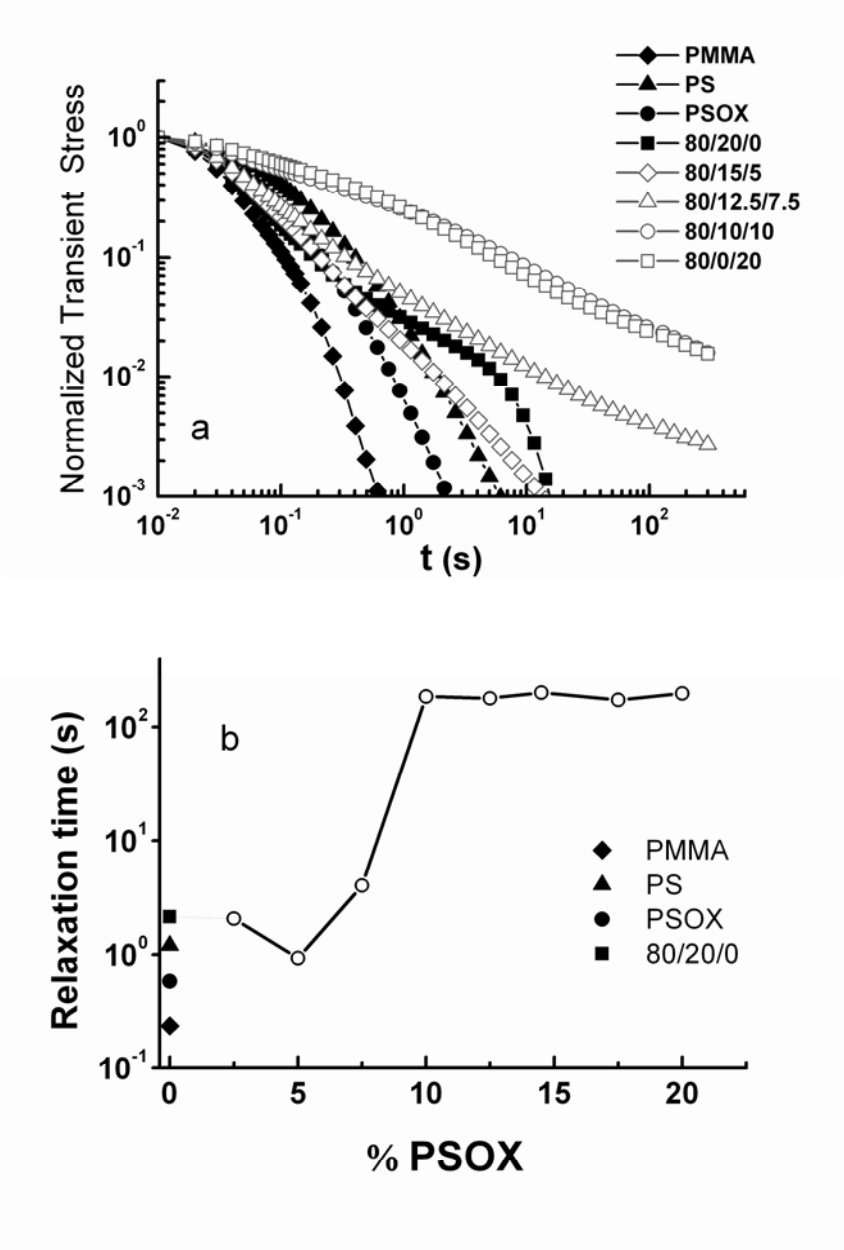

Figure 4.7 - (a) Normalized transient stress for concentrated blends of PMMA/PS/PSOX and their components after cessation of a steady shear flow of 0.1 s^{-1} for 250s, at 230°C. (b) Time taken to blends and their components to relax stress for 2% of the initial value.

Another interesting feature is the fact of the amount of oxazoline group has an important role. The mechanism that causes the very slow relaxation process in the blends with most oxazoline groups is not clear yet. The reduction of the interfacial tension resulting from specific interactions between the oxazoline groups and PMMA could explain the results. In order to clear this, Small Angle Light Scattering, SALS, experiments were performed.

4.2.6. SALS

As mentioned before, in order to avoid the problems associated with multiple scattering, dilute samples (1 wt% of PS or PSOX in PMMA) were prepared for SALS investigations. In these experiments samples being sheared at 2.5 s^{-1} were, after 800 seconds, submitted to a shear rate step to 70 s^{-1}, at which they are maintained for 250 s. After this time, the shear is suddenly removed and the sample is allowed to relax in time.

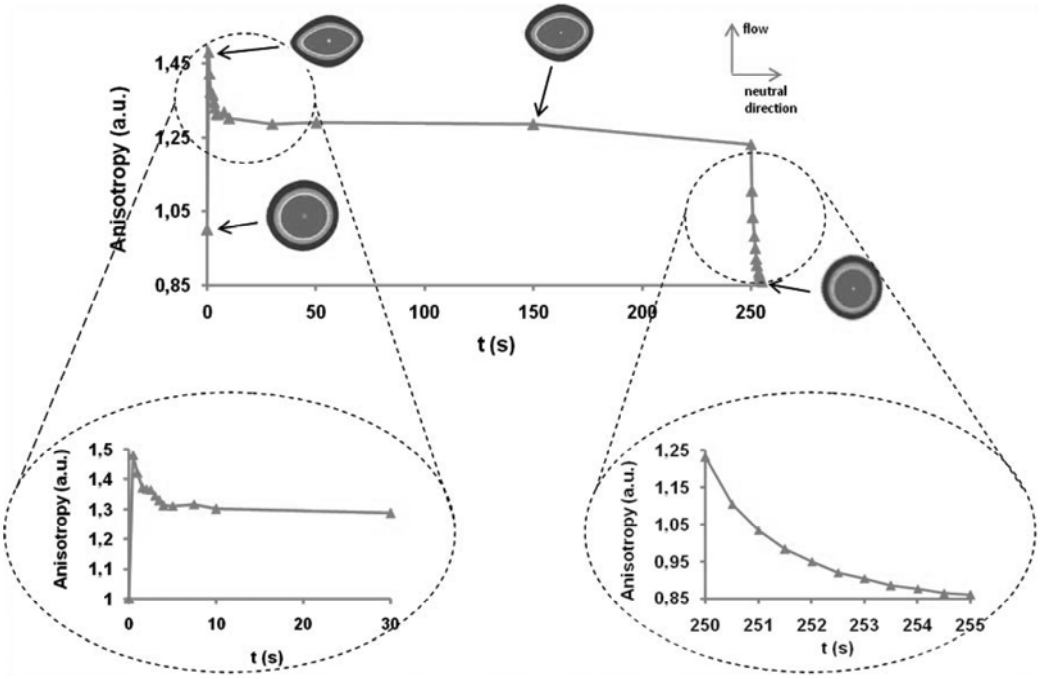

Figure 4.8 - Anisotropy as a function of time for the 99/1/0 blend. A step-up in shear from 2.5 s^{-1} to 70 s^{-1} is performed and the flow is stopped 250 s later. Representative SALS patterns are shown for each stage.

Figure 4.8 shows the results for the 99/1/0 blend and, as expected, the SALS pattern deforms very in the neutral direction, thus indicating that the dispersed phase is being deformed in the flow direction. Moreover, the anisotropy shows an overshoot characteristic of orientation and/or break-up of the droplets. When the flow is stopped the SALS pattern takes about 5 seconds to recover the isotropic shape, *i.e.*, for the stresses to relax completely, which is within the same timescale observed in stress relaxation experiments in shear (Figure 4.7).

Figure 4.9 depicts the results for the 99/0/1 blend and it too shows the existence of an overshoot in the anisotropy, but much smaller than for the 99/1/0 blend. Initially the droplets deforms in the flow direction as was observed for PMMA/PS blend. However, at long times the anisotropy pattern appears slightly deformed in flow direction, a trait that is present even upon the cessation of flow, which is an indication that dispersed phase is slightly deformed in the vorticity direction. Deformation of the dispersed phase in the vorticity direction at relatively high shear rates has been reported by several authors [Hobbie and Migler (1999), Lin *et al.* (2005), Mighri and Huneault (2006), Migler (2000)] in blends whose droplets are more elastic than the matrix. Although this phenomenon depends critically on the difference in the elasticity of the components, this alone cannot explain the observed behaviour because the elasticity ratio between the PSOX and PMMA is relatively low and is even lower than that between PS and PMMA. Thus, the results of Figure 4.9 (deformation on the vorticity direction) can hence be attributed to an increase of elasticity in the interfaces caused by introduction of oxazoline groups (which was already demonstrated in Figure 4.3 a). Even after the cessation of flow, the dispersed phase remains slightly elongated in the vorticity direction during a long time.

These results indicate that the very slow relaxation observed in blend with more oxazoline groups is due to stronger interactions that increase the elasticity of interface. These interactions seem to resist to deformation causing a slower relaxation when flow is stopped.

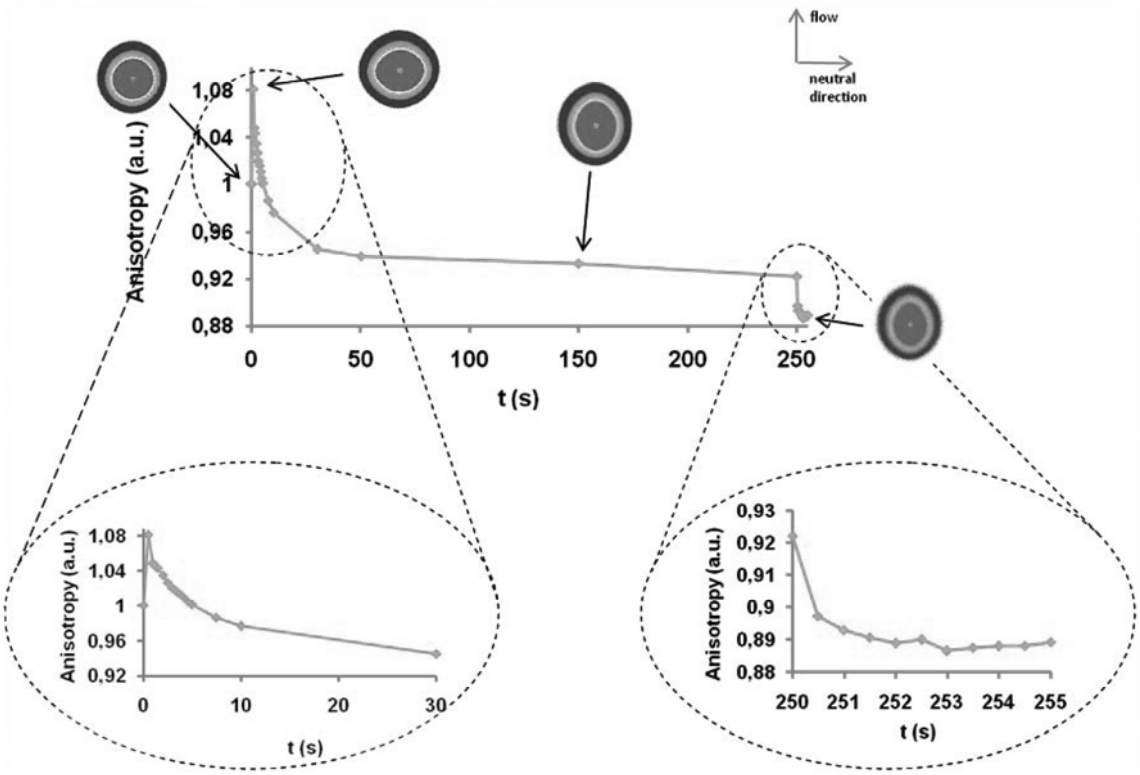

Figure 4.9 - Anisotropy as a function of time for the 99/0/1 blend. A step-up in shear from 2.5s^{-1} to 70s^{-1} is performed and the flow is stopped 250s later. Representative SALS patterns are shown for each stage

4.3 SUMMARY

In this chapter, the role of the interface in the rheological behaviour of a model polymer blends was investigated. Although no chemical bonds between PMMA and PSOX could be detected the rheological results show that in blends containing PS modified with oxazoline the interfaces have a different behaviour. In particular it was observed that the introduction of oxazoline leads to an increase of the relaxation times of the blends. Moreover, above a critical concentration of PSOX the rheological behaviour of the blends almost does not change which is an indication that at this concentration the interface becomes saturated with oxazoline groups. The SALS experiments allowed one to conclude that the addition of PSOX increases the interfacial elasticity leading to droplet deformations in the vorticity direction at high enough shear rates. This increase of interfacial elasticity is due to additional entanglements and interactions that result from introduction of oxazoline groups. Moreover, the results show that these additional entanglements slow down the relaxation of the dispersed phase.

In the previous Chapter it was not clear whether the increase of second relaxation time was mainly due to small deformation of the compatibilized droplets (not observed in the non-compatibilized case because of slip effects) or if there was some more relaxation phenomena at the interface. In this Chapter it became clear that the additional relaxation time has its origin in an increase of elasticity of the interface, which results from additional entanglements and interactions and not in the deformation of the droplets.

In the next Chapter, blends without elastic interfaces will be studied in order to assess if these effects are still present in those cases.

References

Borschig, C., B. Fries, W. Gronski, C. Weis and C. Friedrich, "Shear-induced coalescence in polymer blends - simulations and rheo small angle light scattering", Polymer 41, 3029-3035 (2000).

Fahrlander, M., M. Bruch, T. Menke and C. Friedrich, "Rheological behavior of PS-melts containing surface modified PMMA-particles", Rheol. Acta 40, 1-9 (2001).

Grizzuti, N. and O. Bifulco, "Effects of coalescence and breakup on the steady state morphology of an immiscible polymer blend in shear flow", Rheol. Acta 36, 406-415 (1997).

Hobbie, E. K. and K. B. Migler, "Vorticity elongation in polymeric emulsions", Physical Review Letters 82, 5393-5396 (1999).

Koning, C., M. Van Duin, C. Pagnoulle and R. Jerome, "Strategies for compatibilization of polymer blends", Progress in Polymer Science 23, 707-757 (1998).

Lin, B., F. Mighri, M. A. Huneault and U. Sundararaj, "Effect of premade compatibilizer and reactive polymers on polystyrene drop deformation and breakup in simple shear", Macromolecules 38, 5609-5616 (2005).

Mechbal, N. and M. Bousmina, "Effect of copolymer addition on drop deformation during uniaxial elongation and during relaxation after cessation of flow", Macromolecules 40, 967-975 (2007).

Mighri, F. and M. A. Huneault, "In situ visualization of drop deformation, erosion, and breakup in high viscosity ratio polymeric systems under high shearing stress conditions", J. Appl. Polym. Sci. 100, 2582-2591 (2006).

Migler, K. B., "Droplet vorticity alignment in model polymer blends", J. Rheol. 44, 277-290 (2000).

Sailer, C. and U. A. Handge, "Melt viscosity, elasticity, and morphology of reactively compatibilized polyamide 6/styrene-acrylonitrile blends in shear and elongation", Macromolecules 40, 2019-2028 (2007).

Van Hemelrijck, E., P. Van Puyvelde, S. Velankar, C. W. Macosko and P. Moldenaers, "Interfacial elasticity and coalescence suppression in compatibilized polymer blends", J. Rheol. 48, 143-158 (2004).

Van Puyvelde, P., S. Velankar and P. Moldenaers, "Rheology and morphology of compatibilized polymer blends", Curr. Opin. Coll. Int. Sci. 6, 457-463 (2001).

Vinckier, I., P. Moldenaers, A. M. Terracciano and N. Grizzuti, "Droplet size evolution during coalescence in semiconcentrated model blends", AIChE J. 44, 951-958 (1998).

Yee, M., P. S. Calvao and N. R. Demarquette, "Rheological behavior of poly(methyl methacrylate)/polystyrene (PMMA/PS) blends with the addition of PMMA-ran-PS", Rheol. Acta 46, 653-664 (2007).

CHAPTER 5

Low interfacial elasticity blends: PP/EVOH/ Na^+

It was seen in previous Chapters that the compatibilization of an immiscible polymer blend can lead to the appearance of a long second relaxation time. This relaxation was attributed to additional entanglements and interactions that, due to the compatibilization, take place in the interface. In this Chapter that hypothesis will be tested in blends that are compatibilized in other ways and do not have interfaces as elastic as those in the previous Chapters.

This chapter was adapted from *Ares, A., J. Silva, J. Maia, L. Barral and M. Abad, "Rheomechanical and morphological study of compatibilized PP/EVOH blends." (2009)* Submitted to *Rheologica Acta*. [Appendix D].

5.1 EXPERIMENTAL

5.1.1. Materials

All the materials employed in the study in this chapter are commercial products. The polymers were chosen in order to have an appropriate melt flow index (MFI) for extrusion purposes. Specifically, a bi-oriented film extrusion-grade polypropylene (PP) (Isplen PP044W3F) from REPSOL-YPF was used; this PP has an MFI of 3.02 g/10 min (230°C, 2160 g) and a density of $0.90\ g/cm^3$. The ethylene-vinyl alcohol copolymer (EVOH, grade F101B) was supplied for EVAL Europe (Kuraray Company Ltd, Kuroashiki, Japan); it has an ethylene concentration of 32.9%, MFI of 6.33 g/10 min (230°C, 2160 g), and a density of $1.19\ g/cm^3$. The Na^+ ionomer (Surlyn resin 8528, from Du Pont, Wilmington, DE, USA) is a random ethylene/methacrylic acid copolymer partially neutralized with sodium, with a MFI of 1.10 g/10 min (190°C, 5000 g) and a density of $0.93\ g/cm^3$.

5.1.2. Compounding

Before processing, the EVOH and the Na^+ ionomer were dried in a vacuum oven for 24 h at 80°C and for 8 h at 60°C, respectively. PP/EVOH and PP/EVOH/ionomer blends were prepared in a co-rotating twin-screw extruder (DSE-20; C.W. Brabender Instruments, South Hackensack, NJ, USA) operating at 45 rpm, with a barrel temperature 215°C and a die temperature of 220°C. All the components were premixed by tumbling and were fed simultaneously into the extruder. Binary blends were prepared with 90/10, 80/20, 70/30 and 60/40 (w/w) PP/EVOH, while the ternary blends were prepared by addition of 2-20% ionomer weight in relation to EVOH weight.

5.1.3. Rheometry

All the PP/EVOH blends were characterized both in shear and in elongational flows. The mechanical, thermal, barrier and morphological properties were studied in previous works (Abad et al. 2004; Abad et al. 2005; Lasagabaster et al. 2006).

The samples for shear rheometry were shaped in the form of discs by compression molding at 210°C applying a pressure of 200 bar for 3 minutes. Those for extensional rheometry were also prepared by compression molding in the same conditions but in the shape of strips of 2x6x60 mm (Thickness x Width x Length). Rectangular cross-section has the advantage of easier clamping and lower distortion when clamped, although it makes sample visualization more difficult.

Rheology experiments were performed using a controlled strain rheometer (ARES, TA Instruments) with parallel-plate geometry (25 mm diameter, gap of 1 mm) at 220°C. The steady shear viscosity (η) was measured in a range of shear rates between 10^{-3} to $10\ s^{-1}$. The complex viscosity (η^*), storage modulus (G') and loss modulus (G'') were measured as function of frequency (ω). Dynamic strain sweep tests at fixed frequencies were performed (in fresh samples every time) in order to determine the linear viscoelastic region prior to the frequency sweeps. The frequency sweep measurements were set up inside the viscoelastic region, in a frequency range from 3×10^{-2} to 3×10^{1} rad/s.

The stress relaxation experiments in shear were performed at 220°C again using a parallel-plate geometry (diameter=25 mm) with a 1000 ± 1 μm gap; a shear rate of $1s^{-1}$ during 25 s was applied and the evolution of the shear stress upon cessation of flow was measured.

Experiments in uniaxial extension flow were also performed for all the samples using the modified rotational rheometer, MRR. In all experiments in extension the temperature of silicone oil was 220°C. At this temperature its density ($0.93\ g/cm^3$) roughly matched the density of the samples. The uniaxial extensional measurements were carried out by applying strain rates between approximately 3×10^{-2} and $3\times10^{-1}\ s^{-1}$.

Each experiment was repeated three times and the average values were taken for analysis both in shear and extensional experiments.

The transient uniaxial extensional viscosity in the linear viscoelastic regime (LVE) was calculated from the relaxation spectra obtained from shear oscillatory data at 220°C, and the Trouton ratio as a function of strain for the different blends was calculated.

Again, more details about the experimental techniques can be found in Chapter 2.

5.2 RESULTS AND DISCUSSION

5.2.1. Brief summary about the previous characterization of PP/EVOH blends

In this section, the principal experimental data obtained on mechanical, barrier and morphological properties of the PP/EVOH blends are summarized.

The mechanical and barrier properties of PP/EVOH blends, both non-compatibilized and compatibilized with different amounts of Na^+ ionomer were studied previously to this work [Abad *et al.* (2004)]. In this, the authors determined the tensile properties of the pure components and blends on extruded films. The tensile strength (σ_B) and strain at break point (ε_B) with EVOH and ionomer amount are presented in Figure 5.1a. In both parameters, it is clear that the

compatibilization has a great effect on the properties of the blends since an improvement in mechanical properties is observed with the addition of compatibilizer.

Figure 5.1b shows the effect of EVOH an ionomer addition in the water vapor transmission rate (WVTR) and in the oxygen transmission rate (O_2TR) values of the extruded films. The O_2TR of the PP/EVOH blends decreased with respect to pure PP especially for EVOH contents of 30% and higher, as was expected due to the good oxygen barrier properties of the copolymer. However, the best values were obtained when 5% or more of the compatibilizer was added to the blends.

The dramatic increase in the WVTR with the addition of EVOH was due to its hydrophilic character of the copolymer; however the PP/EVOH films with ionomer concentrations equal or higher than 5% the obtained WVTR values even lower than of the ones obtained for the pure PP.

The relative diameters of EVOH particles were plotted as a function of some ionomer percentage in order to see the effect of copolymer and ionomer in blends morphology. The relative diameters were calculated following Eqn. (5.1), where $d_{60/40}$ corresponds to the biggest diameter of the EVOH particles measured in the 60/40 PP/EVOH blend:

$$d_R = \frac{d_{blend}}{d_{60/40}} \tag{5.1}$$

For 90/10; 80/20 and 60/40 PP/EVOH blends only two formulations were measured, but the behaviour is similar to the 70/30 PP/EVOH blends in which all formulations were represented. It is obvious that the EVOH particle size increases with the addition of EVOH to the blends and that ionomer addition causes a decrease of disperse phase size and a better adhesion between the components, This effect is clearly seen in the SEM micrographs too. Figure 5.1c displays the morphology of the 90/10 and 70/30 PP/EVOH blends compatibilized with a 10% and 20% of Na^+ ionomer.

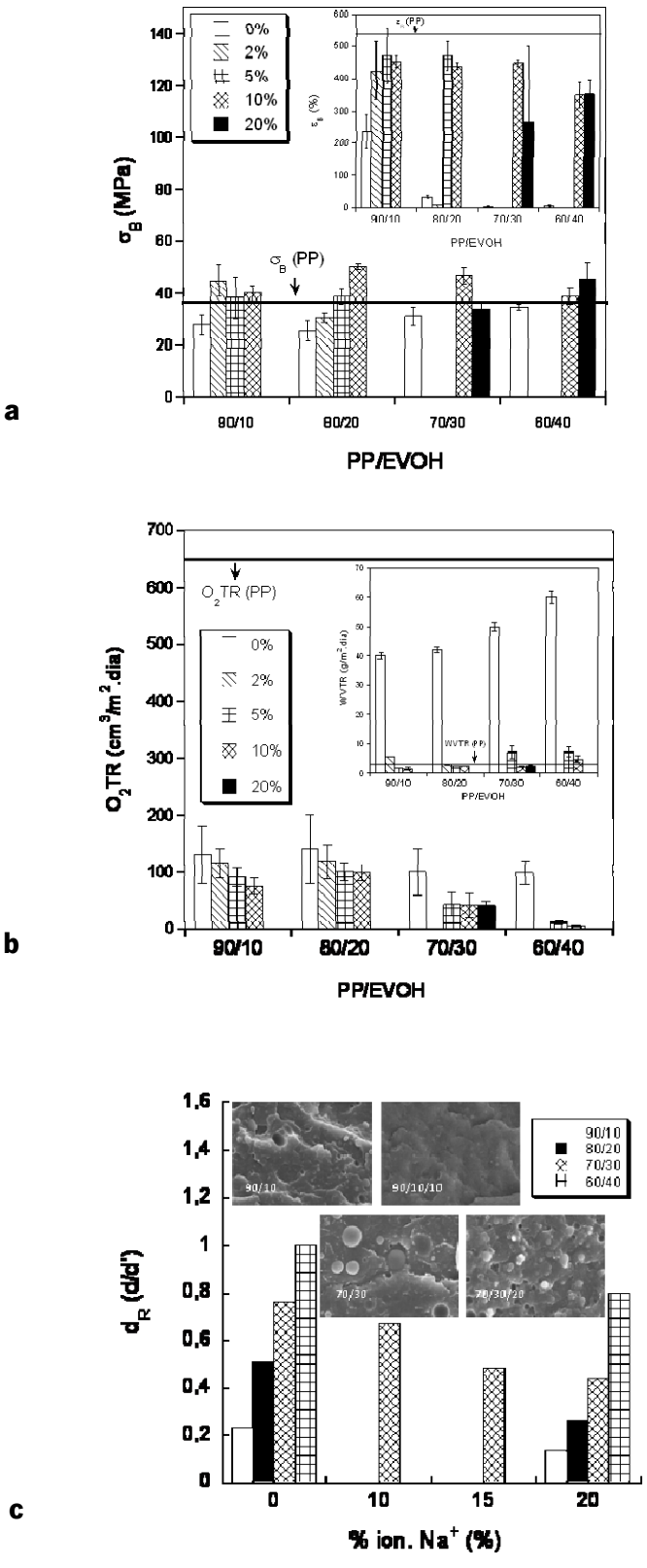

Figure 5.1 - Influence of the EVOH and ionomer amount in different properties; (a) Tensile strength and elongation at break, (b) Oxygen and vapour transmission rate, (c) relative diameter of EVOH particles and morphology (SEM micrographs x1500). Taken from Abad *et al.* (2004).

Thus, from the point of view of the barrier properties, mechanical properties and morphology, the addition of low amounts of Na^+ ionomer was an effective compatibilizer to the PP/EVOH blends. Although acceptable results were obtained for all compatibilized blends, the best cost/properties ratio was obtained for the 90/10/10 PP/EVOH/Na^+ blend because minor amounts of EVOH and ionomer were necessary.

With good compatibilization established, we will now focus on the effect of ionic compatibilization on the rheological properties.

5.2.2. Effect of the EVOH content in the rheology of PP/EVOH blends

Figures 5.2a-e show the rheological behaviour in oscillatory shear and in extension of the binary PP/EVOH blends.

Figure 5.2a depicts the complex viscosity versus frequency and it shows the onset of the Newtonian plateau for pure PP at low frequencies, followed by a mildly shear-thinning behaviour. This behaviour is basically replicated for all the blends, with the absolute value of complex viscosity decreasing with increasing EVOH content. The reason for this is related to the orientation of the EVOH domains inside the PP matrix and the immiscibility of both phases that prevents stress transfer between them and results in interfacial slippage.

This behaviour is replicated by the results for the storage and loss moduli, G' and G'', as can be seen in Figures 5.2b and 5.2c, respectively. An interesting feature is that the crossover between G' and G'' of EVOH is different to that of the other materials. In fact, for EVOH this crossover occurs at a frequency of approximately 0.3 rad/s, while for the other materials it occurs only at frequencies at least one order of magnitude higher.

Figure 5.2d, shows the results in uniaxial extensional rheometry and contrarily to what could be expected, apparently this effect is not as pronounced, which could be due to two reasons; the first is that strain-hardening behaviours of both PP and EVOH (expressed by the Trouton ratio) are very similar and the second is that the experiments for the immiscible blends are extremely hard to perform and the data scatter may be masking any effect.

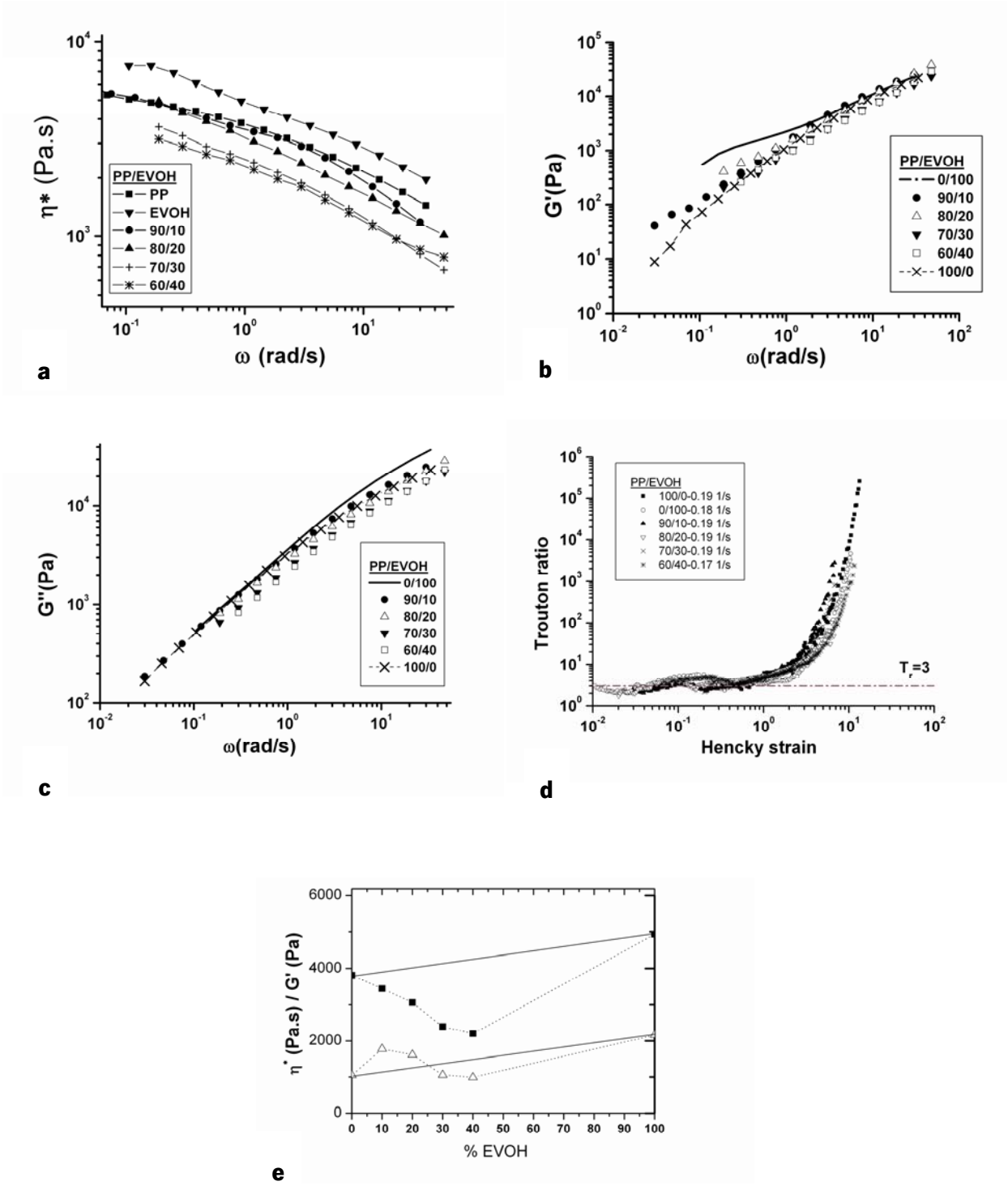

Figure 5.2 - Curves for the binary PP/EVOH blends; (a) Complex viscosity versus frequency, (b) Evolution of the storage modulus (G') with frequency, (c) Evolution of the loss modulus (G'') with frequency (d) Influence of the EVOH content on the Trouton ratio against Hencky strain, (e) Complex Viscosity and G'(Pa) at 1 rad/s versus EVOH percentage.

One unexpected feature of Figure 5.2d is the fact that PP, a linear material, shows an important degree of strain hardening. One explanation for this fact is that as this PP is a commercial polymer with a grade specifically developed for bi-oriented extrusion, and it is likely that it has a complex composition; for example, a small amount of a very high molecular weight component can produce a strong effect on the strain-hardening of linear polymers [Sugimoto *et al.* (2001)]. Unfortunately it was not possible to quantify the molecular weight and molecular weight distribution of PP.

The results of linear viscoelastic studies can provide reliable information on morphology of the blends. The viscoelastic response of the blends at low frequencies can be used for evaluating of the interfacial interaction between phases because the effect of flow induced molecular orientation on viscosity and elasticity becomes less important. The complex viscosity and storage modulus versus blend composition together with the same results calculated using the mixing rule at frequency of 1 rad/s are presented in the Figure 5.2e. The binary blends show negative deviation in the viscosity for all blends and negative deviation of elasticity in blends with 30% and 40% of EVOH. On the basis of Utracki's studies [Utracki (1988)] the negative deviation of the viscosity and elasticity observed for EVOH-rich blends can be attributed to the presence of weak interfacial interaction between phases in these blends.

5.2.3. Effect of the ionomer content in the rheology of PP/EVOH blends

Figure 5.3a shows the complex viscosity as a function of frequency for 90/10 PP/EVOH blend with different amounts of ionomer. With the addition of 2% and 5% of ionomer, a decrease in viscosity is observed thus indicating that the amount of ionomer is not sufficient to compatibilize the blends effectively. With the addition of 10% ionomer, higher values of viscosity than the immiscible blend are observed, which reflects the fact that the extent of the compatibilization is increasing. This is due to the improvements of interfacial adhesion between PP and EVOH, as can be seen in the morphology (Figure 5.3d) and the better EVOH phase dispersion due to the compatibilization. Besides, the improvement of rheological properties of the blends can also be related with the phenomenon of the rough surfaces of extruded non-compatibilized blends

compared to the smooth surfaces of extruded blends compatibilized by Na^+ in melt extrusion process. This is in agreement with the results obtained for barrier and mechanical properties where the best data were obtained for 90/10/10 PP/EVOH/ Na^+ blend.

These results were also confirmed in Figures 5.3b and 5.3c where both moduli for the blend with 2 and 5% ionomer content were lower than for the non-compatibilized blend. For 10% EVOH, however, it is apparent that compatibilization is occurring to a high enough extent as to cause a small but noticeable increase in the moduli. At large frequencies, storage modulus G' and loss modulus G'', slightly increases with Na^+ concentration. At low frequencies the effect of compatibilizer is much more pronounced.

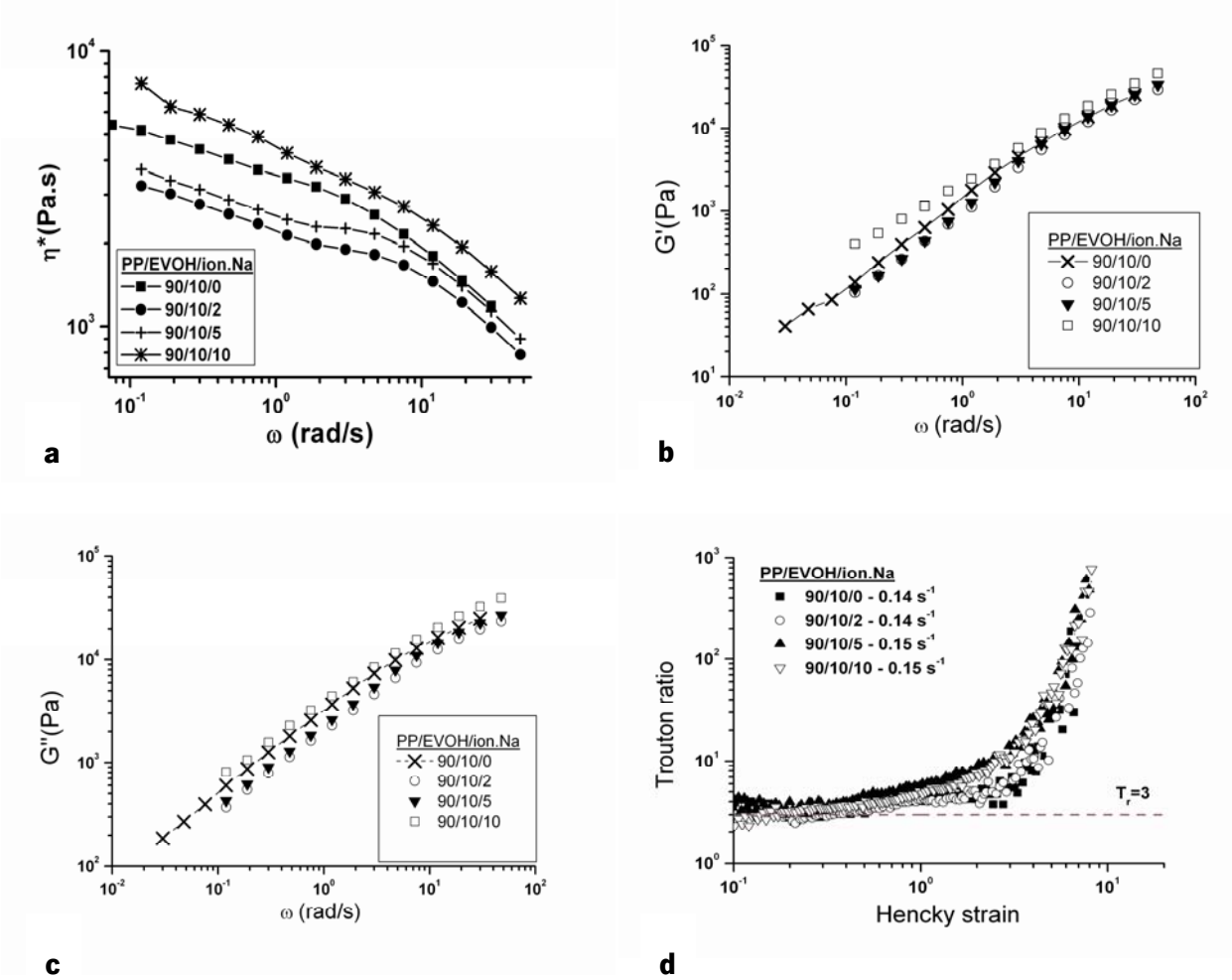

Figure 5.3 - Curves for the 90/10 w/w PP/EVOH blends with different amounts of ionomer; (a) Complex viscosity versus frequency, (b) Evolution of the storage modulus (G') with frequency, (c) Evolution of the loss modulus (G'') with frequency (d) Influence of the ionomer content on the Trouton ratio against Hencky strain.

The results for uniaxial extension (Figure 5.3d) also seem to confirm those in shear, but in this case a noticeable increase in the Trouton ratio can already be seen for the blend with 5% ionomer; in fact, the results are almost the same as for the blend with 10% ionomer. The reason for this behaviour is that in the compatibilized blends the morphology is different; EVOH has better adhesion to the PP matrix, and the average size of the EVOH domains is lower as it was proved in the previous morphology study. With this type of morphology, the effect of extensional flow on the interfacial area is much higher than the one of shear flow, thus yielding a noticeable compatibilization effect at lower ionomer contents, *i.e.*, it induces the strain hardening behaviour even with the addition of small quantities of compatibilizer [Hong *et al.* (2005a), Hong *et al.* (2005b)]. At small strains a good agreement between the experimental data and the linear viscoelastic prediction is evident for all the concentrations of ionomer. At large strains the elongational viscosity increases more rapidly and exceeds the linear viscoelastic prediction. This strain-hardening is more clearly seen with the increase of ionomer amount. All the compatibilized blends are, like their non-compatibilized counterparts, highly strain-hardening, as expected, with the strain-hardening becoming more pronounced as the strain rate increases due to the fact that the reduction of the area of the sample what produces an increase in the interfacial area in both absolute terms and relatively to the sample volume; for an example of this see Figure 5.4a and 5.4b, for the 90/10 w/w PP/EVOH and 90/10/10 w/w PP/EVOH/ion.Na blends, respectively.

Identical results were obtained for 80/20 PP/EVOH blend than for the 90/10 PP/EVOH blend, and, thus, for the sake of simplicity, that data is not included in the text.

For the two blends with 30 and 40% of copolymer the results are also very similar and again only the study of the 60/40 PP/EVOH blend is reported.

Figures 5.5a-d depict the results for the latter blend and show that addition of up to 10% of ionomer clearly has an increasing compatibilizing effect. However, the material with 20% ionomer shows a decrease in both the viscosity (Figure 5.5a) and the linear viscoelastic moduli (Figures 5.5b-c). It is observed that increasing the compatibilizer content enhances interfacial adhesion between two phases, ultimately resulting in increase of resistance to deformation of

compatibilized blends. However, the addition of compatibilizer above a critical concentration (20%) probably gives no more contributions to the increase the interfacial adhesion, *i.e.*, it reaches a saturation stage, and decreases the viscosity of the blends due to the lower viscosity of Na^+ ionomer.

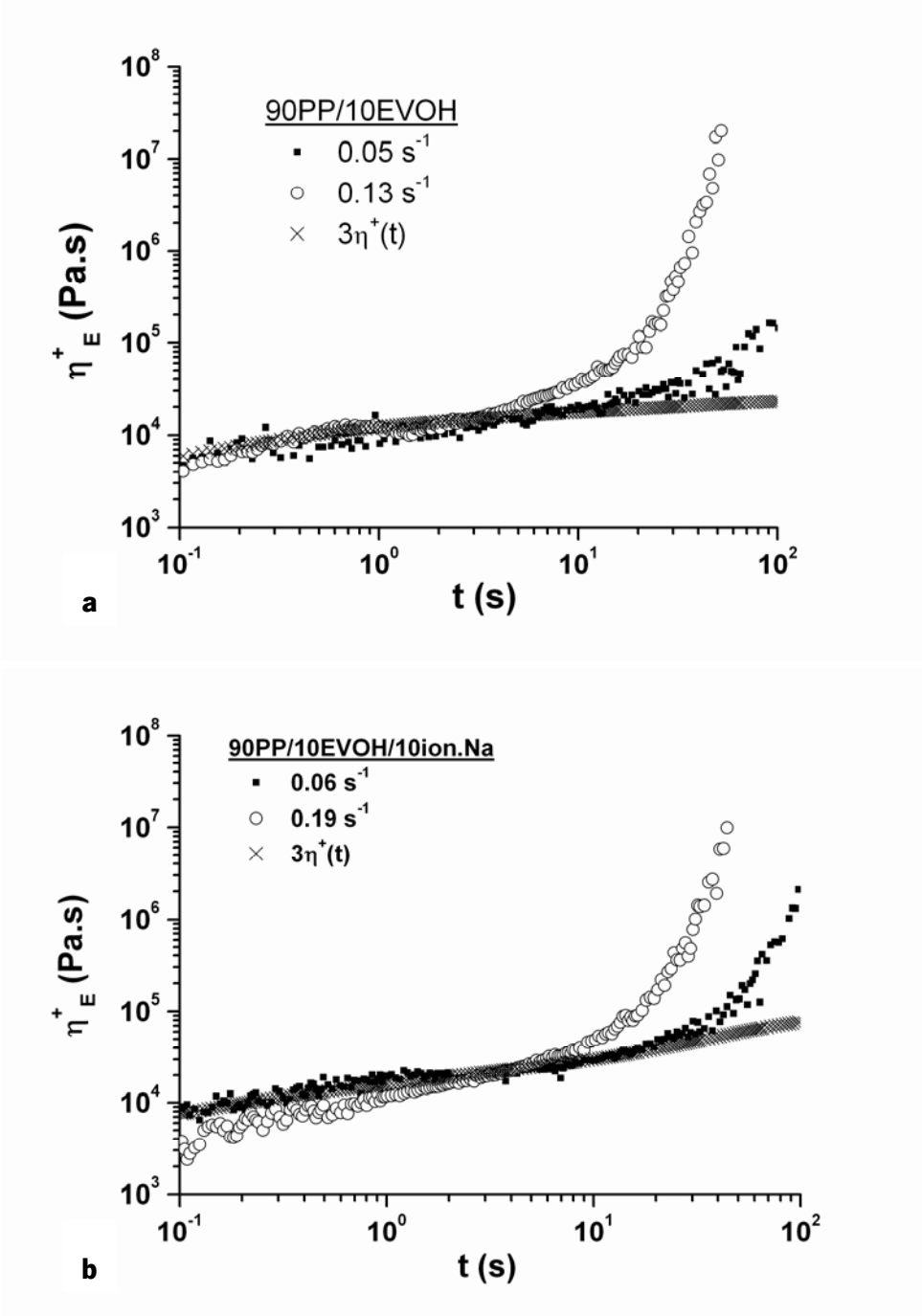

Figure 5.4 - Transient uniaxial extensional viscosity for the 90/10 w/w PP/EVOH blend; (a) 0% of ionomer, (b) 10% of ionomer.

As it was seen for the others blends, the experiments in uniaxial extension (Figure 5.5d) show good compatibilization occurring for lower ionomer contents; in this case the best results were achieved for the 60/40/5 PP/EVOH/Na blend, although compatibilization is also observed for the blends compatibilized with 10 and 20% of ionomer.

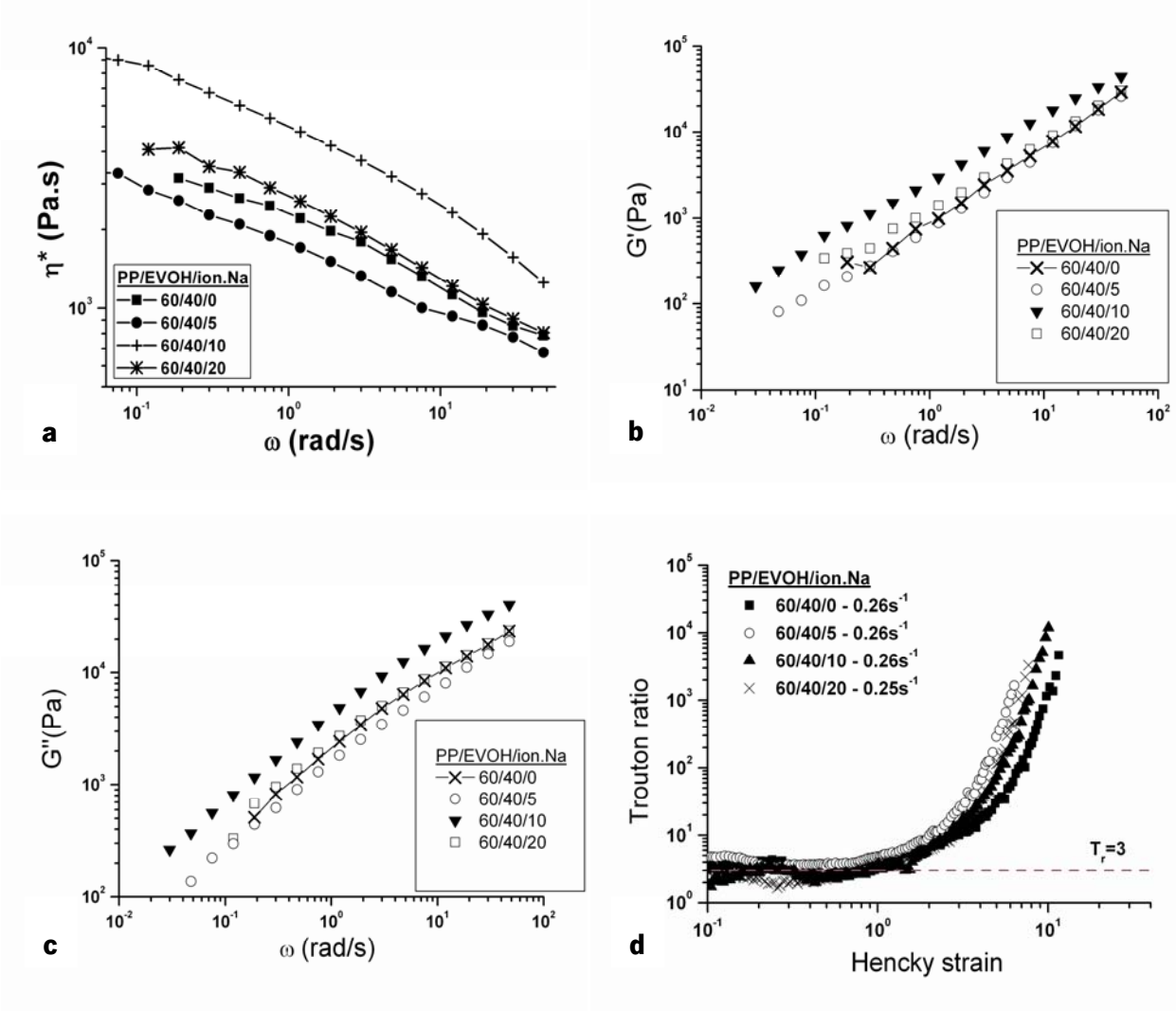

Figure 5.5 - Curves for the 60/40 w/w PP/EVOH blends with different amounts of ionomer; (a) Complex viscosity versus frequency, (b) Evolution of the storage modulus (G') with frequency, (c) Evolution of the loss modulus (G'') with frequency, (d) Influence of the ionomer content on the Trouton ratio against Hencky strain.

5.2.4. Stress relaxation experiments

Shear stress relaxation measurements (Figure 5.6) show that PP relaxes in a single step and EVOH relaxes in two steps which is a consequence of the fact of EVOH is a copolymer. The dispersed phase concentration greatly affects the relaxation behaviour of the blends.

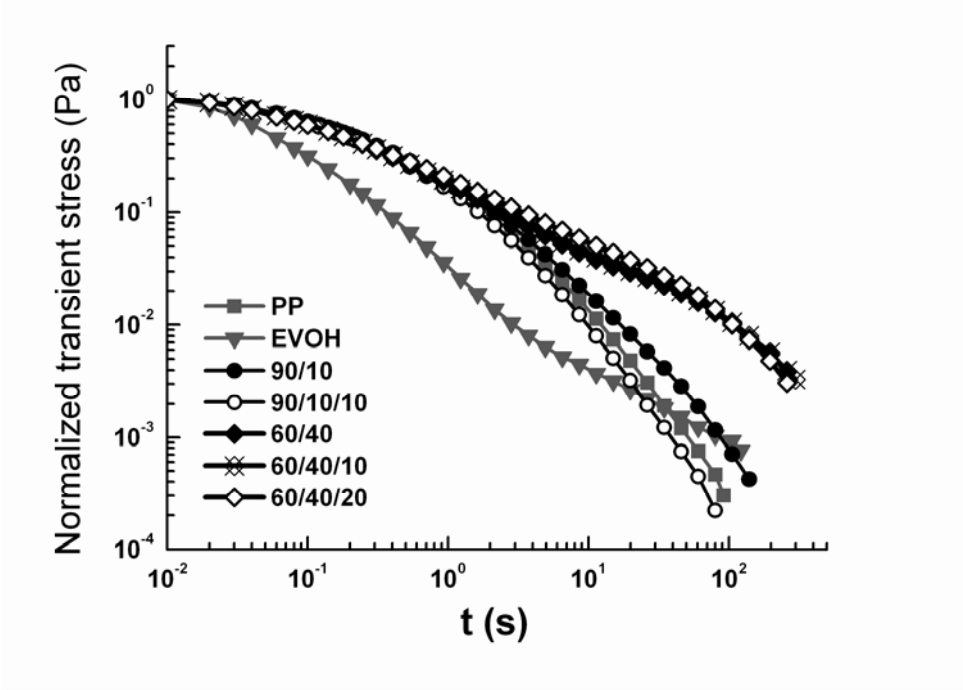

Figure 5.6 - Normalized transient stress for several blends of PP/EVOH, compatibilized and non-compatibilized, and their pure components after a cessation of a shear flow of 1 s^{-1} for 25s at 220°C.

For the blends with 10% EVOH the relaxation curve has a shape similar to that of PP, with the exception of the non-compatibilized blend that shows a slower terminal relaxation thanks to the presence of the non-compatibilized EVOH phase, as expected. For the compatibilized blend the relaxation kinetics is slightly quicker to that of the matrix (PP). This is an inversion in relaxation behaviour after step shear relatively to the previous chapters (the relaxation time increase with the addiction of the compatibilizer). This is probably due to the inversion of the relaxation kinetics of the components (here, the dispersed phase relax faster in the first seconds).

For the 40% EVOH blends, there are two noteworthy features: a) The relaxation is much slower than for any of the two components and b) Its kinetics is basically independent of the blend being

compatibilized or not. In what concerns the former, this happens because the interfacial area, which contributes to relaxation, is higher in more concentrated blends. In what regards the latter, this phenomenon is related to the fact that the interfacial area increases with the amount of EVOH and thus it is expected that the same amount of compatibilizer will yield a much smaller effect in terms of relaxation kinetics for this blend than for the one with 10% EVOH.

Inversely to the Chapters 3 and 4, here the relaxation after a cessation of shear flow experiments show that the introduction of compatibilizer did not increase the relaxation time of blends. This is expected since the strength of ionic bonds decreases with increasing temperature Thus the interfacial interactions and entanglements are not so strong as in those cases.

5.3 SUMMARY

The main conclusions obtained from the rheological study in shear and extensional flows of polypropylene and ethylene-vinyl alcohol copolymer (PP/EVOH) blends compatibilized with Na^+ ionomer can be summarized as follows:

a) The binary PP/EVOH blends show shear thinning behaviour that increases with EVOH amount.

b) A negative deviation behaviour of the viscosity and elasticity was observed for EVOH-rich blends as expected for immiscible blends.

c) For the 90/10 PP/EVOH blend, a 10% of sodium ionomer was necessary to observe the compatibilization effect in shear and extensional flows. The rheological data displayed an increase of the viscosity and moduli for this formulation, which is related with the more uniform morphology of the material and with the improvement of barrier and mechanical properties with respect to the non-compatibilized system. Besides, an increase in Trouton ratio and strain hardening behaviour were obtained with the ionomer addition.

d) The same behaviour was found for 60/40 PP/EVOH blends compatibilized, although a larger ionomer amount was necessary to observe noticeable compatibilization.

e) The stress relaxation experiments showed that the same amount of compatibilizer causes a minor effect, in terms of relaxation kinetics, in blends with high amount of EVOH and that the relaxation kinetics in these is generally much slower than that of any of the individual components, PP and EVOH.

As in the previous chapters, the rheological behaviour of these blends depends of the amount of compatibilizer. However, contrarily to the blends of Chapters 3 and 4, it was observed that the addition of compatibilizer does not have a marked influence in relaxation after a cessation of a shear flow, which is consistent with fact that compatibilization via the addition of a ionomer does not significantly increase the elasticity of interfaces. Thus, the stress relaxation experiments are a very powerful tool to evaluate the elasticity of interfaces, particularly in compatibilized blends.

References

Abad, M. J., A. Ares, L. Barral, J. Cano, F. J. Diez, S. Garcia-Garabal, J. Lopez and C. Ramirez, "Use of a sodium ionomer as a compatibilizer in polypropylene/high-barrier ethylene-vinyl alcohol copolymer blends: The processability of the blends and their physical properties", J. Appl. Polym. Sci. 94, 1763-1770 (2004).

Hong, J. S., K. H. Ahn and S. J. Lee, "Strain hardening behavior of polymer blends with fibril morphology", Rheol. Acta 45, 202-208 (2005a).

Hong, J. S., J. L. Kim, K. H. Ahn and S. J. Lee, "Morphology development of PBT/PE blends during extrusion and its reflection on the rheological properties", J. Appl. Polym. Sci. 97, 1702-1709 (2005b).

Sugimoto, M., Y. Masubuchi, J. Takimoto and K. Koyama, "Melt rheology of polypropylene containing small amounts of high-molecular-weight chain. 2. Uniaxial and biaxial extensional flow", Macromolecules 34, 6056-6063 (2001).

Utracki, L. A., "Viscoelastic Behavior of Polymer Blends", Polym. Eng. Sci. 28, 1401-1404 (1988).

CHAPTER 6

Discussion and conclusions

6.1 DISCUSSION AND CONCLUSIONS

In this work the role of compatibilization on the dynamics of interfaces, particularly in blends with viscosity ratios higher than one, was investigated. The existent analytical models are not able to correctly predict the effect of compatibilization on rheological behaviour of blends, particularly when viscoelastic components and viscosity ratios different than one are involved.

First, PA6/EPM/EPM-g-MA concentrated blends, in which the elasticity of the phases can not be neglected, were investigated. Then, in order to better understand the results and achieve a deeper knowledge about these polymeric systems, SALS was used on optically transparent PMMA/PS/PSOX blends.

In both PA6/EPM/EPM-g-MA and PMMA/PS/PSOX blends major effects of compatibilization in stress relaxation after cessation of flow, both in shear and extension were found. In these blends the introduction of compatibilizer causes a large increase in relaxation times, this behaviour depending on the concentration of compatibilizer. A remarkable fact, that is very clear in PMMA/PS/PSOX, is the existence of a critical concentration above which the addiction of compatibilizer does not change the rheological behaviour of the blend.

The mechanisms causing the increase of relaxation times were investigated. In PA6/EPM blend it was observed, freezing the morphology after a deformation in elongation, that the droplets of compatibilized blends were slightly elongated while in the uncompatibilized blend they were spherical. This deformation of the droplets, which is due to a better adhesion between the phases, could, at least partially, explain the increase of relaxation times. However, the use of SALS in the transparent PMMA/PS/PSOX blends, during shear flows showing that the addiction of high enough concentrations

of oxazoline causes a droplet deformation in the vorticity direction at high shear rates which is an indication of a strong increase in interfacial elasticity. Even after a long time after cessation of flow the dispersed phase remains deformed which leads to conclusion that the additional entanglements and interactions slow down the relaxation. Thus, the increase in relaxation time of PA6/EPM by introduction of compatibilizer should be explained not only by a higher deformation of the droplets but also, and possibly mainly, by entanglements in the interfaces that slow down the relaxation.

This type of behaviour is not universal and depends strongly on the type of compatibilization and the type of interactions that occurs at the interface. The first of the type of blends above was compatibilized through addition of a reactive polymer while in the second one the introduction of the oxazoline groups led to formation of additional physical interactions and in both cases similar rheological behaviour was found. However, if different types of compatibilization are used, the nature of the interactions at the interface changes and so does the rheological behaviour. This was shown for blends of PP/EVOH compatibilized with a Na^+ ionomer. Although, the effect of compatibilization through the presence of the ionomer is effective from the point of view of barrier properties, mechanical properties and morphology, the relaxation of the blends after cessation of flow is not significantly changed by the addiction of compatibilizer. The temperature dependence of strength of ionic bonds explain why the interactions introduced by the compatibilizer the interfaces are not as strong as in the previous blends (at least at high temperatures), and thus do not cause a significant increase of relaxation time after deformation.

Appendix

Appendix A – *Silva, J., A. V. Machado and J. Maia, "Rheological behaviour of high-viscosity emulsions: A comparison between the predictive capabilities of several theoretical models", Journal of the Portuguese Society of Rheology 4, 64-71 (2004).*

Appendix B – *Silva, J., A. V. Machado and J. Maia, "Rheological behavior of compatibilized and non-compatibilized PA6/EPM blends", Rheol Acta 46, 1091-1097 (2007).*

Appendix C – *Silva, J., A. V. Machado, P. Moldenaers, J. Maia, "The effect of interfacial properties on the deformation and relaxation behavior of PMMA/PS blends" (2008)* Submitted to *Journal of Rheology.*

Appendix D – *Ares, A., J. Silva, J. Maia, L. Barral and M. Abad, "Rheomechanical and morphological study of compatibilized PP/EVOH blends." (2008)* Submitted to *Rheologica Acta*.

Appendix A

Silva, J., A. V. Machado and J. Maia, "Rheological behaviour of high-viscosity emulsions: A comparison between the predictive capabilities of several theoretical models", Journal of the Portuguese Society of Rheology 4, 64-71 (2004).

RHEOLOGICAL BEHAVIOUR OF HIGH-VISCOSITY EMULSIONS: A COMPARISON BETWEEN THE PREDICTIVE CAPABILITIES OF SEVERAL THEORETICAL MODELS

*J. M. Silva, A. V. Machado and J. M. Maia**
Department of Polymer Engineering , University of Minho, Campos de Azurém, 4800 Guimarães, Portugal, email: jmaia@dep.uminho.pt

Keywords: Emulsions models; polymer blends; linear viscoelastic behaviour.

Abstract: In the last years, the importance of blends of immiscible polymers has increased with a large number of studies about relationships between rheology and morphology having been developed. In fact, the rheological behaviour of a blend depends not only on the proprieties and proportion of the neat polymers, but also on its morphology and interfacial tension between polymers. In this work we compare the predictive capabilities of the Lee-Park model, an extension of the Doi-Otha model to include fluids with different viscosities, and the Palierne model. For characteristic values of blends of immiscible polymers, the Palierne [1] and Bousmina [2] models give approximately similar predictions for linear viscoelastic data. The Doi-Otha [3] and Lee-Park [4] models are able, in principle, to describe the behaviour of polymer blends for any type of flow and are usually used to predict the transient response of emulsions.

1. INTRODUCTION

The rheology of emulsions, in special, high-viscosity emulsions (for example, incompatible polymer blends in the molten) has been a subject of a great interest owing to the increasing use of polymer blends in industrial applications. This has brought about the need to try to predict the rheological behaviour of the materials, for which purpose several models have been developed. In the early 50's, Oldroyd, taking the pioneer works of Einstein [5] and Taylor [6], developed a model [7][8] that included time-dependent effects to describe rheology of diluted emulsions. The fluids were assumed to be Newtonian and the droplet deformation small. The most interesting extension of the Oldroyd emulsion model is that proposed by Palierne [1], who analyzed the linear viscoelastic behaviour of non-dilute emulsions of viscoelastic droplets in a viscoelastic matrix. Dipole-type particles interactions are considered and effects of particle size distribution are included. The Palierne model describes the complex modulus, G_B^*, of viscoelastic emulsions as a function of the complex moduli of both phases (G_M^* for the matrix and G_I^* for the droplets), the ratio of the interfacial tension and the droplet size and the size distribution, as follows:

$$G_B^* = \frac{1+3\sum_i \phi_i H_i^*(\omega)}{1-2\sum_i \phi_i H_i^*(\omega)} G_M^*(\omega) \tag{1}$$

with

$$H_i^*(\omega) = \frac{4\left(\alpha/R_i\right)\left[2G_M^*(\omega)+5G_I^*(\omega)\right]+\left[G_I^*(\omega)-G_M^*(\omega)\right]\left[16G_M^*(\omega)+19G_I^*(\omega)\right]}{40\left(\alpha/R_i\right)\left[G_M^*(\omega)+G_I^*(\omega)\right]+\left[2G_I^*(\omega)+3G_M^*(\omega)\right]\left[16G_M^*(\omega)+19G_I^*(\omega)\right]} \tag{2}$$

where α is the interfacial tension and ϕ_I is the volume fraction of particles with radius R_i. Starting from the Kerner model [9], for a rheological behaviour of a composite of two elastic bodies, Bousmina [2] derived another expression for G^*

$$G_B^* = G_m^* \frac{2\left(G_I^* + \alpha/R\right) + 3G_M^* + 3\phi\left(G_I^* + \alpha/R - G_M^*\right)}{2\left(G_I^* + \alpha/R\right) + 3G_M^* - 2\phi\left(G_I^* + \alpha/R - G_M^*\right)} \tag{3}$$

where R is the mean radius of the dispersed phase.
A third model was proposed for Doi and Otha [3]. They considered the interface between the two phases and derived a semiphenomenological kinetic equation to describe the time evolution of interfacial area per unit of volume (Q) and its anisotropy (q_{ij}) in a given flow field. The interfacial area and its anisotropy are defined as follows:

$$Q = \frac{1}{V}\int dS \tag{4}$$

$$q_{ij} = \frac{1}{V}\int dS(n_i n_j - \tfrac{1}{3}\delta_{ij}) \tag{5}$$

where n_i denotes the unit normal vector to the interfaces, V the total system volume, and dS an interface element. The constitutive equation obtained by Doi and Otha was later modified by Lee and Park [4] to account for a mismatch in the viscosities of polymers. They proposed the following constitutive equations:

$$\sigma_{ij} = \left(1 + \frac{6(\eta_I - \eta_M)}{10(\eta_I + \eta_M)}\phi\right)\eta_M \dot{\gamma}_{ij} - \alpha q_{ij} - P\delta_{ij} \tag{6}$$

$$\frac{\partial}{\partial t}q_{ij} = -q_{ik}d_{kj} - q_{jk}d_{ki} + \frac{2}{3}\delta_{ij}d_{lm}k_{lm} - \frac{Q}{3}\left(d_{ij} + d_{ji}\right) + \frac{q_{lm}d_{lm}}{Q}q_{ij} - \lambda\frac{\alpha}{\eta_M}Q\,q_{ij} - \lambda\nu\frac{\alpha}{\eta_M}\left(\frac{q_{lm}q_{lm}}{Q}\right)q_{ij} \tag{7}$$

$$\frac{\partial}{\partial t}Q = -d_{ij}q_{ij} - \lambda\mu\frac{\alpha}{\eta_M}Q^2 - \lambda\nu\frac{\alpha}{\eta_M}q_{ij}q_{ij} \tag{8}$$

where η_M is the zero-shear viscosity of matrix, η_I is the zero-shear viscosity of inclusions, P is the hydrostatic pressure, λ is the total relaxation parameter, μ the size relaxation, ν the shape relaxation. The μ parameter is associated to coalescence and so it can be considered zero in small amplitude oscillatory flow because the deformation of dispersed phase is small. Other considerations suggested $\nu = 1 - \phi$, for the same type of flow.
Several researchers [10][11] have reported a negative deviation behaviour (NDB), *i.e.*, when the values of both G' and G'' of the blends are lower than those of either the components (see Figure 1, for a typical example). In this work, the predictions of several models will be

analysed and compared in terms of their predictive capabilities of both the viscoelastic and NDB of the blends.

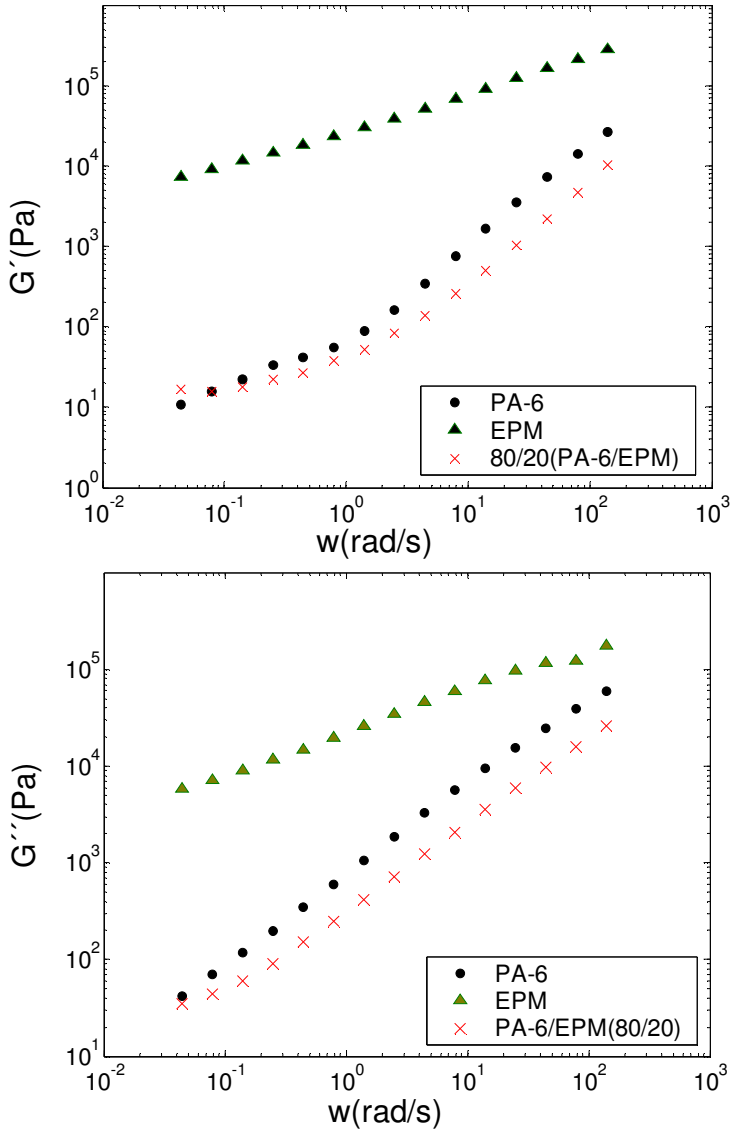

Figure 1 – Storage and dissipative modulus of a PA-6/EPM blend (80/20, w/w) and of their components.

2. INFLUENCE OF EMULSION PARAMETERS ON THE PALIERNE MODEL

Let us consider a two fluids emulsion and suppose that both fluids have a Maxwel-type behaviour according to

$$G^* = \frac{i\omega\eta}{1+i\omega\lambda} \tag{9}$$

We will then start from typical values of the constants and vary them in order to study the influence of each of them on the viscoelastic behaviour. The initial values of the constants are $\lambda_M = \lambda_I = 0.1s$, $\eta_M = \eta_I = 10^6$ Pa.s, $\alpha = 10$ mN/m. Furthermore, we shall assume that all droplets have same radius, $R = 1\mu m$.

Figure 2 shows that the plateau modulus in G' decreases in value but is extended to lower frequencies with increasing radius of the particles of the dispersed phase. The effect of interfacial tension is the opposite since eq. 2 depends on α/R_i. There are no significant effects in G''.

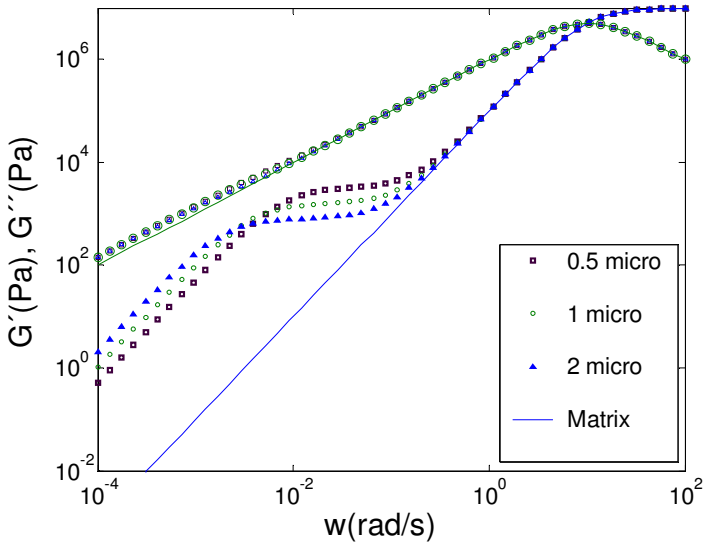

Figure 2 - Dynamic moduli vs frequency. Effect of variation of radius of inclusions. (micro = μm)

On the contrary, the increase of volume fraction of the disperse phase leads to an increase of the G' plateau, as expected, as can be seen in Figure 3; this also shows a slight increase of G'' at low frequencies.

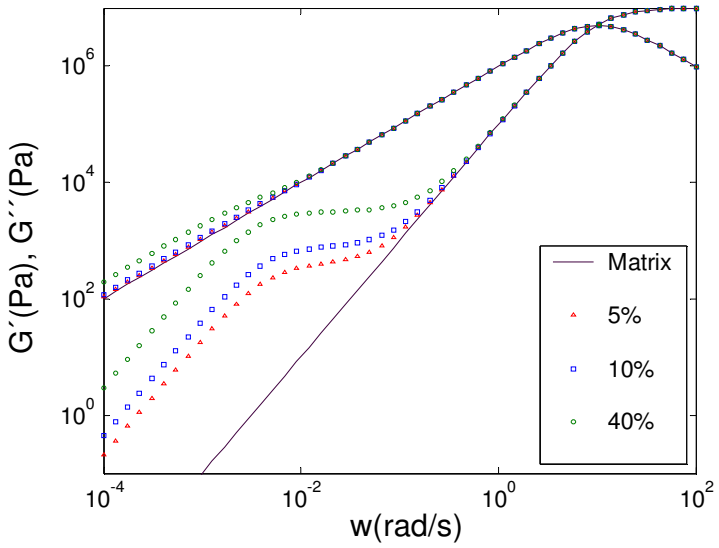

Figure 3 - Dynamic moduli vs frequency. Effect of variation of volume fraction of the disperse phase.

In order to study the influence of the viscosity ratio between the dispersed phase and the matrix, that of the latter was kept constant at 10^6 Pa.s and that of the former was changed from a minimum of 10^5 Pa.s to a maximum of 10^8 Pa.s, thus yielding a ratio varying between 0.1 and 100. Figure 4 shows clearly that there is a marked influence of the viscosity ratio on the value of the plateau in $G^{'}$, which is shifted to lower frequencies and decreases with increasing viscosity ratio.

Finally, when the relaxation time of the disperse phase increases so does the plateau in $G^{'}$ (Figure 5), which was expected due to the increased elasticity levels.

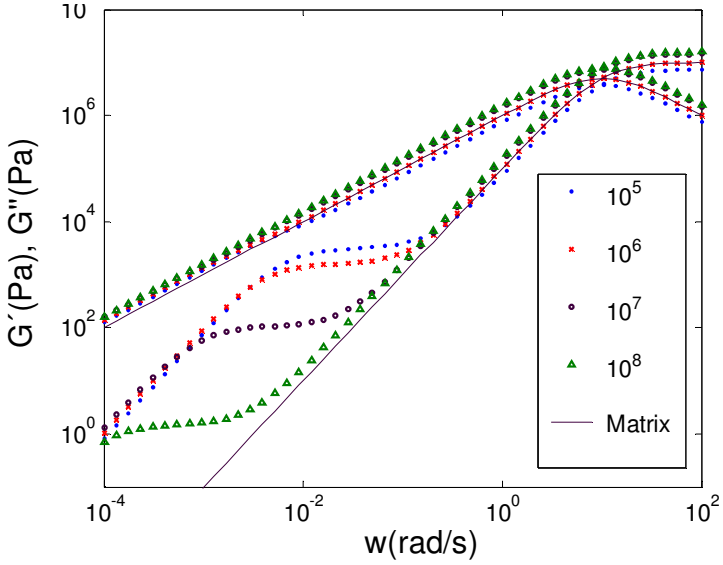

Figure 4 – Dynamic moduli vs frequency. Effect of the zero-shear viscosity of the dispersed phase.

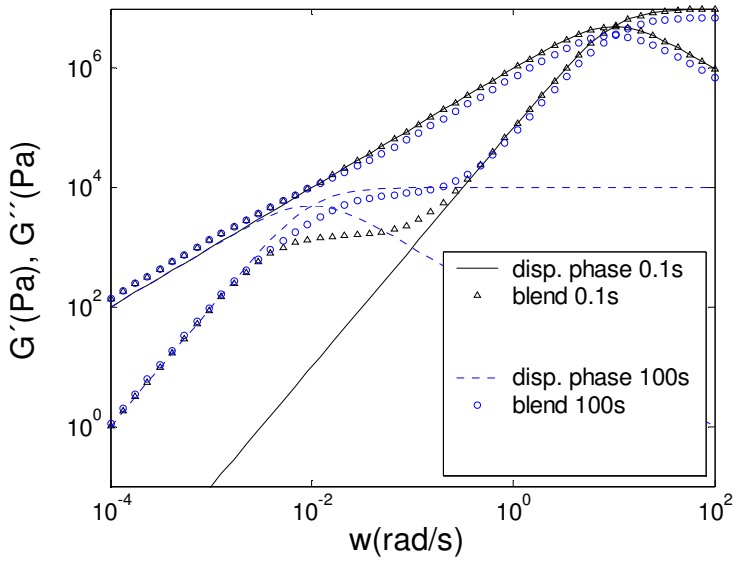

Figure 5 - Dynamic moduli vs frequency. Effect of relaxation time of dispersed phase.

3. COMPARISON BETWEEN THE PALIERNE AND LEE-PARK MODELS

The Bousmina and Palierne models give very similar predictions for typical values of the parameters [2], which is not the case with the predictions of the Lee-Park model. We compared these models varying different parameters.
In the Lee-Park model, the interfacial area, Q, is related to the particle radius by:

$$Q = \frac{6\phi}{R} \tag{10}$$

Figure 6 shows, for both radii, that the plateau modulus in $G^{'}$ predicted by the Lee-Park model is higher than that predicted by the Palierne model.
In what regards other parameters, the Lee-Park model predicts a higher value for plateau in $G^{'}$, for different values of interfacial tension (Figure 7) and shows lower sensibility to variations of the viscosity ratio and volume fraction of dispersed phase than the Palierne model.

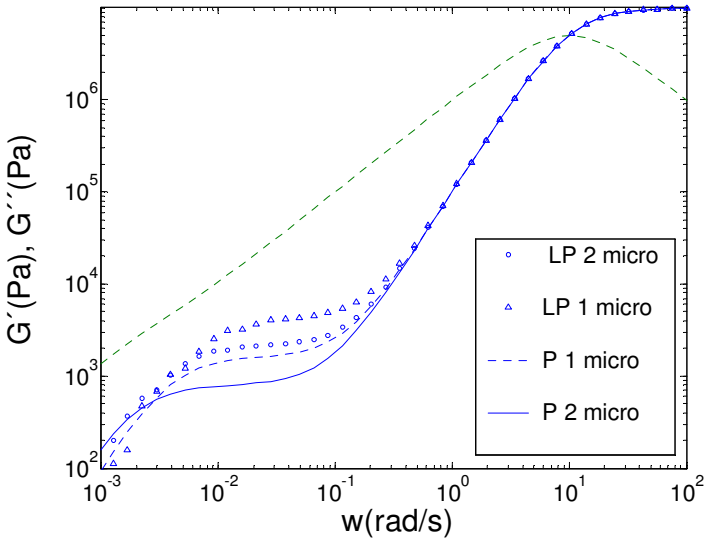

Figure 6 - Dynamic moduli vs frequency. Comparation of models predictions for different radius of inclusions. ($micro = \mu m$, PL- Lee-Park model, P- Palierne model, $\lambda = 0.6$)

Contrarily to the Palierne model, the Lee-Park model has an adjustable parameter: the relaxation total, λ. In Figure 8 it is shown that this parameter affects the width of the $G^{'}$ plateau; when λ increases the width of the plateau modulus in $G^{'}$ decreases.
None of the models is able to predict the rheological proprieties of blends that show a negative deviation behaviour (NBD) that often occurs when slippage at the polymer interfaces occurs. In fact, all the models assume continuity on the interfaces and fail in these cases. Recently, Adhikari and Goveas [12], modifying a Palierne theory, calculated the rheological proprieties for dilute polymer emulsions considering a slip effect. However, this modification to the original Palierne theory is not valid for concentrated polymer emulsions, such as typical polymer blends and, thus, this still constitutes an open problem.

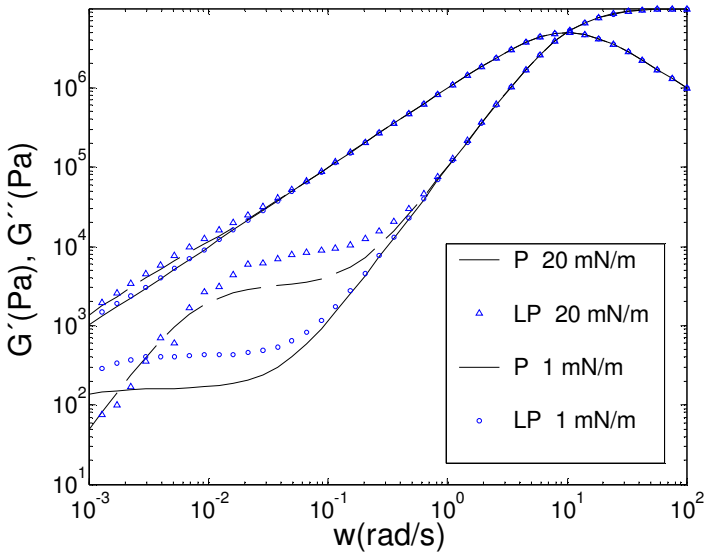

Figure 7 - Dynamic moduli vs frequency. Comparation of models predictions for different values of interfacial tension. (PL- Lee-Park model, P- Palierne model, $\lambda = 0.6$)

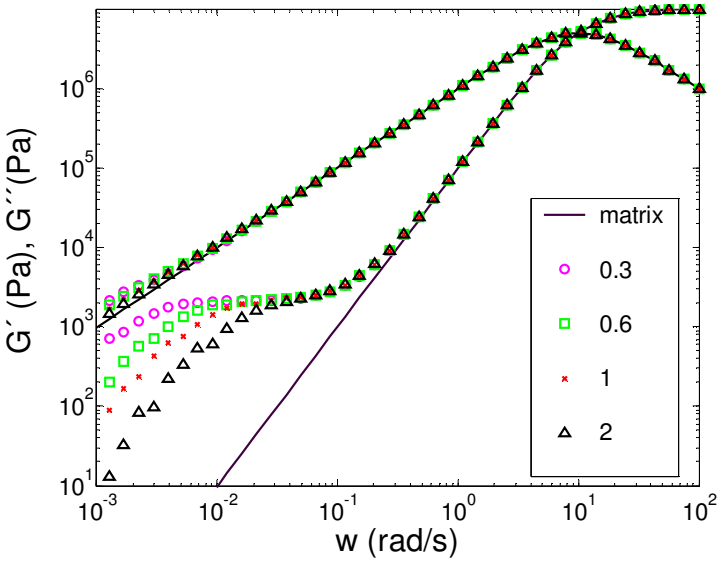

Figure 8 - Dynamic moduli vs frequency. Effect of λ parameter (total relaxation parameter).

4. CONCLUSIONS

The Palierne and Bousmina models give quantitatively similar predictions for $G^{'}$ and G'' of blends in small amplitude oscillatory flows. The Doi-Otha family models present a great advantage, in that they can, in principle, be used to predict the behaviour of a blend in any type of flow, namely, in transient ones. This model also predicts higher values for the plateau in $G^{'}$ than the Palierne model.

None of the models studied in this work is to able to predict the existence of negative deviation behaviour, *i.e.*, when the values of both G' and G'' of the blends are lower than those of either the components, that occurs often; this is a drawback that the future models (or extension of the existing ones) should clearly try to overcome.

5. REFERENCES

[1] Palierne, J. F. (1990). "Linear Rheology of Viscoelastic Emulsions with Interfacial-Tension." Rheol Acta **29**(3): 204-214

[2] Bousmina, M. (1999). "Rheology of polymer blends: linear model for viscoelastic emulsions." Rheol Acta **38**(1): 73-83

[3] Doi, M. and T. Ohta (1991). "Dynamics and Rheology of Complex Interfaces .1." J Chem Phys **95**(2): 1242-1248

[4] Lee, H. M. and O. O. Park (1994). "Rheology and Dynamics of Immiscible Polymer Blends." J Rheol **38**(5): 1405-1425

[5] Einstein, A. (1906). Ann. Physik 19: 289.

[6] Taylor, G. I. (1932). Proc. Roy. Soc. A 138: 41.

[7] Oldroyd, J. G. (1953). Proc. Roy. Soc. London A218: 122.

[8] Oldroyd, J. G. (1955). Proc. Roy. Soc. London A232: 567.

[9] Kerner, E. H. (1956). "The Elastic and Thermo-Elastic Properties of Composite Media." Proceedings of the Physical Society of London Section B **69**(8): 808-813.

[10] Covas, J. A., A. V. Machado, et al. (2000). "Rheology of PA-6/EPM/EPM-g-MA blends along a twin-screw extruder." Advances in Polymer Technology **19**(4): 260-276.

[11] Zhao, R. and C. W. Macosko (2002). "Slip at polymer-polymer interfaces: Rheological measurements on coextruded multilayers." Journal of Rheology **46**(1): 145-167.

[12] Adhikari, N. P. and J. L. Goveas (2004). "Effects of slip on the viscosity of polymer melts." Journal of Polymer Science Part B-Polymer Physics **42**(10): 1888-1904.

[13] Lacroix, C., M. Aressy, et al. (1997). "Linear viscoelastic behavior of molten polymer blends: A comparative study of the Palierne and Lee and Park models." Rheol Acta **36**(4): 416-428

[14] Graebling, D., R. Muller, et al. (1993). "Linear Viscoelastic Behavior of Some Incompatible Polymer Blends in the Melt - Interpretation of Data with a Model of Emulsion of Viscoelastic Liquids." Macromolecules **26**(2): 320-329.

Appendix B

Silva, J., A. V. Machado and J. Maia, "Rheological behavior of compatibilized and non-compatibilized PA6/EPM blends", Rheol Acta 46, 1091-1097 (2007).

Rheol Acta
DOI 10.1007/s00397-007-0201-z

ORIGINAL CONTRIBUTION

Rheological behavior of compatibilized and non-compatibilized PA6/EPM blends

Jorge Silva · Ana Vera Machado · João Maia

Received: 8 June 2006 / Accepted: 26 April 2007

Abstract The rheological properties of PA-6/EPM polymer blends, non-compatibilized and compatibilized with grafted ethylene propylene rubber (EPM-g-MA), have been investigated. Linear and non-linear (relaxation both in shear and extension) experiments were realized. Stress relaxation experiments coupled with scanning electron microscopy (SEM) analysis showed the existence of one relaxation time and non-deformed droplets for the immiscible blend, and two relaxation times and deformed droplets for the compatibilized ones, the second relaxation being more pronounced for higher compatibilizer contents. These results clearly indicate that, despite the high viscosity and elasticity ratios, if high amounts of compatibilizer are added to the blend, interfacial slip is suppressed and a high-enough adhesion between the phases is achieved for the high-viscosity dispersed phase to be deformed.

Keywords Polymer blends · Compatibilization · Interface · Nonlinear rheology · PA-6/EPM blends · Droplet deformation

Introduction

Blending polymers is a relatively cheap way to generate high performance materials. Blends already represent a large fraction of all plastics produced. Their properties depend strongly on the properties of the components and on the morphology, as most of polymer blends of industrial interest are generally immiscible. However, the behavior of interfaces during polymer blend processing is not well understood yet and is the subject of much ongoing research worldwide.

The first model to predict with relative accuracy the dynamic modulus of a two-phase system with viscoelastic components was proposed by Palierne (1990). Although it is only valid for small-amplitude oscillatory flow, it has been shown to be in good agreement with experimental data (e.g., Graebling et al. 1993). To predict the dynamic moduli of the blend using this model, it is necessary to know the dynamic moduli of the matrix and dispersed phase, the interfacial tension, and the size distribution of the droplets. In the Palierne model, the distribution of droplet radius can be substituted by the volumetric mean radius, provided that the polydispersivity index (R_v/R_n) does not exceed the value of 2 (Graebling et al. 1993).

In terms of the response to extensional flows, Delaby et al. (1994, 1995, 1996a, 1996b) studied blends with well-controlled number and size of droplets and viscosity ratios. The authors found that the droplet deforms less than the macroscopic deformation of the sample when it is more viscous than the matrix and more than the matrix (approximately 5:3 times) when it is less viscous, which is in accordance with the theories of Taylor (1934) and Cox (1969) for vanishing interfacial tension. Delaby et al. (1994, 1995, 1996a, 1996b) also used Palierne's linear model to derive a first-order time evolution deformation of the droplet during start-up of flow. Mighri et al. (1997) used a convergent die to generate an apparent elongation flow and showed that the droplet deformation is not only governed by the viscosity ratio but also by the elasticity ratio, defined as the ratio between the relaxation time of the dispersed phase to that of the matrix. They observed that the droplet deformation increases with

Paper presented at the 3rd Annual European Rheology Conference, April 27–29, 2006, Crete, Greece

J. Silva · A. V. Machado · J. Maia (✉)
Department of Polymer Engineering, IPC—Institute for Polymers and Composites, University of Minho,
4800-058 Guimarães, Portugal
e-mail: jmaia@dep.uminho.pt

increasing elasticity of the matrix and decreases with increasing elasticity of the droplet. The elongational properties of acrylonitrile–butadiene–styrene (ABS) polymer melts were investigated by Takahashi et al. (1997) who showed that strain-hardening could be correlated with the deformability of the butadiene particles. The strain hardening of the samples containing hard butadiene particles was strongly reduced in comparison with soft ones because of a length decrease of the region of elongational flow. Oosterlinck et al. (2005), while studying poly(methyl methacrylate)-polystyrene (PMMA-PS) blends subjected to uniaxial elongation flows, verified that the extra stress due to droplet deformation can, in principle, be deduced from extensional rheological measurements. However, experimental studies about the morphological development of immiscible blends during uniaxial elongational flows are rare, and some aspects, mainly those concerned with the influence of elasticity, need to be clarified.

The elongation and subsequent recovery of PS/PMMA blends, as well as the evolution of morphology, were studied by Gramespacher and Meissner (1997) and, more recently, by Mechbal and Bousmina (2004) and Handge and Pötschke (2004). Pronounced differences were observed in the recovery behavior after melt elongation, that of the blends being much larger than that of the blend components. The results suggest that, in polymer blends, there is a fast molecular recovery related with each component and a slow one associated with interfacial tension.

Over the last years, the use of compatibilizers has become a usual practice because the compatibilizers enhance adhesion between the two phases and stabilize the morphology, leading to a finer morphology. Compatibilization can be achieved by different methods, such as the addition of a pre-synthesized copolymer or creating in situ, during the blending process, a third component, often called an interfacial agent, emulsifier, or compatibilizer (Utracki 1994; Datta and Lohse 1996a, b). This component can be a graft or block copolymer, which tends to be located at the interfaces between the two components of the blend.

The first method, ex situ, has the advantage of better control of the molecular architecture of the compatibilizer. However, it requires specific chemical routes and reaction conditions. In the second method, also called reactive blending or in situ compatibilization, the generation of the compatibilizer is performed in situ at the interfaces directly during blending. To generate the copolymer at the interface, both polymers must have reactive groups. For example, the terminal amine groups of PA-6 can react with maleic anhydride groups of the modified polyolefins. Moreover, because the compatibilizer is formed in situ at the interfaces, the problem of getting it there no longer exists. For these reasons, this second method has become very attractive recently. Nevertheless, because the reaction takes place primarily in the interfaces, it is difficult to control the rate of formation, the amount, and the molecular architecture of the compatibilizer.

In addition, the behavior of the interfaces modified by compatibilizers is not well understood yet. Most of the rheological studies in this area deal with the blends compatibilized with a pre-synthesized block copolymers (Van Puyvelde et al. 2001), revealing a new relaxation process in this type of blends. For example, Riemann et al. (1997) showed that the addition of P(S-*b*-MMA) and P(CHMA-*b*-MMA) block copolymers at PS/PMMA blends originates a new relaxation time, τ_β. Moreover, they observed that the addition of a compatibilizer causes a slight increasing of the shape relaxation time,τ_1. Considering non-isotropic interfacial stress in the Palierne model, the authors predicted the relaxation time τ_β. In fact, some studies (Van Hemelrijck et al. 2004) suggest that the concentration of compatibilizer can change along the droplet interface, leading to an extra stress called the Maragoni stress.

It has been reported that the presence of compatibilizers suppresses droplet coalescence (Van Puyvelde et al. 2001; Van Hemelrijck et al. 2004) and reduces or eliminates interfacial slip. For example, Van Puyvelde et al. (2003), studying PA-6/EPR blends, had observed a negative deviation from the log-additivity rule. They observed that the addition of compatibilizer suppresses slip, significantly increasing the viscosity of the blend. Their studies support the hypothesis that the interfacial slip is due to loss of entanglements in the interfacial region.

The scaling laws of Doi and Ohta (1991) on the shear stress were verified experimentally by Iza et al. (2001) for PS/HDPE blends physically compatibilized with copolymers. However, these authors verified that N_1 does not scale with $\dot{\gamma}$ but with $\dot{\gamma}^{\alpha}$, where α is close to 2. Moreover, it was demonstrated that the amount of compatibilizer, as well as its structure, drastically affects the rheological response to a sudden imposition of a shear rate.

Macaúbas et al. (2005), using blends of PP/PS compatibilized with a linear triblock copolymer (styrene–ethylene–butylene–styrene, SEBS), observed that the scaling laws are not valid for the shear stress. They formulated a model using the ideas of Doi and Ohta (1991), Lacroix et al. (1998), and Bousmina et al. (2001) that was able to predict the behavior of non-compatibilized blends for a single step shear. However, the model does not predict the behavior of compatibilized blends. Finally, Silva et al. (2006) observed that the shear behavior of PA-6/EPM blends is altered by in situ compatibilization. They observed that the addition of EPM-g-MA compatibilizer leads to an increase of dynamic moduli, mainly at low frequencies, and to the appearance of a second longer relaxation time in shear.

From the above review, it results quite clear that the rheological behavior of blends (compatibilized and non-

compatibilized) with high viscosity and elasticity ratios is not well understood yet despite their obvious industrial importance. Thus, the main aim of the present work is to understand the role of the in situ compatibilization of these materials, namely, to assess whether the high viscosity, high elasticity droplets of the dispersed phase are viscoelastically deformed under flow, and what the implications in the overall rheological behavior of the materials are.

Experimental

Materials

Several blends of a commercial polyamide-6 (PA-6 Akulon K123), an ethene–propene rubber (EPM Keltan 740) and an ethene–propene rubber modified with maleic anhydride (EPM-g-MA ExxelorVA 1801, containing 0.49 wt% of MA, as determined by Fourier transform infrared (FTIR), were prepared in a twin-screw extruder under the same process conditions. The PA-6 content was kept constant in all blends, but the amount of modified rubber was varied to have different amounts of maleic anhydride in each blend and, thus, various amounts of compatibilizer at the interface. The chemical and morphological characterizations were performed in a previous work (Machado et al. 1999), some data being summarized in Tables 1 and 2. The volume (R_v) and number (R_n) average radii were calculated using Eqs. 1 and 2:

$$R_v = \frac{\sum_i n_i R_i^4}{\sum_i n_i R_i^3} \tag{1}$$

$$R_n = \frac{\sum_i n_i R_i}{\sum_i n_i} \tag{2}$$

where n_i=number of the droplets having radius R_i.

Table 1 Compounding of the blends

Blend (*w*/*w*/*w*)	PA6 (wt%)	EPM (wt%)	EPM-g-MA (wt%)[a]	MA content of rubber phase (wt%)[b]
80:20:0	80	20	0	0
80:15:5	80	15	5	0.13
80:10:10	80	10	10	0.25
80:5:15	80	5	15	0.37
80:0:20	80	0	20	0.49

[a] MA content of EPM-g-MA is 0.49 wt%.
[b] MA content of the rubber phase is the weight average of the combined EPM and EPM-g-MA rubber phases.

Table 2 Morphological characterization of the blends

Blend (*w*/*w*/*w*)	R_v (μm)	R_n (μm)	R_v/R_n
80:20:0	17.6	5.6	3.1
80:15:5	8.25	1.28	6.5
80:10:10	2.35	1.18	2.0
80:5:15	1.78	1.11	1.6
80:0:20	0.36	0.20	1.8

Shear rheometry

The rheological measurements in shear were performed in a Reologica Stress Tech HR rheometer, using a parallel plate geometry (diameter=25 mm) with a 1,000±1 μm gap. Samples were vacuum dried at 80 °C during 12 h before each rheological experiment.

All oscillatory tests were performed at three different temperatures (240, 260, 280 °C) in a nitrogen atmosphere, time sweep measurements at constant frequency having been performed to ensure that neither polymerization nor degradation occurred during the frequency sweep tests (Figs. 1 and 2).

The stress relaxation experiments were performed at 240 °C in a nitrogen atmosphere; a shear rate of 0.1 s^{-1} during 250 s was applied, and the shear stress upon cessation of flow was measured. Because it is likely that the processing of blends causes degradation (by chain scission/crosslinking) of the polyamide to have comparable results for the PA6 and the blends, the former was also extruded under the same conditions as the latter. Thus, all the results shown below are not for virgin PA6, but for extruded PA6.

Extensional rheometry

The extensional rheological measurements were performed on the modified rotational rheometer (MRR) developed by Maia et al. (1999). For start-up extensional measurements, extruded samples (either in a Leistritz twin-screw extruder blends or in a Rosand RH8-2 capillary rheometer–EPM and EPM-g-MA) were used. For extensional relaxation experiments, samples with rectangular cross-section (about 3× 2 mm) necessary to increase the signal were prepared by compression molding. All the samples were vacuum dried at 80 °C during 12 h before the corresponding rheological experiments.

Upon loading onto the rheometer, residual stresses were allowed to relax; once the measured torque decayed to zero, any existing slack was removed, which was followed by another waiting period for residual stress relaxation; only once the measured torque decayed to zero again would the experiment be started. The effective length of each sample

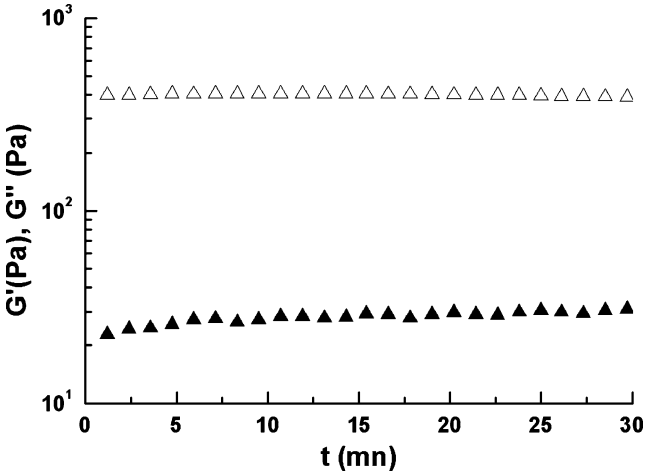

Fig. 1 Dynamic moduli of PA6 measured at a constant frequency (0.1 Hz) at 260 °C in a nitrogen atmosphere

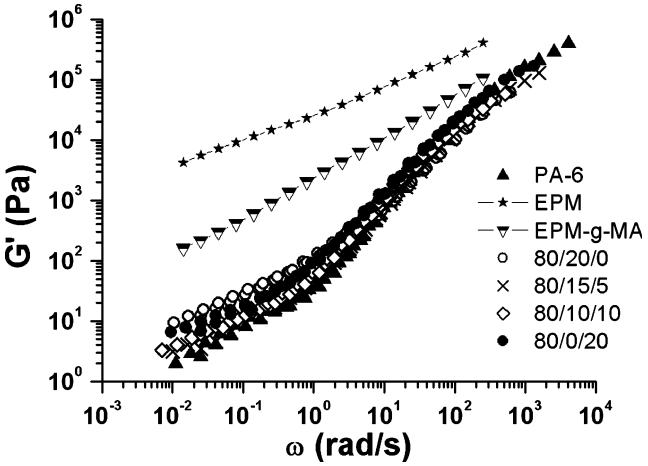

Fig. 3 Storage modulus for several blends of PA6/EPM/EPM-g-MA and their components

was 40 mm, and the diameter varied between 2 and 3 mm, thus, yielding an aspect ratio, L/D, ranging between approximately 13 and 20, which has been shown (Barroso et al. 2002) to be high enough for end effects to be negligible. During all the experiments, the samples were immersed in silicone oil at 240 °C for the dual purpose of temperature control and sagging prevention. The particular details on the experimental technique to measure the stress relaxation after an extensional step strain are given in Barroso and Maia (2002).

The main motivation for performing extensional rheometry experiments on these samples is related to the fact that their viscosity and elasticity ratios are very high (see below) and, therefore, any differences in rheological behavior, especially due to interfacial phenomena, between the immiscible and the compatibilized blends are likely to be better seen in extensional flows than is shear (e.g., Oosterlinck et al. 2005).

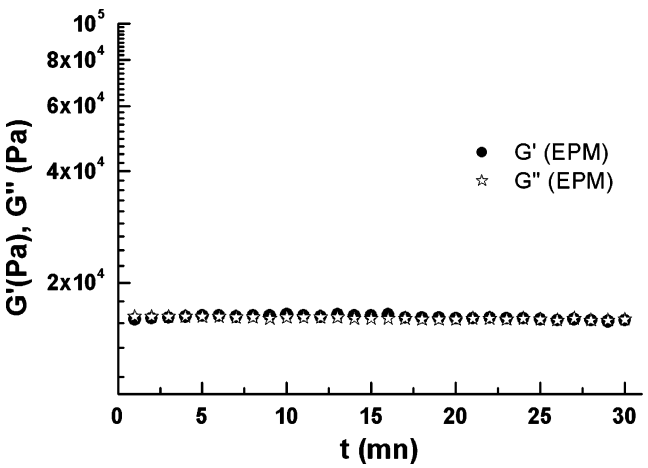

Fig. 2 Dynamic moduli of EPM measured at a constant frequency (0.1 Hz) at 240 °C

Morphology

To study the morphology of samples undergoing extensional deformations, the oil bath was rapidly removed during an experiment and the deformed sample was quenched in liquid nitrogen (the whole process takes only 2 to 3 s) while the deformation is still being imposed. This means that no significant morphological changes, such as droplet relaxation and/or coalescence, should occur during the quenching process. Once solidified, the samples were fractured longitudinally in liquid nitrogen, etched with boiling xylene to remove the rubber from the surface and gold plated; their morphology was studied using a Jeol JSM 6310F scanning electron microscope.

Results and discussion

Figures 3 and 4 show the dynamic moduli of the blends and their components (PA-6, EPM, EPM-g-MA). Time–temperature superposition was performed at a reference temperature of 260 °C for PA-6 and the blends. From the figures, it is possible to observe that the *t*–*T* superposition works well at high frequencies, while at low frequencies, there is some scatter in the data, and it is possible that, especially at the higher temperatures, sample degradation is starting to set in. However, because the experiments were performed in a nitrogen atmosphere, this is not very likely; in addition, because the scatter is not large enough to mask the qualitative behavior of the G′ and G″ curves, the option was made to keep the data.

The figures show that the blends have different qualitative behaviors depending on the amount of compatibilizer. At high frequencies, all the blends except the one with the highest compatibilizer content show an effect commonly known as negative deviation behavior, NDB, which origi-

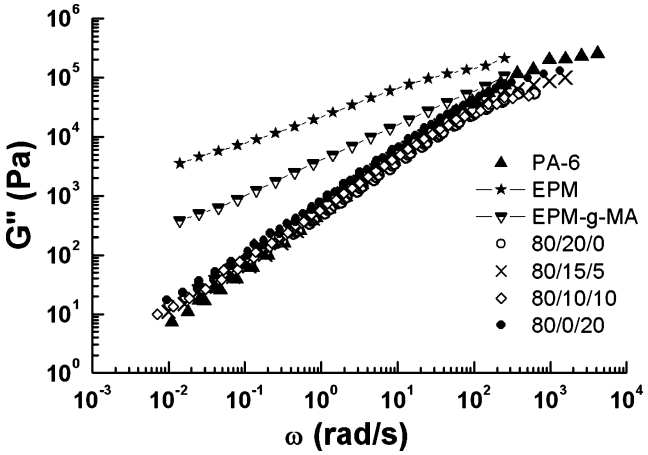

Fig. 4 Dissipative modulus for several blends of PA6/EPM/EPM-g-MA and their components

nates in slip at the interfaces (Utracki 1983; Van Puyvelde et al. 2003) due to poor or insufficient compatibilization between the matrix and the dispersed phase. At low frequencies, an increase in the moduli of the blends can be noticed. This is especially noticeable at very low frequencies where a plateau in G′, which has been related to the size of the particles of the dispersed phase and the amount of compatibilizer at the interfaces (Riemann et al. 1997; Van Hemelrijck et al. 2004), seems to develop.

Again, it could be argued that this plateau could also be attributed to changes in rheological properties of the components during the experiment, e.g., degradation. However, as shown in Figs. 1 and 2, the rheological behavior of PA-6 and EPM remains very much constant in time at the time-scale of the experiments.

Because the viscosity ratios are very high (approximately 50 and 400 between PA6 and EPM, at 3×10^{-3} Hz), the Palierne model is not able to predict, even qualitatively, these results.

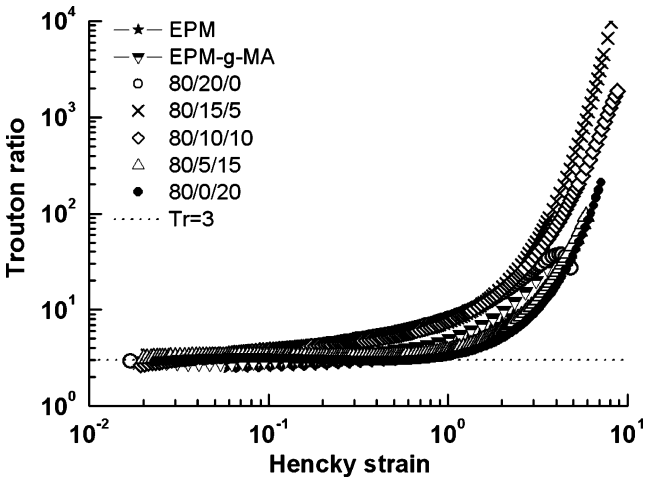

Fig. 5 Trouton ratios for all blends. Strain rates, $\dot{\varepsilon}$: 80/20/0, 0.10 s^{-1}; 80/15/5, 0.11 s^{-1}; 80/10/10, 0.16 s^{-1}; 80/5/15, 0.14 s^{-1}; 80/0/20, 0.13 s^{-1}; EPM, 0.10 s^{-1}; EPM-g-MA, 0.11 s^{-1}

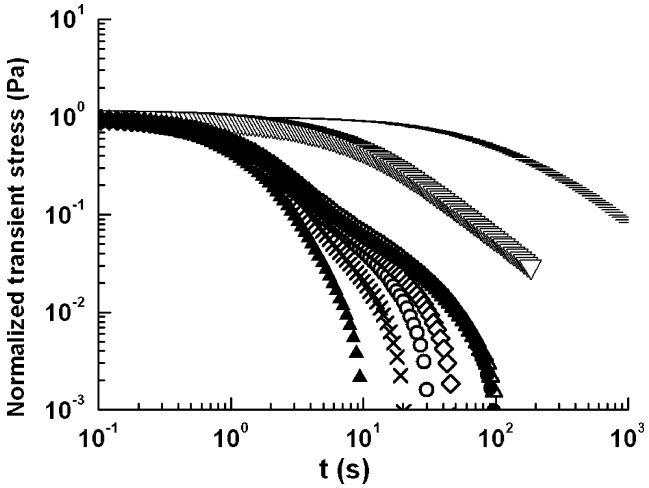

Fig. 6 Normalized transient stress for several blends of PA6/EPM/EPM-g-MA and their components after cessation of a shear flow of 0.1 s^{-1}. *Filled triangle* PA-6, *bar* EPM, *inverted open triangle* EPM-g-MA, *open circle* 80/20/0, *cross* 80/15/5, *diamond* 80/10/10, *open triangle* 80/5/15, *filled circle* 80/0/20

Figure 5 shows the transient Trouton ratios for all the materials in uniaxial extension (except PA6 that was not possible to test due to its low viscosity), the main features being:

(a) All the materials show a pronounced strain hardening due to the existence of a rubber phase. In the non-compatibilized blend, the degree of strain hardening is much smaller than in the remainder, which is a further indication of poor adhesion between the two phases.
(b) The onset of strain hardening is much lower (of the order ε_H=0.1) for the non-compatibilized and the insufficiently compatibilized blends (EPM-g-MA content equal or lower than 10%) than for those with higher MA contents (of the order ε_H=1).

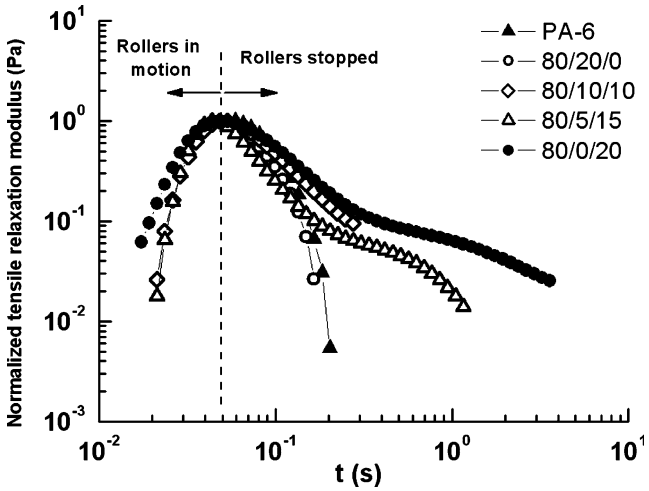

Fig. 7 Normalized relaxation modulus flow for the blends and their components. Strain rates are PA-6, 15.6 s^{-1}; 80/20/0, 0.98 s^{-1}; 80/10/10, 0.98 s^{-1}; 80/5/15, 0.24 s^{-1}; 80/0/20, 0.54 s^{-1}

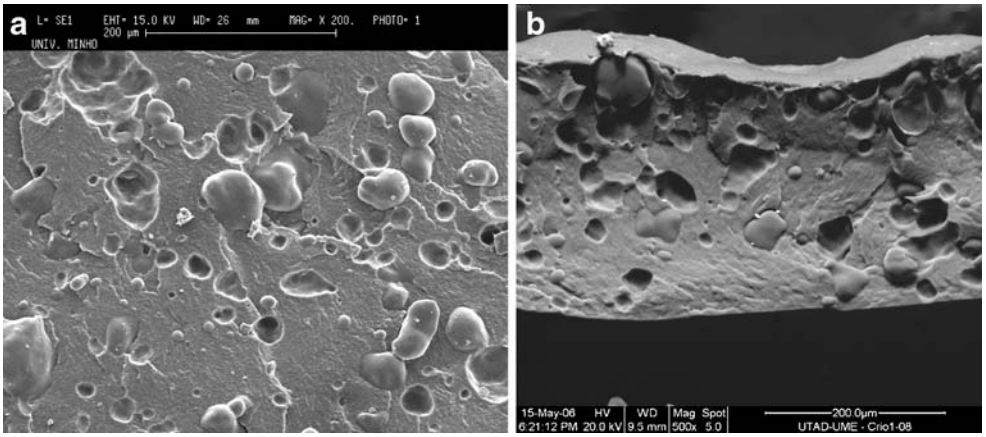

Fig. 8 SEM micrographs of the fracture surfaces of the 80/20/0 blend: **a** non-deformed sample and **b** after extension (the sample was stretched during 5 s at a strain rate of 0.08 s^{-1})

Again, this is presumably due to the better adhesion between the phases; i.e., the presence of the rubber stabilizes the blend and increases the range of linear viscoelastic response (note that the onset of strain hardening for the EPM and EPM-g-MA are very similar to those of the 15 and 20% EPM-g-MA blends).

Shear stress relaxation measurements (Fig. 6) illustrated that all blends relax in two consecutive steps. The first (faster) step should be related with the relaxation of the PA-6 matrix, and the second (slower) step is probably due to relaxation of EPM and/or interfaces. In this case, particle size and interfacial adhesion play a determinant role in the shear stress relaxation function. For the compatibilized blends, the second relaxation time increases in duration with increasing amount of compatibilizer up to a EPM-g-MA content of 15%, which indicates that the effect is related with a better adhesion at the interfaces and saturates at 15% EPM-g-MA concentration. An interesting feature in Fig. 6 is that the second relaxation time of the 80/15/5 blend is slightly shorter than the one of the non-compatibilized blend, which indicates that low compatibilizer amounts are enough to decrease significantly the droplets' average size but not to prevent the slip between the phases.

As in the shear relaxation experiments, in the extensional relaxation (after a step strain) experiments, the compatibilized blends exhibits higher relaxation times (Fig. 7). Once more, the fast relaxation time can be attributed to the PA-6 matrix and the slow one to the interface and/or rubber dispersed phase. This suggests that the presence of slip at the interface inhibits the deformation of dispersed phase droplets and that this effect is corrected with the addition of EPM-g-MA. However, this needs to be confirmed by a morphological analysis of stretched samples on a SEM.

Representative results of the morphological analysis are depicted in Figs. 8 and 9 for the non-compatibilized and the highest compatibilizer content blends, respectively. Figure 8 shows the morphologies of the non-compatibilized blend (a) before extension and (b) quenched during extension, and the similarities are immediately apparent: in both cases, droplets are essential spherical. Thus, there was no (or only negligible) deformation of the rubber phase upon extension due to interfacial slip. In the compatibilized blend, the average droplet size is much smaller, as would be expected, and the morphologies before (Fig. 9a) and after (Fig. 9b) extension are quite different. In the former case, the expected spherical droplet morphology is seen, and in the latter, the droplets are very elongated, but still quite large. This is an indication that the compatibilizer was present in an enough content to make the drag force on the droplets overcome the resistance to flow/deformation of the rubber phase (note that the viscosity ratio is very high in these materials).

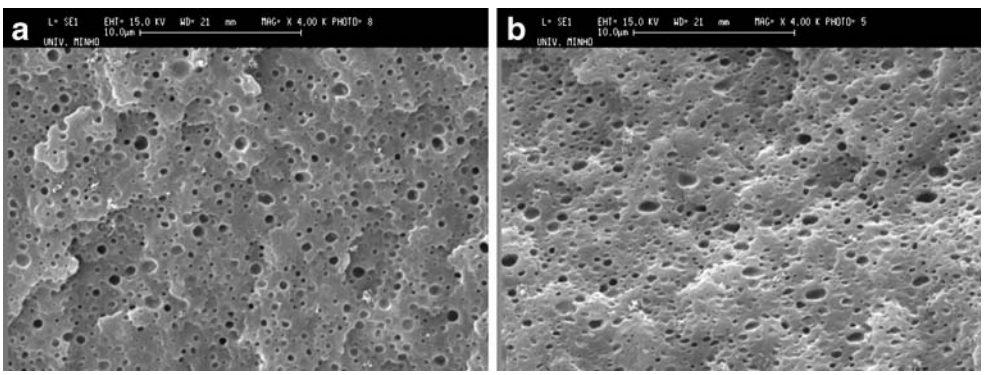

Fig. 9 SEM micrographs of the fracture surfaces of the 80/0/20 blend: **a** non-deformed sample and **b** after extension (the sample was stretched during 5 s at a strain rate of 0.08 s^{-1})

Conclusions

In the present work, the rheological proprieties of immiscible and compatibilized blends with high viscosity and elasticity ratios were studied. Despite this fact, the rubber droplets do not exhibit a rigid sphere-like behavior. In fact, oscillatory shear, uniaxial extension, and stress relaxation experiments (in both shear and extension) showed the existence of one relaxation time for the immiscible blend and two for the compatibilized ones that, in all cases, is more pronounced for higher compatibilizer contents. Together with SEM evidence of the existence of elongated droplets after extension for the compatibilized blends and spherical ones in the non-compatibilized ones, these results clearly indicate that, despite the high viscosity and elasticity ratios, if high enough amounts of compatibilizer are added to the blend, interfacial slip is suppressed and a high-enough adhesion between the phases is achieved for the high-viscosity dispersed phase to be deformed.

Acknowledgment The authors would like to thank to the Foundation for Science and Technology–FCT for awarding one of them (Jorge Silva) a PhD Fellowship (ref. BD/12833/2003) within the framework of Programa Operacional "Ciência, Tecnologia, Inovação" (POCTI) and Programa Operacional Sociedade da Informação (POSI) of the Quadro Comunitário de Apoio III (2000–2006).

References

Barroso VC, Maia JM (2002) Evaluation by means of stress relaxation (after a step strain) experiments of the viscoelastic behavior of polymer melts in uniaxial extension. Rheol Acta 41:257–264

Barroso VC, Covas JA, Maia JM (2002) Sources of error and other difficulties in extensional rheometry revisited: commenting and complementing a recent paper by T. Schweizer. Rheol Acta 41: 154–161

Bousmina M, Aouina M, Chaudhry B, Guenette R, Bretas RES (2001) Rheology of polymer blends: non-linear model for viscoelastic emulsions undergoing high deformation flows. Rheol Acta 40:538–551

Cox RG (1969) Deformation of a drop in a general time-dependent fluid flow. J Fluid Mech 37:601–623

Datta S, Lohse D (1996) Polymeric compatibilizers. Hanser, Munich

Datta S, Lohse D (1996) Polymeric compatibilizers, uses and benefits in polymer blends. Hanser, Munich

Delaby I, Ernst B, Germain Y, Muller R (1994) Droplet deformation in polymer blends during uniaxial elongational flow-influence of viscosity ratio for large capillary numbers. J Rheol 38:1705–1720

Delaby I, Ernst B, Muller R (1995) Drop deformation during elongational flow in blends of viscoelastic fluids. Small deformation theory and comparison with experimental results. Rheol Acta 34:525–533

Delaby I, Ernst B, Muller R (1996a) Drop deformation in polymer blends during elongational flow. J Macromol Sci Phys B35:547–561

Delaby I, Ernst B, Froelich D, Muller R (1996b) Droplet deformation in immiscible polymer blends during transient uniaxial elongational flow. Polym Eng Sci 36:1627–1635

Doi M, Ohta T (1991) Dynamics and rheology of complex interfaces, 1. J Chem Phys 95:1242–1248

Graebling D, Muller R, Palierne JF (1993) Linear viscoelastic behavior of some incompatible polymer blends in the melt-interpretation of data with a model of emulsion of viscoelastic liquids. Macromolecules 26:320–329

Gramespacher H, Meissner J (1997) Melt elongation and recovery of polymer blends, morphology, and influence of interfacial tension. J Rheol 41:27–44

Handge UA, Potschke P (2004) Interplay of rheology and morphology in melt elongation and subsequent recovery of polystyrene/poly (methyl methacrylate) blends. J Rheol 48:1103–1122

Iza M, Bousmina M, Jerome R (2001) Rheology of compatibilized immiscible viscoelastic polymer blends. Rheol Acta 40:10–22

Lacroix C, Grmela M, Carreau PJ (1998) Relationships between rheology and morphology for immiscible molten blends of polypropylene and ethylene copolymers under shear flow. J Rheol 42:41–62

Macaubas PHP, Demarquette NR, Dealy JM (2005) Nonlinear viscoelasticity of PP/PS/SEBS blends. Rheol Acta 44:295–312

Machado AV, Covas JA, Van Duin M (1999) Chemical and morphological evolution of PA-6/Epm/Epm-g-MA blends in a twin screw extruder. J Polym Sci Polym Chem 37:1311–1320

Maia JM, Covas JA, Nobrega JM, Dias TF, Alves FE (1999) Measuring uniaxial extensional viscosity using a modified rotational rheometer. J Non-Newton Fluid Mech 80:183–197

Mechbal N, Bousmina M (2004) Uniaxial deformation and relaxation of polymer blends: relationship between flow and morphology development. Rheol Acta 43:119–126

Mighri F, Ajji A, Carreau PJ (1997) Influence of elastic properties on drop deformation in elongational flow. J Rheol 41: 1183–1201

Oosterlinck F, Mours M, Laun HM, Moldenaers P (2005) Morphology development of a polystyrene/polymethylmethacrylate blend during start-up of uniaxial elongational flow. J Rheol 49:897–918

Palierne JF (1990) Linear rheology of viscoelastic emulsions with interfacial-tension. Rheol Acta 29:204–214

Riemann RE, Cantow HJ, Friedrich C (1997) Interpretation of a new interface-governed relaxation process in compatibilized polymer blends. Macromolecules 30:5476–5484

Silva JM, Machado AV, Maia JM (2006) Transient rheological behaviour of PA6/EPM/EPM-g-MA blends. Adv Mater Forum III 514–516:853–857

Takahashi T, Wu WG, Toda H, Takimoto J, Akatsuka T, Koyama K (1997) Elongational viscosity of ABS polymer melts with soft or hard butadiene particles. J Non-Newton Fluid Mech 68:259–269

Taylor GI (1934) The formation of emulsions in definable fluids of flow. Proc R Soc A 146:501–523

Utracki LA (1983) Melt flow of polymer blends. Polym Eng Sci 23: 602–609

Utracki LA (1994) Encyclopaedic dictionary of commercial polymer blends. ChemTec, Toronto

Van Hemelrijck E, Van Puyvelde P, Velankar S, Macosko CW, Moldenaers P (2004) Interfacial elasticity and coalescence suppression in compatibilized polymer blends. J Rheol 48:143–158

Van Puyvelde P, Velankar S, Moldenaers P (2001) Rheology and morphology of compatibilized polymer blends. Curr Opin Colloid Interface Sci 6:457–463

Van Puyvelde P, Oommen Z, Koets P, Groeninckx G, Moldenaers P (2003) Effect of reactive compatibilization on the interfacial slip in nylon-6/EPR blends. Polym Eng Sci 43:71–77

Appendix C

Silva, J., A. V. Machado, P. Moldenaers, J. Maia, "The effect of interfacial properties on the deformation and relaxation behavior of PMMA/PS blends" (2009) Submitted to *Journal of Rheology.*

The effect of interfacial properties on the deformation and relaxation behavior of PMMA/PS blends

J. Silva, A. V. Machado

Department of Polymer Engineering, I3N—Institute of Nanostructures, Nanomodelling and Nanofabrication, University of Minho, 4800-058 Guimarães, Portugal

P. Moldenaers

Department of Chemical Engineering, Katholieke Universiteit Leuven, W. de Croylaan 46 – B 3001 Heverlee (Leuven),Belguium

J. Maia[a)]

Department of Polymer Engineering, I3N—Institute of Nanostructures, Nanomodelling and Nanofabrication, University of Minho, 4800-058 Guimarães, Portugal

Department of Macromolecular Science and Engineering, Case Western Reserve University, Cleveland, OH 44106-7202

a) Corresponding author

Synopsis

This work aims at studying the role of interface properties on the rheological behavior of uncompatibilized and compatibilized polymer blends. Blends of polymethylmetacrylate, PMMA, with polystyrene, PS, and PS functionalized with oxazoline, PSOX, with concentrations of up to 20 w/w% of the dispersed phase were used. It was observed that until a critical concentration is reached the increase of PSOX content leads to a significant increase of a) the elasticity at low frequencies b) the relaxation time after cessation of flow, both in shear and extension. This points to a likely significant role played by interface elasticity. Since no chemical reactions occur between PMMA and the oxazoline groups of PSOX the latter is probably caused by the creation of additional physical entanglements by the oxazoline groups. Beyond this critical concentration, the amount of PSOX does not have a significant influence on the rheological behavior of the blends, which is an indication that the entanglement density at the interface reaches a maximum and so does its elasticity. In order to gain an insight into the relaxation dynamics of the droplets and interface and their relationship with the rheological behavior of the blends, Small Angle Light Scattering (SALS) was used in diluted blends (1 wt % of the dispersed phase) during step shear. SALS shows a slight deformation of dispersed phase in the

vorticity direction for the 99PMMA/1PSOX blend while the droplets of the 99PMMA/1PS blend deforms in the flow direction only. This result confirms the big increase in the interfacial elasticity.

I. INTRODUCTION

Blending polymers allows for the development of materials with enhanced proprieties with much less effort than that required to synthesize a completely new polymer and blends already represent a large fraction of all plastics produced. For example, in 2001 approximately 10% of all thermoplastics and 75% of all elastomers were processed as blends [Ehrenstein (2001)] and these numbers have grown further in recent years. The properties of the blends depend strongly on the properties of the components, on the interfacial properties and on the final morphology, as most polymer blends of industrial interest are generally immiscible. Usually, the immiscible blends reveal poor interfacial adhesion, their morphology is coarse and unstable and consequently the mechanical properties are bad. To overcome these difficulties and develop materials with the required properties, compatibilization is often required.

Compatibilization can be achieved by different methods, such as through the addition of a pre-synthesized copolymer or by creating chemically and in situ, during the blending process, a third component, often called an interfacial agent, emulsifier, or compatibilizer [Datta and Lohse (1996a), Datta and Lohse (1996b), Utracki (1994)]. This component can be a graft or block copolymer, which tends to be located at the interface between the two components of the blend. The first method, ex situ, has the advantage of better control of the molecular architecture of the compatibilizer. However, it requires specific chemical routes and reaction conditions. In the second method, also called reactive blending or in situ compatibilization, the generation of the compatibilizer is performed in situ at the interface directly during blending. Another strategy to enhance the compatibility of the immiscible blends is by increasing specific interactions between polymers, such as Van der Waals interactions, hydrogen bonding, ion-dipole interaction and ion-ion interactions [He *et al.* (2004), Koning *et al.* (1998)].

Compatibilization increases the interfacial adhesion between the components of the blend [Van Puyvelde *et al.* (2003)], produces a finer morphology, delays the coalescence of the dispersed phase [Van Hemelrijck *et al.* (2004), Van Puyvelde *et al.* (2001)] and increases the interfacial elasticity. As could be expected, these differences in the interfacial proprieties and morphology induce different rheological responses of the blends, when subjected to flow. For example, when submitted to small amplitude oscillatory shear, immiscible binary blends show a higher elasticity in the low frequency

range than that of the combined individual components. The higher value of elasticity of the blends can result in the presence of a secondary plateau at low frequencies in the storage modulus vs frequency curve. That phenomenon is due to the relaxation of the shape of the dispersed phase when shear deformed [Graebling *et al.* (1993), Oosterlinck *et al.* (2005)]. In the case of compatibilized blends, there are several experimental studies that present evidence for an additional relaxation time. This relaxation time can be attributed to the relaxation of Marangoni stresses tangential to the interface between the dispersed phase and the matrix [Riemann *et al.* (1997), Van Hemelrijck *et al.* (2004)]. They are caused by a gradient of interfacial tension, induced by a gradient of compatibilizer concentration at the interface [Van Hemelrijck *et al.* (2004), Van Puyvelde *et al.* (2001)].

A generalized version of the Palierne model [Jacobs *et al.* (1999)], which includes an interfacial shear modulus, predicts this additional relaxation time in compatibilized blends. Several authors [Yee *et al.* (2007); Huo *et al.* (2007); Shi *et al.* (2002); Asthana and Jayaraman (1999)] used this model and obtained good agreement with the experimental data of the compatibilized blends. However, Sailer and Handge (2007), studying blends of PA 6/SAN compatibilized with styrene-acrylonitrile-maleic anydrid terpolymer (SAN-MA)concluded that the generalized Palierne model could not be fitted to the experimental data for reasonable values of interfacial tension and interfacial shear modulus.

In what concerns the behavior of immiscible polymer blends when subjected to extensional flows, some studies are available in the literature, but in much less quantity than for shear flows. The elongation and subsequent recovery of poly(methylmethacrylate)-polystyrene (PMMA/PS) blends, as well as the evolution of the morphology, were studied by Gramespacher and Meissner (1997) and, more recently, by Mechbal and Bousmina (2004) and Handge and Potschke (2004). In terms of recovery after melt elongation, the results suggest that, as in shear flows, there is a fast molecular recovery related with each component and a slow one associated with interfacial tension. In terms of elongational flow, Mechbal and Bousmina (2004) observed that the behavior of a PMMA/PS (95/5) blend is mainly dominated by the matrix. Oosterlinck *et al.* (2005), while also studying PMMA/PS blends subjected to uniaxial elongational flows, verified that the extra stress due to droplet deformation can, in principle, be deduced from extensional rheological measurements.

Experimental studies about the behavior of compatibilized blends in extensional flows are even less abundant. Mechbal and Bousmina (2007) studied the effect of the diblock

copolymer addition on the rheology and morphology development during uniaxial elongation and during relaxation after cessation of flow on a PMMA/PS blend with viscosity ratio lower than 1. They observed that when the concentration of the copolymer is above a critical concentration, the interface becomes saturated, the droplets are less deformed and the relaxation is slower. They postulated that this behavior is due to local entanglements, which resist deformation. Moreover, it was concluded that if the molecular weight of copolymer is smaller than the critical molecular weight of entanglement of both PS and PMMA then the copolymer does not affect the stress relaxation behavior.

Also, rheological transient shear experiments have shown that the compatibilization has an important effect on rheological properties [Iza *et al.* (2001), Macaubas *et al.* (2005), Silva *et al.* (2007)], which suggest a large contribution of the modified interface to the overall behavior.

In the previous work by the present authors [Silva *et al.* (2007)] it was shown that the relaxation behavior after both shear and extensional deformations of blends of polyamide-6, PA6, and highly elastic ethylene-propylene copolymer, EPM, varied markedly between immiscible and compatibilized blends. Although all materials showed a two-step relaxation process, the difference in time scale of the second slower process between the immiscible and the compatibilized was very large (nearly two orders of magnitude). Morphological analysis showed that the dispersed EPM droplets were not elongated in the uncompatibilized blend, but were slightly elongated in the highly compatibilized one, despite the fact that the viscosity ratios were very high in both cases (in excess of 10 for the compatibilized blend and of 100 for the uncompatibilized one). Although at the time the second relaxation process was attributed to the relaxation of the EPM droplets, the role of the compatibilizer at the interface on the relaxation mechanism still remains unanswered. Thus, the main aim of this work is to complement the previous one through the study of the linear and non-linear viscoelastic and rheo-optical behavior of PS/PMMA and PSOX/PMMA polymer blends. It is neither known nor expected a priori that any chemical reaction between oxazoline and PMMA occurs. Nevertheless, it is expected that the oxazoline groups promote new physical interactions that change the dynamic of interface. Thus, the characteristics of the interface and the subsequent deformation and relaxation mechanisms will be investigated. The main reason for this choice of polymers was that it is expected that they will allow the relative effect of interface structure to be studied in details since they are both optically transparent, which facilitates rheo-optical measurements. The components are also relatively inelastic, thus allowing disperse

phase elasticity to be negligible while still showing relatively high viscosity ratios (between 2 and 4 at the relevant shear and extension rates) so that the dispersed phase deformation is still relatively small.

II. EXPERIMENTAL

A. Materials

The blend components are commercial grades of polymethylmethacrylate (PMMA, Altuglas VSE UVT, MFI 27g/10min at 230ºC with 3.8Kg) and polystyrene (PS, Solarene G116, MFI 2.3g/10min at 200ºC with 5Kg). The oxazoline functionalized polystyrene (PSOX, Epocros RPS-1005, 6-10 g/10 min at 200ºC with 5Kg) (FIG. 1) was provided by Nippon Shokubai. In the PSOX the weight of oxazoline groups corresponds to 1.9% of the total weight.

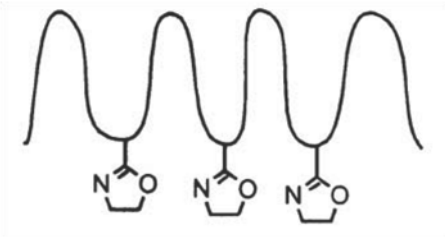

FIG. 1. Schematic of a PS chain functionalized with oxazoline.

B. Compounding

A series of blends of PMMA/PS/PSOX were prepared in this work. The concentration of the PMMA matrix was keep constant (80 w/w%) while those of PS and PSOX were varied from a maximum of PS and no PSOX (80/20/0 PMMA/PS/PSOX) to the opposite situation, i.e., 20 w/w% of PSOX and no PS (80/0/20 PMMA/PS/PSOX). Moreover, two diluted blends (99/1/0 PMMA/PS/PSOX and 99/0/1 PMMA/PS/PSOX) were also prepared. A Haake batch mixer at a set temperature of 210 ºC and a rotor speed of 80 rpm was used to compound the blends. The sample was removed from the mixer after a mixing time of 600 s.

C. Morphology

The morphology of all the blends was analyzed by SEM (Scanning Electron Microscopy). The samples were fractured in liquid nitrogen and then the PS/PSOX

phase was removed in cyclohexane at 50ºC during 1h. The morphology of the blends was studied, after gold plating the samples, using a Jeol JSM 6310F Scanning Electron Microscope.

D. Rheometry

The rheological measurements were performed in an ARES rheometer (TA Instruments). Samples were vacuum dried at 80ºC during 12h before each rheological experiment. Since degradation may occur during blend preparation, in order to have comparable results for the pure components and the blends, the former were also subjected to the same processing conditions in the mixer.

Oscillatory tests were performed for the pure components and blends at 230ºC, using a parallel-plate geometry with a $1000 \pm 1\ \mu m$ gap. For the samples with lowest moduli 50 mm plates were used in order to increase the signal, whilst for the remainder 25 mm diameter plates were used. Stress relaxation experiments after shear were performed at 230 ºC using the same geometry; a shear rate of 0.1 s^{-1} during a time interval of 250 s, which is enough to reach the steady state, was applied and the evolution of the shear stress upon cessation of flow was measured.

The extensional rheological measurements were performed on the MRR (Modified Rotational Rheometer) developed by Maia *et al.* (1999) at 205 ºC (the highest temperature at which the sample yielded a strong enough signal to be measured). For both extensional start-up and relaxation extensional experiments, samples with rectangular cross-section (about 3×2 mm), prepared by compression molding, were used in order to increase the signal (force) measured by the rheometer. Upon loading onto the rheometer, residual stresses were first allowed to relax; once the measured torque decayed to zero any existing slack was removed and once again the stresses were allowed to relax. The effective length of each sample was 40 mm and the diameter varied between 2 and 3 mm, thus yielding an aspect ratio, L/D, ranging between approximately 13 and 20. This has been shown [Barroso *et al.* (2002)] to be high enough for shear-related end-effects to be negligible. During all experiments the samples were immersed in silicone oil at the test temperature for the dual purpose of temperature control and sagging prevention. The particular details on the experimental technique to measure the stress relaxation after an extensional step strain are given in Barroso and Maia (2002) and Barroso *et al.* (2003).

E. Small Angle Light Scattering (SALS)

Small angle light scattering measurements (SALS) were performed to study the deformation of the droplets and the interface. Light emerging from a He-Ne laser ($\lambda = 633\ nm$) is sent through the sample that is contained within a Linkam shear cell (CSS 450). The anisotropy of the SALS patterns can be quantified calculating a second moment tensor from the measured light intensity on the 2D CCD array. Then, the anisotropy, ε, is given by the difference between the eigenvalues of this tensor [Borschig *et al.* (2000)]:

$$\varepsilon(\dot{\gamma}, t) = \frac{\left[\left(\int d\vec{q} q_x q_x I(q, \dot{\gamma}, t) - \int d\vec{q} q_y q_y I(q, \dot{\gamma}, t)\right)^2 + 4 \int d\vec{q} q_x q_y I(q, \dot{\gamma}, t)^2\right]^{0.5}}{\int d\vec{q} I(q, \dot{\gamma}, t)} \quad (1)$$

This calculation was done using in house developed SalsSoftware from K. U. Leuven. To avoid multiple scattering only the diluted blends (99/1/0 and 90/0/1) were used in the SALS experiments. The experiments were performed at 230ºC.

III. RESULTS AND DISCUSSION

A. Viscosity ratios of the pure components

Fig. 2a shows the steady state and the complex viscosities of the pure components as functions of shear rate and frequency, respectively. These materials are thermorheologically simple and thus the Cox-Mertz rule is valid. Fig. 2b shows the viscosity ratios between the two polystyrenes (with and without oxazoline) and the PMMA matrix at 230 ºC. At low frequencies the viscosity ratios between PS and PMMA and PSOX and PMMA are 3.8 and 1.6, respectively. They decrease as the frequency increases reaching values approaching unity at high frequencies. This behavior means that the stress relaxation experiments (which were performed after the imposition of a shear rate of 0.1 s^{-1}) were performed in blends of relatively high viscosity ratios.

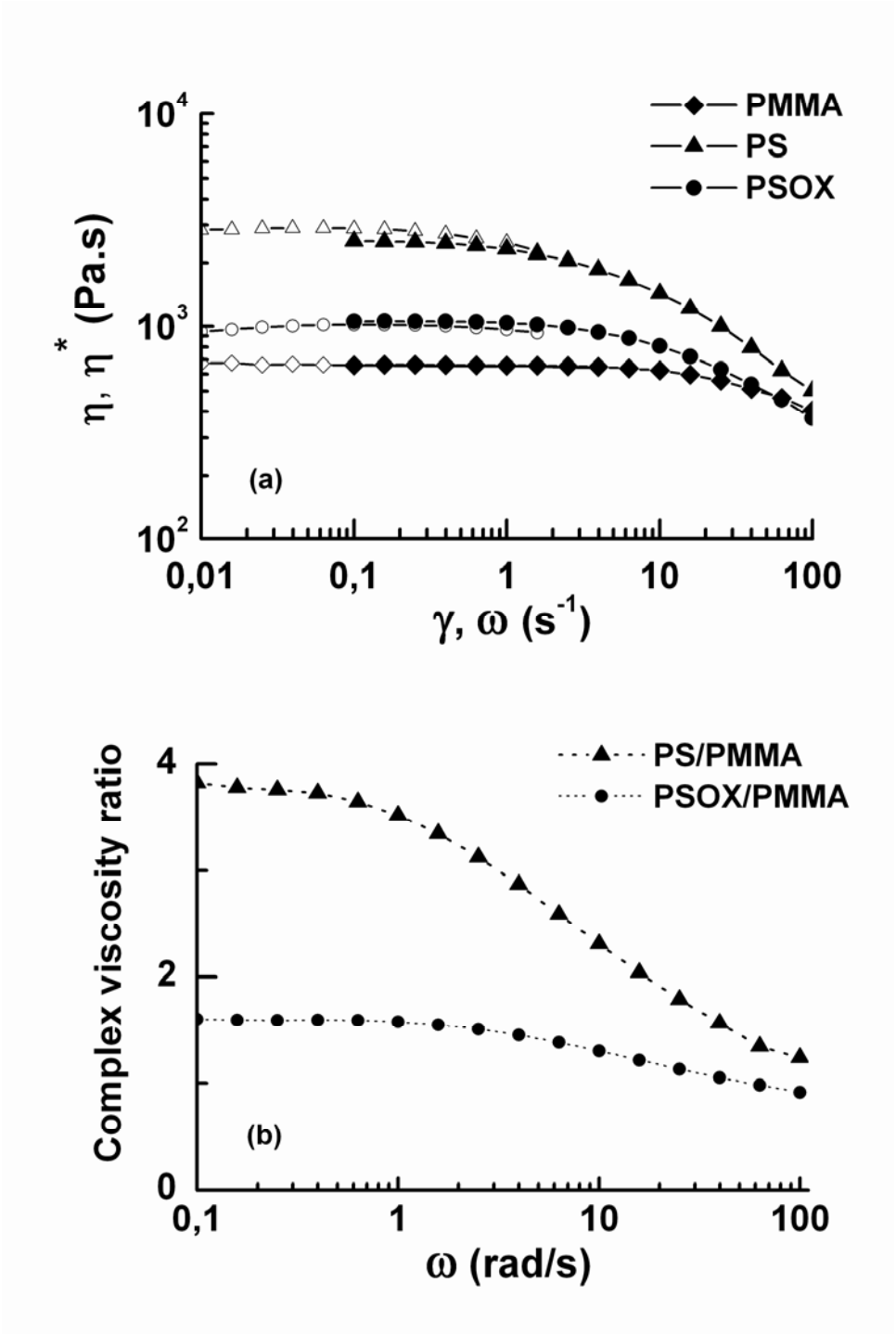

FIG. 2. (a) Viscosities of the pure components at 230ºC. The open symbols are the steady shear viscosity; the full symbols are the complex viscosity. (b) Viscosity ratios at 230ºC.

B. Blend morphology

The morphology of the blends after the mixing process was analyzed by SEM. The blends with 20% dispersed phase show similar morphologies. They exhibit droplet-matrix morphology with similar droplet sizes, R_n varying between 0.3 and 0.4 μm and

R_v/R_n between 1.6 and 1.8. The dilute blends (with 1% of dispersed phase), also show droplet-matrix morphology but with smaller droplet sizes (R_n=0.09 μm for both 99/1/0 and 99/0/1 and R_v/R_n=1.1 and 1.2 for 99/1/0 and 99/0/1, respectively).

Since the process conditions were the same for all blends, the differences in the morphology of the diluted and concentrated blends is due to the fact that in the former are less prone to coalescence than the latter (in the uncompatibilized blends) because the probability of collision of two droplet is lower and because the dynamic equilibrium is established at lower droplet sizes [Grizzuti and Bifulco (1997), Vinckier ***et al.*** (1998)].

C. Linear Viscoelastic behavior

The dynamic storage and loss moduli of the three pure components and the concentrated blends, at 230ºC, are shown in the Figures 3a) and b) respectively. The PMMA/PS blend shows a shoulder in G', which is a typical behavior for an immiscible polymer blend. Moreover, their dynamic moduli can be fitted to the Palierne model. In the blends containing modified polystyrene it was observed that the increase of PSOX concentration causes an increase of the dynamic moduli at low frequencies. In G' this increase is very large when the PSOX concentration goes from 7.5 to 10% wt and remains nearly constant thereafter, thus indicating that there may exist a critical concentration of PSOX above which there are no significant changes in rheological behavior as a function of %PSOX added. Moreover, the observed plateau (also previously observed by other authors in compatibilized blends, e.g., Yee et al. (2007), Sailer and Handge (2007) and Fahrlander et al. (2001)), suggests that the extra interactions at the interface play a crucial role in the rheological behavior, inclusively being more important than the average size and size distribution of the dispersed phase. Thus, it seems that the amount of oxazoline has an important role in the elasticity of the interfaces.

This behavior cannot be explained by the relaxation of droplets of the dispersed phase only. For example, if one tries to fit any form of the Palierne model to the data of the blends with higher concentrations of PSOX, the obtained values of the interfacial tension are totally unrealistic.

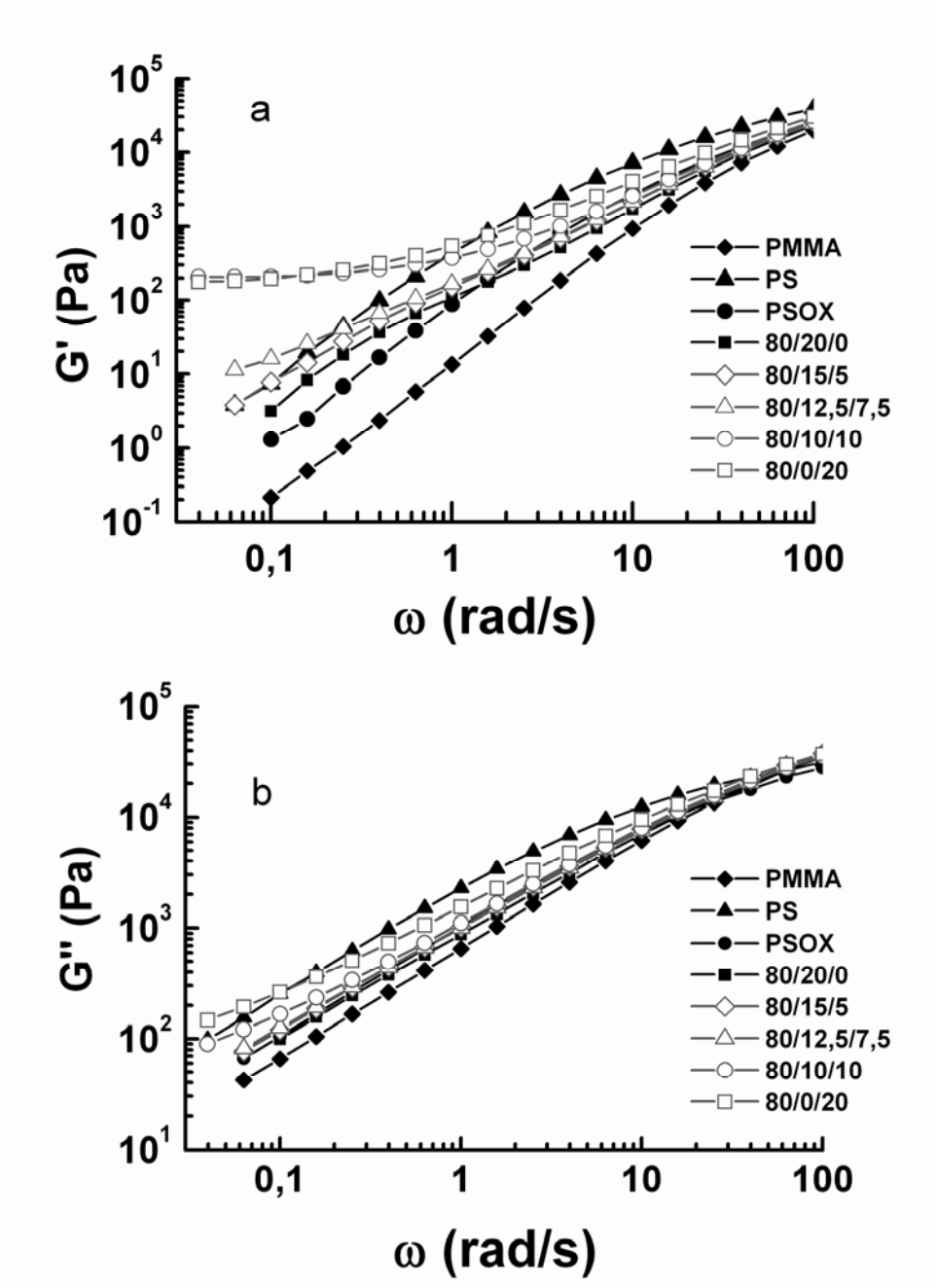

FIG. 3. Moduli for PMMA, PS, PSOX and the blends at 230ºC. (a) Storage and (b) loss moduli.

The elongational measurements, the results of which are depicted in Fig. 4 for the samples with highest concentrations of PS and PSOX, show that while the 80/20/0 blend follows linear viscoelastic behavior, the 80/0/20 blend exhibits strong strain hardening, which is in broad agreement with the results in oscillatory shear. Again the

interfacial contribution in 80/0/20 blend clearly seems to be much higher than in case of 80/20/0 blend.

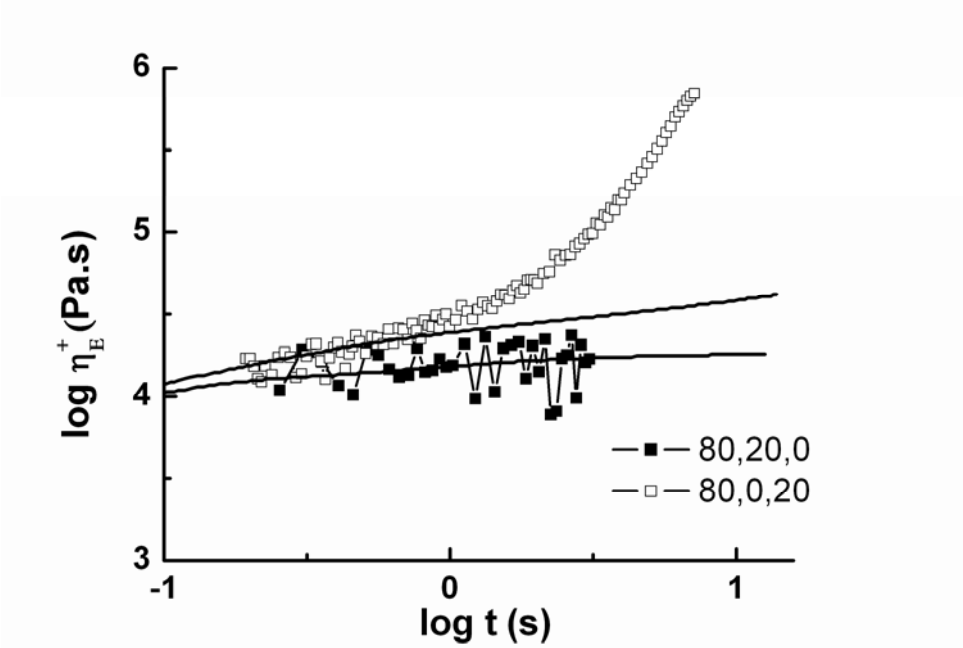

FIG. 4. Transient uniaxial extensional viscosity at 205ºC for 80/20/0 and 80/0/20 blends (strain rates of 0,46s^{-1} and 0,24s^{-1} respectively) and corresponding curves (solid lines) for the linear viscoelastic regime.

These results indicate that some chemical reaction or additional physical interaction occur in blends containing PSOX. In order to study the possibility of the existence of new chemical species or interactions in PMMA/PSOX blends, a FTIR analysis was performed.

D. FTIR

It is known that oxazaline groups react with carboxylic acids, acid anhydrides and phenolic hydroxyls. However, no chemical reaction is known to occur between oxazoline and methacrylate groups. To verify whether the introduction of PSOX leads to formation of new chemical species and to investigate the occurrence of new additional physical interactions between oxazoline and PMMA FTIR was used.

After compression of a small sample of each blend (80/20/0 and 80/0/20), FTIR spectra were recorded in transmittance mode (Fig. 5). These are very similar, indicating that no reaction took place when oxazoline groups were present. Thus, from FTIR it is possible to state that during blending there was no formation of new chemical species at the

interface, or the amount that could be formed was so low that can not be detected by this technique. Likewise, the spectra can not allow conclude the existence of additional physical interactions.

Figure

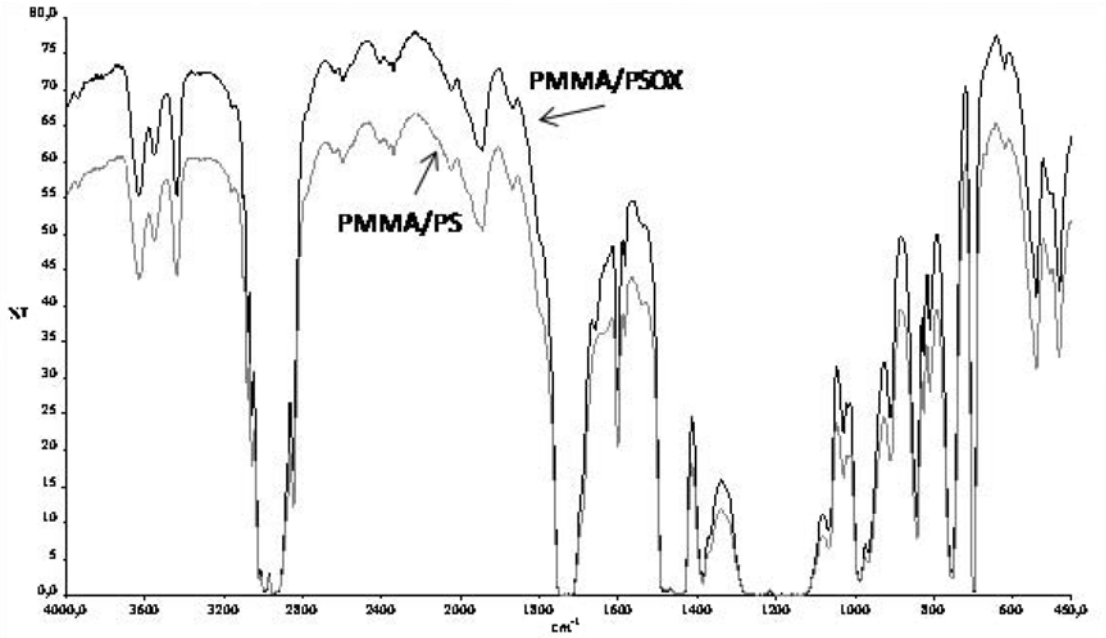

FIG. 5. FTIR spectra of PMMA/PS and PMMA/PSOX blends.

However, it is known that specific interactions between polymer chains result in a change of the mixing enthalpy, resulting in a decrease of the interfacial tension and increase in the interphase thickness [Koning *et al.* (1998)]. Thus, the occurrence of hydrogen bonds and Van der Waals interactions between PMMA and PSOX, for example, may play a compatibilizing role in the mixtures through the enhancement of the interactions at the interface.

E. Relaxation after cessation of flow

At this point is not clear whether the plateau at low frequencies in G' and strain hardening behavior in extension observed for 80/0/20 blend is due to a larger deformation of the droplets and/or to existence of strong physical interactions at the interface of the 80/0/20 blend that are not present in the 80/0/20 blend. One way to determine for sure whether these results are really due to interfacial effects is to

perform stress relaxation experiments after flow and compare the relaxation kinetics of the PMMA/PS blend and the blends containing PSOX.

The aim is to test the elasticity of the interfaces while deforming the disperse phase droplets as little as possible. This can be better achieved in extension than in shear. Hence, stress relaxation experiments after a step uniaxial extension were performed. The results (see Fig. 6) show that the 80/20/0 blend follows essentially the relaxation of matrix, as expected, while the blend with PSOX shows a second relaxation process. At long times the relaxation modulus of the 80/0/20 blend becomes higher than the relaxation modulus of the PSOX dispersed phase. Thus, this clearly shows that there is strong stress build-up at the interface in these systems that may even surpass that inside the droplets. This effect was attributed previously [Silva *et al.* (2007)] to the long term relaxation of the highly elastic disperse phase, but clearly the present results indicate that the interface may play at least a similar role. Mechbal and Bousmina (2007) investigating compatibilized blends observed that much slower stress relaxation is obtained at higher copolymer compatibilizer concentrations, i.e., above a critical concentration of saturation of the interface. This effect was attributed to entanglements in the interfaces.

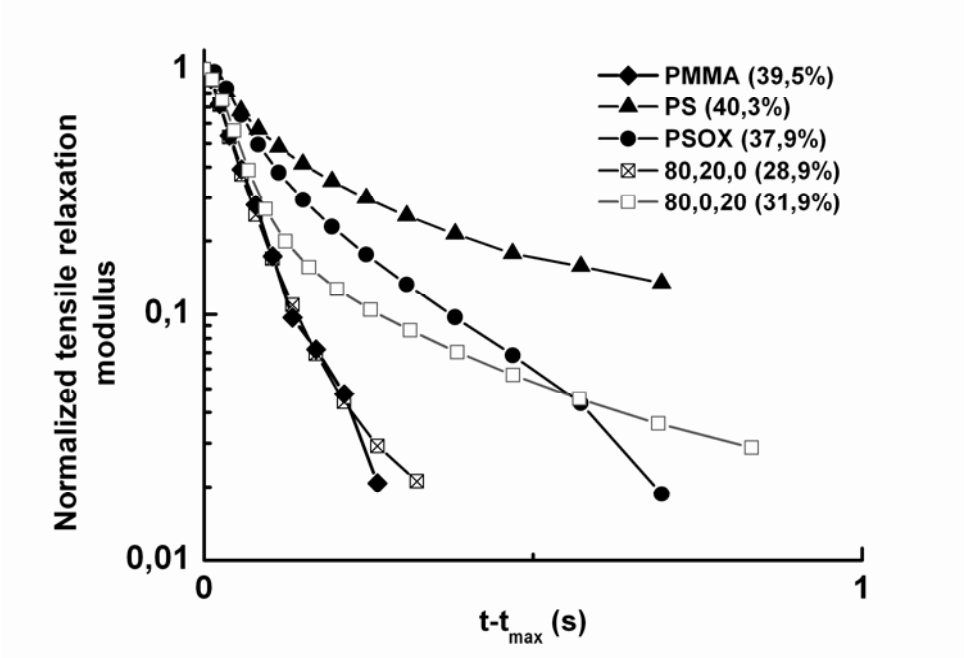

FIG. 6. Normalized transient extensional stress for concentrated blends of PMMA/PS/PSOX and their components after a step extension, at 205ºC. The difference between time and time that corresponding to maximum stress is represented in x-axis. The stress is normalized by its maximum. The Hencky strains, in percentage, applied to each sample are as shown.

The results for the relaxation behavior after steady shear, for a number of blends with varying PS and PSOX ratios, (Fig. 7a) indicate that, at long times, all blends relax slower than the pure components which is a consequence of the relaxation of the dispersed phase and/or interfaces. The blend without PSOX (80/20/0) shows a well-defined two-step relaxation process: a first fast relaxation due to the molecular relaxation of the PMMA matrix followed by a second one slower related with the shape relaxation of the PS droplets. With the introduction of the PSOX the relaxation in two-steps becomes less evident. In fact the shape of the curves and the increase of the relaxation times indicate that there are additional relaxation mechanisms (interfacial relaxation) which are characteristic of compatibilized blends (an additional relaxation time was predicted indirectly by Van Hemelrijck *et al.* (2004), Van Puyvelde *et al.* (2001) from the calculation of the relaxation spectra of compatibilized blends).

Fig. 7b shows the time necessary for the reduced relaxation modulus to decrease to 2% of the original value (dubbed, for simplicity, “relaxation” time) vs. the concentration of PSOX. It is clear that the increase of the “relaxation” time with increase of concentration of PSOX is not linear. At very low PSOX concentrations the relaxation decreases slightly relatively to that of the immiscible blend but then increases rapidly between 5 w/w% and 10 w/w%, at which point it becomes independent of the concentration of PSOX in the dispersed phase. Like the results in storage modulus, these also reveal the existence of a critical concentration for PSOX (the existence of a critical concentration for compatibilizer was reported by Mechbal and Bousmina (2007)). Moreover, the blends above the critical concentration exhibit a very slow relaxation process lasting of the order of several minutes. Again, these results are consistent with the plateau in G’ observed in the linear viscoelastic measurements. Even neither new chemical bonds (see FTIR results above) nor significant morphological changes were found, these results indicate that PSOX is indeed acting as a compatibilizer, albeit a physical one.

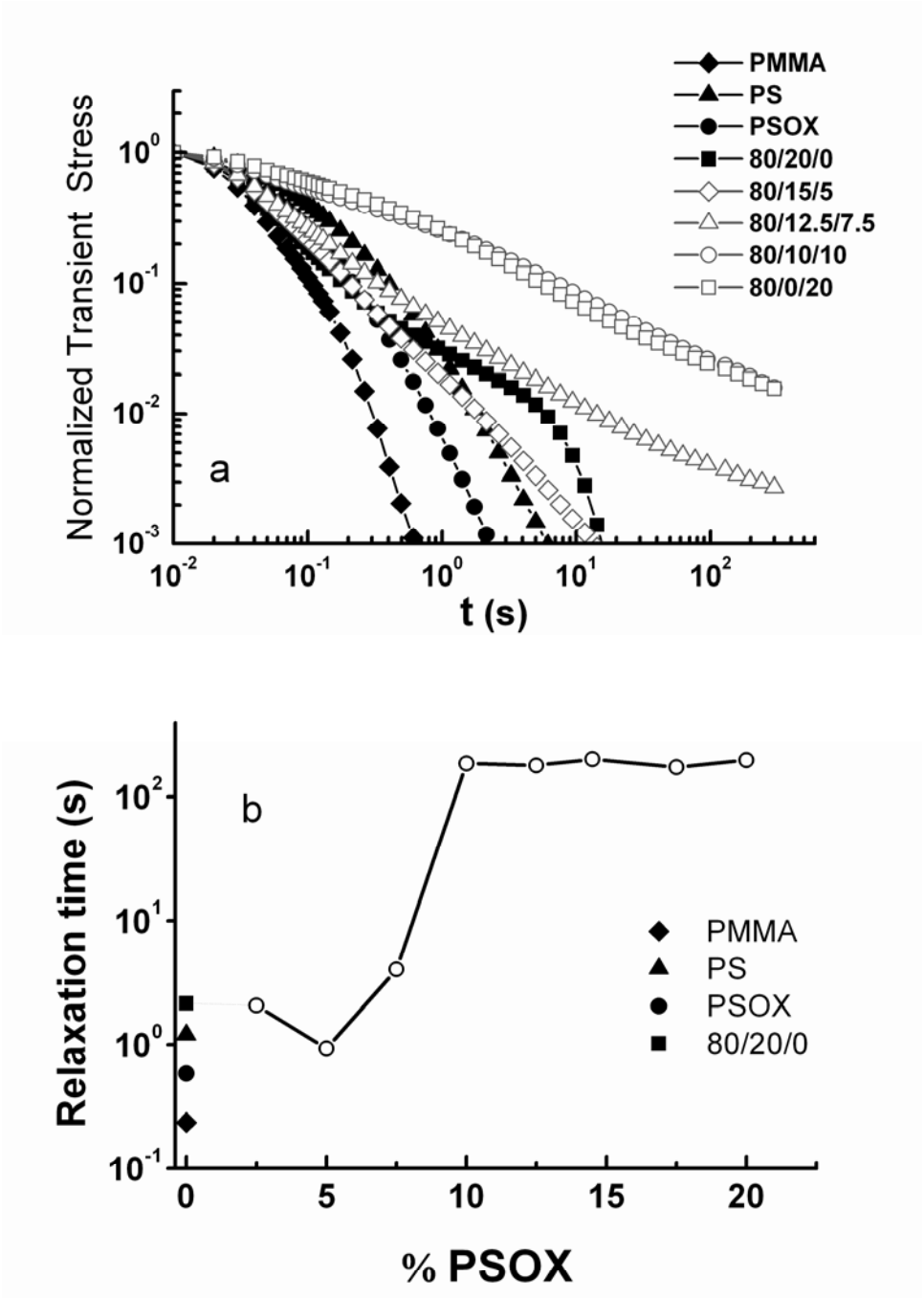

FIG. 7. (a) Normalized transient stress for concentrated blends of PMMA/PS/PSOX and their components after cessation of a steady shear flow of $0.1s^{-1}$ for 250s, at 230ºC. (b) Time taken by the blends and their components to relax stress for 2% of the initial value.

Another interesting feature is the fact of the amount of oxazoline group has an important role. The mechanism that causes the very slow relaxation process in the blends with most oxazoline groups is not clear yet. The reduction of the interfacial

tension resulting from specific interactions between the oxazoline groups and PMMA can explain the results. In order to clear this, Small Angle Light Scattering, SALS, experiments were performed.

F. SALS

As mentioned before, in order to avoid the problems associated with multiple scattering, dilute samples (1 wt% of PS or PSOX in PMMA) were prepared for SALS investigations. In these experiments samples being sheared at 2.5 s^{-1} were, after 800 seconds, submitted to a shear rate step to 70 s^{-1}, at which they are maintained for 250 s. After this time, the shear is suddenly removed and the sample is allowed to relax in time.

Fig. 8 shows the results for the 99/1/0 blend and, as expected, the SALS pattern deforms very in the neutral direction, thus indicating that the dispersed phase is being deformed in the flow direction. Moreover, the anisotropy shows an overshoot characteristic of orientation and/or break-up of the droplets. When the flow is stopped the SALS pattern takes about 5 seconds to recover the isotropic shape, *i.e.*, for the stresses to relax completely, which is within the same timescale observed in stress relaxation experiments in shear (Fig. 4).

Fig. 9 depicts the results for the 99/0/1 blend and it too shows the existence of an overshoot in the anisotropy, but much smaller than for the 99/1/0 blend. Initially the droplets deforms in the flow direction as was observed for PMMA/PS blend. However, at long times the anisotropy pattern appears slightly deformed in flow direction, a trait that is present even upon the cessation of flow, which is an indication that dispersed phase is slightly deformed in the vorticity direction. Deformation of the dispersed phase in the vorticity direction at relatively high shear rates has been reported by several authors [Hobbie and Migler (1999), Lin *et al.* (2005), Mighri and Huneault (2006), Migler (2000)] in blends whose droplets are more elastic than the matrix. Although this phenomenon depends critically on the difference in the elasticity of the components, this alone cannot explain the observed behavior because the elasticity ratio between the PSOX and PMMA is relatively low and is even lower than that between PS and PMMA. Thus, the results of Fig. 9 (deformation on the vorticity direction) can hence be attributed to an increase of elasticity in the interfaces caused by introduction of oxazoline groups (which was already demonstrated in Fig. 3a). Even after the

cessation of flow, the dispersed phase remains slightly elongated in the vorticity direction during a long time.

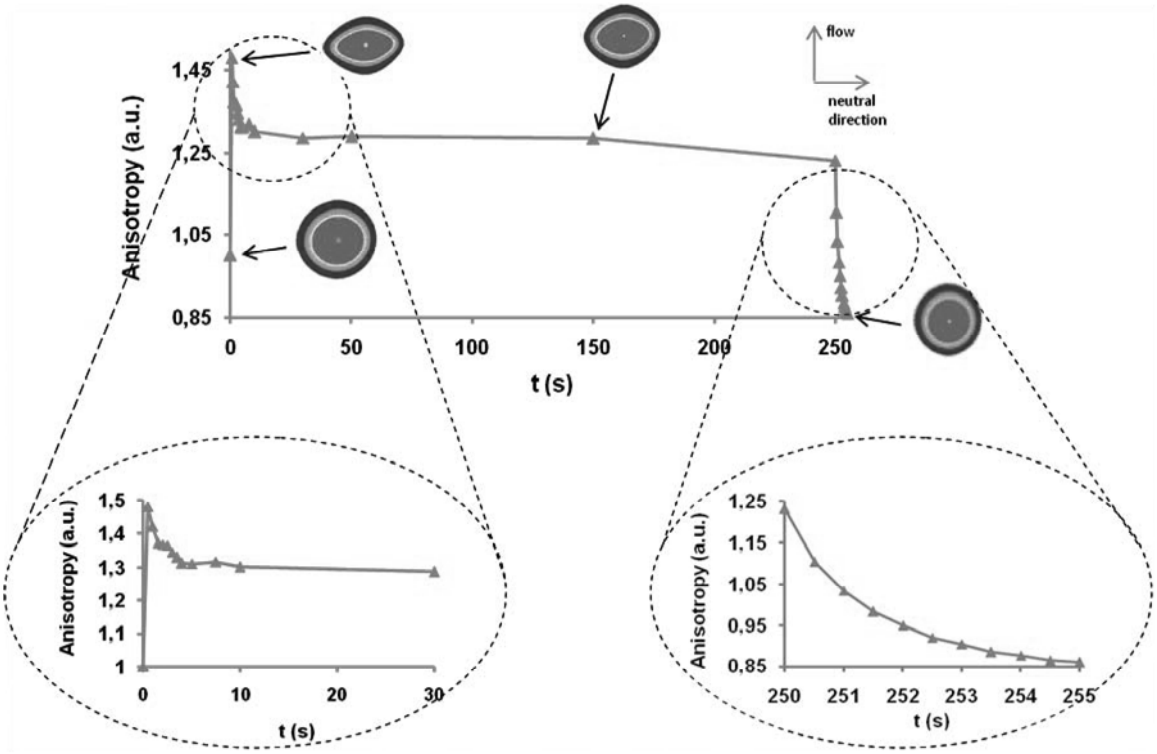

FIG. 8. Anisotropy as a function of time for the 99/1/0 blend. A step-up in shear from $2.5s^{-1}$ to $70s^{-1}$ is performed and the flow is stopped 250s later. Representative SALS patterns are shown for each stage.

These results indicate that the very slow relaxation observed in blend with more oxazoline groups is due to stronger interactions that increase the elasticity of interface. These interactions seem to resist to deformation causing a slower relaxation when flow is stopped.

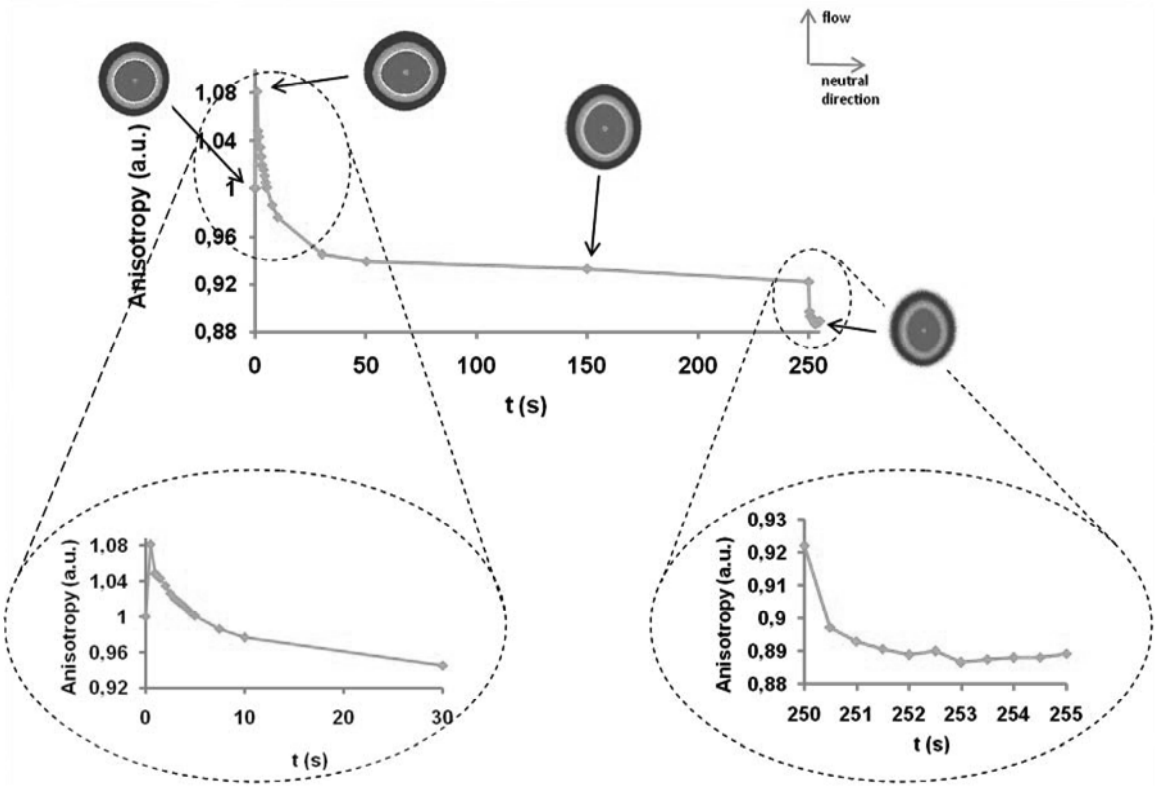

FIG. 9. Anisotropy as a function of time for the 99/0/1 blend. A step-up in shear from $2.5s^{-1}$ to $70s^{-1}$ is performed and the flow is stopped 250s later. Representative SALS patterns are shown for each stage.

IV. CONCLUSIONS

In this work, we studied the role of the interface in the rheological behavior of polymer blends. With this purpose and in order to minimize the contribution of the deformation of the dispersed phase without making it so viscous that no deformation occurred, PMMA/PS and PMMA/PSOX blends with viscosity ratios slightly higher that 1 were used. Although no chemical bonds between PMMA and PSOX could be detected the rheological results show that in blends containing PS modified with oxazoline the interfaces have a different behavior. In particular it was observed that the introduction of oxazoline leads to an increase of the relaxation times of the blends. Moreover, above a critical concentration of PSOX the rheological behavior of the blends almost does not change which is an indication that at this concentration the interface becomes saturated with oxazoline groups. The SALS experiments allow to conclude that the addition of PSOX increases the interfacial elasticity leading to droplet deformations in

the vorticity direction at high enough shear rates. This increase of interfacial elasticity is due to additional entanglements and interactions that result from introduction of oxazoline groups. Moreover, the results show that these additional entanglements slow down the relaxation of the dispersed phase.

As a more general conclusion it can be said that even in the case of blends of industrial interest, normally having viscosity ratios of 1 or above, the behavior of the interface is crucial and therefore these emulsions cannot be treated as suspensions of hard spheres.

ACKNOWLEDGMENTS

This study was possible thanks to the Foundation for Science and Technology–FCT for awarding Jorge Silva with a PhD Fellowship (ref. BD/12833/2003) within the framework of Programa Operacional “Ciência, Tecnologia, Inovação” (POCTI) and Programa Operacional Sociedade da Informação (POSI) of the Quadro Comunitário de Apoio III (2000–2006). The authors also wish to thank Loic Hilliou for helpful discussions.

References

Asthana, H. and K. Jayaraman, "Rheology of reactively compatibilized polymer blends with varying extent of interfacial reaction," Macromolecules **32**, 3412-3419 (1999).

Barroso, V. C., J. A. Covas and J. M. Maia, "Sources of error and other difficulties in extensional rheometry revisited: commenting and complementing a recent paper by T. Schweizer," Rheol. Acta **41**, 154-161 (2002).

Barroso, V. C. and J. M. Maia, "Evaluation by means of stress relaxation (after a step strain) experiments of the viscoelastic behavior of polymer melts in uniaxial extension," Rheol. Acta **41**, 257-264 (2002).

Barroso, V. C., S. P. Ribeiro and J. M. Maia, "Stress relaxation after a step strain in uniaxial extension of polyisobutylene and polyethylene," Rheol. Acta **42**, 345-354 (2003).

Borschig, C., B. Fries, W. Gronski, C. Weis and C. Friedrich, "Shear-induced coalescence in polymer blends - simulations and rheo small angle light scattering," Polymer **41**, 3029-3035 (2000).

Datta, S. and D. Lohse, *Polymeric compatibilizers* (Hanser, Munich, 1996a).

Datta, S. and D. Lohse, *Polymeric compatibilizers, uses and benefits in polymer blends* (Hanser, Munich, 1996b).

Ehrenstein, G. W., *Polymeric Materials: Structure-Properties-Applications* (Hanser, Munich, 2001).

Fahrlander, M., M. Bruch, T. Menke and C. Friedrich, "Rheological behavior of PS-melts containing surface modified PMMA-particles," Rheol. Acta **40**, 1-9 (2001).

Graebling, D., R. Muller and J. F. Palierne, "Linear Viscoelastic Behavior of Some Incompatible Polymer Blends in the Melt - Interpretation of Data with a Model of Emulsion of Viscoelastic Liquids," Macromolecules **26**, 320-329 (1993).

Gramespacher, H. and J. Meissner, "Melt elongation and recovery of polymer blends, morphology, and influence of interfacial tension," J. Rheol. **41**, 27-44 (1997).

Grizzuti, N. and O. Bifulco, "Effects of coalescence and breakup on the steady state morphology of an immiscible polymer blend in shear flow," Rheol. Acta **36**, 406-415 (1997).
Handge, U. A. and P. Potschke, "Interplay of rheology and morphology in melt elongation and subsequent recovery of polystyrene/poly(methyl methacrylate) blends," J. Rheol. **48**, 1103-1122 (2004).
He, Y., B. Zhu and Y. Inoue, "Hydrogen bonds in polymer blends," Progress in Polymer Science **29**, 1021-1051 (2004).
Hobbie, E. K. and K. B. Migler, "Vorticity elongation in polymeric emulsions," Physical Review Letters **82**, 5393-5396 (1999).
Huo, Y. L., G. Groeninckx and P. Moldenaers, "Rheology and morphology of polystyrene/polypropylene blends with in situ compatibilization," Rheol. Acta **46**, 507-520 (2007).
Iza, M., M. Bousmina and R. Jerome, "Rheology of compatibilized immiscible viscoelastic polymer blends," Rheol. Acta **40**, 10-22 (2001).
Jacobs, U., M. Fahrlander, J. Winterhalter and C. Friedrich, "Analysis of Palierne's emulsion model in the case of viscoelastic interfacial properties," J. Rheol. **43**, 1495-1509 (1999).
Koning, C., M. Van Duin, C. Pagnoulle and R. Jerome, "Strategies for compatibilization of polymer blends," Progress in Polymer Science **23**, 707-757 (1998).
Lin, B., F. Mighri, M. A. Huneault and U. Sundararaj, "Effect of premade compatibilizer and reactive polymers on polystyrene drop deformation and breakup in simple shear," Macromolecules **38**, 5609-5616 (2005).
Macaubas, P. H. P., N. R. Demarquette and J. M. Dealy, "Nonlinear viscoelasticity of PP/PS/SEBS blends," Rheol. Acta **44**, 295-312 (2005).
Maia, J. M., J. A. Covas, J. M. Nobrega, T. F. Dias and F. E. Alves, "Measuring uniaxial extensional viscosity using a modified rotational rheometer," J. Non-Newtonian Fluid Mech. **80**, 183-197 (1999).
Mechbal, N. and M. Bousmina, "Effect of copolymer addition on drop deformation during uniaxial elongation and during relaxation after cessation of flow," Macromolecules **40**, 967-975 (2007).
Mechbal, N. and M. Bousmina, "Uniaxial deformation and relaxation of polymer blends: relationship between flow and morphology development," Rheol. Acta **43**, 119-126 (2004).
Mighri, F. and M. A. Huneault, "In situ visualization of drop deformation, erosion, and breakup in high viscosity ratio polymeric systems under high shearing stress conditions," J. Appl. Polym. Sci. **100**, 2582-2591 (2006).
Migler, K. B., "Droplet vorticity alignment in model polymer blends," J. Rheol. **44**, 277-290 (2000).
Oosterlinck, F., M. Mours, H. M. Laun and P. Moldenaers, "Morphology development of a polystyrene/polymethylmethacrylate blend during start-up of uniaxial elongational flow," J. Rheol. **49**, 897-918 (2005).
Riemann, R. E., H. J. Cantow and C. Friedrich, "Interpretation of a new interface-governed relaxation process in compatibilized polymer blends," Macromolecules **30**, 5476-5484 (1997).
Sailer, C. and U. A. Handge, "Melt viscosity, elasticity, and morphology of reactively compatibilized polyamide 6/styrene-acrylonitrile blends in shear and elongation," Macromolecules **40**, 2019-2028 (2007).
Shi, D., Z. Ke, J. H. Yang, Y. Gao, J. Wu and J. H. Yin, "Rheology and morphology of reactively compatibilized PP/PA6 blends," Macromolecules **35**, 8005-8012 (2002).
Silva, J., A. V. Machado and J. Maia, "Rheological behavior of compatibilized and non-compatibilized PA6/EPM blends," Rheol. Acta **46**, 1091-1097 (2007).
Utracki, L. A., *Encyclopaedic dictionary of commercial polymer blends* (ChemTec, Toronto, 1994).

Van Hemelrijck, E., P. Van Puyvelde, S. Velankar, C. W. Macosko and P. Moldenaers, "Interfacial elasticity and coalescence suppression in compatibilized polymer blends," J. Rheol. **48**, 143-158 (2004).
Van Puyvelde, P., Z. Oommen, P. Koets, G. Groeninckx and P. Moldenaers, "Effect of reactive compatibilization on the interfacial slip in nylon-6/EPR blends," Polym. Eng. Sci. **43**, 71-77 (2003).
Van Puyvelde, P., S. Velankar and P. Moldenaers, "Rheology and morphology of compatibilized polymer blends," Curr. Opin. Coll. Int. Sci. **6**, 457-463 (2001).
Vinckier, I., P. Moldenaers, A. M. Terracciano and N. Grizzuti, "Droplet size evolution during coalescence in semiconcentrated model blends," AIChE J. **44**, 951-958 (1998).
Yee, M., P. S. Calvao and N. R. Demarquette, "Rheological behavior of poly(methyl methacrylate)/polystyrene (PMMA/PS) blends with the addition of PMMA-ran-PS," Rheol. Acta **46**, 653-664 (2007).

Appendix D

Ares, A., J. Silva, J. Maia, L. Barral and M. Abad, "Rheomechanical and morphological study of compatibilized PP/EVOH blends." (2009) Submitted to *Rheologica Acta*.

Rheomechanical and morphological study of compatibilized PP/EVOH blends.

Ana Ares[1]*, Jorge Silva[2], Joao M. Maia[2], Luis Barral[1], María J. Abad[1]

1. Grupo de Polímeros, Departamento de Física, EUP-Ferrol, Universidad de A Coruña, EUP, Avda. 19 Febrero s/n, 15405 Ferrol, Spain
2. I3N - Institute for Nanostructures, Nanomodeling and Nanofabrication, Department of Polymer Engineering, University of Minho 4800-058 Guimarães, Portugal

Abstract

In order to find the relationships between processibility and properties of the polypropylene / ethylene-vinyl alcohol copolymer (PP/EVOH) blends, their rheological behavior, in both shear and extensional flows, was studied and related with mechanical, morphological and barrier properties of the materials. The nonlinear viscoelastic behavior in shear was also analyzed. The data showed that the rheological parameters (viscosity, loss modulus, storage modulus, extensional viscosity and Trouton ratio) improved with the addition of low quantities of sodium ionomer copolymer used as compatibilizer. At the same time, the overall properties of the PP/EVOH blends, improved as result of the compatibilizer addition. The morphological analysis showed the changes in the material properties were related with a more uniform distribution of EVOH particles in the PP matrix. The rheological data obtained allowed us to choose the optimal range for EVOH and ionomer contents, especially in terms of combining good processing characteristics with the good final properties.

Keywords Polypropylene/EVOH blends, extensional Rheology, nonlinear viscoelastic behaviour, compatibilization, mechanical properties, barrier properties

*Correspondence to: Ana Ares, Grupo de Polímeros, Departamento de Física, E.U.P.-Ferrol, Universidad de A Coruña, Avda. 19 Febrero, s/n. 15405-Ferrol; Spain
E-mail: aares@udc.es Fax: 981337401

Introduction

One of the limiting properties of polymeric materials in the food packaging field is their inherent permeability to low molecular weight substances, i.e. gases, moisture and organic vapors. Despite the existence of excellent high barrier materials to gases in oxygen-sensitive food packaging applications, including ethylene-vinyl alcohol copolymers (EVOH), polyamides or polyesters, some of these materials are, for instance, easily plasticized by moisture or do not thermoseal well; consequently, they are more commonly blended with hydrophobic polymers like, polypropylene or polyethylene, or encapsulated in multilayer structures between these hydrophobic polymers. Thus in the last years, much attention has been paid to the study of polypropylene/ethylene-vinyl-alcohol copolymer blends (López-Rubio et al. 2005; Lohfink and Kamal 1993; Kamal et al. 1995; Fisher et al. 2000) due to their great potential interest for the food packaging industry. Polypropylene, PP, is cheap, has good mechanical properties, low density and low permeability to moisture but as a disadvantage, it has high permeability to gases like oxygen. On the other hand, ethylene-alcohol vinyl copolymers, EVOH, show low permeability to oxygen, carbon dioxide and hydrocarbons but their properties are very sensitive to moisture levels (Yeh et al. 2005; Zhang et al. 2001; Kalfoglou et al. 1998). The PP/EVOH blends are an interesting route to improve the PP barrier properties with an easier processibility than the EVOH copolymers and with a reduced cost. (Abad et al. 2004, Abad et al. 2005, Lasagabaster et al. 2006). Although there is a large available bibliography about the properties of these blends and their compatibilization (Macknight and Earnest 1981, Lohfink and Kamal 1993, Walling and Kamal 1996, Garmabi et al. 1998, Demarquete and Kamal 1998, Yeo et al. 2001, López-Rubio et al. 2003), an in-depth study about their rheological properties had not been realized yet. Besides, from the point of view of the PP/EVOH blends processibility, the study of the rheological properties in extensional flow is very interesting to predict the material behavior during their processing using thermoforming or blow molding techniques.

In a previous study, the improvement on the mechanical properties and the barrier properties of PP/EVOH blends using low contents of a copolymer partially neutralized with sodium as compatibilizer (Abad et al. 2004) was measured and related with changes in the morphology of the blends. However, rheological effects of the compatibilizer incorporation to the PP/EVOH blends are a matter that has not been

discussed yet in detail. These rheological parameters are especially important in the principal polymer processing techniques for packaging applications such as blow injection molding, thermoforming or film blowing. Moreover, several studies report that compatibilization of the polymer blends can affect the nonlinear viscoelastic behavior in shear (Iza et al. 2001, Macaubas et al. 2005, Silva et al. 2007).

The main aim of the current work is to complete the last one with the evaluation of the influence of EVOH and ionomer Na^+ content on the shear and extensional flow behavior of PP/EVOH blends, since in order to optimize the compatibilization of the blends and their subsequent industrial application, the study of the rheological properties in both shear and extensional flows is of great importance (Filipe et al. 2006). The nonlinear viscoelastic behavior in shear was also analyzed in order to investigate if compatibilization affects the behavior of the blends in this regime.

Experimental

Materials

All the materials employed in this study are commercial products, the polymers having been chosen in order to have an appropriate melt flow index (MFI) for extrusion purposes. Specifically, a bi-oriented film extrusion-grade polypropylene (PP) (Isplen PP044W3F) from REPSOL-YPF was used; this PP has an MFI of 3.02 g/10 min (230ºC, 2160 g) and a density of 0.90 g/cm^3. The ethylene-vinyl alcohol copolymer (EVOH, grade F101B) was supplied for EVAL Europe (Kuraray Company Ltd, Kuroashiki, Japan); it has an ethylene concentration of 32.9%, an MFI of 6.33 g/10 min (230ºC, 2160 g), and a density of 1.19 g/cm^3. The Na^+ ionomer (Surlyn resin 8528, from Du Pont, Wilmington, DE, USA) is a random ethylene/methacrylic acid copolymer partially neutralized with sodium, with a MFI of 1.10 g/10 min (190ºC, 5000 g) and a density of 0.93 g/cm^3.

Sample preparation

Before processing, the EVOH and the Na^+ ionomer were dried in a vacuum oven for 24 h at 80ºC and for 8 h at 60ºC, respectively. PP/EVOH and PP/EVOH/ionomer blends were prepared in a co-rotating twin-screw extruder (DSE-20; C.W. Brabender

Instruments, South Hackensack, NJ, USA) operating at 45 rpm, with a barrel temperature 215ºC and a die temperature of 220ºC. All the components were premixed by tumbling and were fed simultaneously into the extruder. Binary blends were prepared with 90/10, 80/20, 70/30 and 60/40 (w/w) PP/EVOH, while the ternary blends were prepared by addition of 2-20% ionomer weight in relation to EVOH weight.

The samples for shear rheometry were shaped in the form of discs or strips by compression molding at 210ºC applying a pressure of 200 bar for 3 minutes. Those for extensional rheometry were also prepared by compression molding in the same conditions but in the shape of strips of 2x6x60 mm (Thickness x Width x Length). Rectangular cross-section has the advantage of easier clamping and lower distortion when clamped, although it makes sample visualization more difficult.

Special care was taken to ensure that all the samples had a uniform cross-section and were free of voids and air bubbles. Compression molding also ensures that the residual stresses are minimized but, nevertheless, all the samples were allowed to relax in the rheometers after loading prior to the experiments starting.

Characterization techniques

All the PP/EVOH blends were characterized both in shear and in elongational flows. These experiments continue the previous works made by the authors, in which the mechanical, thermal, barrier and morphological properties of the blends were studied (Abad et al. 2004; Abad et al. 2005; Lasagabaster et al. 2006)

Rheology experiments were performed using a controlled strain rheometer (ARES, TA Instruments) with parallel-plate geometry (25mm diameter, gap of 1 mm) at 220ºC. The complex viscosity (η^*), storage modulus (G') and loss modulus (G'') were measured as function of frequency (ω). Dynamic strain sweep tests at fixed frequencies were performed (in fresh samples every time) in order to determine the linear viscoelastic region prior to the frequency sweeps. The frequency sweep measurements were set up inside the viscoelastic region, in a frequency range from $3x10^{-2}$ to $3x10^{1}$ rad/s.

The stress relaxation experiments in shear were performed at 220 ºC again using a parallel-plate geometry (diameter=25 mm) with a 1000 ± 1 μm gap; a shear rate of $1s^{-1}$ during 25 s was applied and the evolution of the shear stress upon cessation of flow was measured.

Experiments in uniaxial extension flow were also performed for all the samples using a modified rotational rheometer, MRR, built in-house and described elsewhere (Maia et al. 1999, Barroso et al. 2002, Barroso et al. 2003). All experiments in extension were performed at 220ºC. High temperature silicone oil was used as supporting medium (in order to compensate for gravity and buoyancy effects) and also for temperature control purposes. At the measuring temperature its density (0,93g/cm^3) roughly matched the density of the samples, so that sagging and swelling of the samples were negligible.

The uniaxial extensional measurements were carried out by applying strain rates between approximately $3x10^{-2}$ and $3x10^{-1}$ s^{-1}. The strain rates here described are true strain rates obtained by image analysis of the evolution with time of the sample cross-section at the rollers, filmed with a digital camera (Maia et al. 1999) and resorting to an image analysis software package. This is a necessary procedure because as was demonstrated elsewhere (Barroso et al. 2002), for this type of rheometers in general the true strain rates are not identical to the theoretical strain rates calculated from the velocity of the pulling rollers due to a variety of end-effects, including slip at the rollers. For this reason the strain rates are very similar between different blends but not exactly equal.

In order to ensure that the samples were stress free at the beginning of each experiment, once loaded onto the MRR they were allowed to relax at the test temperature. Any sagging shown was then removed and any residual stress allowed to relax, again, before the experiment was started (Barroso et al. 2002). This dwell time served also the purpose to stabilize the sample temperature inside the oil bath. Each experiment was repeated three times and the average values were taken for analysis both in shear and extensional experiments.

The transient uniaxial extensional viscosity in the linear viscoelastic regime (LVE) was calculated from the relaxation spectra obtained from shear oscillatory data at 220ºC, and the Trouton ratio as a function of strain for the different blends was calculated.

Results and discussion

Brief summary about the previous characterization of PP/EVOH blends

In this section, the principal experimental data obtained on mechanical, barrier and morphological properties of the PP/EVOH blends are summarized to explain the need of the rheological study and to compare the data obtained with the other properties.

The mechanical and barrier properties of PP/EVOH blends, both non-compatibilized and compatibilized with different amounts of Na^+ ionomer were studied in a previous paper (Abad et al. 2004) In these works, the tensile properties of the pure components and blends had been determined on extruded films. The tensile strength (σ_B) and strain at break point (ε_B) with EVOH and ionomer amount are presented in Figure 1a. In both parameters, it is clear that the compatibilization has a great effect on the properties of the blends since an improvement in mechanical properties is observed with the compatibilizer addition.

Figure 1b shows the effect of EVOH an ionomer addition in the water vapor transmission rate (WVTR) and in the oxygen transmission rate (O_2TR) values of extruded films. The O_2TR of the PP/EVOH blends decreased with respect to pure PP especially for EVOH contents of 30% and higher, as we expected due to the good oxygen barrier properties of copolymer. However, the best values were obtained when 5% or more of the compatibilizer was added to the blends.

The dramatic increase in the WVTR with the addition of EVOH was due to its hydrophilic character of the copolymer; however the PP/EVOH films with ionomer concentrations equal or higher than 5% the obtained WVTR values even lower than of the ones obtained for the pure PP.

The relative diameters of EVOH particles were plotted as a function of some ionomer percentage (Fig. 1c) in order to see the effect of copolymer and ionomer in blends morphology. The relative diameters were calculated following equation 1, where $d_{60/40}$ corresponds to the biggest diameter of the EVOH particles measured in the 60/40 PP/EVOH blend:

$$d_R = \frac{d_{blend}}{d_{60/40}} \quad (Eq.\ 1)$$

For 90/10; 80/20 and 60/40 PP/EVOH blends only two formulations were measured, but the behavior is similar to the 70/30 PP/EVOH blends in which all formulations were represented. It is obvious that the EVOH particle size increases with the addition of EVOH to the blends and that the ionomer addition causes a diminution of disperse phase size and a better adhesion between the components, This effect is clearly seen in the SEM micrographs too. The figure 1c displays the morphology of the 90/10 and 70/30 PP/EVOH blends compatibilized with a 10% and 20% of Na^+ ionomer.

Thus, from the point of view of the barrier properties, mechanical properties and morphology, the addition of low amounts of Na+ ionomer was effective to

compatibilizer the PP/EVOH blends. And although acceptable results were obtained for all compatibilized blends, the best cost/properties ratio was obtained for the 90/10/10 PP/EVOH/Na^+ blend because minor amounts of EVOH and ionomer were necessary. However to complete this work, it is necessary to study the processibility of these materials in depth.

Effect of the EVOH content in the rheology of PP/EVOH blends

Figures 2a-d shows the rheological behavior in oscillatory shear and in extension of the binary PP/EVOH blends.

Figure 2a shows complex viscosity versus frequency, it is shows the onset of the Newtonian plateau for pure PP at low frequencies, followed by a mildly shear-thinning behavior. This behavior is basically replicated for all the blends, with the absolute value of complex viscosity decreasing with increasing EVOH content. The reason for this is related to the orientation of the EVOH domains inside the PP matrix and the immiscibility of both phases that prevents stress transfer between them and results in interfacial slippage.

This behavior is replicated by the results for the storage and loss moduli, G' and G'', as can be seen in Figure 2b. An interesting feature is that the crossover between G' and G'' of EVOH is different to that of the other materials. In fact, for EVOH this crossover occurs at a frequency of approximately 0.3 rad/s, while for the other materials it occurs only at frequencies at least one order of magnitude higher.

Figure 2c, shows the results in uniaxial extensional rheometry and contrarily to what could be expected, apparently this effect is not as pronounced due to two reasons; the first is that strain-hardening behaviors of both PP and EVOH (expressed by the Trouton ratio) are very similar and the second is that the experiments for the immiscible blends are extremely hard to perform and the data scatter may be masking any effect.

One unexpected feature of Figure 2c is the fact that PP, a linear material, shows an important degree of strain hardening. One explanation for this fact is that as this PP is a commercial polymer with a grade specifically developed for bi-oriented extrusion, and it is likely that it has a complex composition; for example, a small amount of a very high molecular weight component can produce a strong effect on the strain-hardening of linear polymers (Sugimoto et al. 2001). Unfortunately it was not possible to quantify the molecular weight and molecular weight distribution of the PP.

The results of linear viscoelastic studies can provide reliable information on microstructure of the blends. The viscoelastic response of the blends at low frequencies can be used for evaluating of the interfacial interaction between phases because the effect of flow induced molecular orientation on viscosity and elasticity becomes less important. The complex viscosity and storage modulus versus blend composition together with the same results calculated using the mixing rule at frequency of 1rad/s are presented in the Figure 2d. The binary blends show negative deviation in the viscosity for all blends and negative deviation of elasticity in blends with 30% and 40% of EVOH. On the basis of Utracki's studies (Utracki 1988) the negative deviation of the viscosity and elasticity observed for EVOH-rich blends can be attributed to the presence of weak interfacial interaction between phases in these blends.

Effect of the ionomer content in the rheology of PP/EVOH blends

The compatibility of inmiscible blends was investigated from the variation of rheological property by adding compatibilizer and then compared with the properties previously obtained.

Figure 3a shows the complex viscosity as a function of frequency for 90/10 PP/EVOH blend with different amounts of ionomer. With the addition of 2% and 5% of ionomer, a decrease in viscosity is observed thus indicating that the amount of ionomer is not sufficient to compatibilize the blends effectively. With the addition of 10% ionomer, higher values of viscosity than the immiscible blend are observed, which reflects the fact that the extent of the compatibilization is increasing. This is due to the improvements of interfacial adhesion between PP and EVOH, as can be seen in the morphology (Figure 1c) and the better EVOH phase dispersion due to the compatibilization. Besides, the improvement of rheological properties of the blends can also be related with the phenomenon of the rough surfaces of extruded non-compatibilized blends compared to the smooth surfaces of extruded blends compatibilized by Na^+ in melt extrusion process. This is in agreement with the results obtained for barrier and mechanical properties where the best data were obtained for 90/10/10 PP/EVOH/Na^+ blend.

These results were also confirmed in Figure 3b where both moduli for the blend with 2 and 5% ionomer content were lower than for the non-compatibilized blend. For 10% EVOH, however, it is apparent that compatibilization is occurring to a high enough

extent as to cause a small but noticeable increase in the moduli. At large frequencies, storage modulus G' and loss modulus G'', slightly increases with Na^+ concentration. At low frequencies the effect of compatibilizer is much more pronounced.

The results for uniaxial extension (Figure 3c) also seem to confirm those in shear, but in this case a noticeable increase in the Trouton ratio can already be seen for the blend with 5% ionomer; in fact, the results are almost the same as for the blend with 10% ionomer. The reason for this behavior is that in the compatibilized blends the morphology is different; EVOH has better adhesion to the PP matrix, and the average size of the EVOH domains is lower as it was proved in the previous morphology study. With this type of morphology, the effect of extensional flow on the interfacial area is much higher that the one of shear flow, thus yielding a noticeable compatibilization effect at lower ionomer contents, *i.e.*, it induces the strain hardening behavior even with the addition of small quantities of compatibilizer (Hong et al. 2005). At small strains a good agreement between the experimental data and the linear viscoelastic prediction is evident for all the concentrations of ionomer. At large strains the elongational viscosity increases more rapidly and exceeds the linear viscoelastic prediction. This strain-hardening is more clearly seen with the increase of ionomer amount. All the compatibilized blends are, like their non-compatibilized counterparts, highly strain-hardening, as expected, with the strain-hardening becoming more pronounced as the strain rate increases due to the fact that the reduction of the area of the sample what produces an increase in the interfacial area in both absolute terms and relatively to the sample volume; for an example of this see Figure 4a and 4b, for the 90/10 w/w PP/EVOH and 90/10/10 w/w PP/EVOH/ion.Na blends, respectively.

Identical results were obtained for 80/20 PP/EVOH blend than for the 90/10 PP/EVOH blend, and, thus, for the sake of simplicity, that data is not included in the text.

For the two blends with 30 and 40% of copolymer the results are also very similar and again only the study of the 60/40 PP/EVOH blend is reported.

Figures 5a-c depict the results for the latter blend and show that addition of up to 10% of ionomer clearly has an increasing compatibilizing effect. However, the material with 20% ionomer shows a decrease in both the viscosity (Figure 5a) and the linear viscoelastic moduli (Figure 5b). It is observed that increasing the compatibilizer content enhances interfacial adhesion between two phases, ultimately resulting in increase of resistance to deformation of compatibilized blends. However, the addition of compatibilizer above a critical concentration (20%) probably gives no more

contributions to the increase the interfacial adhesion, *i.e.*, it reaches a saturation stage, and decreases the viscosity of the blends due to the lower viscosity of Na^+ ionomer.
As was seen for the others blends, the experiments in uniaxial extension (Figure 5c) show good compatibilization occurring for lower ionomer contents; in this case the best results were achieved for the 60/40/5 PP/EVOH/Na blend, although compatibilization is also observed for the blends compatibilized with 10 and 20% of ionomer.

Stress relaxation experiments

Shear stress relaxation measurements (Fig. 6) show that PP relaxes in a single step and EVOH relaxes in two steps which is a consequence of the fact of EVOH is a copolymer. The dispersed phase concentration greatly affects the relaxation behavior of the blends.
For the blends with 10% EVOH the relaxation curve has a shape similar to that of PP, with the exception of the non-compatibilized blend that shows a slower terminal relaxation thanks to the presence of the non-compatibilized EVOH phase, as expected. For the compatibilized blend the relaxation kinetics is very similar (albeit slightly quicker) to that of the matrix (PP), which is a sign of good compatibilization.
For the 40% EVOH blends, there are two noteworthy features: a) The relaxation is much slower than for any of the two components and b) Its kinetics is basically independent of the blend being compatibilized or not. In what concerns the former, this happens because the interfacial area, which contributes to relaxation, is higher in more concentrated blends. In what regards the latter, this phenomenon is related to the fact that the interfacial area increases with the amount of EVOH and thus it is to be expected that the same amount of compatibilizer will yield a much smaller effect in terms of relaxation kinetics for this blend than for the one with 10% EVOH.
This behavior is related with the data obtained for the other properties; for 90/10 and 80/20 PP/EVOH blends a lower amount of ionomer than in 70/30 and 60/40 PP/EVOH blends is necessary in order to obtain good mechanical and barrier properties and a good morphology,.

Conclusions

The principal conclusions obtained from the rheological study in the shear and extensional flows of polypropylene and ethylene-vinyl alcohol copolymer (PP/EVOH) blends compatibilized with Na^+ ionomer, can be summarized as follows:

a) The binary PP/EVOH blends show shear thinning behaviour that increases with EVOH amount.

b) A negative deviation behavior of the viscosity and elasticity was observed for EVOH-rich blends as expected for immiscible blends.

c) For the 90/10 PP/EVOH blend, a 10% of sodium ionomer was necessary to observe the compatibilization effect in shear and extensional flows. The rheological data displayed an increase of the viscosity and moduli for this formulation, which is related with the more uniform morphology of the material and with the improvement of barrier and mechanical properties respect to the non-compatibilized system. Besides, an increase in Trouton ratio and strain hardening behavior were obtained with the ionomer addition.

d) The same behavior was found for 60/40 PP/EVOH blends compatibilized, although a larger ionomer amount was necessary to observe noticeable compatibilization.

e) The stress relaxation experiments showed that the same amount of compatibilizer causes a minor effect, in terms of relaxation kinetics, in blends with high amount of EVOH and that the relaxation kinetics in these is generally much slower than that of any of the individual components, PP and EVOH.

In summary, from the rheological experiments, we can conclude that the optimal amount of compatibilizer is around 10% measured with respect to EVOH quantity. This fact is similar to the conclusion obtained from the morphology, mechanical and barrier properties. The sodium ionomer was proven to be an adequate compatibilizer for the PP/EVOH blends because it was possible to improve the global properties of the materials at the same time that the processibility of the blends was maintained. Besides, the good extensional properties of the blends made them suitable to use in packaging industry with its usual processing techniques as thermoforming or blow molding

Acknowlegdements

Financial support for this work was provided by the Secretaría Xeral de Investigación e Desenrolo, Xunta de Galicia, through grant XUGA-PGIDT02TM17201PR and the

Portuguese government through FCT – Foundation for Science and Technology, through grant BD/12833/2003.

REFERENCES

Abad MJ, Ares A, Barral L, Cano J, Diez FJ, García-Garabal S, López J, Ramírez C (2004) Use of a sodium ionomer as compatibilizer in polypropylene/high-barrier ethylene-vinyl alcohol copolymer blends: The processability of the blends and their physical properties. J Appl Polym Sci 94(4):1763-1770

Abad MJ, Ares A, Barral L, Eguizábal JI (2005) Influence of the ethylene-(methacrylic acid)-Zn^{2+} ionomer on the thermal and mechanical properties of blends of poly(propylene) (PP)/ethylene-(vinyl alcohol) copolymer (EVOH). Polym Internat 54(4): 673-678

Barroso VC, Covas JA, Maia JM (2002) The Uniaxial Elongation Rheometer RME - six years of experience. Comments. Sources of error and other difficulties in extension rheometry revisited: commenting and complementing a recent paper by T. Schweizer. Rheol Acta 41(1-2): 154-161

Barroso VC, Ribeiro SP, Maia JM (2003) Unusual extensional behaviour of a polystyrene/HIPS blend. Rheol Acta 42(5): 483-490

Demarquete NR, Kamal MR (1998) Influence of maleation of polypropylene on the interfacial properties between polypropylene and ethylene-vinyl alcohol copolymer. J Appl Polym Sci 70(1): 75-87

Filipe S, Cidade MT, Maia JM (2006) Uniaxial extensional flow behaviour of immiscible and compatibilized polypropylene/liquid crystalline polymer blends. Rheol Acta 45(3): 281-289

Garmabi H, Demarquette NR, Kamal MR (1998) Effect of temperature and compatibilizer on interfacial tension of PE/PA-6 and PP/EVOH. Intern Polym Process XIII 13 (2): 183-191

Hong JS, Ahn KH, Lee SJ (2005) Strain hardening behaviour of polymer blends with fibril morphology. Rheol Acta 45(2): 202-208

Hong JS, Kim JL, Ahn KH, Lee SJ (2005) Morphology development of PBT/PE blends during extrusion and its reflection on the rheological properties. J Appl Polym Sci 97(4): 1702-1709

Ismail H, Halimatudahliana A, Nasir M (2002) The effect of various compatibilizers on mechanical properties of polystyrene/polypropylene blends. Polym Test 21(2):163-170

Iza M, Bousmina M, Jerome R (2001) Rheology of compatibilized immiscible viscoelastic polymer blends. Rheol Acta 40: 10-22

Kalfoglou NK, Samios CK, Papadopoulou CP (1998) Compatibilization of poly(ethylene-co-vinyl alcohol) (EVOH) and EVOH-HDPE blends: structure and properties. J Appl Polym Sci 68(4): 589-596

Lasagabaster A, Abad MJ, Barral L, Ares A (2006) FTIR study on the nature of water sorbed in polypropylene (PP)/ethylene-vinyl alcohol copolymer (EVOH) films. Eur Polym J 42(11): 3121-3132.

López-Rubio A, Hernández-Muñoz P, Gímenez E, Yamamoto T, Gavara R, Lagarón JM (2005) Gas barrier changes and morphological alterations induced by retorting in ethylene vinyl alcohol-based food packaging structures. J Appl Polym Sci 96(6): 2192-2202

López-Rubio A, Lagarón JM, Giménez E, Cava D, Hernández-Muñoz P, Yamamoto T, Gavara R (2003) Morphological alterations induced by temperature and humidity in ethylene-vinyl alcohol copolymers. Macromolecules 36(25): 9467-9476

Lohfink GW, Kamal MR (1993) Morphology and permeability in extruded polypropylene/ethylene-vinyl alcohol copolymer blends. Polym Eng Sci 33(21): 1404-1420

Maia JM, Covas JA, Nóbrega JM, Dias TF, Alves FE (1999) Measuring uniaxial extensional viscosity using a modified rotational rheometer. J Non-Newt Fluid Mech 80 (2,3), 183-197

Macaubas PHP, Demarquette NR, Dealy JM (2005) Nonlinear viscoelasticity of PP/PS/SEBS blends. Rheol Acta 44(3): 295-312

Macknight, Earnest TR (1981) Structure and properties of ionomers. Macrom Reviews 16: 41-122

Silva J, Machado AV, Maia JM (2007) Rheological behavior of compatibilized and non-compatibilized PA6/EPM blends. Rheol Acta 46(8): 1091-1097

Sugimoto M, Masabuchi Y, Takimoto J, Koyama K (2001) Melt Rheology of Polypropylene Containing Small Amounts of High-Molecular-Weigth Chain.2. Uniaxial and Biaxial Extensional Flow. Macromol 34(17): 6056-6063

Utracki LA (1988) Viscoelastic behaviour of polymer blends. Polym Eng Sci 28(21): 1401-1404

Walling N, Kamal MR (1996) Phase morphology and properties of injection molded polypropylene/ethylene-vinyl alcohol copolymer blends. Adv Polym Techn 15(4): 269-288

Yeh JT, Yao WH, Du Q, Chen CC (2005) Blending and barrier properties of blends of modified polyamide and ethylene vinyl alcohol copolymer. J Polym Sci Part B: Polym Phys 43(5): 511-521

Yeo JH, Lee CH, Park CS, Lee KY, Nam JD, Kim SW (2001) Rheological, morphological, mechanical and barrier properties of PP/EVOH blends. Adv Polym Techn 20(3): 191-201

Zhang Z, Britt IJ, Tung MA (2001) Permeation of oxygen and water vapor through EVOH films as influenced by relative humidity. J Appl Polym Sci 82(8): 1866-1872

FIGURE CAPTIONS

Figure 1. Influence of the EVOH and ionomer amount in different properties; (a) Tensile strength and elongation at break, (b) Oxygen and vapour transmission rate, (c) relative diameter of EVOH particles and morphology (SEM micrographs x1500)

Figure 2. Curves for the binary PP/EVOH blends; (a) Complex viscosity versus frequency, (b) Evolution of the storage modulus (G') and loss modulus (G'') with frequency, (c) Influence of the EVOH content on the Trouton ratio against Hencky strain, (d) Complex Viscosity and G'(Pa) at 1 rad/s versus EVOH percentage.

Figure 3. Curves for the 90/10 w/w PP/EVOH blends with different amounts of ionomer; (a) Complex viscosity versus frequency, (b) Evolution of the storage modulus (G') and loss modulus (G'') with frequency, (c) Influence of the ionomer content on the Trouton ratio against Hencky strain.

Figure 4. Transient uniaxial extensional viscosity for the 90/10 w/w PP/EVOH blend; (a) 0% of ionomer, (b) 10% of ionomer.

Figure 5. Curves for the 60/40 w/w PP/EVOH blends with different amounts of ionomer; (a) Complex viscosity versus frequency, (b) Evolution of the storage modulus (G') and loss modulus (G'') with frequency, (c) Influence of the ionomer content on the Trouton ratio against Hencky strain.

Figure 6. Normalized transient stress for several blends of PP/EVOH, compatibilized and non-compatibilized, and their pure components after a cessation of a shear flow of $1s^{-1}$ for 25s at 220ºC.

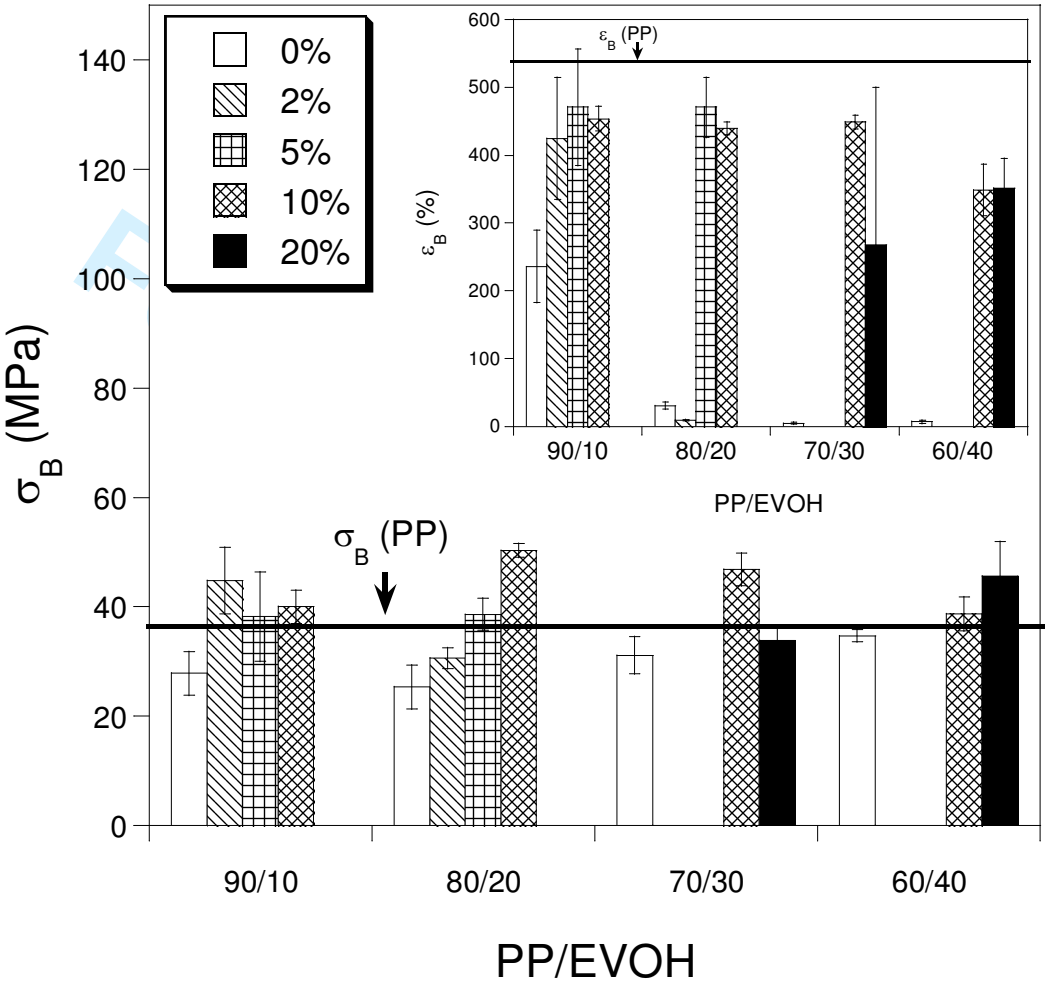

Fig. 1a

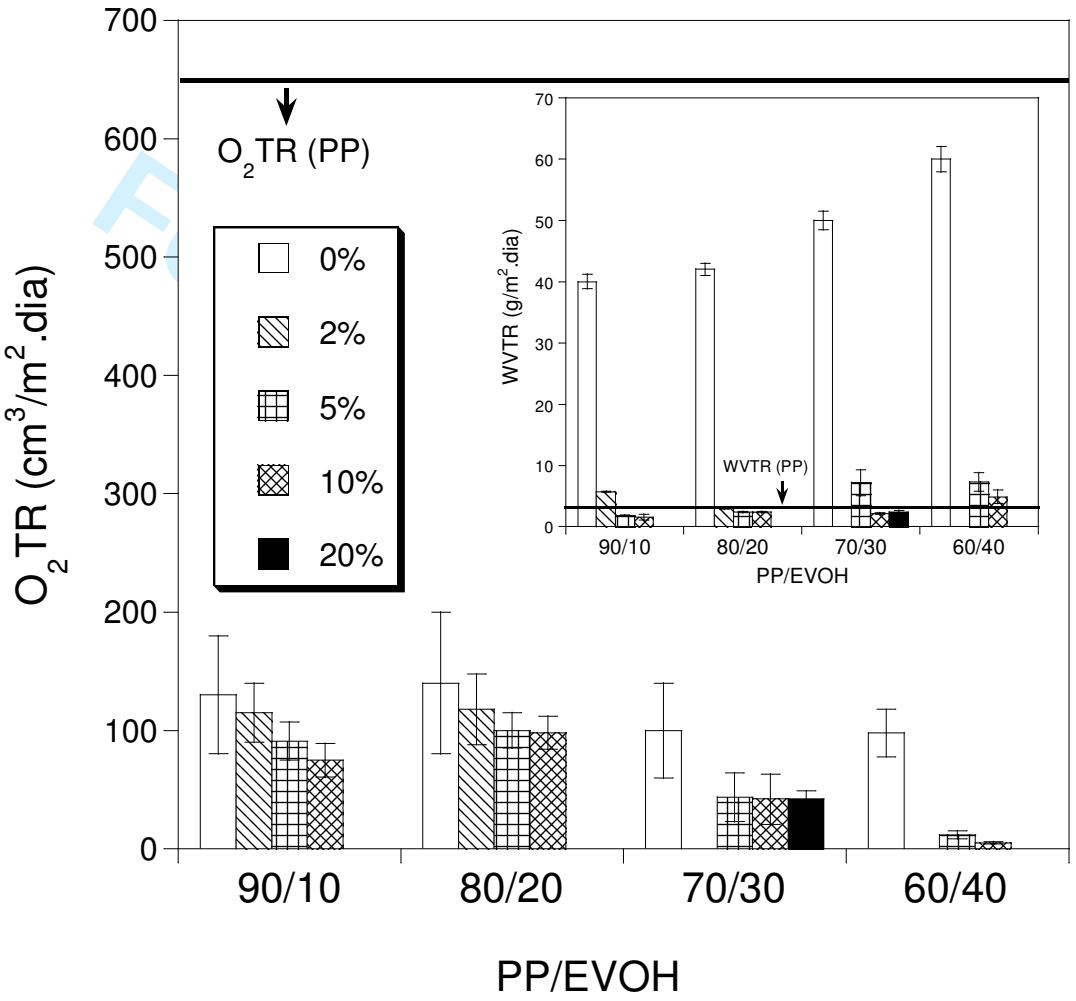
700
600
500
400
300
200
100
0
O2TR (PP)
0%
2%
5%
10%
20%
O2TR (cm3/m2.dia)
90/10
80/20
70/30
60/40
PP/EVOH
WVTR (g/m2.dia)
WVTR (PP)
70
60
50
40
30
20
10
0
90/10
80/20
70/30
60/40
PP/EVOH

Fig. 1b

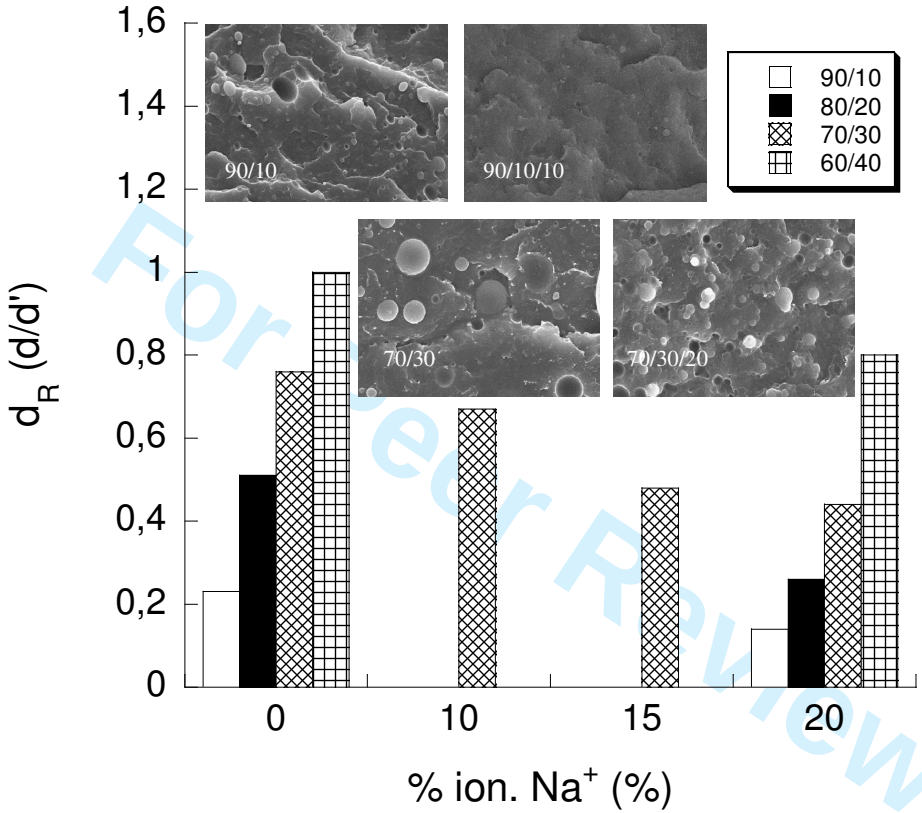

Fig. 1c

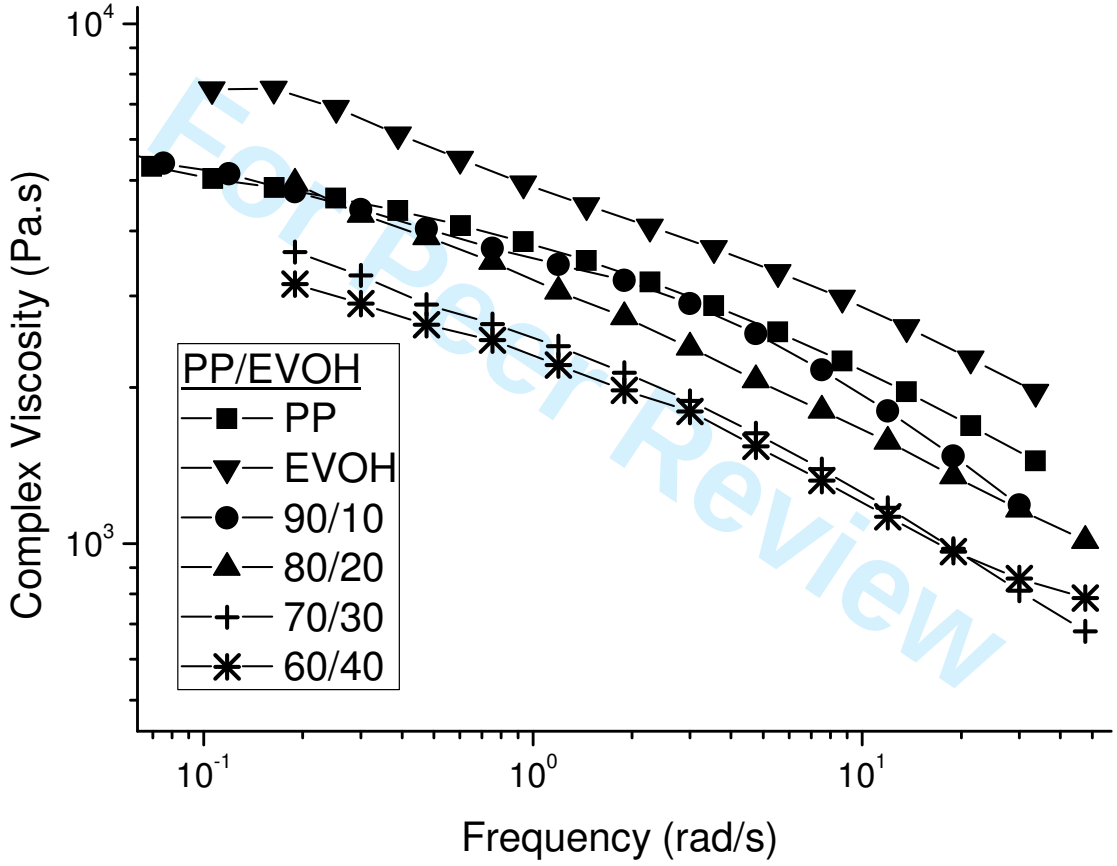

Fig. 2a

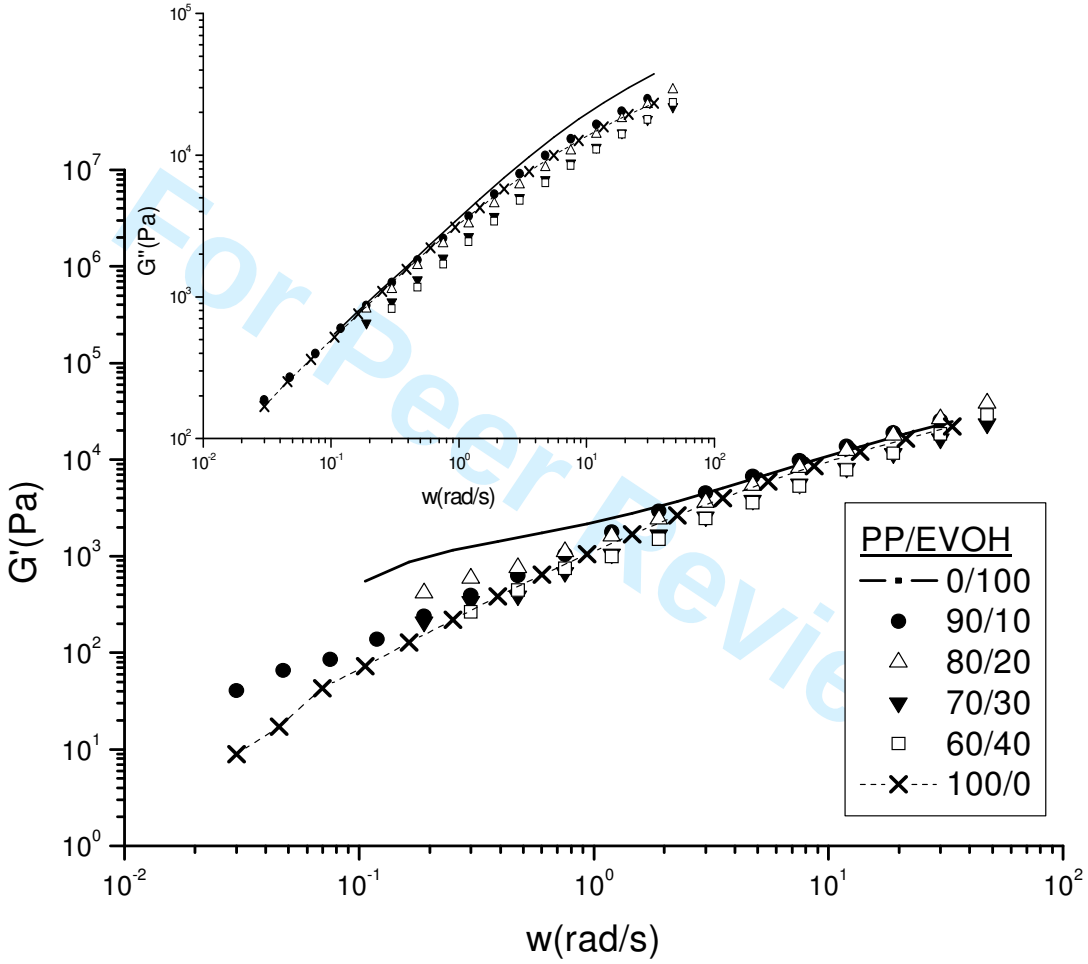

Fig. 2b

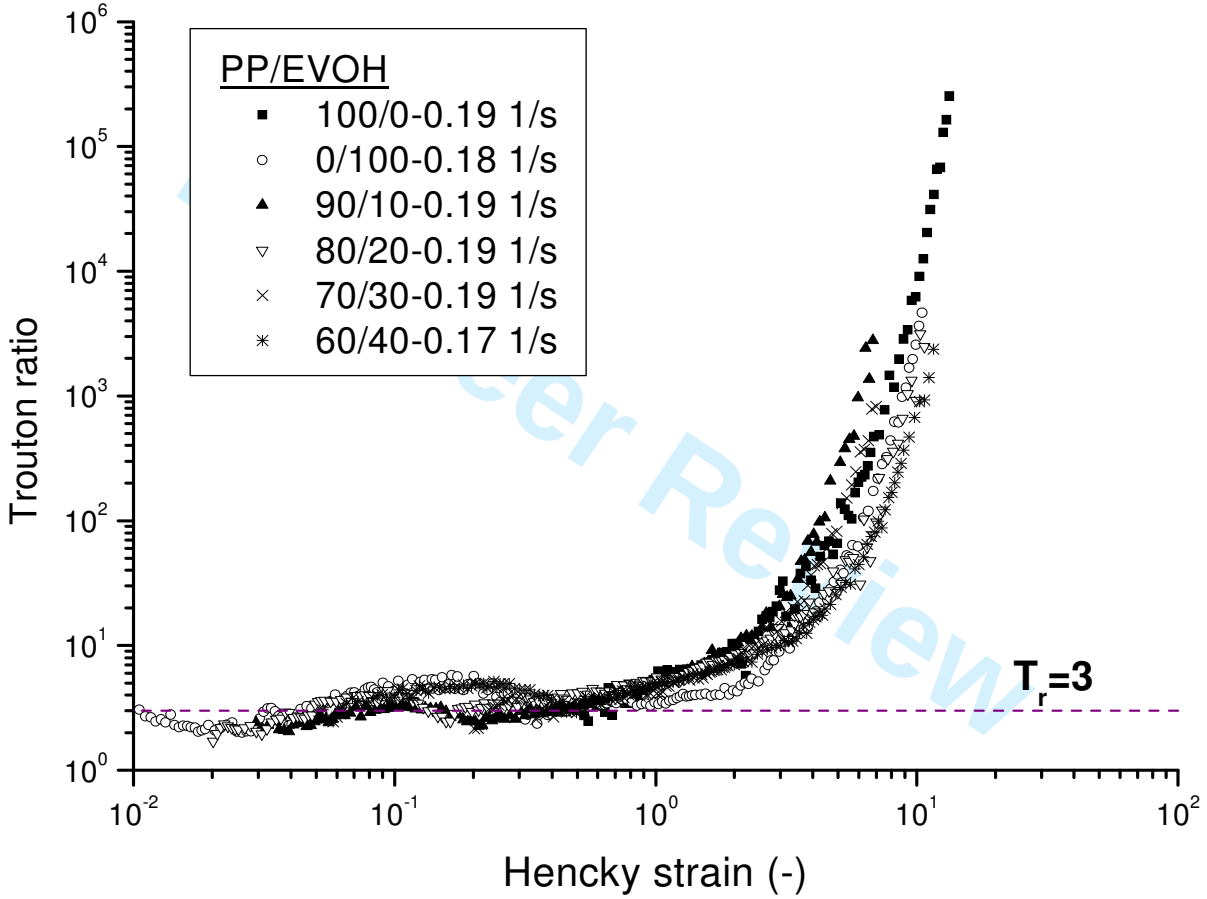
PP/EVOH
100/0-0.19 1/s
0/100-0.18 1/s
90/10-0.19 1/s
80/20-0.19 1/s
70/30-0.19 1/s
60/40-0.17 1/s
Trouton ratio
Hencky strain (-)
T_r=3

Fig. 2c

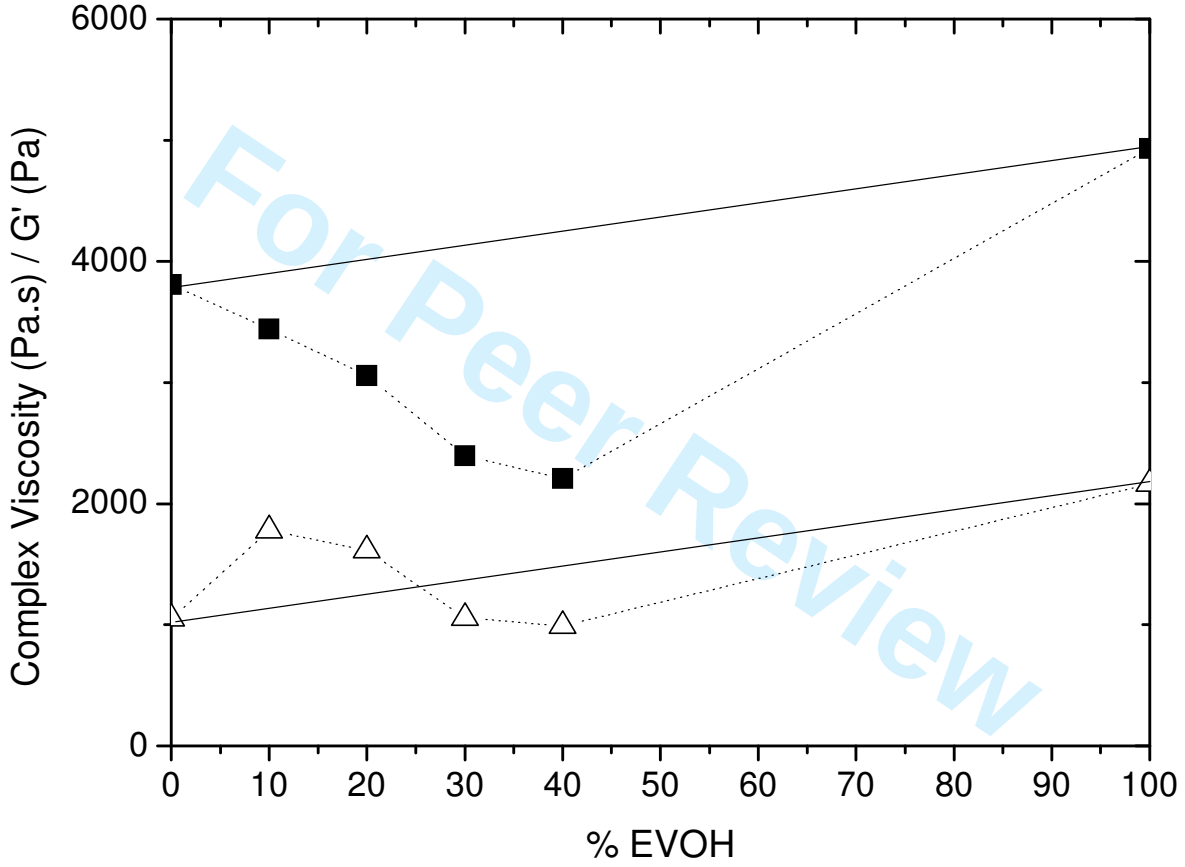

Fig. 2d

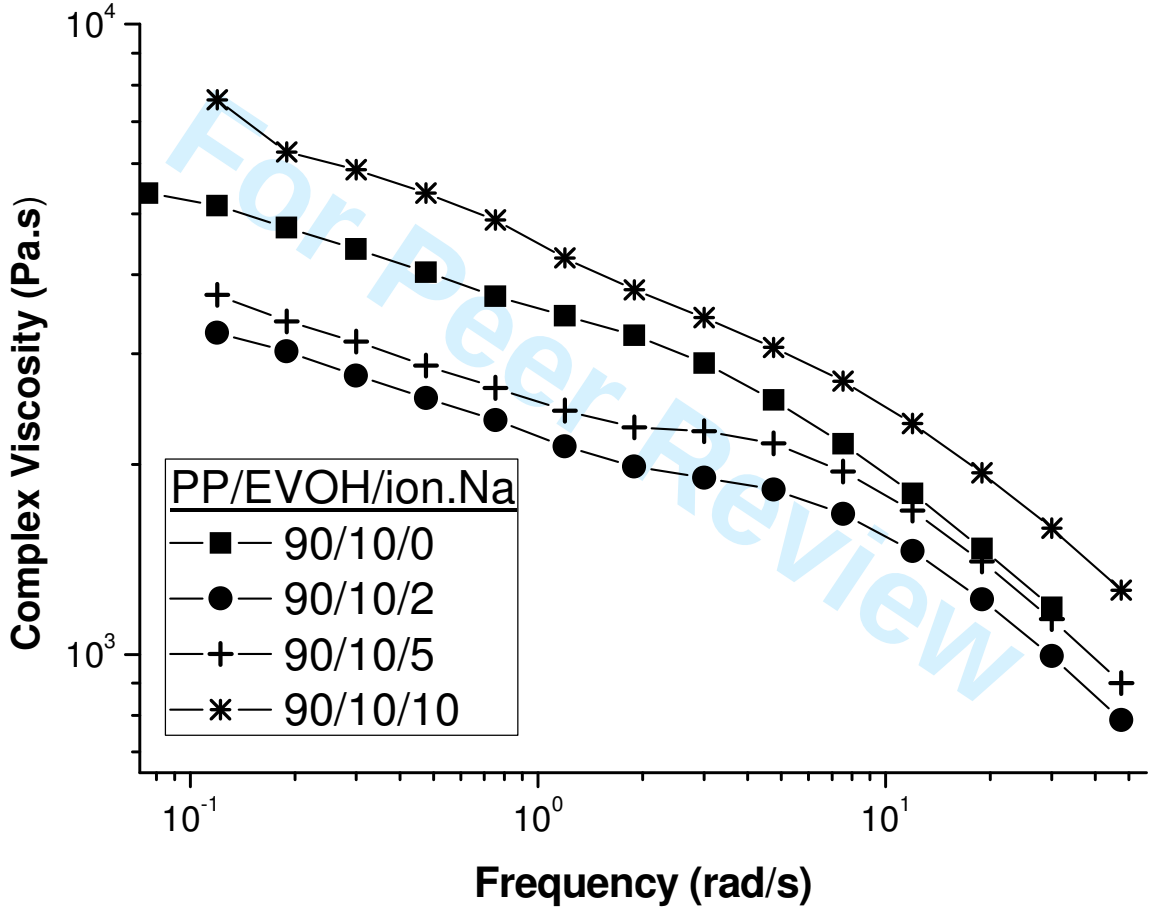
Complex Viscosity (Pa.s)
Frequency (rad/s)
PP/EVOH/ion.Na
90/10/0
90/10/2
90/10/5
90/10/10
For Peer Review

Fig. 3a

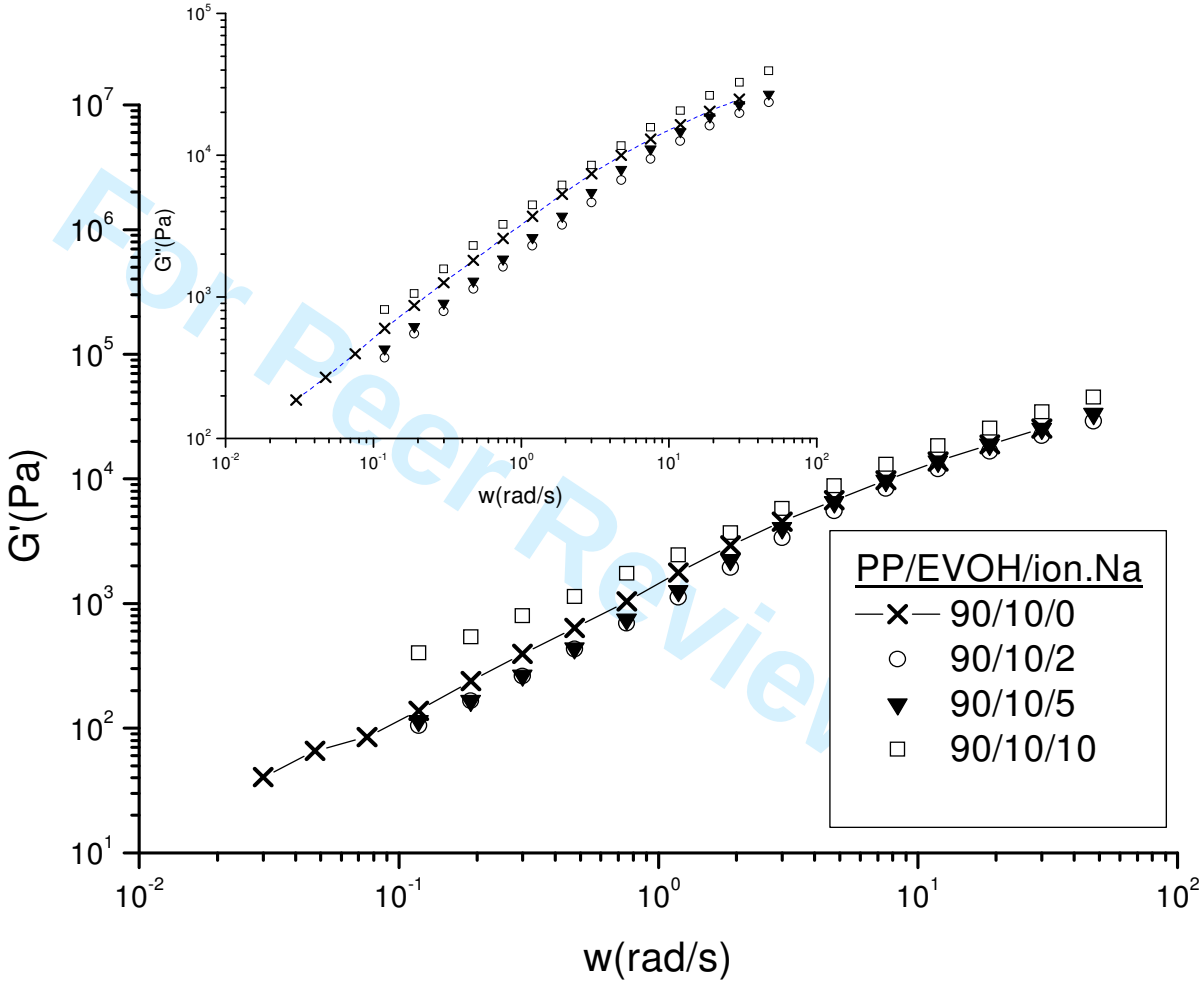

Fig. 3b

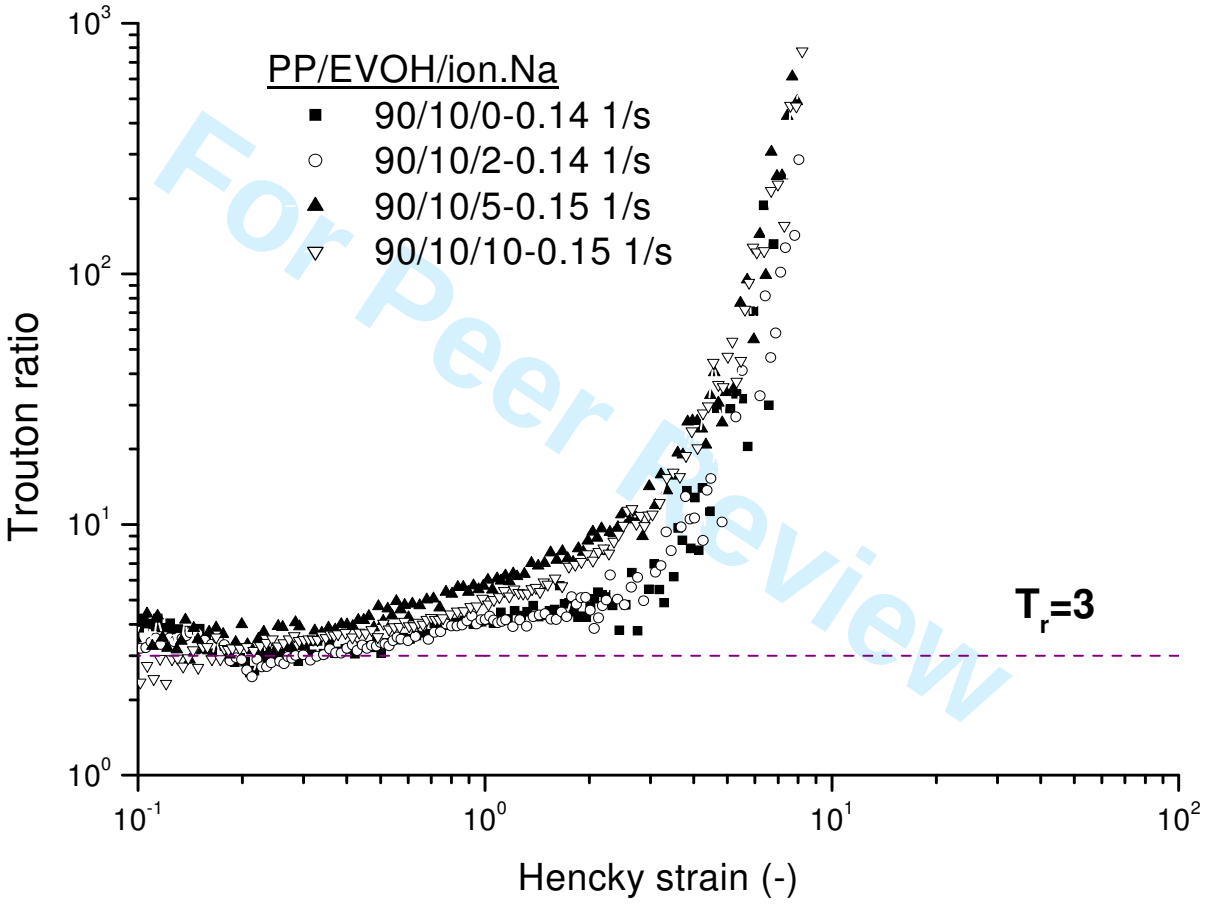

Fig. 3c

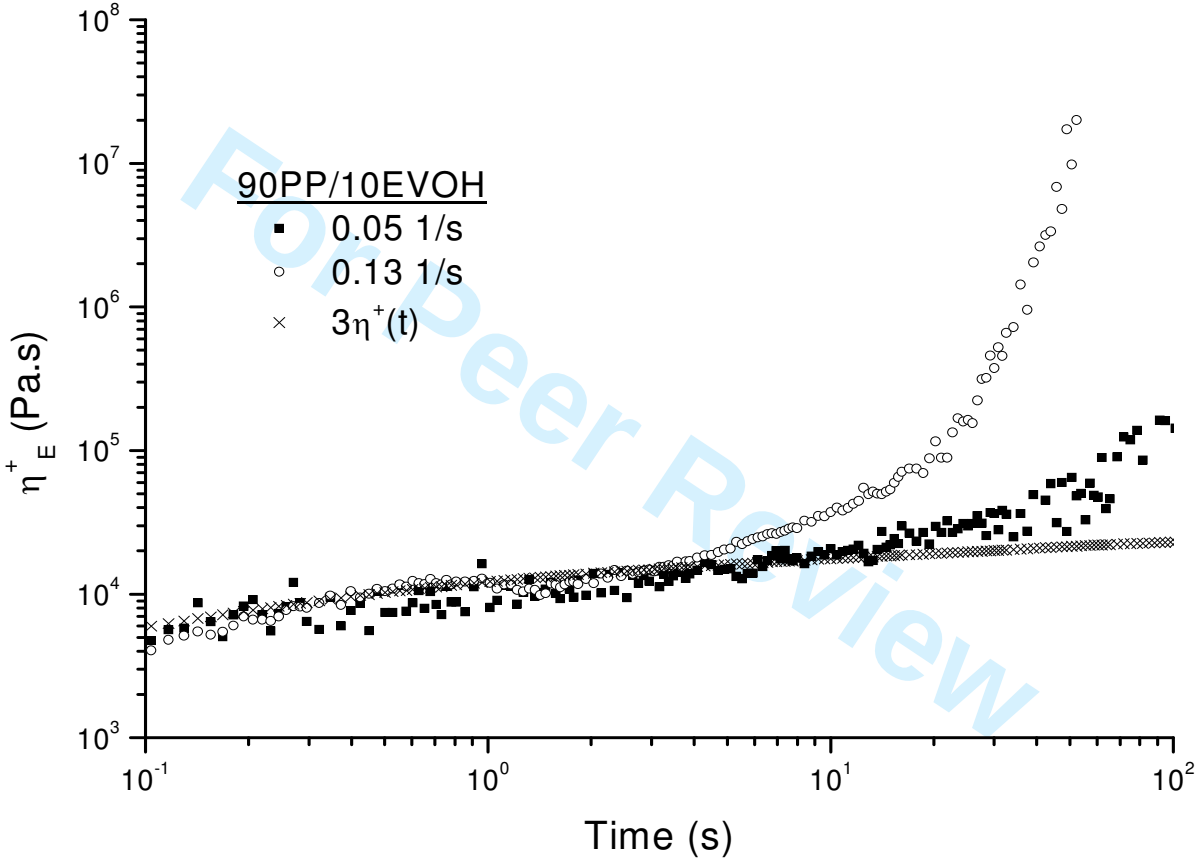

Fig. 4a

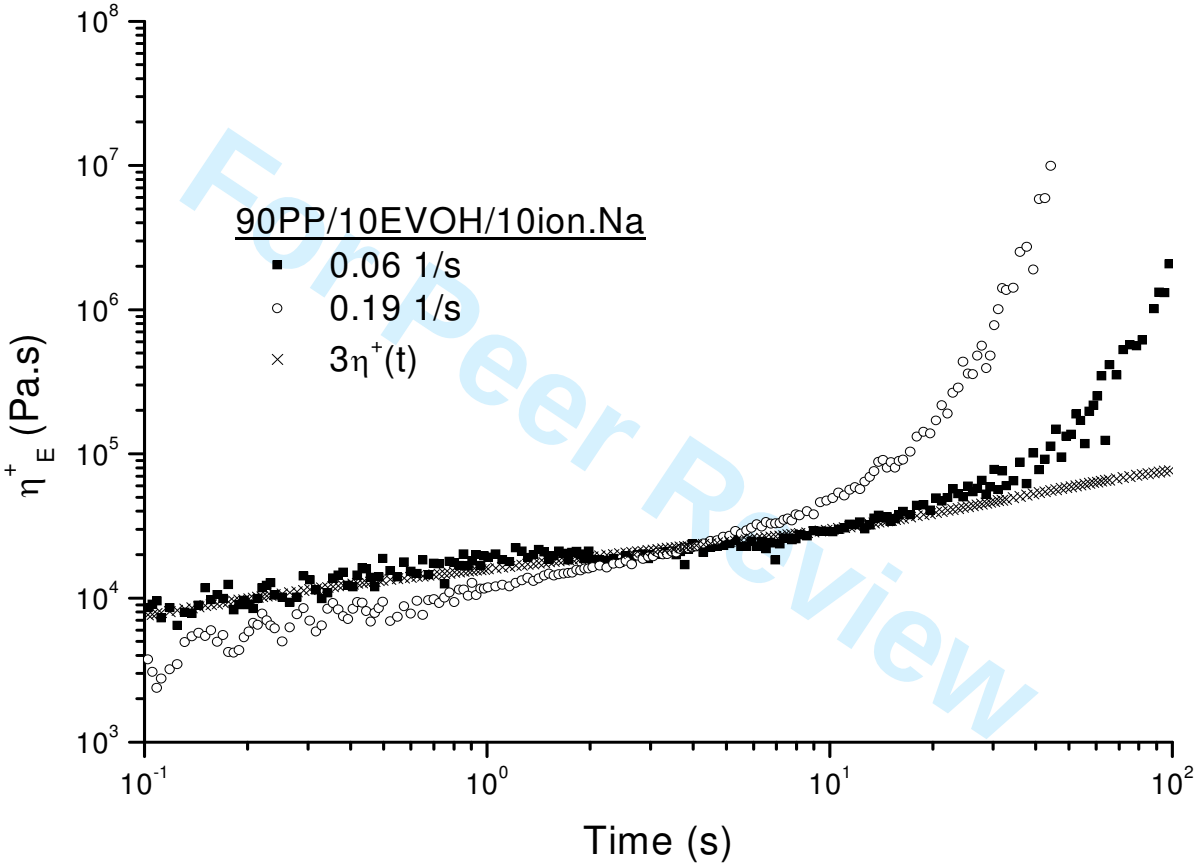

Fig. 4b

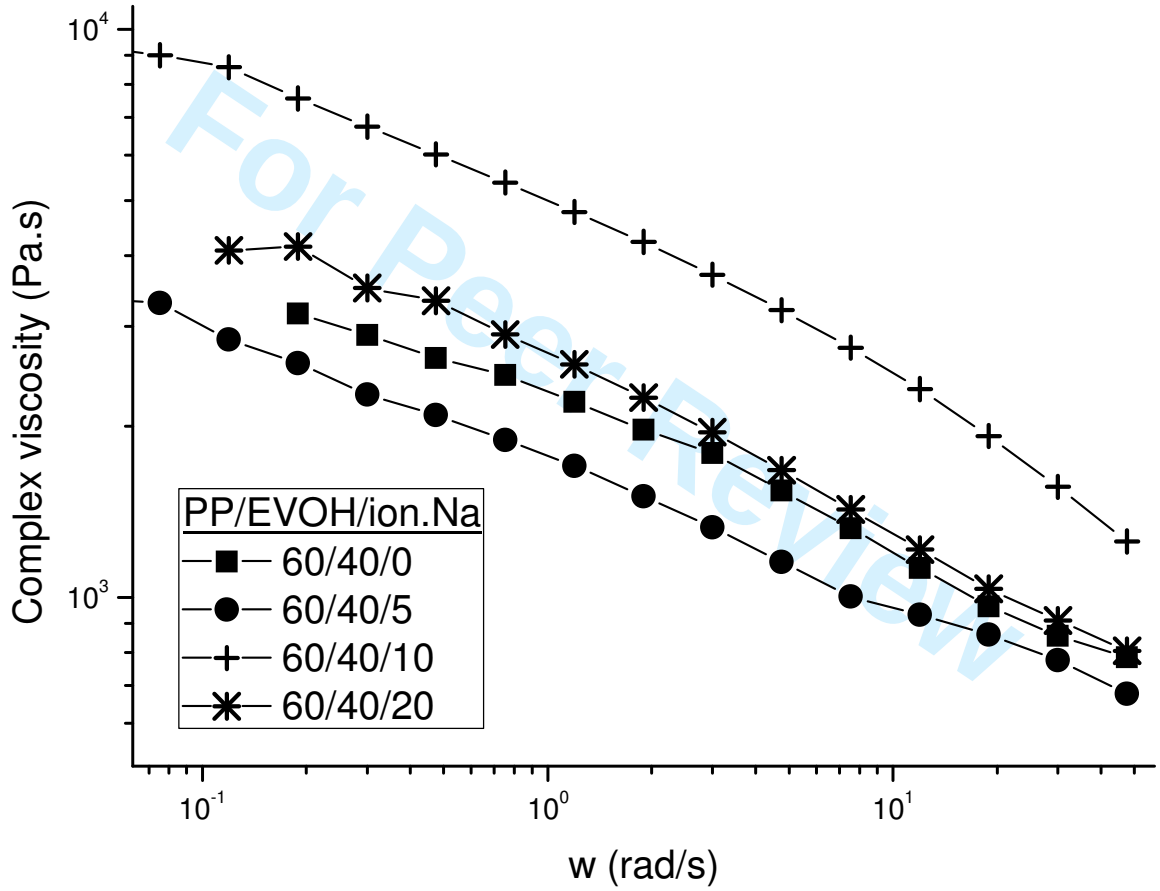

Fig.5a

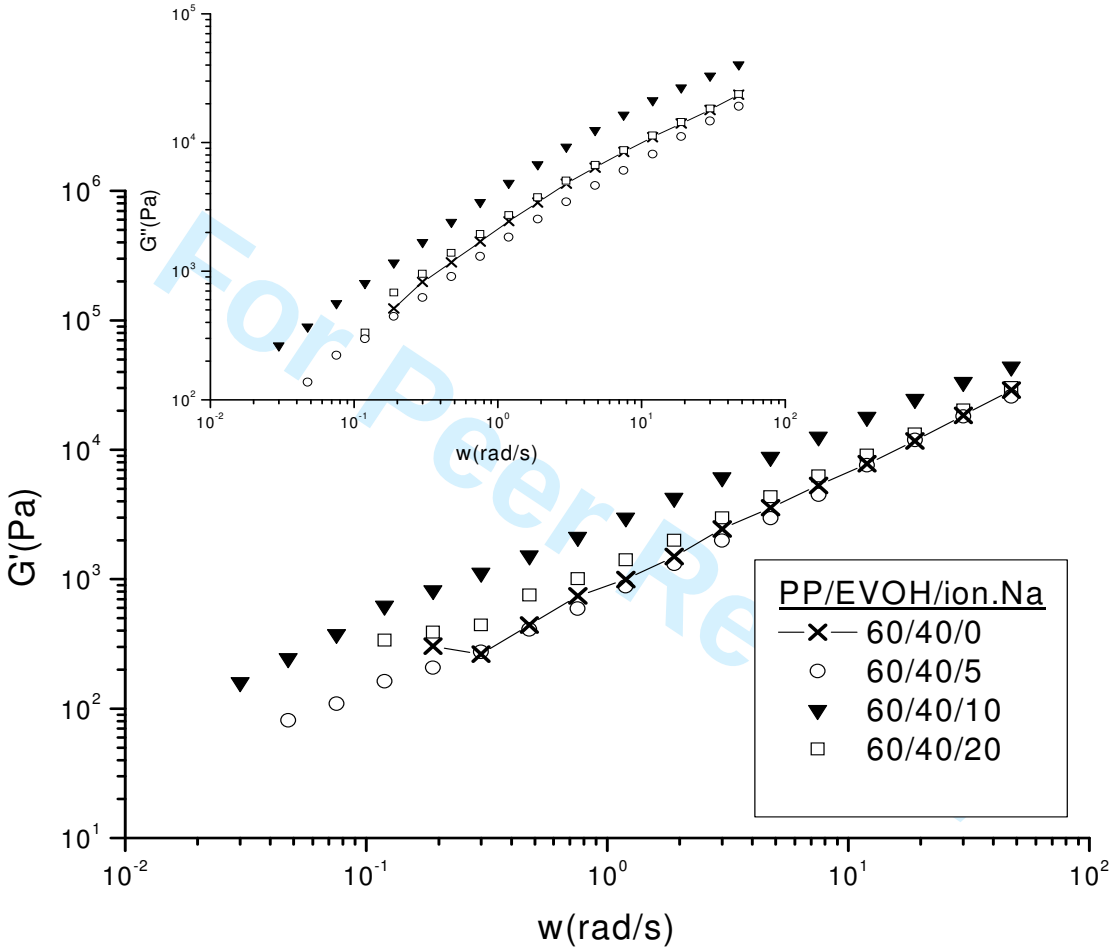

Fig.5b

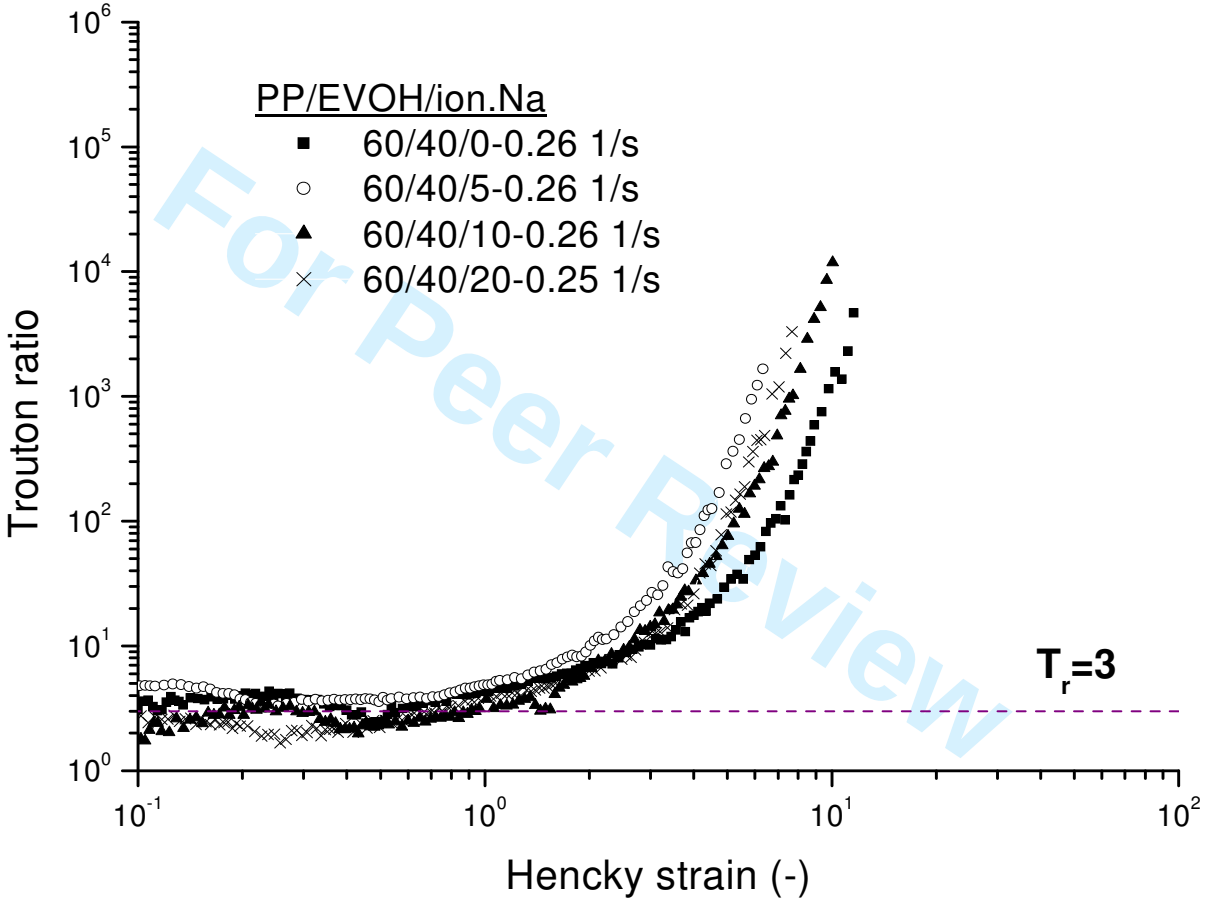

Fig.5c

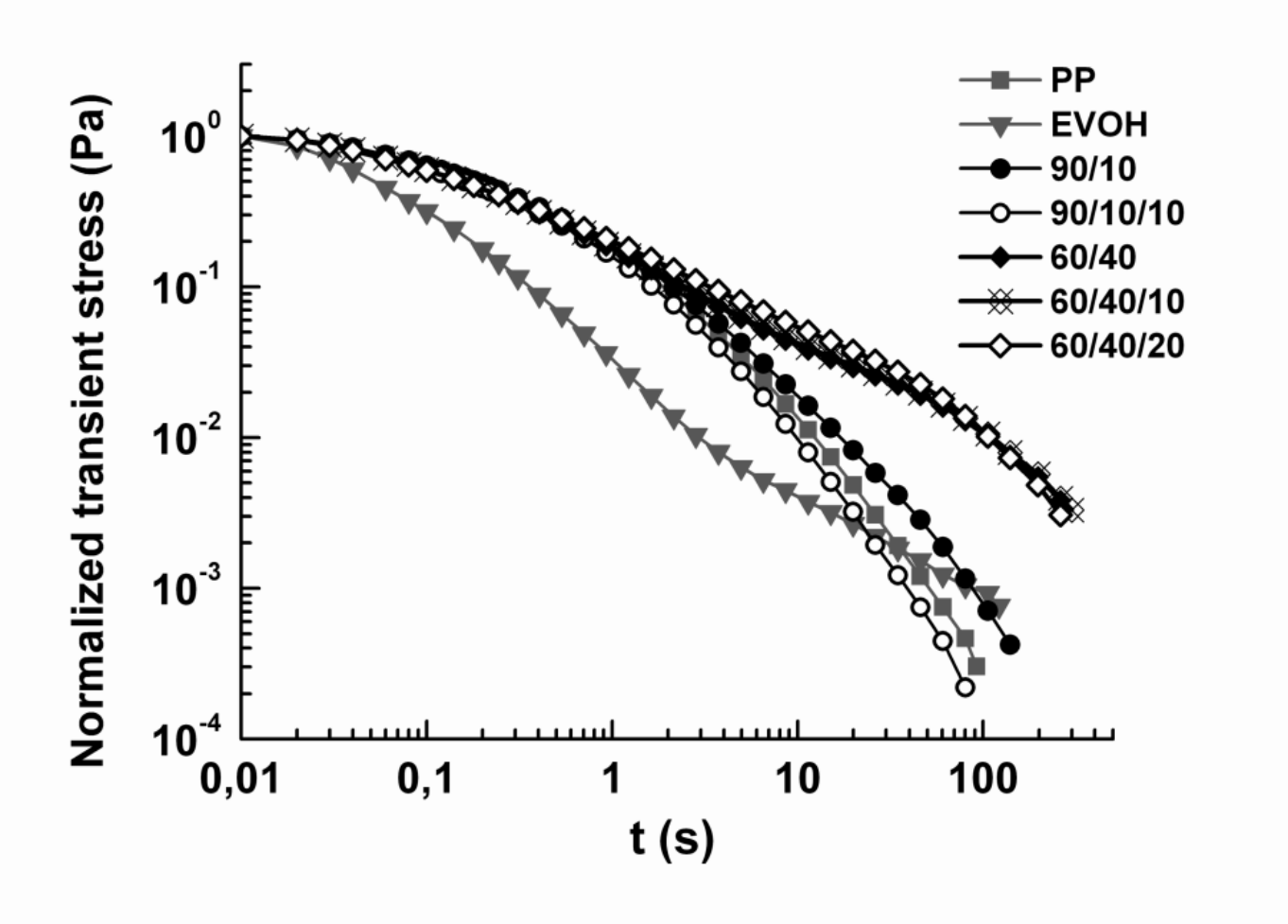
Normalized transient stress (Pa)
10^{0}
10^{-1}
10^{-2}
10^{-3}
10^{-4}
0,01
0,1
1
10
100
t (s)
PP
EVOH
90/10
90/10/10
60/40
60/40/10
60/40/20

Fig.6